Berichte des Forschungszentrums Jülich 3922

2nd ANKE Workshop on „Strangeness Production in pp and pA Interactions at ANKE“

Held at the Petersburg Nuclear Physics Institute (PNPI), Gatchina, Russia on June 21/22, 2001.

Markus Büscher, Vera Kleber,
Pawel Kulessa, Mikhail Nekipelov

Berichte des Forschungszentrums Jülich ; 3922
ISSN 0944-2952
Institut für Kernphysik Jül-3922

Zu beziehen durch: Forschungszentrum Jülich GmbH · Zentralbibliothek
52425 Jülich · Bundesrepublik Deutschland
☎ 02461/61-5220 · Telefax: 02461/61-6103 · e-mail: zb-publikation@fz-juelich.de

Preface

The workshop on "Strangeness Production in pp and pA Interactions at ANKE" was held at the *Petersburg Nuclear Physics Institute (PNPI)* in Gatchina, Russia on June 21/22, 2001. During the workshop the latest experimental data on K^+-meson production in proton-nucleus and elementary proton-proton interactions obtained at the ANKE spectrometer at the proton synchrotron COSY of the *Forschungszentrum Jülich (FZJ)* were intensively discussed. About 25 scientists mostly from Russia and Germany joined the workshop and 20 talks were presented.

This booklet contains copies of the transparencies shown during the workshop as well as short summaries of each talk. These presentations focussed on yet unpublished data from ANKE which are still under analysis. For completeness and in order to give the reader an overview about the accomplished results from ANKE, also copies of already published articles are supplied as the first section of these proceedings. The outstanding result up to now is the measurement of deep-subthreshold K^+ production in proton carbon collisions. These data reveal a high degree of collectivity in the target nuclei.

The workshop benefitted greatly from financial support by the Deutsche Forschungsgemeinschaft (DFG)[1], the German Ministry for Education and Research (BMBF)[2], the Russian Foundation for Fundamental Research (RFFI)[3] and the board of management of the FZJ which is gratefully acknowledged.

Last but not least we would like to thank the local organizers, Dr. V. Koptev and colleagues, for the technical organization of the meeting. We enjoyed very much the hospitality at *PNPI* which led to a stimulating atmosphere with extremely lively and fruitful discussions.

Jülich, October 2001

Markus Büscher

---

[1] 436 RUS 113/444, 436 RUS 113/561

[2] WTZ-RUS-684-00, WTZ-RUS-685-00

[3] 99-02-04034, 99-02-18179a

Contents

2^{nd} ANKE workshop on "Strangeness production in pp and pA interactions at ANKE" June 21/22, 2001 PNPI, Gatchina

Thursday, June 21: K^+-production in proton-nucleus collisions

		Chairperson: V. Koptev
10:00	*A.A. Vorobyev*	Welcome
10:10	*M. Büscher (FZJ)*	Status of K^+-measurements with ANKE at COSY-Jülich
10:40	*R. Koch (FZJ)*	Luminosities during ANKE experiments (A dependence)
		V. Koptev
11:30	*M. Nekipelov (PNPI, FZJ)*	Data on K^+-production in pA collisions from ANKE
12:00	*A. Sibirtsev/M. Büscher (FZJ)*	Compilation of existing data
12:30	Discussion:	Experimental situation in K^+-production from nuclei
		W. Cassing
14:30	*Z. Rudy*	Results of CBUU calculations
15:00	*E.Ya. Paryev (INR)*	Folding-model calculations I
15:30	*A. Sibirtsev (FZJ)*	Folding-model calculations II
16:00	*M. Büscher (FZJ)*	First results of the ROC-model calculations
		W. Cassing
16:40	Discussion:	What have we learned about K^+-production in nuclei?
17:15	*V. Koptev (PNPI)*	Future K^+-measurements with ANKE
17:45	*M. Hartmann (FZJ)*	Measurements with the K^--detection system
19:00	*Dinner*	

Friday, June 22: ANKE experiments on ω, $a_0(980)/f_0(980)$, Λ and Σ production

		H. Ströher
10:00	*V. Kleber (FZJ)*	Results of the measurements on pp $\rightarrow da_0^+(980)$
10:40	Discussion:	Which further experimental information is needed from ANKE?
11:10	*M. Büscher (FZJ)*	Planned $a_0(980)/f_0(980)$ measurements at ANKE
		H. Ströher
12:00	*P. Kravchenko(PNPI)*	Measurement of the Λ/Σ ratio at ANKE
12:30	Discussion	
13:00	*V. Chernyshev (ITEP)*	Status of the pellet target for ANKE
		M. Büscher
15:00	*S. Barsov (PNPI)*	Data on ω-meson production on neutron targets from ANKE
15:30	*A. Mussgiller (FZJ)*	Target-near counters for spectator tagging
	A. Mussgiller (FZJ)	Future spectator and vertex counters for ANKE
16:15	*I. Saluzhenko (ITEP)*	NN correlations: Pauli principle and FSI
16:45	*H. Ströher (FZJ)*	Long-term perspectives, final discussion

List of participants

	Name	Institution	e-mail
1	V. Abaev	PNPI, Gatchina	abaev@mail.pnpi.spb.ru
2	S. Barsov	PNPI, Gatchina	barsov@mail.pnpi.spb.ru
3	M. Büscher	FZ Jülich	m.buescher@fz-juelich.de
4	W. Cassing	Univ. Giessen	Wolfgang.Cassing@theo.physik.uni-giessen.de
6	V. Chernyshev	ITEP, Moscow	chernychov@vitep5.itep.ru
7	A. Getalov	PNPI, Gatchina	getalov@mail.pnpi.spb.ru
8	M. Hartmann	FZ Jülich	m.hartmann@fz-juelich.de
9	V. Kleber	FZ Jülich	v.kleber@fz-juelich.de
10	R. Koch	FZ Jülich	r.koch@fz-juelich.de
11	V. Koptev	PNPI, Gatchina	koptev@mail.pnpi.spb.ru
12	P. Kravtchenko	PNPI, Gatchina	kravch@reco3.pnpi.spb.ru
13	A. Kudryavstsev	ITEP, Moscow	kudryavt@heron.itep.ru
14	P. Kulessa	FZ Jülich	p.kulessa@fz-juelich.de
15	S. Manaenkov	PNPI, Gatchina	sman@mail.pnpi.spb.ru
16	S. Mikirtychiants	PNPI, Gatchina	mkrtch@mail.pnpi.spb.ru
17	A. Mussgiller	FZ Jülich	a.mussgiller@fz-juelich.de
18	M. Nekipelov	FZJ, PNPI	m.nekipelov@fz-juelich.de
19	E. Paryev	INR Moscow	Paryev@al20.inr.troitsk.ru
20	Z. Rudy	Jagellonian Univ.	ufrudy@cyf-kr.edu.pl
21	I. Seluzhenkov	ITEP, Moscow	seluzhen@heron.itep.ru
22	A. Sibirtsev	FZ Jülich	a.sibirtsev@fz-juelich.de
23	H. Ströher	FZ Jülich	h.stroeher@fz-juelich.de
24	M. Zhalov	PNPI, Gatchina	

Photos taken during the workshop

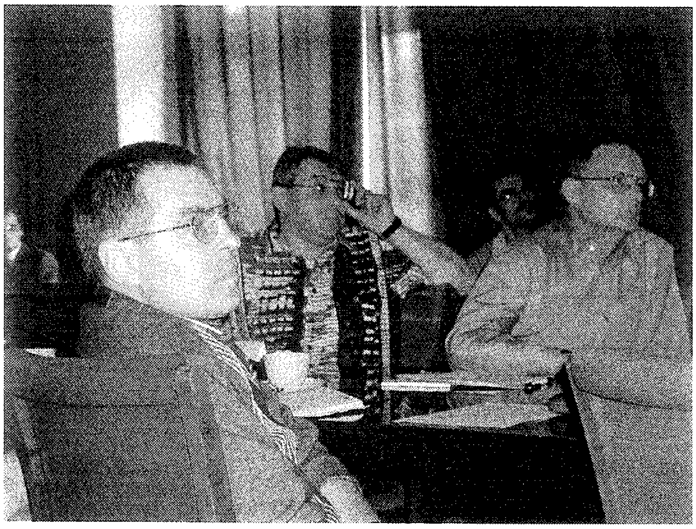

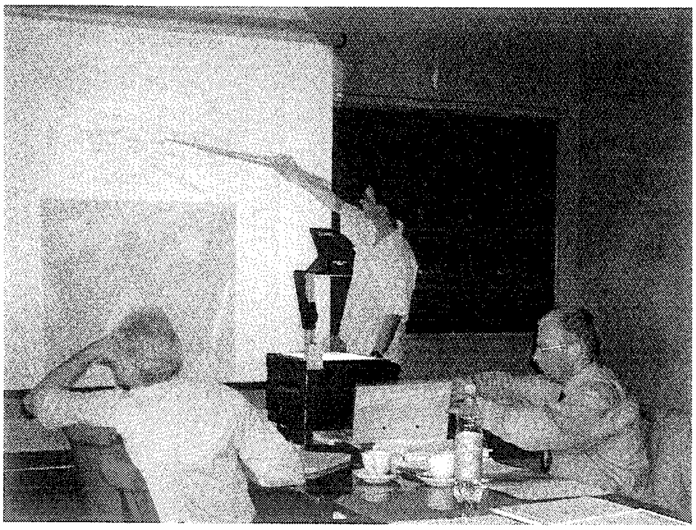

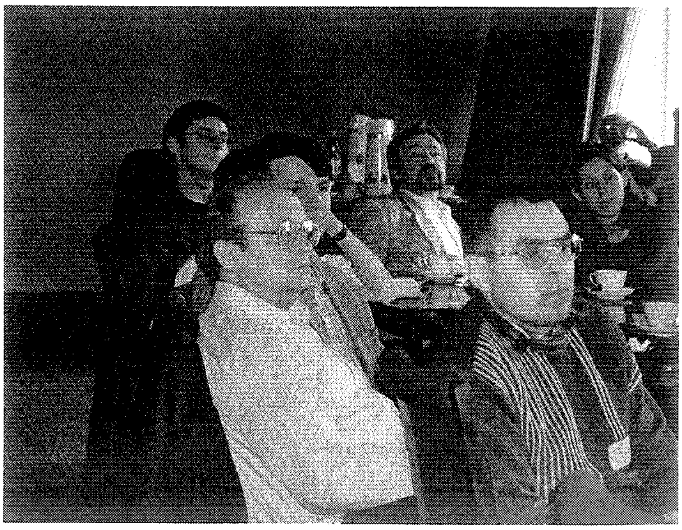

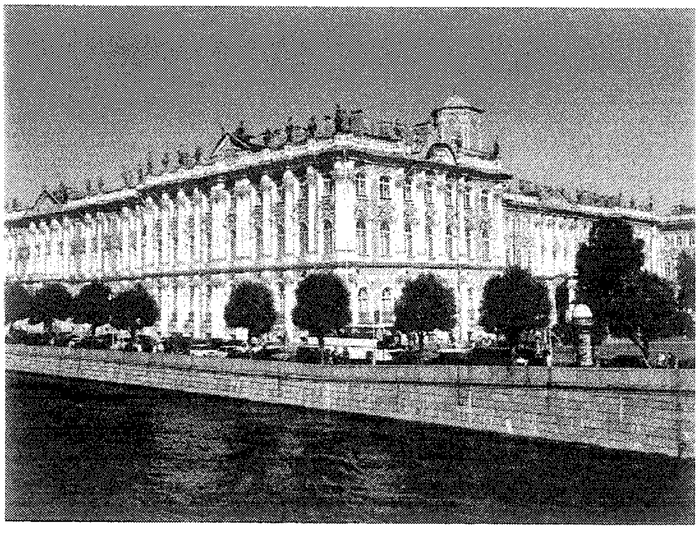

Identification of K^+-mesons from subthreshold pA collisions with ANKE at COSY-Jülich

M. Büscher[a], H. Junghans[a], V. Koptev[b], M. Nekipelov[b], K. Sistemich[a], H. Ströher[a], S. Barsov[b], G. Borchert[a], W. Borgs[a], M. Debowski[c], W. Erven[d], R. Esser[e,1], P. Fedorets[f], D. Gotta[a], M. Hartmann[a], V. Hejny[a], A. Kacharava[g,h], H.R. Koch[a], V. Komarov[g], P. Kulessa[i], A. Kulikov[g], G. Macharashvili[g,h], S. Merzliakov[g], S. Mikirtychiants[b], H. Müller[c], A. Mussgiller[a], R. Nellen[a], M. Nioradze[h], H. Ohm[a], A. Petrus[g], F. Rathmann[a], Z. Rudy[i], R. Schleichert[a], Chr. Schneider[c], O.W.B. Schult[a], H.J. Stein[a], I. Zychor[j]

[a]*Institut für Kernphysik, Forschungszentrum Jülich, 52425 Jülich, Germany*

[b]*High Energy Physics Department, Petersburg Nuclear Physics Institute, 188350 Gatchina, Russia*

[c]*Institut für Kern- und Hadronenphysik, Forschungszentrum Rossendorf, D-01474 Dresden*

[d]*Zentralinstitut für Elektronik, Forschungszentrum Jülich, 52425 Jülich, Germany*

[e]*Institut für Kernphysik, Universität zu Köln, Zülpicher Str. 77, 50937 Köln, Germany*

[f]*Institute for Theoretical and Experimental Physics, Cheremushkinskaya 25, 117259 Moscow, Russia*

[g]*Laboratory of Nuclear Problems, Joint Institute for Nuclear Research, 141980 Dubna, Russia*

[h]*High Energy Physics Institute, Tbilisi State University, University Street 9, 380086 Tbilisi, Georgia*

[i]*Institute of Physics, Jagellonian University, Reymonta 4,30059 Cracow, Poland*

[j]*The Andrzej Soltan Institute for Nuclear Studies, 05400 Swierk, Poland*

Abstract

The spectrometer ANKE has been put into operation at the accelerator COSY of the Forschungszentrum Jülich in spring 1998. An initial scientific goal is to study K^+-production in pA collisions at subthreshold energies far below the free NN-threshold at $T_p = 1.58$ GeV. This requires the identification of K^+-mesons in a background of pions and protons, about 10^6 times more intense. In this paper the sophisticated detection system and the software procedures for kaon identification are described. With the help of TOF, energy-loss and range measurements as well as the track information from wire chambers, it is possible to measure $\mathrm{d}^2\sigma/\,\mathrm{d}\Omega\,\mathrm{d}p$ for deep subthreshold K^+ production at beam energies down to $T_\mathrm{p} = 1.0$ GeV.

PACS: 29.40.-n; 25.40.-h

Key words: K^+-meson detection; Subthreshold K^+-production

1 Introduction

The production of K^+-mesons in proton-nucleus reactions at beam energies below the free nucleon-nucleon threshold ($T_\mathrm{p} = 1.58$ GeV), so-called subthreshold production presently is a topic of strong interest [1–4]. Since K^+-mesons have a long mean free path in the nuclear medium it is expected that valuable information about short-range correlations in nuclei can be extracted from these studies. Further research goals are insights into the reaction dynamics, different production mechanisms and the properties of the produced kaons inside the nuclear environment. In a recent theoretical paper [3] it has been pointed out that the existing data still do not allow to draw unambiguous conclusions about the above mentioned issues. Differential spectra are needed in a wide momentum range for different target nuclei and beam energies. This is particularly the case at beam energies below 1.2 GeV since so far only total cross sections have been measured there [1].

The great challenge of kaon studies at beam energies far below the NN-threshold is the fact that the production cross sections are extremely small. Furthermore, the produced K^+-mesons have a short life time and, thus, a very compact detection system is mandatory, in particular at low kaon momenta. The magnetic spectrometer ANKE [5–10] and its detectors have been built and optimized for such measurements.

In order to get realistic estimates on the K^+ and background rates at ANKE, calculations were performed using the Rossendorf-Collision (ROC) model [11]. Figure 1 shows the result of these model calculations for proton-carbon collisions. The production cross sections shown in the figure are integrated over the angular range $\vartheta = 0 \ldots 10^\circ$ — roughly corresponding to the angular acceptance of ANKE [6,10]. It can be seen that the background of protons and

---

[1] Now working at: Saint-Gobain Crystals & Detectors GmbH, 42929 Wermelskirchen, Germany.

pions stays nearly constant whereas the kaon cross section dramatically decreases as the energy approaches the absolute threshold ($T_p = 0.75$ GeV for carbon); at $T_p = 1.0$ GeV, the lowest energy of our measurements up to now, the K^+/π^+ ratio is as small as $\sim 10^{-6}$. Note that the cross sections presented in Fig. 1 are momentum integrated. Most of the produced protons are above the momentum range measured at ANKE. Thus, in the spectra presented in Sect. 3.1, the number of pions and protons is approximately equal. However, high-momentum protons can hit structure material, e.g., the pole shoes of the spectrometer magnet and produce secondary particles. In fact, those turned out to be the most severe source of background, see Sect. 3.2.

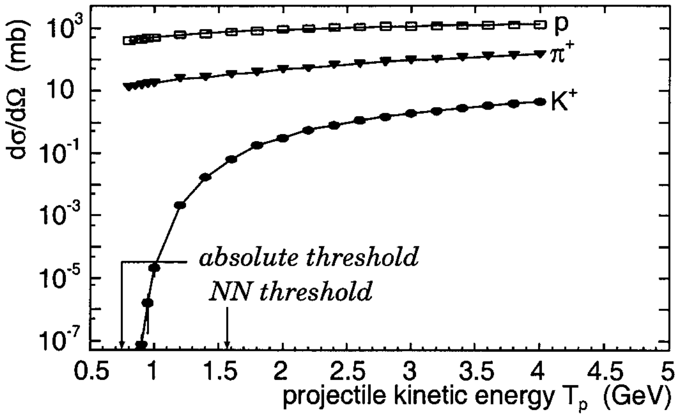

Fig. 1. Predicted momentum-integrated cross sections for the production of K^+ mesons and background particles in proton-carbon collisions into emission angles $\vartheta < 10°$. The calculations were made using the Rossendorf-Collision (ROC) model [11].

The spectrometer ANKE has been described in detail in [9]. Therefore, in this paper only a brief overview of the setup and its detection systems for K^+-mesons is given. The procedures for data analysis are described and it is shown how momentum distributions of kaons from proton-nucleus collisions at beam energies as low as 1.0 GeV are obtained.

2 Description of the experimental setup

2.1 Principles of K^+-Identification with ANKE

For the identification of K^+-mesons the following criteria are used at ANKE:

- ANKE provides a momentum focusing of the ejectiles (Sect. 2.2). This is used to define the K^+-momenta and serves as an important means to suppress the background of pions and protons in range telescopes (Sect. 2.3.2).

- A fast on-line trigger system based on start- and stop detectors of a time-of-flight setup allows the selection of particles with certain momenta and emission angles at the target. Narrow time-of-flight (TOF) gates can be defined for the identification of pions, kaons and protons, respectively (Sect. 2.3).
- Range telescopes in the focal surface of the spectrometer dipole discriminate pions, kaons and protons with the same momenta due to their different energy losses. Passive degraders in the telescopes between the scintillation counters enhance the discrimination efficiency (Sects. 2.3.2 and 3.1).
- The K^+-mesons are stopped in the range telescopes. Their decay with a lifetime of $\tau = 12.4$ ns provides an effective criterion for the identification of these mesons via the detection of delayed signals (Sects. 2.3.2 and 3.1).
- The tracks of the ejectiles are measured with multi-wire proportional chambers (MWPCs) (Sect. 2.3.1). From this information the emission angles at the target are deduced and a suppression of background not originating from the target is possible (Sect. 3.2).

2.2 The ANKE spectrometer

The ANKE spectrometer [7–10] is located at the internal target position TPA of the cooler synchrotron COSY-Jülich. It consists of three dipole magnets — two smaller ones (D1 and D3, see Fig. 2) to guide the circulating COSY beam and a C-shaped spectrometer magnet (D2) with a large gap height of 20 cm. Between D1 and D2, space for the installation of various internal targets is available. For the measurements described here, triangular-shaped foil targets made of carbon (polycrystalline diamond), copper and gold were suspended from frames [9]. The target dimensions typically are 2 mm (width at base glued to the frame), 20 mm (length) and 0.04–15 mg/cm^2 (thickness). D2 has an angular acceptance of $\Delta\Omega \approx 50$ msr for ejectiles emitted under forward angles $\vartheta \approx 0°$. Furthermore, the flight path of the ejectiles between target and the focal-surface detectors is short ($l \approx 150 \ldots 400$ cm) so that kaons reach the detectors with a probability of ~ 30 % in spite of their short lifetime.

Each of the range telescopes located at the focal-surface was optimized for a certain kaon-momentum range, see Sect. 2.3.2. Therefore, when changing the beam energy to measure the K^+-momentum spectra for different projectile energies, one must keep constant *i)* the field in the ANKE magnets and *ii)* the relative locations of target and D2 so that the momenta of the ejectiles hitting a certain telescope remain constant. Consequently, the radius of curvature and the deflection angle of the circulating COSY beam changes in all three dipoles with varying beam energy. This can be compensated by a movement of the spectrometer dipole D2 perpendicular to the direction of the undisturbed COSY beam [9]. For the measurements described in this paper, all three magnets were operated at a fixed field strength of $B = 1.30$ T (measure-

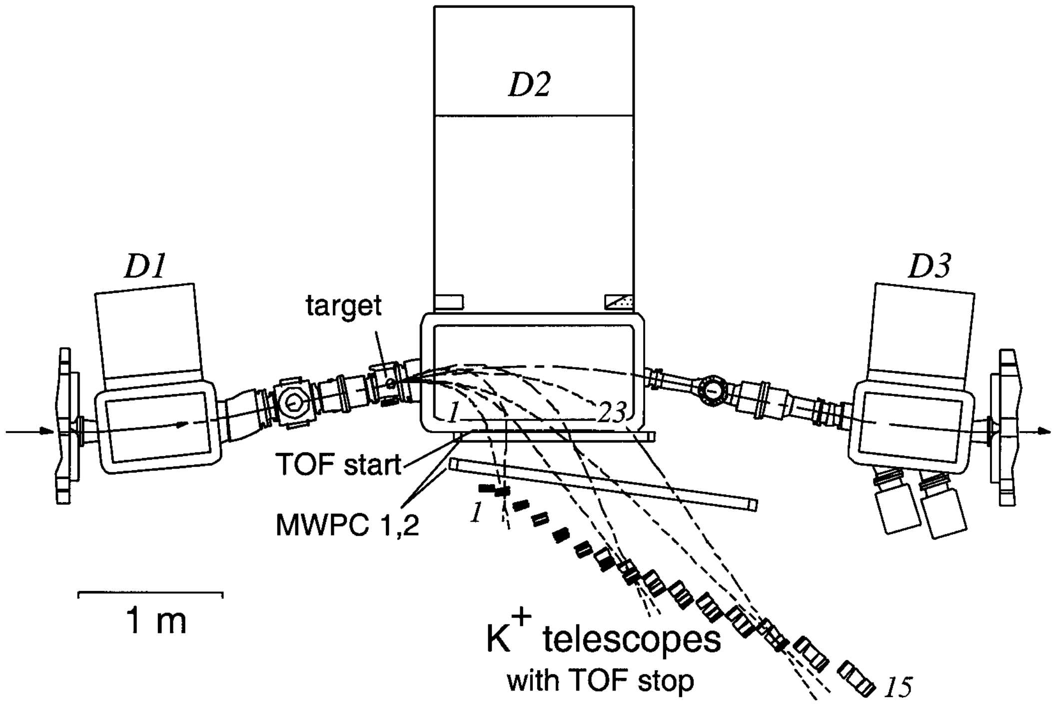

Fig. 2. Top view of the ANKE spectrometer and detectors used for K^+ identification. The dashed lines show trajectories of ejectiles with different momenta and horizontal emission angles of $\vartheta \pm 10°$. The numbers indicate the positions of the 23 start counters and the 15 telescopes.

ment of the K^+-production cross sections) or at the maximum achievable field strength in D2 of $B = 1.57$ T (calibration measurements for the time-of-flight detectors). The lower field strength used for the cross-section measurements was chosen in order to avoid too large deflection angles of the COSY beam at low beam energies. The resulting deflection angles in D1, $\alpha = 10.1° \ldots 5.5°$ at $T_p = 1.0 \ldots 2.3$ GeV, are in any case smaller than the maximum value of 10.6° permitted by the bellows of the vacuum system, see [9] for details.

Ray-tracing calculations [10] show that at $B = 1.30$ T the K^+ telescopes cover a momentum range of $p \approx 110 \ldots 525$ MeV/c. The horizontal angular acceptance of D2 for which the focusing properties are still sufficient to allow kaon identification in the telescopes is $\vartheta \approx -15° \ldots +15°$, cf. Sect. 2.3. The vertical acceptance is given by the gap height of D2 and varies between $\phi \approx \pm 7°$ for the lowest momenta and $\pm 3.5°$ (highest). The heights of all detectors were chosen such that they cover the full vertical acceptance of the spectrometer dipole.

2.3 K^+-detection system

The schematic layout of the K^+-detection system at ANKE is sketched in Fig. 3. It is rigidly connected to the spectrometer dipole D2 and consists of three major components: *i)* 23 TOF-start counters (*PILOT-U, Nuclear Enterprises*) close to the vacuum window (made of 500 μm Al) at the right-hand side of D2. The counters are positioned as close as possible to the exit window in order to maximize the distance to the TOF-stop counters. Each start counter has a horizontal angular acceptance of $2^\circ - 6^\circ$ depending on the ejectile momenta. All scintillators are 27 cm high and 5 cm wide. Their thickness has been chosen as a compromise between sufficient light output and little small-angle scattering. It increases from 0.5 mm (counters 1, 2) for the low momentum detectors to 1.0 mm (counters 3—5) and 2.0 mm for higher momenta. Each scintillator is read out on both ends by a photomultiplier. *ii)* The tracking system to reconstruct ejectile trajectories consisting of two multi-wire proportional chambers (MWPC 1, 2). They are located in front of all detector components except the TOF-start counters in order to minimize distortions of the ejectile trajectories due to small-angle scattering. *iii)* 15 range telescopes which are placed along the focal surface of D2. The horizontal angular acceptance of each telescope varies from $\pm 1^\circ$ to $\pm 15^\circ$ depending on the on- or off-line coincidences with the corresponding start counters. Each telescope is composed of TOF-stop, ΔE, veto scintillation counters (*BC408, Bicron*), which are read out by photomultipliers on both sides, and two passive degraders made of copper. Telescopes 9–15 also contain lucite Čerenkov counters. For a detailed description of the telescopes see Sect. 2.3.2.

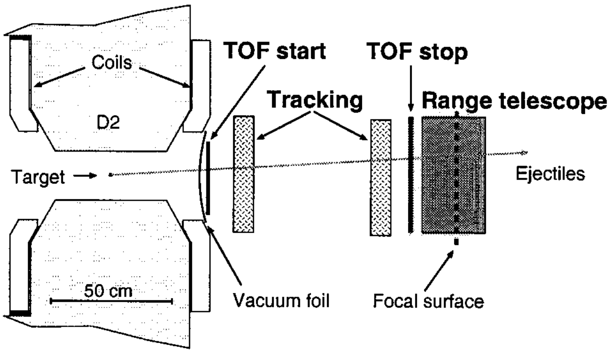

Fig. 3. Simplified layout of the detection system used for the subthreshold K^+-studies at ANKE (looking in the direction of the circulating COSY beam).

The precise time information from the start, stop, ΔE and veto counters (see Sect. 3.1 for values of the time resolution) is achieved by constant-fraction discriminators and mean timers both specifically developed for this purpose [12]. In addition, the vertical spatial information in each scintillator is obtained from the time difference of both phototubes. The resolution for the stop detectors is better than 30 mm (FWHM). With one specially built VME-module for each stop counter it is possible to set a common TOF gate (length variable between 3 ns and 23 ns) in coincidence with up to 16 individually adjustable start-stop combinations [12]. In this way corridors of acceptable start-stop combinations can be defined through which the K^+-mesons from the target should pass. A total of 16 VME modules is needed for the ANKE on-line TOF trigger which allows to select pions, kaons or protons already during data taking.

2.3.1 Multi-wire proportional chambers

The two MWPCs [13,14] of the ANKE K^+-detection system have been built in a modular design at the Forschungszentrum Rossendorf and differ only in the dimension of the sensitive planes and the diameter of the anode wires (see Table 1). The arrangement of the sensitive wires in the planes, vertical and inclined by +30° and −30°, respectively, allows to determine the space coordinates of the particle track in the wire chamber. Together with the knowledge of the magnetic field of the D2 magnet one can reconstruct the momentum and emission angle of the particle at the target position. The necessary accuracy of the reconstructed momentum $\Delta p/p$ is 2–3% for pions. This can be achieved with a wire spacing of 2.54 mm. An intrinsic resolution $\sim$ 0.7 mm between the inclined and vertical planes has been determined in test measurements [13].

Table 1
Properties of MWPC 1 and MWPC 2.

	MWPC1	MWPC2
Gas mixture	70% Ar : 30% CO_2	
No. of anode planes	3	
Arrangement of anode wires	vertical and +30° und −30° inclined	
HV anodes	0 V	
max. HV cathodes	−3000 V	
Wire spacing	2.54 mm	
Distance anode-cathode	5 mm	
No. of wires per plane	512	768
Anode wires	20 μm tungsten	25 μm tungsten
Cathode material	18 μm mylar foil	23 μm mylar foil
Sensitive area	35·130 cm^2	60·196 cm^2

The readout of the chambers is performed using a highly integrated front-end system based on two chips which were developed at the Rutherford Appleton Laboratory (RAL) [15]. The analog chip RAL 118 amplifies and discriminates the signal. The digital chip RAL 111 on the one hand provides the proper delay of the signal using a digital shift register. This is necessary since the signal of the MWPCs must be stored until the system trigger has been generated. On the other hand, RAL 111 digitizes the signals and performs zero suppression. The latter leads to a huge data reduction since in a typical event only around 2% of the wires have a signal and only the numbers of those wires are sent to the subsequent data-aquisition system. Thus during the K^+-measurements particle fluxes of about 5000 s^{-1} per wire could be handled by the readout system. A more detailed description of the complete readout system can be found in [16].

The drift time of electrons in the used gas mixture is 80 ns at most [17]. Therefore no restrictions are expected when the chamber is operated at a maximal particle flux of 10^6 s^{-1}. To minimize the number of multiple hits the width of the readout gate is set to 110 ns.

2.3.2 The K^+ range telescopes

The K^+-telescopes are positioned along the focal surface of D2 perpendicular to the trajectories of ejectiles which leave the target in the forward direction, $\vartheta = 0^\circ$. Each detector covers a limited momentum range given by its width of 10 cm and the dispersion of D2. The values for the momentum acceptances which are shown in the right column of Table 2 were calculated for ejectiles emitted at 0° from the target and neglecting small angle scattering in the vacuum foils and the detector components.

Figure 4a) shows momentum distributions for three telescopes which were obtained from data on π^+-production in proton-carbon collisions and from corresponding GEANT simulations. For the reconstruction of the pion momenta from the wire-chamber information, a simple box-field approach has been applied in which the trajectories in front of and behind the effective field of D2 are described by straight lines. The ejectile momenta are determined by calculating a circular arc with a constant radius of curvature connecting these straight lines. The fact that each of the telescopes is hit by ejectiles within a rather limited momentum range of $\Delta p/p = 7 - 24\%$, provided they originate from the target at angles less than $\sim 15^\circ$ (see right column of Table 2), allows to exploit the different ranges and energy losses of ejectiles with different masses for the K^+-identification, see Sect. 3.1 for details.

Figure 4b) shows momentum distributions for telescope #13 and the individual start counters. It can be seen that particles which traverse start counters #10–21 have a small momentum spread, $\Delta p/p \approx 8\%$. The lowest counters also detect fast ejectiles which are emitted from the target at large angles $\vartheta \leq 30^\circ$. Since they miss the well-defined field region of D2 they are only

Table 2
Dimensions of the telescope components used for the measurements at $B = 1.30$ T. In addition, telescopes #9–15 contain 5 cm thick lucite Čerenkov counters between stop and degrader I. The momentum ranges covered by each telescope are given in the last column.

	Height	Thickness [cm]					Momentum range
Telescope	[cm]	Stop	Degr.I	ΔE	Degr.II	Veto	[MeV/c]
1	52	0.3	—	0.5	0.2	1.0	110–140
2	57	0.5	—	0.5	0.2	1.0	140–160
3	62	1.0	—	1.0	0.2	1.0	160–182
4	67	1.0	—	1.0	0.8	1.0	182–205
5	77	1.0	0.1	1.5	0.8	1.0	205–227
6	82	1.0	0.11–0.37	2.0	0.8	1.0	227–252
7	88	1.0	0.26–0.58	2.0	1.6	1.0	252–280
8	94	1.0	0.43–0.82	3.0	1.3	1.0	280–310
9	100	1.0	0.11–0.57	3.0	1.0	1.0	310–340
10	100	1.0	0.49–1.08	3.0	1.5	1.0	340–370
11	100	1.0	1.06–1.78	3.0	1.7	1.0	370–400
12	100	1.0	1.70–2.57	4.0	1.0	1.0	400–430
13	100	1.0	2.56–3.49	4.0	1.0	1.0	430–460
14	100	1.0	3.23–4.34	5.0	2.0	1.0	460–490
15	100	1.0	4.20–5.37	5.0	2.0	1.0	490–525

slightly deflected so that their momentum distributions smear out. Indicated in the figure is the range of valid start counters which are accepted by the on-line TOF trigger. For these counters, corresponding to horizontal emission angles $|\vartheta| \leq 12°$, the imaging properties of D2 are sufficient to detect ejectiles with well defined momenta.

The telescopes consist of vertically oriented scintillators and copper degraders. The thicknesses of all components were determined with the help of GEANT simulations [17,18] for K^+-identification. The results of the simulations were verified for a sample telescope by test measurements with pion, kaon and proton beams from the 10 GeV proton synchrotron at ITEP, Moscow [4]. Table 2 shows the thicknesses of all components used during the measurements described here. The first counter in each telescope is the TOF-stop counter, see Fig. 5, followed by 5 cm thick lucite Čerenkov counters (in telescopes #9–15 only) for the suppression of fast pionic and leptonic background. During data analysis it turned out that these counters provide no additional back-

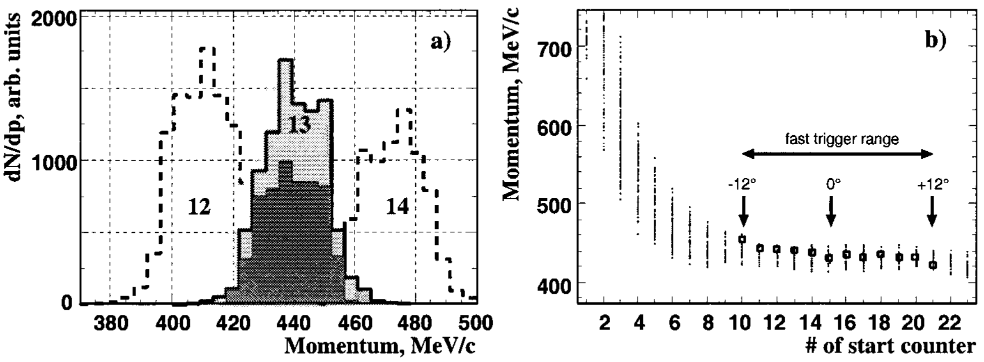

Fig. 4. **a)** Momentum distribution of pions from p(2.3GeV)C $\rightarrow$ π^+X reactions emitted at angles $\leq 10°$ and detected in telescopes #13 (light shaded histogram), 12 and 14 (dashed). For comparison the result of a GEANT simulation is given (dark shaded, scaled down by an arbitrary factor). **b)** Simulated momentum ranges for the individual start counters and telescope #13. For the simulation horizontal emission angles of even up to 30° were permitted. The central arrow indicates the start counter which detects particles emitted at 0° at this setting of the beam energy and field strength in D2; the range of start-stop combinations accepted by the fast trigger is indicated by the horizontal bar. Also shown by the open squares are the mean ejectile momenta calculated from TOF spectra, see Sect. 3.1 for details.

ground suppression. Thus they were not used in the current analysis for kaon identification.

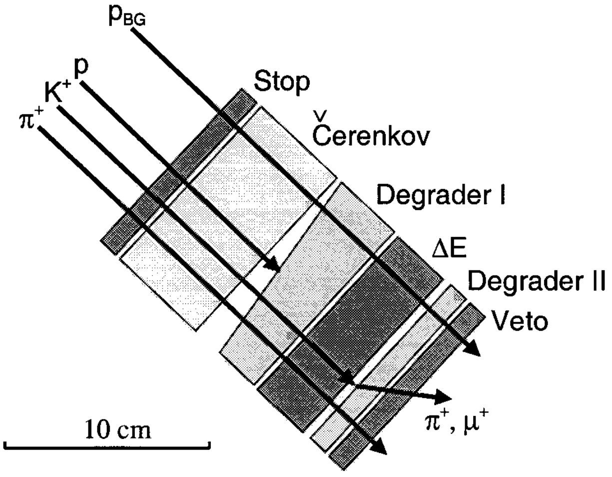

Fig. 5. Sketch of telescope #13. The ranges of pions, kaons and protons originating from the target as well as scattered protons (p_{BG}) with the same velocity (i.e. TOF) as kaons are indicated. See text for a detailed description of detector components.

The function of degrader I is twofold: first, it stops protons originating from the target and prevents them from entering the ΔE counter. Second, it slows down kaons such that they are stopped at the far end of the ΔE counter or in the second degrader. This results in a large K^+ energy loss in the ΔE counter which helps to separate them from pions and scattered protons, see Sect. 3.1. The tapered shape of degrader I accounts for the momentum dispersion along the focal surface of D2: From the left to the right edge of each telescope the degrader thickness increases in correspondence with the ejectile momentum. In order to minimize the range spread for kaons, each telescope is positioned such that the first degrader is located in the focal plane where the momentum spread of the ejectiles is smallest. Pions from the target pass through the counters and degraders almost unaffected due to their high velocity and result in small energy losses in all counters. The thicknesses of degrader I have carefully been fine tuned during calibration measurements (by adding thin copper sheets) at $T_\mathrm{p} = 2.3$ GeV where the kaon rate is sufficiently high to identify them without the help of the energy-loss spectra in the ΔE counter, see Sect. 4.

Kaons which are stopped in the ΔE counter or in the second degrader decay with a lifetime of $\tau = 12.4$ ns. Their decay products, μ^+ or π^+ emitted isotropically, can reach the veto counter and result in signals which are characteristically delayed with respect to K^+-signals in the stop or ΔE counters of the same telescope. This provides an additional criterion for K^+-identification which becomes particularly important for low beam energies. This method based on the detection of delayed decay muons was already applied previously in the measurement of total cross sections at beam energies between 0.8 and 1.0 GeV [1].

The most problematic background is caused by secondary protons produced on the pole shoes of D2 or in the vacuum chamber. This contains a component with the same time-of-flight as the kaons and thus approximately twice their momenta. Such protons ($\mathrm{p_{BG}}$), which are also indicated in Fig. 5, pass through all detectors of a telescope. The thicknesses of degrader II were chosen larger than necessary to prevent kaons from reaching the veto counter: they also slow down the background protons such that their energy loss in the veto counter significantly increases beyond that of the koan-decay products. Selection of events with small energy losses in the veto counters thus is an additional criterion for kaon identification since their decay muons and pions are minimum ionizing.

3 Data analysis

3.1 Examples of scintillator spectra

Examples of time-of-flight (TOF) distributions between the stop counter of telescope #13 and the different start counters are shown in Figure 6. The data were taken during a calibration run with high field strength in D2 ($B =$ 1.57 T). During data taking an open on-line TOF trigger was chosen such that pions, protons and scattered particles are visible in the spectra. Most of the spectra show two distinct peaks for pions and protons originating from the target which have well defined momenta, $p \approx 430 - 460$ MeV/c, see Table 2 and Fig. 4. From the spectra an average time resolution of $\sim$ 650 ps (FWHM) for target pions in the central region — start counters #10–21, corresponding to horizontal emission angles $|\vartheta| \leq 12°$ — has been deduced. The shift of the proton peaks towards smaller flight times and the larger width ($\sim$ 1000 ps) for the lower start-counter numbers is due to the momentum spread shown in Fig. 4b) which causes a variation of the proton velocities. This is not the case for pions since, due to the low mass, their velocity is close to the speed of light. For start-counters with numbers below 5, the two peaks disappear and a broad TOF distribution develops because of the high-momentum protons, see Fig. 4b). The pions are suppressed here because of inefficiencies of the first few start counters for high momentum pions. In start counter #23 the peak of protons from the target is reduced for the following reasons: the average ejectile momenta (and ranges) are smaller, see Fig. 4b), and the effective counter thickness is increased due to the smaller entrance angle into the telescope. This prevents part of the target protons from reaching the ΔE counter. Since a signal in this counter was required in the on-line trigger only the fastest protons can be detected and the proton rate is reduced. This effect also has an influence on the spectra of start counters #18–21. Here the width of the proton peak is reduced from 1000 ps down to 500 ps.

The separation of the pion- and proton-TOF peaks in Fig. 6 allows to calculate the average momentum of the ejectiles originating from the target. The deduced values for start counters #10–21 are presented as the open squares in Fig. 4b) and agree with the momenta from ray-tracing calculations using GEANT. Remember that the TOF spectra from Fig. 6 were obtained at a field strength of $B = 1.57$ T in D2 (field setting used for the TOF calibrations) whereas the momentum ranges in Fig. 4 are given for $B = 1.30$ T (field setting used for the cross-section measurements). Thus the momenta from TOF were multiplied by the ratio of the field strengths 1.30/1.57 in order to allow a comparison with the GEANT simulations.

Fig. 7 shows the energy-loss spectra which were measured simultaneously with the TOF spectra of Fig. 6. They allow to determine the detection efficiencies for pions in the start counters assuming that the energy-loss distributions can be fitted by Landau distributions. Values of $\sim$ 95% were obtained, except for the first two start counters which are only 0.5 mm thick. In this case the efficiencies are below 50%. For kaons the detection efficiencies are higher and very close to 100%. The efficiencies are taken into account when normalizing the number of identified kaons to known pion-production cross sections.

Figure 8a) shows the combined TOF distribution for the stop counter of telescope #13 and start counters #10–21 from Fig. 6. The time resolution for

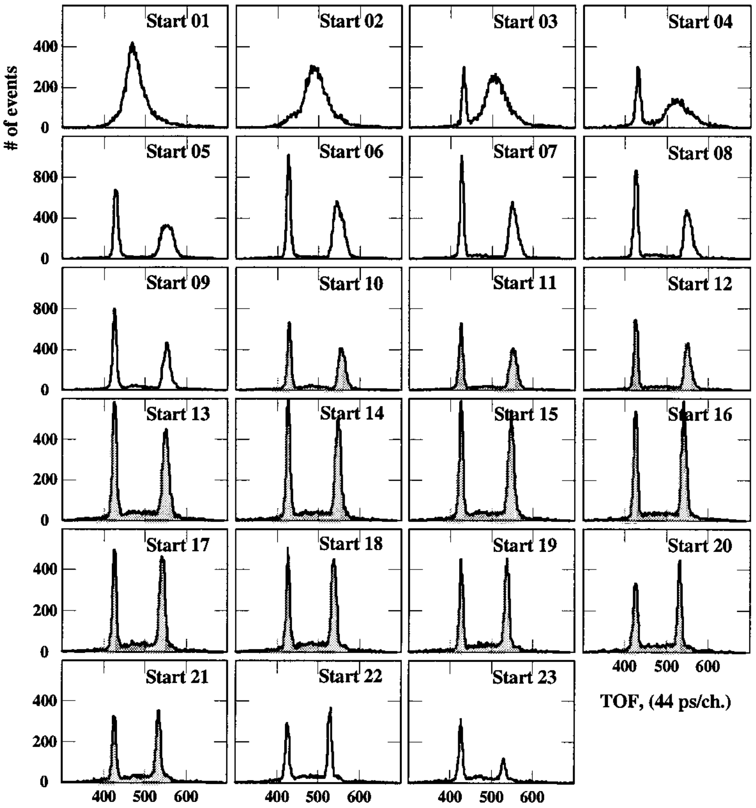

Fig. 6. Time-of-flight spectra at an incident proton energy $T_p = 1.5$ GeV between stop counter #13 and start counters # 1–23. The data presented in this figure were obtained during a dedicated calibration run with open trigger at $B = 1.57$ T with a carbon target. The range of "valid" start counters for this particular stop counter, see Fig. 4b), is indicated by the shaded histograms.

pions in Fig. 8a) amounts to 650 ps (FWHM), as in case of the individual spectra from Fig. 6. Due to the different lengths of the flight paths for each start counter, the values of the TOF difference between pions and protons vary, which causes a smearing of the proton peak in the sum spectrum.

In principle, the observed time resolution should allow a clear separation of pions (protons) and kaons. The TOF difference between pions and kaons (peak-to-peak) amounts to $\sim 8\sigma$; assuming a pure gaussian distribution one would expect a pion suppression much better than the requested 10^6. Such a huge suppression is, however, not achieved in the experiment due to background produced in secondary hadronic interactions. The flat background in Fig. 8 is mainly caused by fast protons emitted from the target at small angles. These protons can hit the pole shoes of D2 or structure material of the vacuum chamber and produce secondary particles which then can reach the telescopes. Such secondary particles are not focussed by D2 and, hence, do not have well defined momenta. Therefore, they result in a broad background distribution in the TOF spectra. Indicated by the shaded area in the sum spectra of Fig. 8 and the following ones are the regions where kaons are expected. This serves

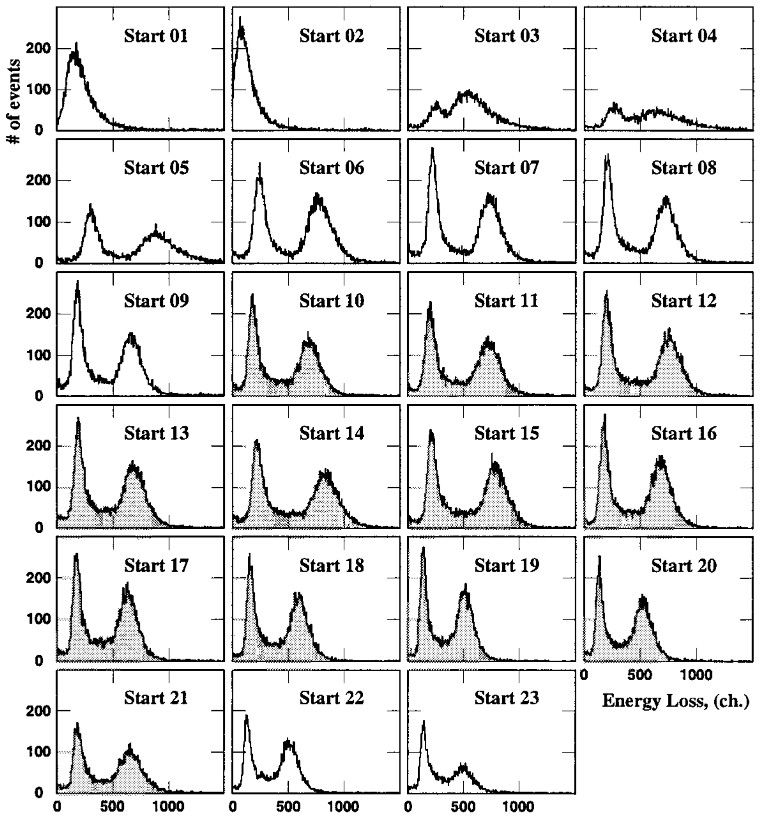

Fig. 7. Energy-loss spectra for the same start-stop combinations as in Fig. 6.

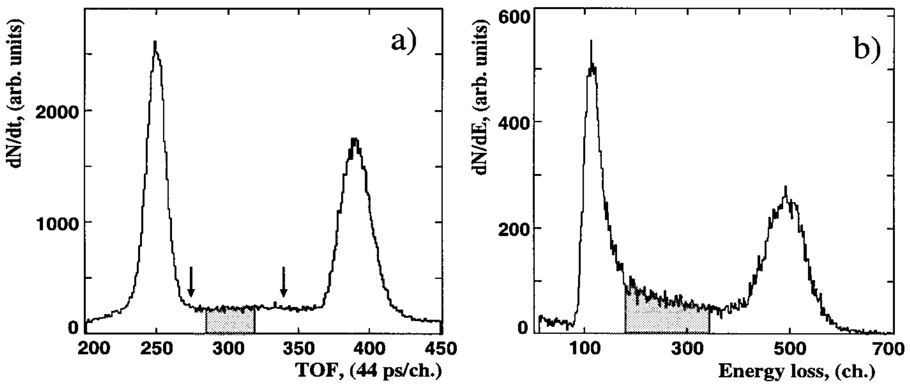

Fig. 8. **a)** TOF and **b)** amplitude spectra of stop counter #13 in coincidence with start counters # 10–21. The approximate position of the gates for the off-line kaon identification are indicated by the shaded areas (see text). Arrows mark the narrowest TOF gates used for on-line event selection. The data were obtained at $B = 1.57$ T with a carbon target.

for illustration only since in the process of kaon identification, individual gates were used for each start-stop combination (i.e. spectra in Fig. 6). The same applies for *all other* scintillator time and amplitude spectra.

Figure 8b) shows the energy-loss distribution in stop counter #13 for ejectiles detected in coincidence with start counters #10–21. As for the TOF spectrum of Fig. 8a) the raw spectrum shows two peaks from pions and protons from the target and a broad background distribution. The ratio of the energy losses of protons and pions is ~ 4.5 as expected from the Bethe-Bloch formula. Consequently, only a moderate separation of pions and kaons (expected energy-loss ratio ~ 1.7) can be achieved from the amplitude signals. Since the lower edge of the pion energy-loss distribution is clearly visible in Fig. 8b), the detection efficiency for pions is larger than 98%. The same high efficiency has been obtained for kaons since the gate indicated in the figure is rather wide.

Figure 9a) shows the energy-loss distribution in the ΔE counter of telescope #13. The data were obtained at $B = 1.30$ T. Since protons from the target are stopped in the Čerenkov counter or in the first degrader there is only one peak from target pions and a broad background distribution from secondary particles visible in the spectrum. As explained in Sect. 2.3.2, the first degraders are used to optimize the energy loss of kaons in the ΔE counters. The solid histogram in Fig. 9b) shows the corresponding energy-loss spectrum for kaons (identified as described later in Sect. 3.4). During the measurements it has been checked whether slight modifications of the degrader thicknesses can improve the kaon-to-background separation. For this purpose the kaon energy loss should be as large as possible (better separation from target pions), while keeping the width of the distributions small (optimization of the kaon to scattered-background ratio). It turned out that the optimization procedure for most telescopes resulted in thicknesses at which the kaons pass through the ΔE counter and are stopped in the second degrader. As an example the corresponding distribution is shown by the dashed histogram in Fig. 9b).

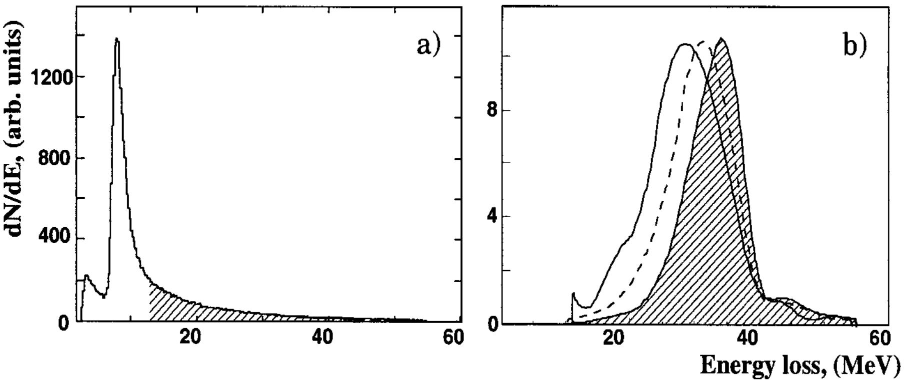

Fig. 9. Energy-loss spectra for ΔE-counter #13 in coincidence with start counters #10–21. **a)** Raw spectrum, the gate for kaons is located above $\Delta E \sim 13$ MeV. **b)** Kaon spectra taken during optimization of degrader I. The values of the tapered degrader thickness are: *i)* 2.76–3.69 cm (solid histogram, initial value from simulation calculations), *ii)* 2.66–3.59 cm (dashed histogram), and *iii)* 2.56–3.49 cm (shaded histogram, optimum thickness given in Table 2). All data were obtained at $T_{\mathrm{p}} = 2.0$ GeV and $B = 1.30$ T with a carbon target.

As explained in Sect. 2.3.2, the time information from the veto counter is a particularly effective criterion for kaon identification. If the kaons are stopped in the second degrader one expects that only their decay muons and pions can reach the veto counter with a time delay characteristic for the K^+-lifetime of 12.4 ns. Figure 10 shows the distribution of the time difference of particle detection in the veto and stop counters of telescope #13. One can clearly see a peak from particles directly passing through the second degrader (pions and secondary protons). In addition, there are delayed events visible which can be attributed to the decay products of K^+-mesons stopped in the second degrader, see Sect. 3.4. The on-line trigger for the accumulation of the K^+-data at low projectile energies rejected prompt events and admitted only those with a delay > 1.3 ns (channel 30). Off line a threshold of > 2.3 ns (channel 55) was set.

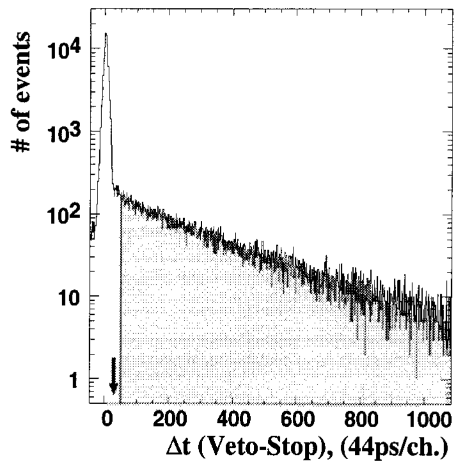

Fig. 10. Time difference between detection of particles in veto- and stop counter of telescope #13. To make the spectrum more illustrative, kaon gates were applied in the scintillator spectra described above and only particles were accepted which vertically come from the target plane (see next section). The arrow shows the location of the gates used during the measurements whereas the off-line cut is indicated by the shaded area, see text for details. The data were obtained at $T_\mathrm{p} = 2.3$ GeV and $B = 1.30$ T with a carbon target.

The use of the full scintillator information (TOF, energy loss in start, stop, ΔE and veto counters plus selection of delayed events in the veto counter) allows for a clear separation of the kaons from pions and protons originating from the target even at the lowest beam energy $T_\mathrm{p} = 1.0$ GeV. However, the background from secondary particles scattered at the pole shoes of D2 cannot sufficiently be suppressed. This is only possible by using the information from the wire chambers on the direction of the ejectiles as explained in the following section.

3.2 Background suppression using the MWPC information

As indicated in Fig. 11 by the dashed line, particles from the target within the angular acceptance passing through the first MWPC at some vertical coordinate y are expected to have a certain vertical angle ϑ (which is measured with the second chamber). All ejectiles undergo multiple scattering in the vacuum foil of D2 and in detector components. This causes some smearing $\Delta\vartheta$ of the expected vertical angular distributions of particles from the target, for example $\Delta\vartheta_{\mathrm{K}^+}$. In contrast to target ejectiles, scattered protons $\mathrm{p_{BG}}$ in general have larger angular differences $\Delta\vartheta\mathrm{p_{BG}}$. Thus the vertical MWPC information can very efficiently be used for the suppression of scattered particles.

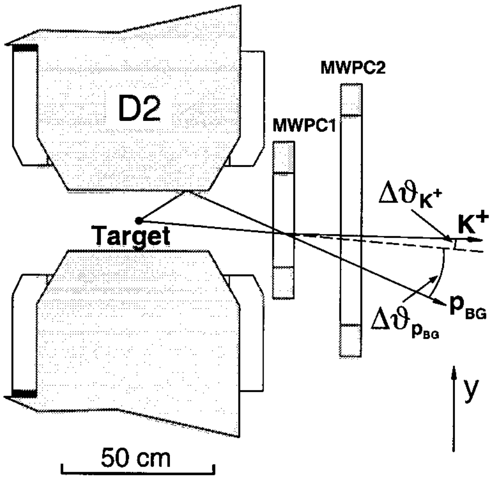

Fig. 11. Ejectiles from the target and scattered background in general have different vertical angles behind the spectrometer. See text for details.

Fig. 12 shows the vertical angular distributions $\Delta\vartheta$ for the remaining K^+-candidates after applying all cuts in the scintillator spectra described above. At the highest beam energy shown in the figure, $T_\mathrm{p} = 2.0$ GeV, there is a clear peak around $\Delta\vartheta = 0$ corresponding to ejectiles from the target. These particles can be identified as kaons, see Sect. 3.4. Only very few events from background particles are still visible. With decreasing beam energy the background surviving the scintillator cuts becomes significantly more important. The broad bumps at both sides of the target peak are mainly from ejectiles scattered at the pole pieces of D2 whereas background events underneath the peak must originate from the same vertical plane in which the target is located. The spectra from Fig. 12 are, for illustration, summed over all valid start counters. However, for identification of the K^+-mesons and for background suppression, the gates around the peak at $\Delta\vartheta = 0$ were optimized for each individual start-stop combination. It will be shown in Sect. 3.4 that for $Tp = 1.0$ GeV the remaining background underneath the peak is smooth and can be subtracted in order to determine the number of kaon events in each telescope. This is particularly important for measurements far below threshold.

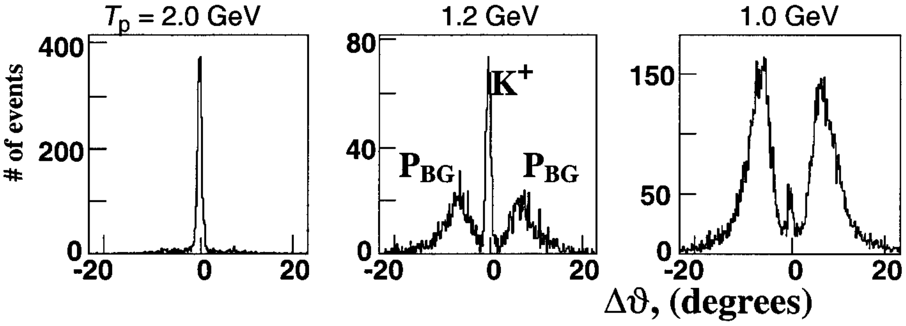

Fig. 12. Distribution of vertical angles measured with the two MWPC's after applying the K^+-cuts in the scintillator spectra of telescope #11. The spectra show a clear peak of kaons originating from the target. Background from scattered particles is also visible. The spectra were measured with a carbon target at three different beam energies.

In addition to the cuts on the vertical distributions from Fig. 12, in the horizontal direction (vertically oriented wires) events are only accepted if the responding wires are inside a corridor defined by trajectories connecting the edges of the individual start and stop counters. This criterion further helps to suppress scattered background, accidental coincidences and chamber noise. The width of these allowed corridors typically is 40...100 wires (10...25 cm).

3.3 Effectiveness of different criteria

In this section we briefly summarize the effectiveness of the most important cuts presented in Sects.3.1 and 3.2 for beam energies T_p = 1.0 and 2.3 GeV. At 2.3 GeV an on-line trigger based only on the TOF information was used which reduces the background and, thus, the amount of data written to tape, by about one order of magnitude. All other criteria, including narrower TOF gates, were applied off-line. The efficiencies of these criteria are summarized in Table 3.

At T_p = 1.0 GeV the background-to-kaon ratio is much larger than at 2.3 GeV. Thus, a stronger on-line trigger, based on TOF measurements and the (delayed) time signal from the veto counters, was used which drastically reduces the amount of data written to tape. During the off-line analysis subsequently stronger criteria were applied. In some cases two criteria were applied at the same time so that the combined efficiencies are shown in the table.

Table 3
Effectiveness of the individual cuts for $T_p = 2.3$ GeV. The numbers presented in columns "K$^+$" and "B.g." are the probabilities that K$^+$-mesons or background particles, accepted by the preceding criteria, are within the gate corresponding to the criterion described in the first two columns of the same line. (†for kaons with emission angles $|\vartheta| \leq 12°$; *see Fig.18 for efficiencies of the individual telescopes)

Criterion	Shown by	K$^+$	B.g.
Valid start counters (on-line)	Shaded spectra in Fig.6	$1.0^\dagger$	0.25
TOF (on-line)	Arrows in Fig.8a)	1.0	0.11
TOF (off-line)	Shaded area in Fig.8a)	0.99	0.29
Vertical direction	Fig.12	0.99	0.11
Delayed veto	Shaded area in Fig.10	0.2^*	$< 10^{-3}$
All		0.2	$< 3.5 \cdot 10^{-6}$

Table 4
Same as Table 3 for $T_p = 1.0$ GeV.

Criterion	Shown by	K$^+$	B.g.
Valid start counters (on-line)	Shaded spectra in Fig.6	$1.0^\dagger$	0.25
TOF & delayed veto (both on-line)	Arrows in Fig.8a) Arrow in Fig.10	0.22	0.002
TOF (off-line) & vertical direction	Shaded area in Fig.8a) Fig.12	0.99	0.002
Delayed veto (off-line)	Shaded area in Fig.10	0.92	0.3
Narrower TOF cuts & Amplitude in ΔE counters	See Sect.3.4 Shaded area in Fig.9a)	0.6^*	0.05
All		0.12	$6 \cdot 10^{-8}$

3.4 Identification of K^+-mesons

Figure 13 shows the remaining events when analysis gates are set on *i)* TOF between start- and stop counters (Fig. 6), *ii)* amplitude information of all scintillation counters (e.g. Figs. 7, 8b, 9), *iii)* time difference between veto- and stop counters of one telescope (Fig. 10) and *iv)* MWPC information (Fig. 12). Due to the moderately large cross sections for kaon production at $T_p = 2.3$ GeV, clear peaks without background in the vertical-angle and TOF distributions are seen. The vertical-angle distribution (a) proves that the particles are directly coming from the target region and the TOF peak (b) is located at the position were kaons are expected. An exponential fit to the time distribution in the veto counters yields a value of $\tau = 12.0 \pm 0.3$ ns, consistent with the expected 12.4 ns.

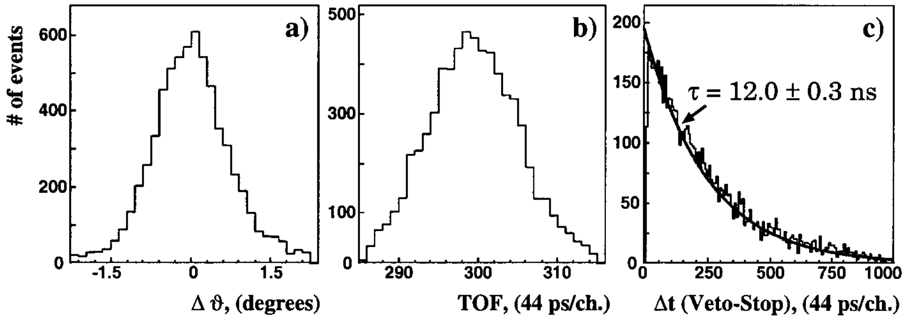

Fig. 13. **a)** Vertical angular distribution of K^+-events (c.f. Fig. 12). **b)**TOF distribution (c.f. Fig. 8a)). **c)** Time difference of detection in the veto and stop counters (c.f. Fig. 10); the spectrum has been shifted such that the gate for kaon detection is located at channel #0. All data were taken at $T_p = 2.3$ GeV with a carbon target. For illustration and in order to increase the number of events, the spectra shown in this section are summed over all valid start-stop combinations by properly shifting the distributions for each individual combination.

Figure 14 shows the same spectra as in Fig. 13 but now for the lowest beam energy, $T_p = 1.0$ GeV. Except for the beam energy, all other experimental conditions and software gates remain unchanged. Neglecting the now visible background, the location of the kaon distributions and, in the case of the vertical angle distributions, also the shape is the same as for the high energy where the production cross section is approx. 10^5 times larger.

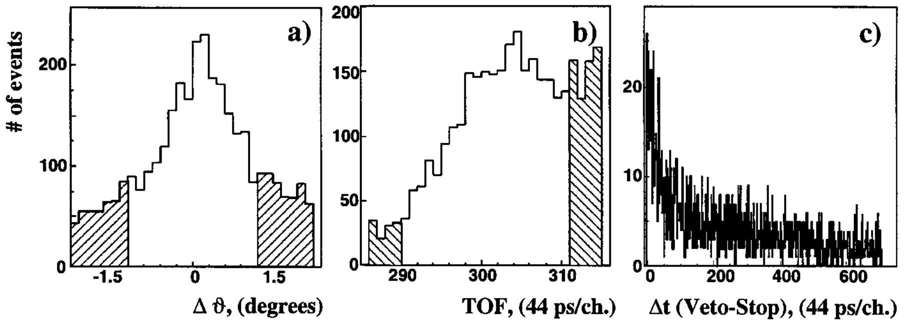

Fig. 14. Same as Fig. 13 but for $T_p = 1.0$ GeV. Indicated in **a)** and **b)** by the shaded areas are the angular and TOF cuts on background events which were used to determine the shape of the background distributions in Fig. 15.

In order to determine the number of detected kaons one has to subtract the background underneath the kaon peaks. The analyses show that this background has a smooth behaviour. As an example, in Fig. 15 the distributions of background events in the vertical-angle, TOF and Δt(veto – stop) spectra is shown. In particular, the vertical-angle distribution is constant in the region of the kaon peak and, thus, the background subtraction can be done by assuming a linear shape of the background in Fig. 14a).

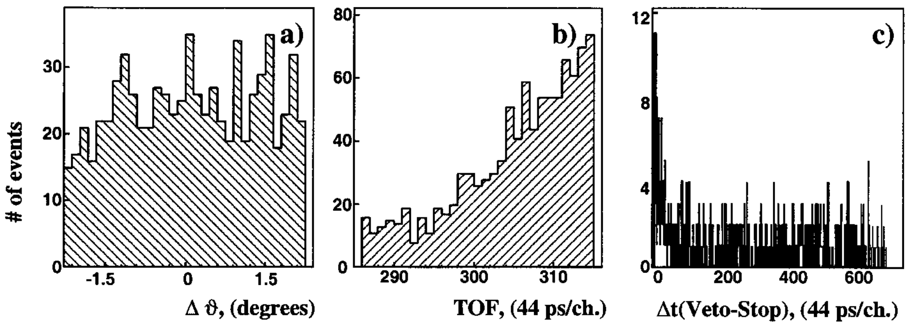

Fig. 15. **a)** Same as Fig. 14a) for background events within the outside gates of the K^+-TOF distribution from Fig. 14b). **b)** Same as Fig. 14b) for background events at the sides of the angular distribution from Fig. 14a). **c)** Same as Fig. 14c) for the events from a).

The remaining kaon distributions after background subtraction are shown in Fig. 16. Both the width of the TOF distribution as well as the exponential slope in the veto counter agree with the (clean) data at $T_{\rm p} = 2.3$ GeV.

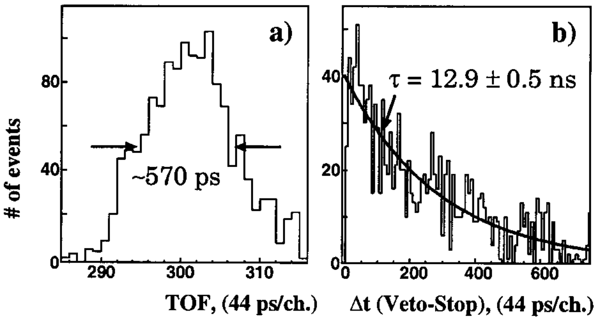

Fig. 16. Same as Fig. 14b) and c) after background subtraction.

4 K^+-momentum spectra

It has been shown in the previous sections that, after applying all criteria on TOF, energy losses and the MWPC information, K^+-mesons can be identified even at $T_{\rm p} = 1.0$ GeV. From the number of observed kaons in each telescope one can deduce momentum spectra, since the telescopes are placed along the focal surface of the spectrometer dipole. In order to obtain the double differential cross sections $\mathrm{d}^2\sigma/\,\mathrm{d}\Omega\,\mathrm{d}p$ for K^+-mesons produced at $\vartheta \sim 0°$, the kaon-detection efficiencies in each telescope have to be corrected for. The cross sections can then be obtained by normalizating to the number of identified π^+-mesons, which were measured in parallel, and to the known π^+-production cross sections. Further corrections, like e.g. for the different solid angles covered by each telescope and the acceptance gaps between them, are not necessary since they are identical for pions and kaons.

At ANKE, we have the possibility to directly determine the K$^+$-detection efficiencies in the telescopes through measurements at high beam energy, $T_\mathrm{p} = 2.3$ GeV. Due to the rather large kaon-production cross section, it is sufficient to use for K$^+$-identification the TOF and the MWPC information *only*. Under these conditions, the efficiencies for kaon (and pion) detection result from the efficiencies of the involved detetors (TOF-start and -stop, MWPC's) which are well known and close to 100%, see Sect. 3. The upper spectra of Fig. 17 show the vertical-angle and TOF distributions of the events fulfilling these criteria. In both cases a peak of kaon events can be seen on top of a flat background distribution. The shape of this background has been determined in independent analyses: *i)* The data taken at 1.0 GeV were used where the cross sections are so small that, with the TOF/MWPC gates, "contaminations" from kaons can be neglected. *ii)* Events from the sides of the kaon distributions were used, see shaded areas of Fig. 14. In both cases the background distributions are almost linear. However, for background subtraction, different background shapes were taken into account and the uncertainties have been included into the errors for the detection efficiencies.

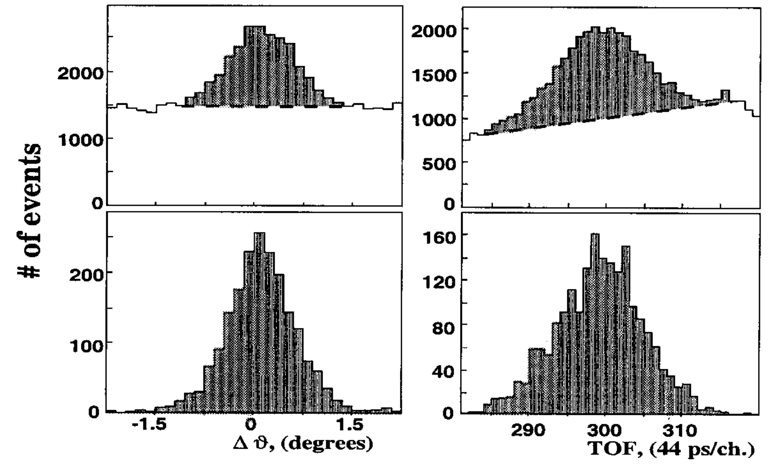

Fig. 17. Same as Fig. 13a) and b) but for telescope #13 only. Upper spectra: gates on TOF and vertical angles only (the gate widths correspond to the ranges of the two histograms). The background is indicated by the solid lines. Lower spectra: all criteria for K$^+$-identification applied (as in Fig. 13). The number of entries in the histograms cannot directly be compared to Fig. 13 since a different data set was used.

The lower spectra in Fig. 17 show the remaining K$^+$-events when *all criteria* (same as used in Sect. 3.4) for kaon identification are applied. In case of telescope #13, shown in the figure, approximately 10% of the kaons "survive" the cuts. The efficiencies — which are equal to the ratio of identified kaons with full gates and TOF/MWPC gates only — could be determined for telescopes 3–15. The corresponding numbers are shown in Fig. 18a) (for the first two telescopes the high background level of scattered particles does not permit to identify kaons with the TOF/MWPC gates only). The detection effiencies are in range of $\sim 10 \ldots 30\%$. The main kaon losses are due to a probability of only about 30% that a decay muon or pion enters the veto counter (limited solid angle), to kaon-scattering out of the telescopes in the first degrader and to hadronic interactions in the telescopes. The decreasing efficiency from telescopes #6 to #15 is caused by increasing thicknesses of the detectors and degraders. The step between #8 and #9 is due to the Čerenkov counters installed in telescopes #9–15; between telescopes #12 and #13 there is, for technical reasons, a significant increase of the distance between the ΔE and veto counters. In the lowest telescopes higher thresholds in the ΔE counters had to be used for kaon identification in order to suppress scattered background which leads to decreasing efficiencies.

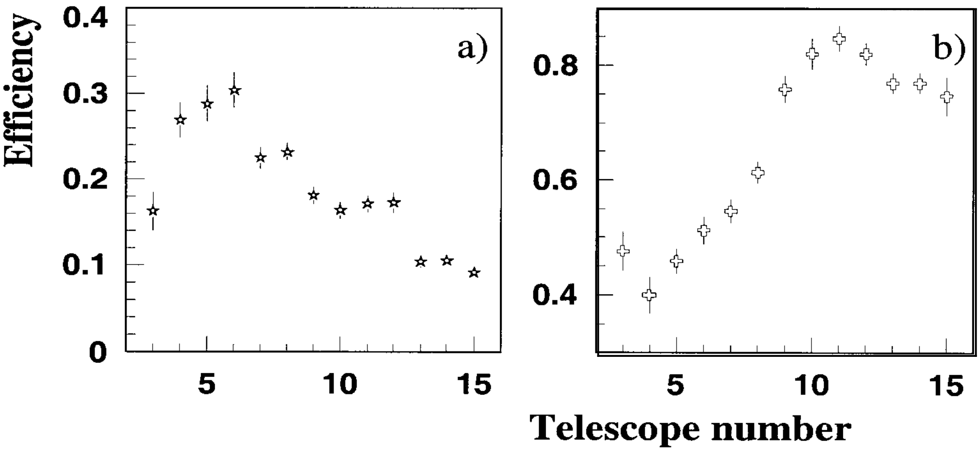

Fig. 18. a) Measured K$^+$-detection efficiencies in the individual telescopes. b) Correction factors which take into account the losses of K$^+$-counts due to the narrow TOF and energy-loss gates used in the off-line analysis at 1.0 GeV.

The cuts set on the spectra in the analysis of the data obtained at the lowest projectile energies were narrower than those for $T_{\mathrm{p}} = 2.3$ GeV in order to suppress background as efficiently as possible. This leads to an additional loss of kaon events. Consequently, the obtained numbers of kaons at low energies also have to be corrected for the efficiencies shown in Fig. 17b) which were determined through a comparison of the numbers of identified K$^+$-mesons at 2.3 GeV with wide and narrow TOF and energy-loss gates.

Figure 19 shows the number of identified K$^+$-mesons in each telescope corrected for the efficiencies from Fig. 18. Except for the above mentioned corrections for decay-in-flight and the different momentum bites and solid angles covered by the individual telescopes, the spectrum shown in the figure is proportional to the double-differential cross section $\mathrm{d}^2\sigma/\mathrm{d}\Omega\mathrm{d}p$ for kaons produced in p(1.0GeV) $+^{12}$ C $\rightarrow$ K$^+$X reactions and emitted into forward angles $\vartheta \leq 12°$.

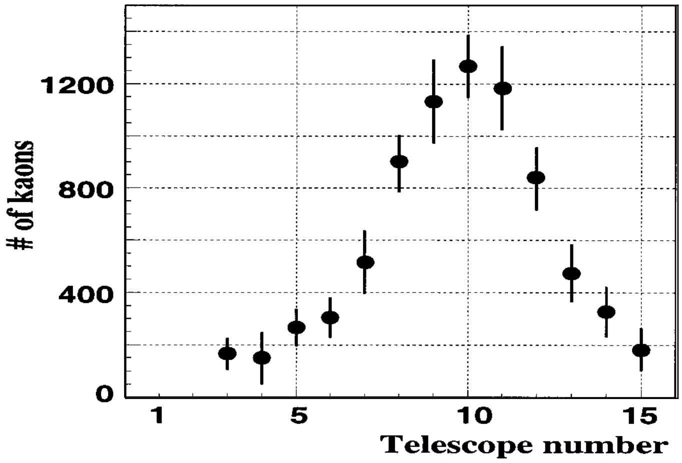

Fig. 19. Momentum distribution of K^+-mesons produced in a carbon target at T_p = 1.0 GeV. The numbers are not corrected for losses from decay-in-flight between target and stop counters and the different momentum bites of the telescopes (see Table 2). The error bars include the statistical uncertainties as well as the ones from the telescope-efficiency calibration.

5 Outlook

First measurements of K^+-momentum distributions in pA collisions at emission angles around 0° have been performed with the ANKE spectrometer at beam energies in the range $T_p = 1.0 \ldots 2.3$ GeV. It has been shown that ANKE and its K^+-detection system allow to identify the kaons out of a 10^6 times higher background of pions, protons and scattered particles. In order to extract double differential cross sections from the number of identified kaons shown in Fig. 19, one still has to correct for decay-in-flight between target and stop counters (30 to 36% of the kaons reach the counters) and the different momentum bites covered by the telescopes. Absolute normalization of the cross sections will be obtained from a comparison of π^+-data taken at ANKE with known π^+-production cross sections [19,20]. The results of the corresponding analysis procedures will be presented in forthcoming publications.

Acknowledgements

We would like to acknowledge the support we received for performing these first measurements at the ANKE spectrometer. The COSY-accelerator crew did an excellent job during beam-preparation and the experiments. Financial support from the following funding agencies was of indispensable help: Georgia (Department of Science and Technology), Germany (BMBF: grants WTZ-RUS-649-96, WTZ-RUS-666-97, WTZ-RUS-685-99, WTZ-POL-007-99; DFG: 436 RUS 113/337, 436 RUS 113/444, 436 RUS 113/561, State of North-Rhine

Westfalia), Poland (Polish State Committee for Scientific Research: 2 P03B 101 19), Russia (Russian Ministry of Science, Russian Academy of Science: 99-02-04034, 99-02-18179a) and European Community (INTAS-98-500).

References

[1] V.P. Koptev et al., *JETP* **67**, 2177 (1988).

[2] S. Schnetzer et al., *Phys. Rev.* **C 40**, 640 (1989); A. Shor et al., *Nucl. Phys.* **A 514**, 717 (1990); W. Cassing et al., *Phys. Lett.* **B 238**, 25 (1990); H. Müller, K. Sistemich, *Z. Phys.* **A 344**, 197 (1992); A.A. Sibirtsev, M. Büscher, *Z. Phys.* **A 347**, 191 (1994); W. Cassing et al., *Z. Phys.* **A 349**, 77 (1994); A.A. Sibirtsev, *Phys. Lett.* **B 359**, 29 (1995); M. Büscher et al., *Z. Phys.* **A 355**, 93 (1996); M. Debowski et al., *Z. Phys.* **A 356**, 313 (1996); A.A. Sibirtsev et al., *Z. Phys.* **A 358**, 357 (1997); A. Badala et al., *Phys. Rev. Lett.* **80**, 4863 (1998); Yu.T. Kiselev et al., *J. Phys.* **B 25**, 381 (1999).

[3] E.Ya. Paryev, *Eur. Phys. J.* **A 5**, 307 (1999).

[4] M. Büscher et al., *Z. Phys.* **A 351**, 333 (1995).

[5] W. Borgs et al., *COSY Proposal no. 18* (1991), unpublished.

[6] M. Büscher, Ph.D. Thesis, Universität zu Köln (1992).

[7] M. Büscher et al., *Proc. Int. Conf. on Mesons and Nuclei at Intermediate Energies*, Dubna, Russia, May 3–7, 1994, World Scientific Publishing, editors M.K.Khankhasayev and Z.B.Kurmanov, ISBN 981-02-1787-0, p.446 (1994).

[8] O.W.B. Schult et al., *Nucl. Phys.* **A 583**, 629 (1995).

[9] S. Barsov et al., *Nucl. Instr. Meth.* **A 462/3**, 364 (2001).

[10] S. Barsov et al., *Proc. 16th Int. Conf. on Magnetic Technology*, Sept. 26 – Oct. 2, 1999, Ponte Vedra Beach, USA, *Trans. Appl. Superconductivity* **10**, 1 (2000); H.J. Stein et al., *Rev. Scient. Instr.* in print.

[11] H. Müller, *Z. Phys.* **A 339**, 409 (1991).

[12] R. Schleichert, Ph.D. Thesis, Technische Hochschule Aachen (1996).

[13] L. von Horn, Ph.D. Thesis, Universität zu Köln (1996).

[14] H. Junghans, Ph.D. Thesis, Universität zu Köln (1999).

[15] M. French et al., *Nucl. Instr. and Meth.* **A 343**, 222 (1994).

[16] W. Erven et al., *IEEE Trans. Nucl. Sci.* **45**, 852 (1998).

[17] A. Schneider, Ph.D. Thesis, Universität zu Köln (1998).

[18] A. Franzen, Ph.D. Thesis, Universität zu Köln (1996).

[19] V.V. Abaev et al., *J. Phys.* **G14** 903 (1988).

[20] J. Papp et al., *Phys. Rev. Lett.* **34** 601 (1975).

VOLUME 87, NUMBER 2 PHYSICAL REVIEW LETTERS 9 JULY 2001

Forward K^+ Production in Subthreshold pA Collisions at 1.0 GeV

V. Koptev,[1] M. Büscher,[2] H. Junghans,[2] M. Nekipelov,[1,2] K. Sistemich,[2] H. Ströher,[2] V. Abaev,[1] H.-H. Adam,[3] R. Baldauf,[4] S. Barsov,[1] U. Bechstedt,[2] N. Bongers,[2] G. Borchert,[2] W. Borgs,[2] W. Bräutigam,[2] W. Cassing,[5] V. Chernyshev,[6] B. Chiladze,[7] M. Debowski,[8] J. Dietrich,[2] M. Drochner,[4] S. Dymov,[9] J. Ernst,[10] W. Erven,[4] R. Esser,[11,*] P. Fedorets,[6] A. Franzen,[2] D. Gotta,[2] T. Grande,[2] D. Grzonka,[2] G. Hansen,[12] M. Hartmann,[2] V. Hejny,[2] L. v. Horn,[2] L. Jarczyk,[13] A. Kacharava,[9] B. Kamys,[13] A. Khoukaz,[3] T. Kirchner,[8] S. Kistryn,[13] F. Klehr,[12] H. R. Koch,[2] V. Komarov,[9] S. Kopyto,[2] R. Krause,[2] P. Kravtsov,[1] V. Kruglov,[9] P. Kulessa,[2,15] A. Kulikov,[9,14] V. Kurbatov,[9] N. Lang,[3] N. Langenhagen,[8] I. Lehmann,[2] A. Lepges,[2] J. Ley,[11] B. Lorentz,[2] G. Macharashvili,[7,9] R. Maier,[2] S. Martin,[2] S. Merzliakov,[9] K. Meyer,[2] S. Mikirtychiants,[1] H. Müller,[8] P. Munhofen,[2] A. Mussgiller,[2] V. Nelyubin,[1] M. Nioradze,[7] H. Ohm,[2] A. Petrus,[9] D. Prasuhn,[2] B. Prietzschk,[8] H. J. Probst,[2] D. Protic,[2] K. Pysz,[15] F. Rathmann,[2] B. Rimarzig,[8] Z. Rudy,[13] R. Santo,[3] H. Paetz gen. Schieck,[11] R. Schleichert,[2] A. Schneider,[2] Chr. Schneider,[8] H. Schneider,[2] G. Schug,[2] O. W. B. Schult,[2] H. Seyfarth,[2] A. Sibirtsev,[2] J. Smyrski,[13] H. Stechemesser,[12] E. Steffens,[16] H. J. Stein,[2] A. Strzalkowski,[13] K.-H. Watzlawik,[2] C. Wilkin,[17] P. Wüstner,[4] S. Yashenko,[9] B. Zalikhanov,[9] N. Zhuravlev,[9] P. Zolnierczuk,[13] K. Zwoll,[4] and I. Zychor[18]

[1]*High Energy Physics Department, Petersburg Nuclear Physics Institute, 188350 Gatchina, Russia*
[2]*Institut für Kernphysik, Forschungszentrum Jülich, D-52425 Jülich, Germany*
[3]*Institut für Kernphysik, Universität Münster, W.-Klemm-Strasse 9, D-48149 Münster, Germany*
[4]*Zentralinstitut für Elektronik, Forschungszentrum Jülich, D-52425 Jülich, Germany*
[5]*Institut für Theoretische Physik, Universität Gießen, H.-Buff-Ring 16, D-35392 Gießen, Germany*
[6]*Institute for Theoretical and Experimental Physics, Cheremushkinskaya 25, 117259 Moscow, Russia*
[7]*High Energy Physics Institute, Tbilisi State University, University Street 9, 380086 Tbilisi, Georgia*
[8]*Institut für Kern- und Hadronenphysik, Forschungszentrum Rossendorf, D-01474 Dresden, Germany*
[9]*Laboratory of Nuclear Problems, Joint Institute for Nuclear Research, 141980 Dubna, Russia*
[10]*Institut für Strahlen- und Kernphysik, Universität Bonn, Nußallee 14, D-53115 Bonn, Germany*
[11]*Institut für Kernphysik, Universität zu Köln, Zülpicher Strasse 77, D-50937 Köln, Germany*
[12]*Zentralabteilung Technologie, Forschungszentrum Jülich, D-52425 Jülich, Germany*
[13]*Institute of Physics, Jagellonian University, Reymonta 4, 30059 Cracow, Poland*
[14]*Dubna Branch, Moscow State University, 141980 Dubna Moscow Region, Russia*
[15]*The Henryk Niewodniczanski Institute of Nuclear Physics, Radzikowskiego 152, PL-31342, Cracow, Poland*
[16]*Physikalisches Institut II, Universität Erlangen-Nürnberg, Erwin-Rommel-Strasse 1, D-91058 Erlangen, Germany*
[17]*Physics Department, UCL, Gower Street, London WC1 6BT, United Kingdom*
[18]*The Andrzej Soltan Institute for Nuclear Studies, PL-05400 Swierk, Poland*

(Received 3 April 2001; published 21 June 2001)

K^+-meson production in pA ($A = \mathrm{C, Cu, Au}$) collisions has been studied using the ANKE spectrometer at an internal target position of the COSY-Jülich accelerator. The complete momentum spectrum of kaons emitted at forward angles, $\vartheta \leq 12°$, has been measured for a beam energy of $T_p = 1.0$ GeV, far below the free NN threshold of 1.58 GeV. The spectrum does not follow a thermal distribution at low kaon momenta and the larger momenta reflect a high degree of collectivity in the target nucleus.

DOI: 10.1103/PhysRevLett.87.022301 PACS numbers: 25.40.Ve, 13.75.Cs, 29.40.−n

A central topic of hadron physics is the influence of the nuclear medium on elementary processes. This question can be studied by measuring the production of mesons in nuclei using projectiles with energies below the threshold for free NN collisions (so-called subthreshold production). These processes necessarily involve cooperative effects of the nucleons inside the target nucleus. The investigation of K^+ production is particularly well suited for this purpose since the meson is relatively heavy so that its production requires strong medium effects. Furthermore, the K^+ scatters little in nuclear matter so that its final-state interactions are expected to be small.

Proton-induced K^+ production at subthreshold energies has been studied at several accelerators. Total cross sections have been measured at the Petersburg Nuclear Physics Institute (PNPI) synchrocyclotron for targets between Be and Pb and projectile energies T_p from 0.8 to 1.0 GeV [1]. The results were discussed in terms of different models [1–5], in particular, of single- or two-step reactions involving the creation of an intermediate pion. It was concluded that additional experimental data were needed for an unambiguous determination of the reaction mechanism and the extraction of the information on nuclear-medium effects. Inclusive differential cross sections for pA interactions have been studied at BEVALAC [6], SATURNE [7], and CELSIUS [8]. Partial momentum spectra have been obtained at laboratory emission angles of 10°, 15°, 35°, 40°, 60°, 80°, and 90°, at projectile energies down to 1.2 GeV, and evidence for the dominance of the two-step processes has been observed at the lowest T_p. Subthreshold production has also been studied at the Institute of Theoretical and Experimental Physics (Moscow, Russia) synchrotron [9], where kaons with high momenta were identified at projectile proton energies of 1.75 to 2.6 GeV, and in heavy-ion reactions at GANIL [10] and GSI [11].

The COoler SYnchrotron COSY-Jülich [12], which provides proton beams in the range $T_p = 0.04\text{–}2.65$ GeV, is well suited for the study of K^+ production. In measurements with very thin windowless internal targets, secondary processes of the produced mesons can be neglected. Subthreshold K^+ production was a prime motivation for building the ANKE spectrometer [13,14] within one straight section of the COSY ring. It consists of three dipole magnets $D1\text{–}D3$, see Fig. 1, which separate forward-emitted reaction products from the circulating proton beam and allow a determination of their emission angles and momenta. The layout of the device, including detectors and the data-acquisition (DAQ) system, was optimized for the study of K^+ spectra down to $T_p = 1.0$ GeV. This is a very demanding task because of the small K^+ production cross sections, e.g., 39 nb for pC collisions at 1.0 GeV [1]. Kaons have to be identified in a background of secondary protons and pions which is up to 10^6 times more intense. K^+ identification is described in detail in [15,16]; only basic features of the procedures are summarized here.

The COSY ring was filled with $2\text{–}4 \times 10^{10}$ protons per cycle and cycle times were typically 30 s. The protons were accelerated to 1.0 GeV on an orbit below the target and then raised by steerers such that the rate in the ANKE detectors was kept constant and on a level that could be handled by the DAQ system. Thin strip targets of C (polycrystalline diamond), Cu, and Au with thicknesses of 40–1500 μg/cm^2 were used. Reaction products were detected with an array of 15 range telescopes positioned along the focal surface. The time of flight (TOF) was measured with 0.5 to 2 mm thick start scintillators (23 detectors of 5 cm width) and 1 cm thick (10 cm wide) stop scintillators which are components of the telescopes; see Fig. 1. Because of the momentum focusing of the dipole $D2$, the telescopes can be used to identify different ejectiles via their ranges: protons are stopped before reaching the ΔE counters, K^+ mesons come to rest before the veto counters, while pions give signals in all detectors. Copper degraders are used to slow down the kaons in front of the ΔE counters (degrader 1) and prevent them from reaching the veto counters (degrader 2). Pions and muons from the decay of stopped kaons are emitted isotropically, and partially detected in the veto counter, with a characteristic delay corresponding to the kaon lifetime $\tau = 12.4$ ns. The multiwire proportional chambers MWPC 1 and 2 allow one to determine the ejectile tracks and hence separate particles originating from the target from scattered background, e.g., from the pole shoes of $D2$. Applying the criteria (i) TOF, (ii) energy losses in the scintillation counters, (iii) delayed signals in the veto counters, and (iv) track origin in the target, it is possible to identify unambigously K^+ mesons [15]. Criteria (i) and (iii) were applied on-line to decrease the amount of data written to tape.

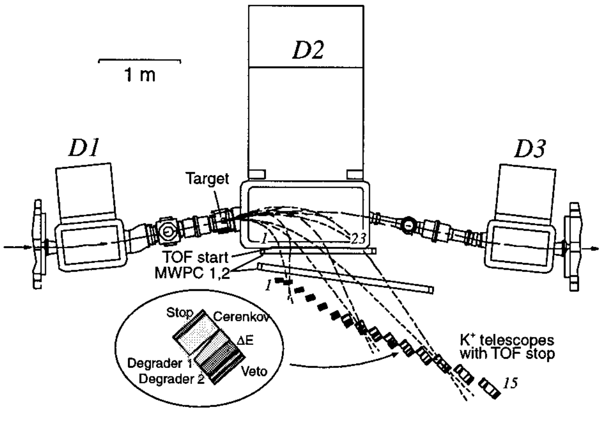

FIG. 1. Top view of the ANKE spectrometer in the COSY ring and detectors used for K^+ identification. The inset shows the components of one of the range telescopes. Typical kaon trajectories are indicated. Details can be found in [13–16].

The typical number of identified K^+ mesons, $N^K_{\mathrm{tel}(i)}$, in one telescope i during a four days run on C was 100. Since each telescope covers a given momentum range, the $N^K_{\mathrm{tel}(i)}$ determine directly the momentum distribution. The accepted momentum bites range from 13% at the low-momentum side of the telescope array ($\sim$150 MeV/c) to 7% for high momenta ($\sim$510 MeV/c). The vertical angular acceptance of ANKE varies between $\vartheta_{\mathrm{V}} = \pm 7°$ and $\pm 3.5°$ for the low- and high-momentum telescopes, respectively. In the horizontal direction, ejectiles with emission angles $|\vartheta_{\mathrm{H}}| \leq 12°$ were accepted by the on-line TOF-trigger system [15].

Double differential cross sections for K^+ production were obtained from $N^K_{\mathrm{tel}(i)}$ by comparison with the number of pions $N^{\pi}_{\mathrm{stop}(i)}$ detected in the stop counters of the same telescope, which were measured in dedicated calibration runs. The ratio of K^+ and π^+ counts was corrected for the different detection efficiencies ϵ and normalized to the corresponding luminosities (deduced from count rates M^{π} and M^K in monitor counters; see below) and to the cross sections of π^+ production in pC interactions in the forward direction at 1.0 GeV [17–19]. Because of their much larger production cross section, pions can be identified applying only criteria (i) and (iv). The cross section is thus given by

$$\begin{aligned} \frac{d^2\sigma^K}{d\Omega\, dp} &= \frac{d^2\sigma^{\pi}}{d\Omega\, dp} \, \frac{N^K_{\mathrm{tel}(i)}}{N^{\pi}_{\mathrm{stop}(i)}} \, \frac{M^{\pi}}{M^K} \, \frac{1}{\epsilon}, \\ \epsilon &= \frac{\epsilon^K_{\mathrm{tel}(i)} \epsilon^K_{\mathrm{MWPC}(i)} \epsilon^K_{\mathrm{decay}}}{\epsilon^{\pi}_{\mathrm{stop}(i)} \epsilon^{\pi}_{\mathrm{MWPC}(i)} \epsilon^{\pi}_{\mathrm{decay}}}, \end{aligned} \tag{1}$$

where $\epsilon^K_{\mathrm{tel}(i)}$ is the K^+-identification efficiency of the ith telescope including the detection probability for the decay muons and pions. Only events where veto counter signals were delayed by at least 2.5 ns with respect to those of the stopped kaons were considered. The efficiencies, $\epsilon^K_{\mathrm{tel}(i)} \sim$ 0.1–0.3, were obtained from a calibration run at $T_p =$ 2.3 GeV, where K^+ production is significantly larger [15].

The average pion detection efficiencies are $\epsilon^{\pi}_{\mathrm{stop}(i)} =$ 0.98. The MWPC efficiencies ϵ_{MWPC} are in the range 0.97–0.99 both for pions and kaons. $\epsilon^K_{\mathrm{decay}}$ and $\epsilon^{\pi}_{\mathrm{decay}}$ take into account losses in flight between target and stop counters; they were determined by simulations as 0.30–0.36 for kaons and 0.85–0.88 for pions. Relative monitoring of the proton beam interacting with the target nuclei A (M^K_A and M^{π}_A) was done with an accuracy of 2% using fourfold coincidences of stop counters 2, 3, 4, and 5, which in this arrangement directly look to the target detecting ejectiles bypassing the spectrometer dipole $D2$.

Our double differential cross section for K^+ production in proton-carbon interactions at $T_p = 1.0$ GeV is shown in Fig. 2(a). In contrast to measurements at higher energies [6–9,20], ANKE reveals, for the first time, a complete momentum spectrum at deep subthreshold energies.

The *low-momentum* part of the K^+ spectrum in Fig. 2(b) cannot be described by a thermal distribution, $E/p^2\, d^2\sigma/dp\, d\Omega \propto \exp(-T^{\star}/T_0)$, where $T^{\star}$ is the K^+ kinetic energy in the beam-proton nucleus system. Such distributions had been assumed to deduce total cross sections from earlier measurements with limited momentum intervals [6–8,20].

A high degree of collectivity is needed in the target nucleus to allow K^+ production far below the free NN threshold; i.e., the number of target nucleons involved must be significantly larger than 1 [1–5]. Alternatively, high intrinsic momenta of the participating target nucleon(s) are required to supply the missing energy for subthreshold kaon production. This is particularly the case for the *high-momentum* part of the kaon spectrum: internal momenta of a single nucleon of at least $p_N \sim 350(550)$ MeV/c would be needed in order to produce kaons in the forward direction with momenta of $p_K \sim 260(500)$ MeV/c. High momentum components above ~500 MeV/c are essentially due to many-body correlations in the nucleus [21].

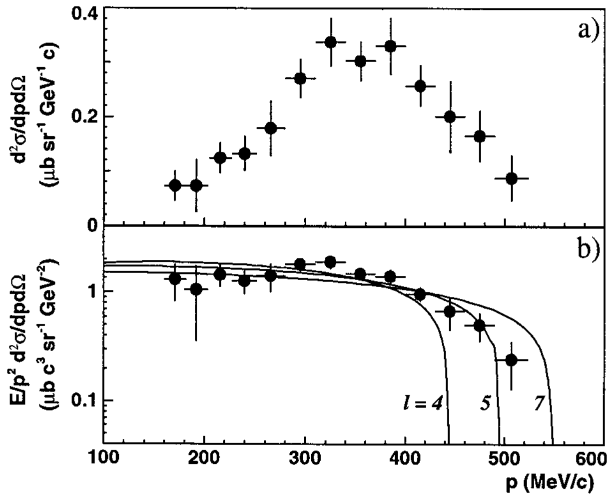

FIG. 2. (a) Double differential K^+-production cross section for the $p(1.0\ \mathrm{GeV})^{12}\mathrm{C} \rightarrow K^+(\vartheta \leq 12^{\circ})X$ reaction as a function of the K^+ momentum. (b) Same data plotted as invariant cross section. The error bars are purely statistical. The overall normalization uncertainty is estimated to be 10%. The solid lines describe the behavior of the invariant cross section within a phase-space approximation [Eq. (2)].

To get a rough estimate of the number of participating nucleons, we describe the invariant cross section within a phase-space approximation. This method has previously been applied to K^+-production data [20] in order to compare spectra obtained under different kinematical conditions [6,7,20]. The invariant cross section for the $p + (lN) \rightarrow (lN) + \Lambda + K^+$ reaction is then

$$\frac{E}{p^2}\frac{d^2\sigma}{dp\,d\Omega} \propto \frac{\sqrt{(s_l - m_\Lambda^2 - l^2 m_N^2)^2 - 4m_\Lambda^2 l^2 m_N^2}}{s_l}, \qquad (2)$$

where m_Λ and m_N are the Λ and nucleon masses, respectively. l is the number of nucleons involved in the interaction and

$$s_l = s + m_K^2 - 2E_K(T_p + [l + 1]m_N) + 2p_K p_p \cos\theta_K\,. \qquad (3)$$

m_K, E_K, p_K, and θ_K are the kaon mass, total energy, momentum, and emission angle, respectively, while T_p and p_p denote the beam energy and momentum. s is the square of the center-of-mass energy of the incident proton and the l target nucleons. The solid lines in Fig. 2(b) show the momentum dependence of the invariant cross section from Eq. (2) for $l = 4, 5, 7$. Although this neglects the intrinsic motion of the l target nucleons, it shows that kaon production at $T_p = 1.0$ GeV can be understood only in terms of cooperative effects with the effective number of nucleons involved in the interaction being ~5–6. It has been suggested [1–5] that such cooperative effects can be described in terms of multistep mechanisms or high-momentum components in the nuclear wave function.

It has also been pointed out [1–5] that the mechanism of subthreshold K^+ production might be identified from the A dependence of the production cross section. The total cross sections measured at PNPI in the energy range $T_p = 0.8$–1.0 GeV scale as $\sigma_{\mathrm{tot}} \propto A^1$ [1]. This behavior has been interpreted in terms of a two-step mechanism with the formation of an intermediate π meson.

We used targets of widely different masses to determine the A dependence of the differential cross sections. All measurements were carried out with the same geometry and detection system at ANKE and the same proton beam settings. The ratios of the kaon-production cross sections for various nuclei as a function of kaon momentum $\sigma_A^{K^+}/\sigma_C^{K^+}$ are therefore equal to the corresponding ratios of kaon count rates in the individual telescopes, normalized to the pion cross-section ratio at a momentum of

507 ± 17 MeV/c detected in telescope No. 15:

$$\left(\frac{\sigma_A^K}{\sigma_C^K}\right)_{(i)} = \left(\frac{N_A^K}{N_C^K}\right)_{(i)} \frac{M_C^K}{M_A^K} \left(\frac{N_C^\pi}{N_A^\pi}\right)_{(15)} \frac{M_A^\pi}{M_C^\pi} \left(\frac{\sigma_A^\pi}{\sigma_C^\pi}\right)_{(15)} . \quad (4)$$

The cross-section ratios for producing pions with momenta around 500 MeV/c in the forward direction in pA collisions were measured to better than 10% by several groups in the 0.73–4.2 GeV energy range [16–19]. All uncertainties from the efficiency correction ϵ in Eq. (1) cancel out for such ratios. The results for Cu/C and Au/C are shown in Fig. 3.

The ratios are almost independent of the K^+ momentum. The solid lines in Fig. 3 indicate fits with constant values; $R(\mathrm{Cu/C}) = 4.0 \pm 0.3$ and $R(\mathrm{Au/C}) = 6.8 \pm 0.8$. These values should be compared to the expected ratios if the cross sections scaled as A^1: $R(\mathrm{Cu/C}) \sim 5$ and $R(\mathrm{Au/C}) \sim 16$. Our data show a significantly weaker A dependence with an exponent closer to 2/3. This is in contrast to the behavior of the total cross sections at the same beam energy found in [1], where kaon production was described in terms of the two-step mechanism. It is possible that, due to rescattering of the produced kaons in the target nucleus out of the angular acceptance of ANKE, there is a kaon deficiency at high momenta and small angles. Since this effect should be stronger for heavier targets, it might account for the weaker A dependence of the differential cross section.

Summarizing, we have measured small-angle K^+ production at $T_p = 1.0$ GeV, which is far below the free NN threshold. The low-momentum part of the K^+ spectrum does not follow a thermal distribution whereas the high-momentum part reveals a high collectivity of the target nucleus. Within a simple kinematical model, about 5–6 nucleons are needed to allow kaon production with momenta $p_K \sim 500$ MeV/c. Alternatively, intrinsic momenta of at least $p_N \sim 550$ MeV/c are required if such kaons are produced in a collision with a single target nucleon. The target-mass dependence of the differential cross sections shows a scaling significantly weaker than those of the total cross sections [1]. The latter have been interpreted in terms of two-step K^+ production. It remains to be shown by microscopic calculations whether this finding is due to rescattering effects of the kaons in the target nucleus or whether it is a reflection of single-step kaon production with high-momentum components in the nuclear wave function.

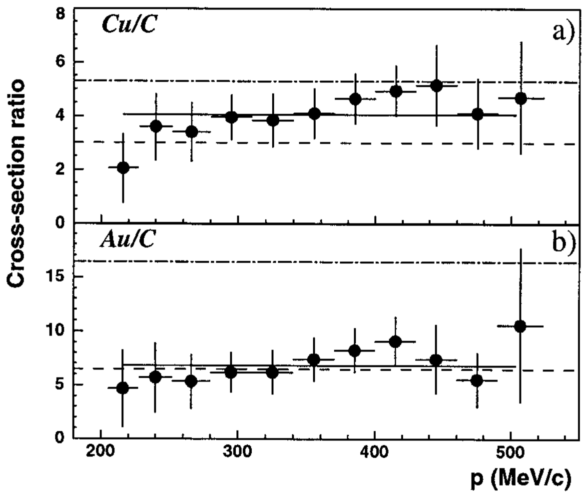

FIG. 3. Ratios of the K^+ production cross sections for Cu/C and Au/C as a function of the kaon momentum. The solid horizontal lines indicate a fit by a constant value. The dashed lines illustrate the ratios if the cross sections scale like $A^{2/3}$ (dashed line) and A^1 (dash-dotted line).

We acknowledge the assistance we received in performing these measurements at the ANKE spectrometer. Financial support from the following funding agencies was of indispensable help for building ANKE, its detectors, and DAQ: Georgia (Department of Science and Technology), Germany (BMBF: Grants No. WTZ-RUS-649-96, No. WTZ-RUS-666-97, No. WTZ-RUS-685-99, No. WTZ-POL-007-99; DFG: Grants No. 436 RUS 113/337, No. 436 RUS 113/444, No. 436 RUS 113/561, State of North-Rhine Westfalia), Poland (Polish State Committee for Scientific Research: 2 P03B 101 19), Russia (Russian Ministry of Science, Russian Academy of Science: 99-02-04034, 99-02-18179a), and European Community (INTAS-98-500).

---

*Present address: Saint-Gobain Crystals & Detectors GmbH, 42929 Wermelskirchen, Germany.

[1] V. P. Koptev *et al.*, JETP **67**, 2177 (1988).
[2] W. Cassing *et al.*, Phys. Lett. B **238**, 25 (1990).
[3] H. Müller and K. Sistemich, Z. Phys. A **344**, 197 (1992).
[4] A. A. Sibirtsev and M. Büscher, Z. Phys. A **347**, 191 (1994).
[5] E. Ya. Paryev, Eur. Phys. J. A **5**, 307 (1999).
[6] S. Schnetzer *et al.*, Phys. Rev. C **40**, 640 (1989).
[7] M. Debowski *et al.*, Z. Phys. A **356**, 313 (1996).
[8] A. Badalà *et al.*, Phys. Rev. Lett. **80**, 4863 (1998).
[9] Yu. T. Kiselev *et al.*, J. Phys. B **25**, 381 (1999).
[10] J. Julien *et al.*, Phys. Lett. B **264**, 269 (1991).
[11] P. Senger and H. Ströbele, J. Phys. G **25**, R59 (1999).
[12] R. Maier, Nucl. Instrum. Methods Phys. Res., Sect. A **390**, 1 (1997).
[13] M. Büscher *et al.*, Phys. Scr. RS **21**, 23 (1993).
[14] S. Barsov *et al.*, Nucl. Instrum. Methods Phys. Res., Sect. A **462**, 364 (2001).
[15] M. Büscher *et al.*, Nucl. Instrum. Methods Phys. Res., Sect. A (to be published).
[16] S. Barsov *et al.*, Acta Phys. Pol. B **31**, 2159 (2000).
[17] D. R. F. Cochran *et al.*, Phys. Rev. D **6**, 3085 (1972).
[18] J. Papp *et al.*, Phys. Rev. Lett. **34**, 601 (1975).
[19] V. V. Abaev *et al.*, J. Phys. G **14**, 903 (1988); **31**, 2159 (2000).
[20] M. Büscher *et al.*, Z. Phys. A **355**, 93 (1996).
[21] H. Nifenecker and J. A. Pinston, Prog. Part. Nucl. Phys. **23**, 271 (1989).

Status of K^+ measurements with ANKE at COSY–Jülich

M.Büscher

Institut für Kernphysik
Forschungzentrum Jülich
52425 Jülich
Germany

Workshop on "Strangeness production in pp and pA interactions at ANKE"

June, 21/22, 2001
PNPI, Gatchina

- Thanks to the local organizers !!
- Proceedings

Copies of transparencies
Written contributions (~1 page) → V.Kleber, P.Kulessa
List of participants

- Schedule
- Goals (M.B.'s viewpoint)

Status of K^+-studies with ANKE Publication
Theoretical interpretation of pA data
Ideas for further experiments?
.....and..... (input from YOU)?

[redacted]

- 'History' (achievements) of subthreshold K^+-studies with ANKE

(1st)

Workshop on "a_0 Physics with ANKE"
July 13/14, 2000
ITEP, Moscow

Thursday, July 13

		Chairperson: V. Chernyshev
10:00		Welcome
10:10	*M. Büscher (FZJ)*	Status of ANKE and planned measurements on pp → da_0^+
10:40	*Yu. Kalashnikova (ITEP)*	Scalar mesons: Why they are interesting
11:10	*L. Kondratyuk (ITEP)*	Properties of the $a_0/f_0(980)$ mesons
11:40	*V. Grishina (INR)*	a_0 production at COSY energies
		L. Kondratyuk
13:30	*J. Haidenbauer (FZJ)*	Description of the $a_0/f_0(980)$ mesons with the Jülich model
14:00	*A. Kudryavtsev (ITEP)*	Perspectives of a_0^- studies
14:30	*V. Tarasov (ITEP)*	A possibility for direct measurements of a_0/f_0 mixing
14:50	*B. Kerbikov (ITEP)*	Superallowed a_0/f_0 mixing
		H. Ströher
16:00	Round-table discussion:	Perspectives of the a_0^+ studies with ANKE
17:00	Dinner	

Friday, July 14

		M. Büscher
10:00	*V. Kleber (FZJ)*	Simulations for the a_0^+ studies with ANKE
10:30	*N. Lang (Münster)*	Status of the cluster-jet target
11:00	*V. Komarov (JINR)*	The ANKE forward detectors and luminosity monitoring
11:50	*Chr. Leim (FZJ)/* *G. Macharashvili(JINR)*	Preparation of the forward Cerenkov counters
12:10	*H. Junghans (FZJ)*	Data-analysis software
12:30	*I. Lehmann (FZJ)*	Luminosity monitoring with the spectator counters
14:00	Excursion to experimental facilities of ITEP	
		K. Sistemich
15:00	*V. Chernyshev (ITEP)*	Future activities at ITEP/Status of the pellet target
15:30	*H. Ströher (FZJ)*	Future activities at ANKE
		M. Büscher
16:30	Concluding discussion:	Future activities, responsibilities, ...

2nd ANKE workshop on "Strangeness production in pp and pA interactions at ANKE" June 21/22, 2001 PNPI, Gatchina

Thursday, June 21: K⁺-production in proton-nucleus collisions

		Chairperson: V. Koptev
10:00	*A.A. Vorobyev* (to be conf.)	Welcome
10:10	*M. Büscher (FZJ)*	Status of K^+-measurements with ANKE at COSY-Jülich
10:40	*R. Koch (FZJ)*	Luminosities during ANKE experiments (A dependence)
11:00	*Coffee*	
		V. Koptev
11:30	*M. Nekipelov (PNPI, FZJ)*	Data on K^+-production in pA collisions from ANKE
12:00	*A. Sibirtsev/M. Büscher (FZJ)*	Compilation of existing data
12:30	Discussion:	Experimental situation in K^+-production from nuclei
13:00	*Lunch*	
		W. Cassing
14:30	*Z. Rudy*	Results of CBUU calculations
15:00	*E.Ya. Paryev (INR)*	Folding-model calculations I
15:30	*A. Sibirtsev (FZJ)*	Folding-model calculations II
16:00	*M. Büscher (FZJ)*	First results of the ROC-model calculations
16:30	*Coffee*	
		W. Cassing
16:40	Discussion:	What have we learned about K^+-production in nuclei?
17:15	*V. Koptev (PNPI)*	Future K^+-measurements with ANKE
17:45	*M. Hartmann (FZJ)*	Measurements with the K^--detection system
19:00	*Dinner*	

Friday, June 22: ANKE experiments on ω, $a_0(980)/f_0(980)$, Λ and Σ production

		H. Ströher
10:00	*V. Kleber (FZJ)*	Results of the measurements on $pp \to da_0^+(980)$
10:40	Discussion:	Which further experimental information is needed from ANKE?
11:10	*M. Büscher (FZJ)*	Planned $a_0(980)/f_0(980)$ measurements at ANKE
11:30-	*Coffee*	
		H. Ströher
12:00	*P. Kravchenko(PNPI)*	Measurement of the Λ/Σ ratio at ANKE
12:30	Discussion	
13:00	*V. Chernyshev (ITEP)*	Status of the pellet target for ANKE
13:30	*Lunch*	
		M. Büscher
15:00	*S. Barsov (PNPI)*	Data on ω-meson production on neutron targets from ANKE
15:30	*A. Mussgiller (FZJ)*	Target-near counters for spectator tagging
	A. Mussgiller (FZJ)	Future spectator and vertex counters for ANKE
16:15	*H. Ströher (FZJ)*	Long-term perspectives, final discussion

Monday

- excursion to PNPI exp facilities
- final discussion

COoler SYnchrotron $T_{max} = 2.7$ GeV

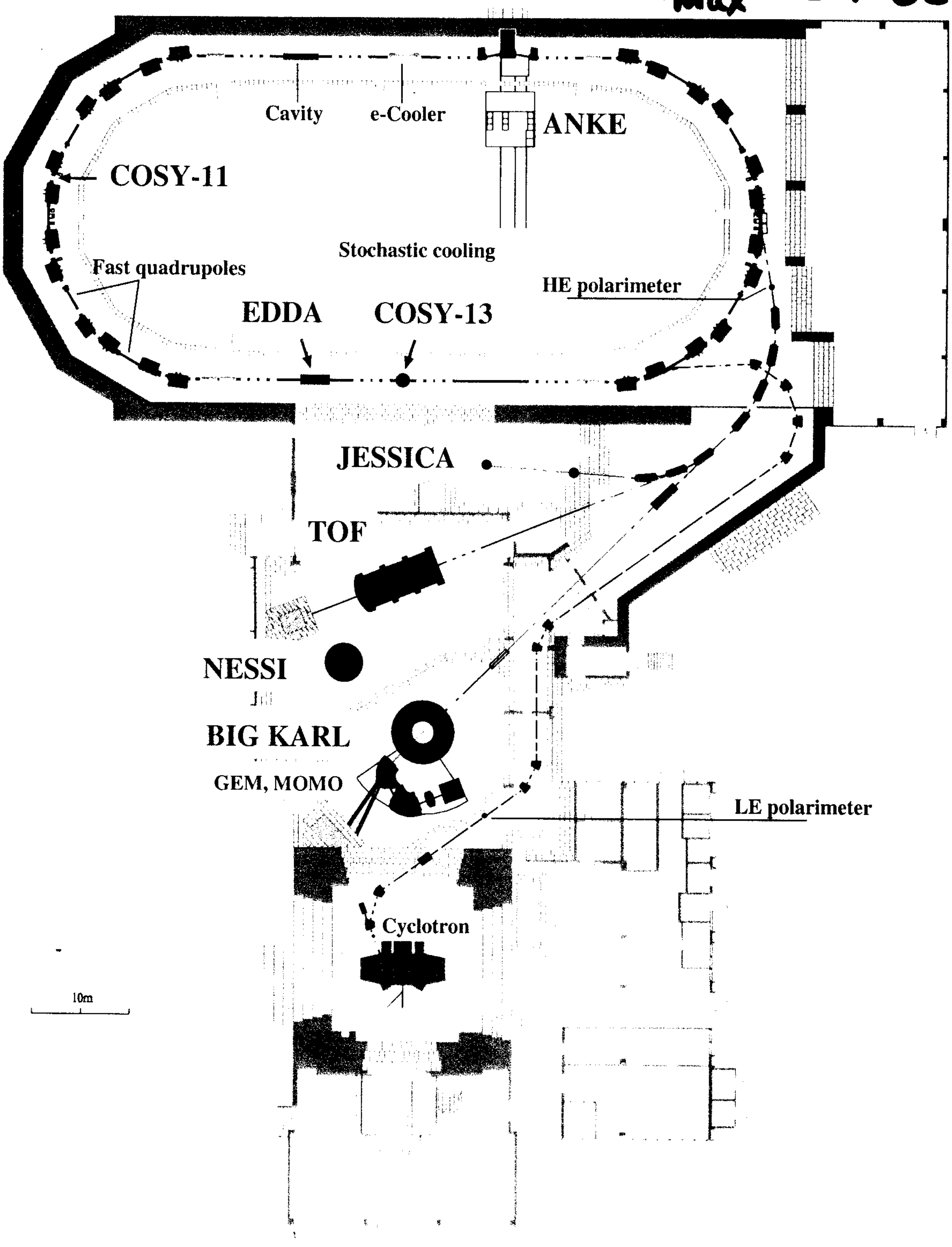

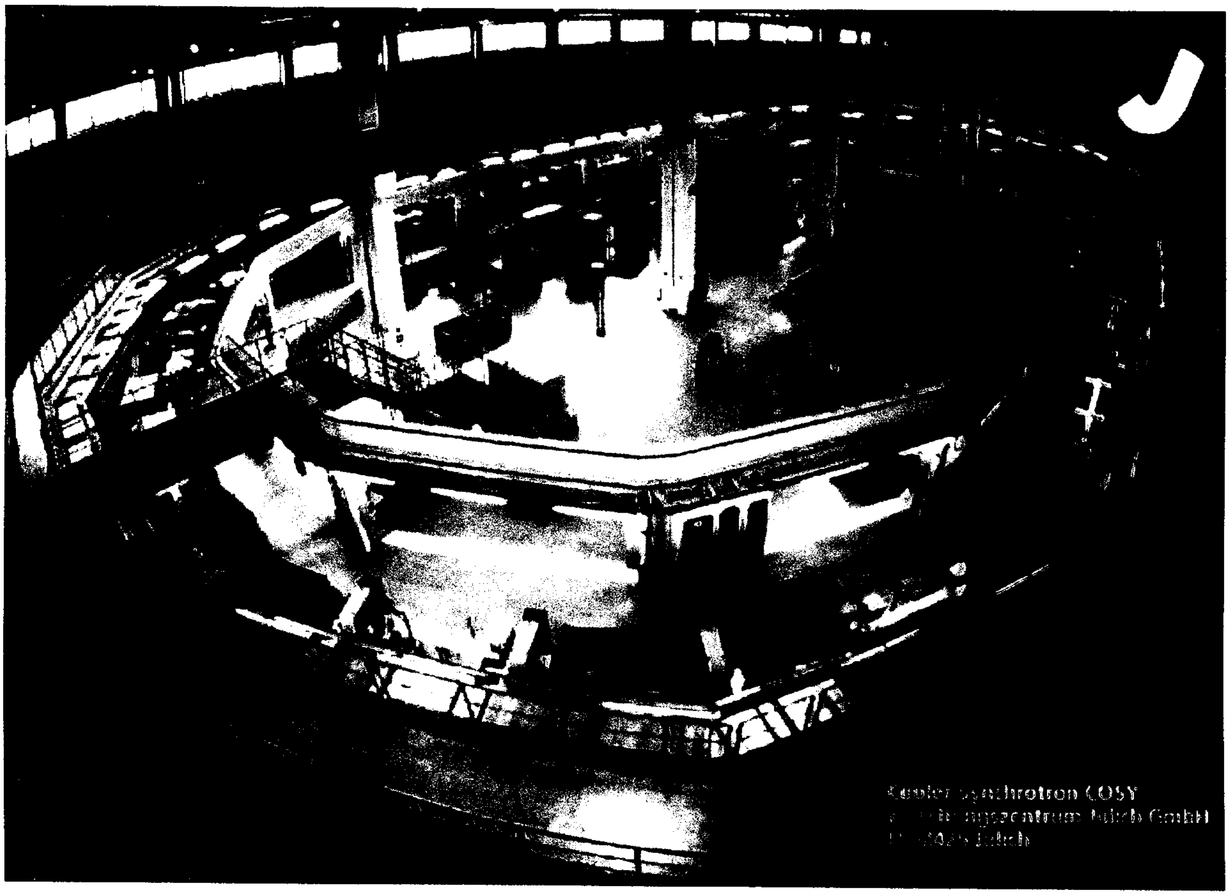
Cooler synchrotron COSY
Forschungszentrum Jülich GmbH
D-52425 Jülich

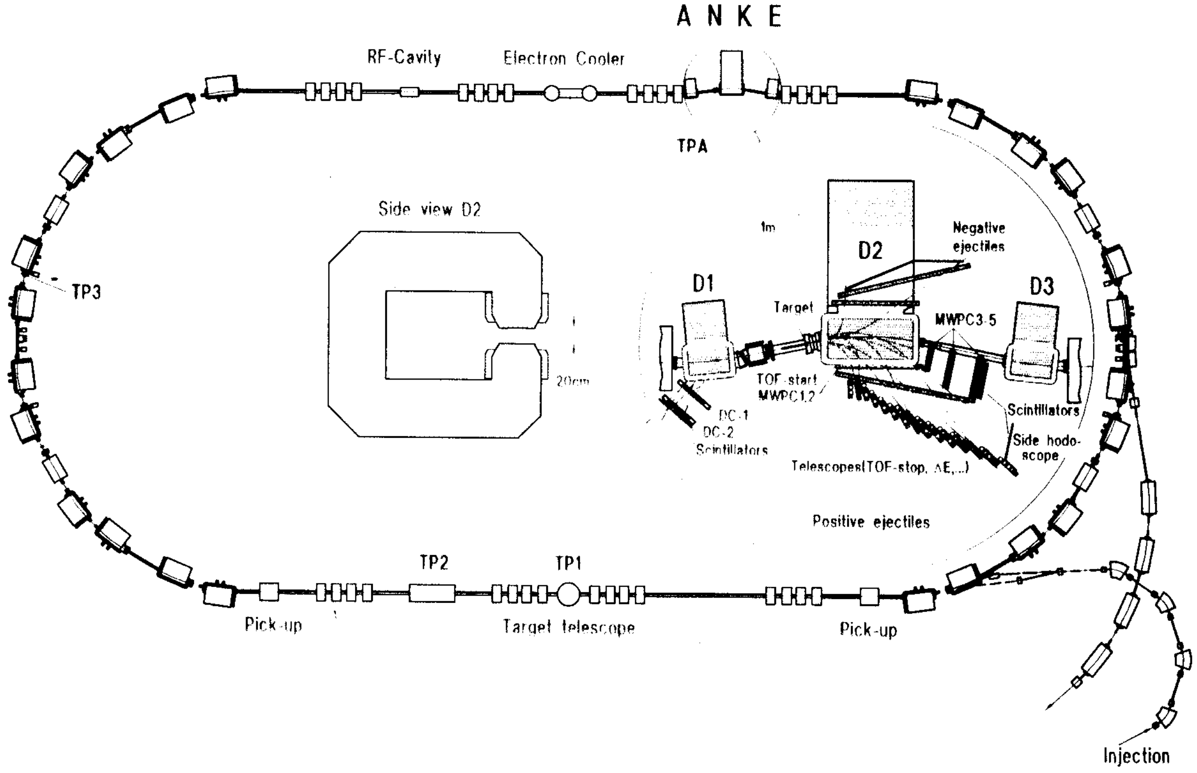
ANKE
RF-Cavity
Electron Cooler
TPA
Side view D2
20cm
1m
D2
Negative ejectiles
D1
D3
Target
MWPC3-5
TOF-start
MWPC1,2
DC-1
DC-2
Scintillators
Scintillators
Side hodo-scope
Telescopes(TOF-stop, ΔE,...)
Positive ejectiles
TP3
TP2
TP1
Pick-up
Target telescope
Pick-up
Injection

Spring 1989

Letter of Intent

for a

Threshold Physics Facility at TP2 in COSY

W. Borgs, D. Gotta, H.R. Koch, W. Oelert, H. Ohm, O.W.B. Schult,
H. Seyfarth, K. Sistemich
Institut für Kernphysik, Kernforschungsanlage Jülich, Postfach 1913,
5170 Jülich, F.R. Germany

F. Hinterberger
Institut für Strahlen– und Kernphysik der Universität Bonn, Nußallee 14–16,
5300 Bonn, F.R. Germany

Summary

It is intended to build a facility for studies of ejectiles under very small angles at the internal target place TP2 of COSY. A system of three dipole magnets is envisaged to separate the ejectiles out of the projectile beam (which experiences a closed orbit bump). This Threshold Physics Facility will enable a large variety of experiments, especially at threshold, with thin targets and the circulating cooled or uncooled beam.

Example for experiments:

Subthreshold K^+ production in proton–nucleus interaction has been studied for proton energies between 800 and 1000 MeV impinging on targets of various nuclei from Be to Pb.

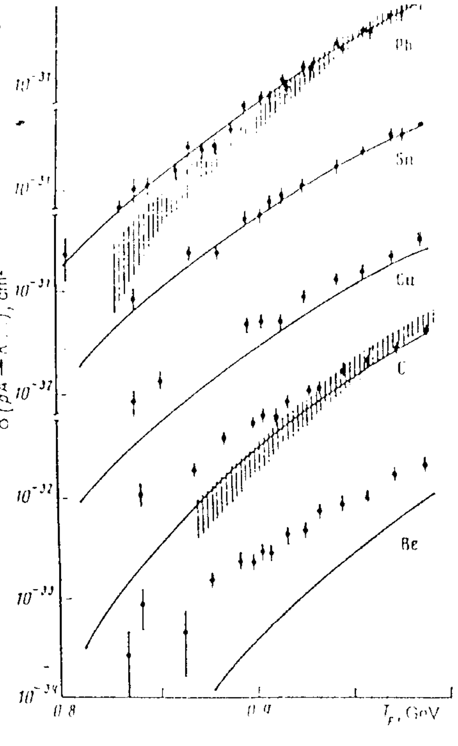

PUPI data

Fig. 4: Inclusive K^+ production cross sections measured [8] during the bombardment of various targets with protons. The full line is the prediction of the mean field model [9] and the hatched regions give the cross sections obtained with the assumption of a two-step K^+ production mechanism [8] where the first step is π production.

K^+ production:

expected cross sections

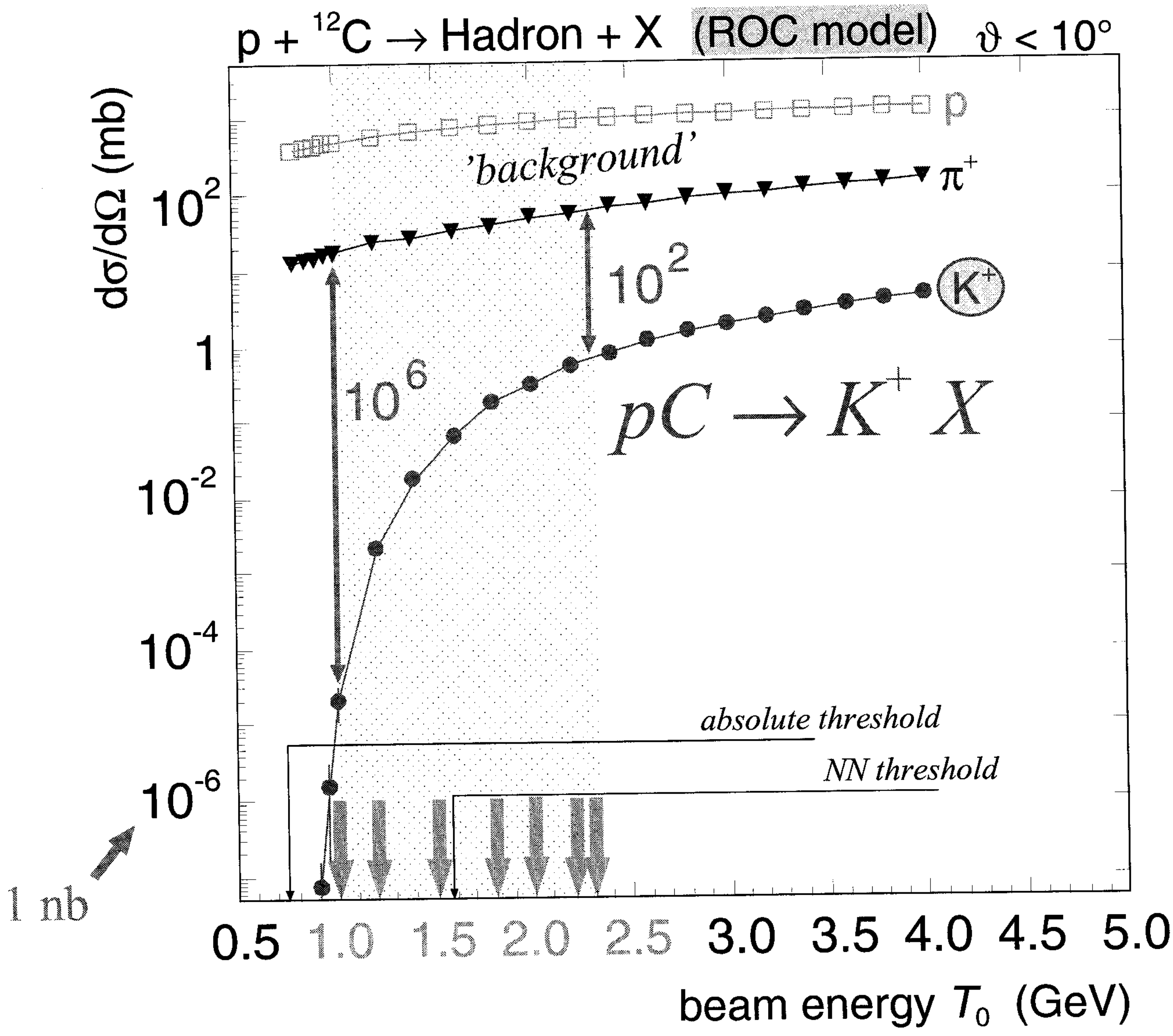

- *Calibration of the detectors: T = 2.3 GeV*
- *Measurement of $d^2\sigma/d\Omega dp$: T=1.0...2.3 Ge*

M.Büscher, 5/01

1990 : Plans for ANKE

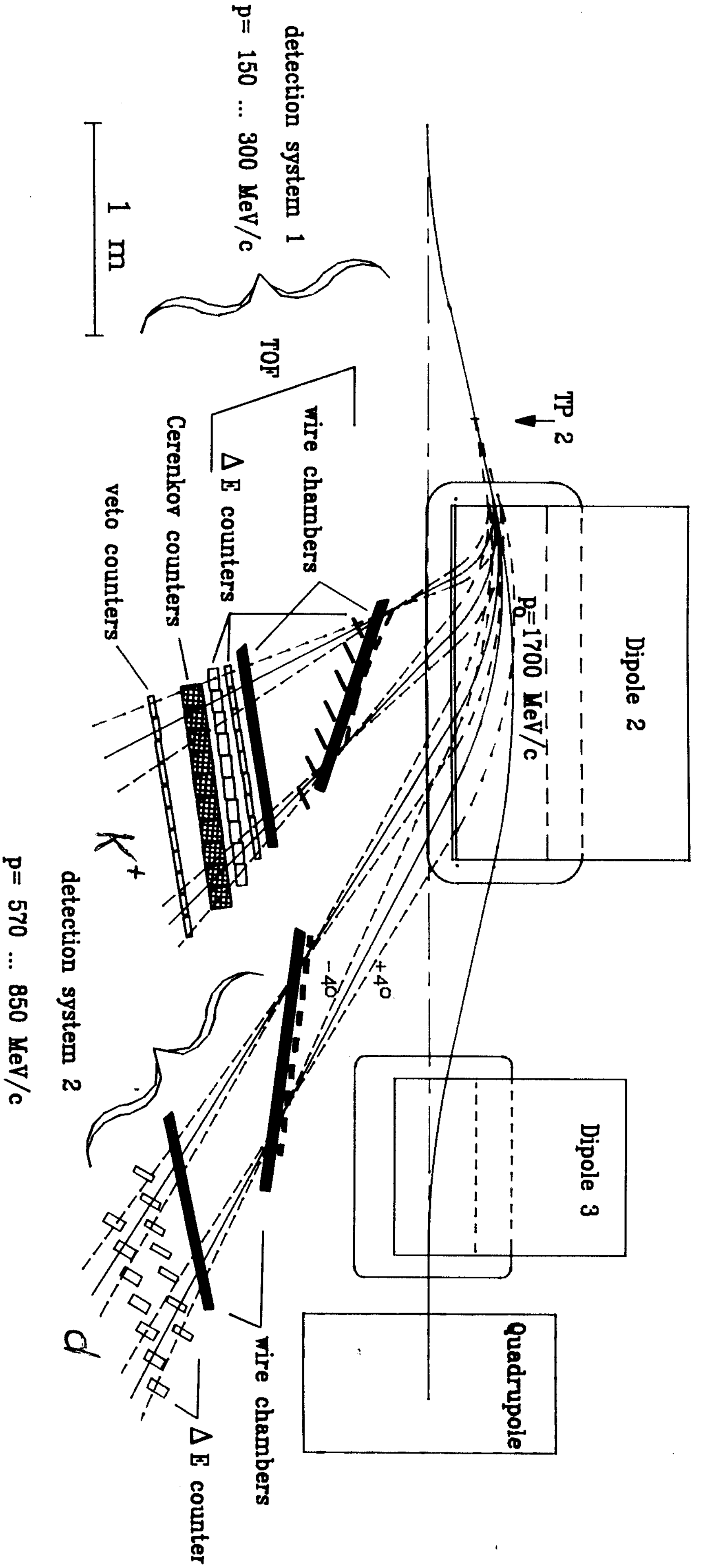

10/1991

Revised COSY Proposal/~~Letter of Intent~~

Title of Experiment Study of the Subthreshold K^+ Production with a 0^0 Facility at TP2 in COSY

For Lab. use
Exp No.:
COSY
18

Collaborators	
W. Borgs, M. Büscher, D. Gotta, D. Grzonka, H.R. Koch, W. Oelert, H. Ohm, O.W.B. Schult, H. Seyfarth, K. Sistemich, K.H. Watzlawik	IKP, KFA Jülich, Germany
J. Ernst, F. Hinterberger	ISKP Univ. Bonn, Germany
L. Jarczyk, B. Kamys, St. Kistryn, A. Kozela, J. Smyrski, A. Strzalkowski	Inst. of Phys., Jagellonian Univ., Cracow, Poland
S. Dienel, K.W. Leege, H. Müller, Chr. Schneidereit	ZfK Rossendorf, Dresden, Germany
S.V. Dshemuchadze, V.I. Komarov, V. Lyachenko F. Nichitiu, V. Travkin, B.Zh. Zalyhanov, N.I. Zhuravlev	JINR Dubna, Moscow, USSR
V. Koptev, V. Abaev	LNPI Gatchina, USSR
P. Birien	EP Division, CERN, Geneva, Switzerland
W. Cassing	Inst.f.Theo.Phys., Univ. Gießen, Germany
H. Dombrowski, R. Santo	IKP, Univ. Münster, Germany

Spokesman for collaboration: Name: K. Sistemich

Address: Institut für Kernphysik, Forschungszentrum Jülich
Postfach 1913, W-5170 Jülich, Germany

Telephone: 02461-613100 Computer Mail Address: KPH 208 at DJU KFA 11

Type of beam (p,d,polarization) p cooled or uncooled	Momentum range (MeV/c) 1500 - 2400	Intensity or internal reaction rate (particles per second) minimum needed 10^7	maximum useful 10^{11}
Type of target H_2,D_2,C,Cu,Pb etc. jet, ribbon	Total number of beam particles needed 10^{16} (4 W)	Earliest date of installation end of 1993	Safety aspects (if any)

What equipment, floorspace etc. is expected from KFA/IKP

0^0 Facility at TP2

↳ "ANKE"

Z. Phys. A 356, 313-325 (1996)

ZEITSCHRIFT
FÜR PHYSIK A
© Springer-Verlag 1996

Subthreshold K^+ production in proton-nucleus collisions

M. Dębowski[1,5], R. Barth[1], M. Boivin[3], Y. Le Bornec[2], M. Cieślak[5], M. P. Comets[2], P. Courtat[2], R. Gacougnolle[2], E. Grosse[1], T. Kirchner[2*], J. M. Martin[2], D. Miśkowiec[1], C. Müntz[4], E. Schwab[1], P. Senger[1], C. Sturm[4], B. Tatischeff[2], A. Wagner[4], W. Waluś[5] N. Willis[2], R. Wurzinger[3], J. Yonnet[3], A. Zghiche[3],**

[1] Gesellschaft für Schwerionenforschung, D-64291 Darmstadt, Germany
[2] Institute de Physique Nucléaire, IN2P3 CNRS, F-91406 Orsay, France
[3] Laboratoire National Saturne, F-91191 Gif-sur-Yvette Cedex, France
[4] Technische Hochschule Darmstadt, D-64289 Darmstadt, Germany
[5] Jagiellonian University, PL-30059 Kraków, Poland

Received: 4 April 1996 / Revised version: 4 July 1996
Communicated by V. Metag

Abstract. Double differential K^+ cross sections have been measured in p+C collisions at 1.2, 1.5 and 2.5 GeV beam energy and in p+Pb collisions at 1.2 and 1.5 GeV. The K^+ spectrum taken at 2.5 GeV can be reproduced quantitatively by a model calculation which takes into account first chance proton-nucleon collisions and internal momentum with energy distribution of nucleons according to the spectral function. At 1.2 and 1.5 GeV beam energy the K^+ data excess significantly the model predictions for first chance collisions. When taking secondary processes into account the results of the calculations are in much better agreement with the data.

measurements at
SATURNE

→ talks by
→ A. Sibirtsev / H. Büscher

VOLUME 80, NUMBER 22 PHYSICAL REVIEW LETTERS 1 JUNE 1998

Subthreshold Production of Low Momentum K^+ in p + C at 1.2 GeV

A. Badalà,[1] R. Barbera,[1,2] M. Bassi,[2] A. Bonasera,[3] M. Gulino,[1,2] F. Librizzi,[1] A. Mascali,[2] A. Palmeri,[1] G. S. Pappalardo,[1] F. Riggi,[1,2] A. C. Russo,[1] G. Russo,[1,2] R. Turrisi,[1] V. Dunin,[4] C. Ekström,[5] G. Ericsson,[6] B. Höistad,[7] J. Johansson,[7] T. Johansson,[7] L. Westerberg,[5] J. Zlomaczhuk,[7] and A. Sibirtsev[8]

[1]*INFN, Sezione di Catania, Corso Italia 57, I95129 Catania, Italy*
[2]*Dipartimento di Fisica dell'Università di Catania, Corso Italia 57, I95129 Catania, Italy*
[3]*Laboratorio Nazionale del Sud, Viale Andrea Doria, Catania, Italy*
[4]*Joint Institute for Nuclear Research, Dubna, 108000 Moscow, Russia*
[5]*The Svedberg Laboratory, Uppsala University, Box 533, S-75121 Uppsala, Sweden*
[6]*Department of Neutron Research, Uppsala University, Box 535, S-75121 Uppsala, Sweden*
[7]*Department of Radiation Sciences, Uppsala University, Box 535, S-75121 Uppsala, Sweden*
[8]*Institut für Theoretische Physik, Universität Giessen, D-35392 Giessen, Germany*

(Received 31 October 1997)

The double differential cross section of low momentum kaons (≤ 0.3 GeV/c) from p + C collisions at subthreshold bombarding energies has been for the first time measured by the use of the CLAMSUD magnetic spectrometer installed at the CELSIUS storage ring. Invariant cross sections extracted from the data show a source rapidity shifted below the nucleon-nucleon rapidity, in agreement with the existence of multistep processes in the K^+ production cross section. The total cross section of the inclusive reaction $^{12}C(p, K^+)$ at 1.2 GeV was extracted and compared with recent data systematics as a function of the proton bombarding energy. [S0031-9007(98)06266-8]

PACS numbers: 25.40.Ve, 25.40.Qa

K^+-telescope test at ITEP (1994)

Z. Phys. A 355, 93–100 (1996)

ZEITSCHRIFT
FÜR PHYSIK A

K^+-meson production in pBe interactions at T_p = 2.9 GeV

M. Büscher[1], R. Eßer[1], A. Franzen[1], L.v. Horn[1], D. Kopyto[1], H. Ohm[1], H. Seyfarth[1], K. Sistemich[1], H. Müller[2], B. Prietzschk[2], B. Rimarzig[2], C. Schneider[2], C. Schneidereit[2], A. Akindinov[3], M. Chumakov[3], V. Demechin[3], V. Ergakov[3], A. Gerasimov[3], V. Goryachev[3], Y. Kiselev[3], V. Kostromin[3], A.A. Sibirtsev[3,4], V. Sopov[3], V. Tchernyshev[3], V. Kruglov[4], A. Petrus[4], V. Koptev[5], S. Mikirtychyants[5]

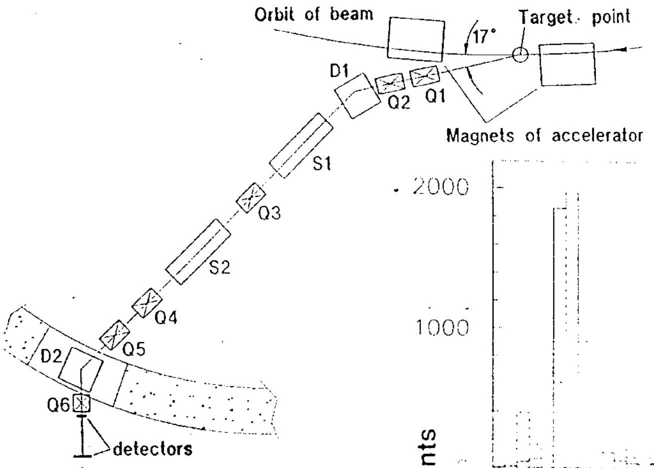

p, π, K

p = 545 MeV/c

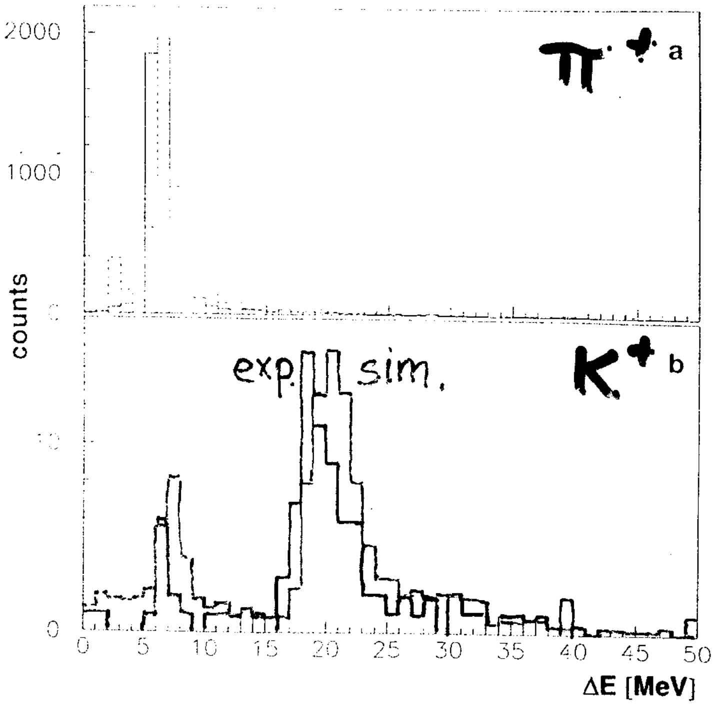

Fig. 5a,b. ΔE spectra of (a) pions and (b) kaons. The measured and simulated spectra are shown as *solid* and *dashed lines*, respectively

	TOF	$A_{\rm stop}$	$\tilde{C}$	ΔE	total
π^+	0.0037	0.13(0.13)	0.10	0.035(0.034)	$3 \cdot 10^{-7}$
p	0.0044	0.01(0.001)	1.00	0.0003(0.0005)	$3 \cdot 10^{-7}$

background suppression

K^+ *identification:*

Range telescopes

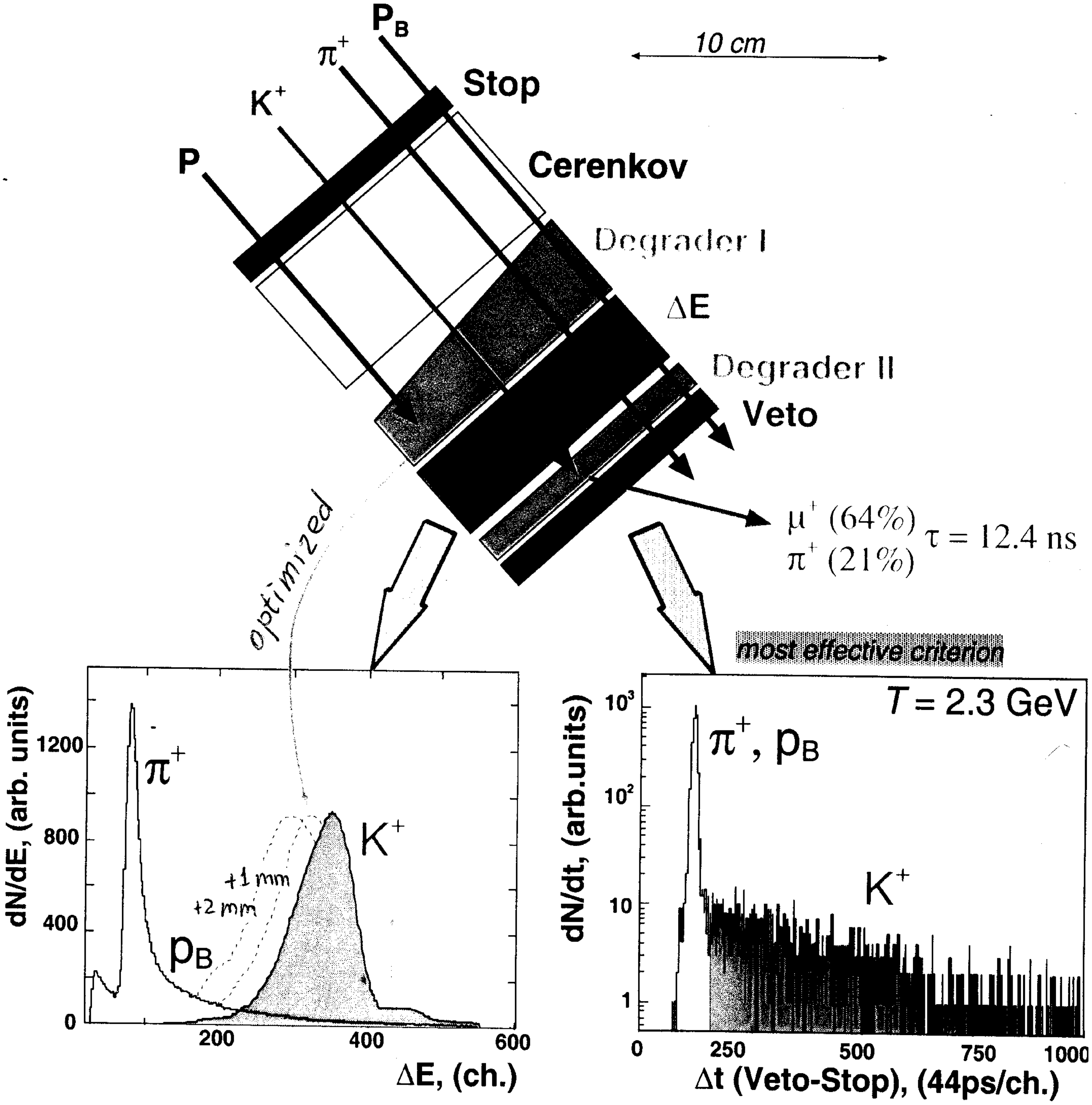

Kaon identification by detecting delayed muons...

(V. Koptev et al., Gatchina, ~1980)

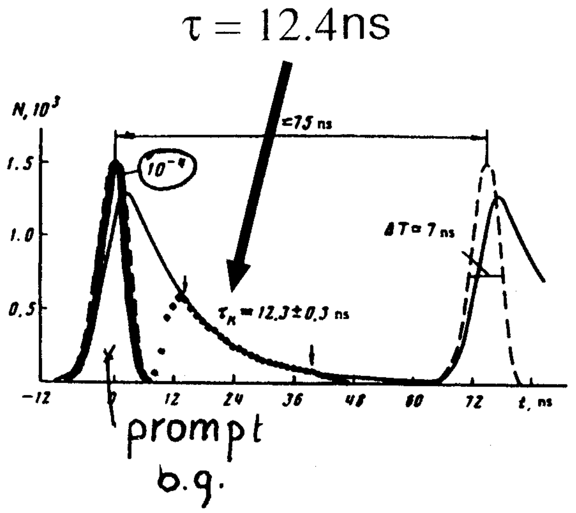

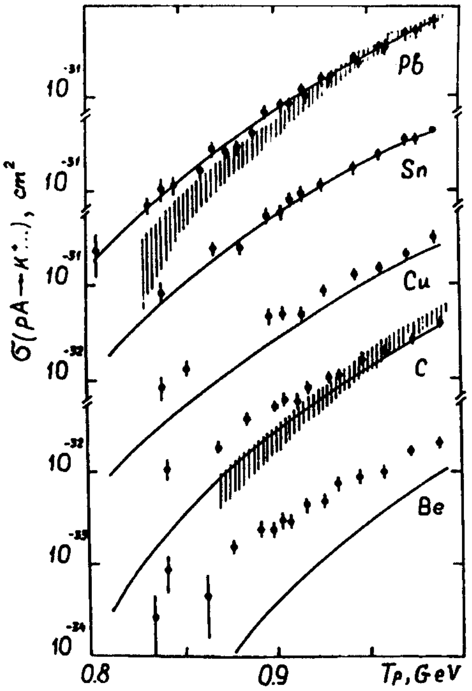

T = 0.8 ... 1.0 GeV
σ = 0.25 ... 550 nb

Magnetic spectrometer ANKE

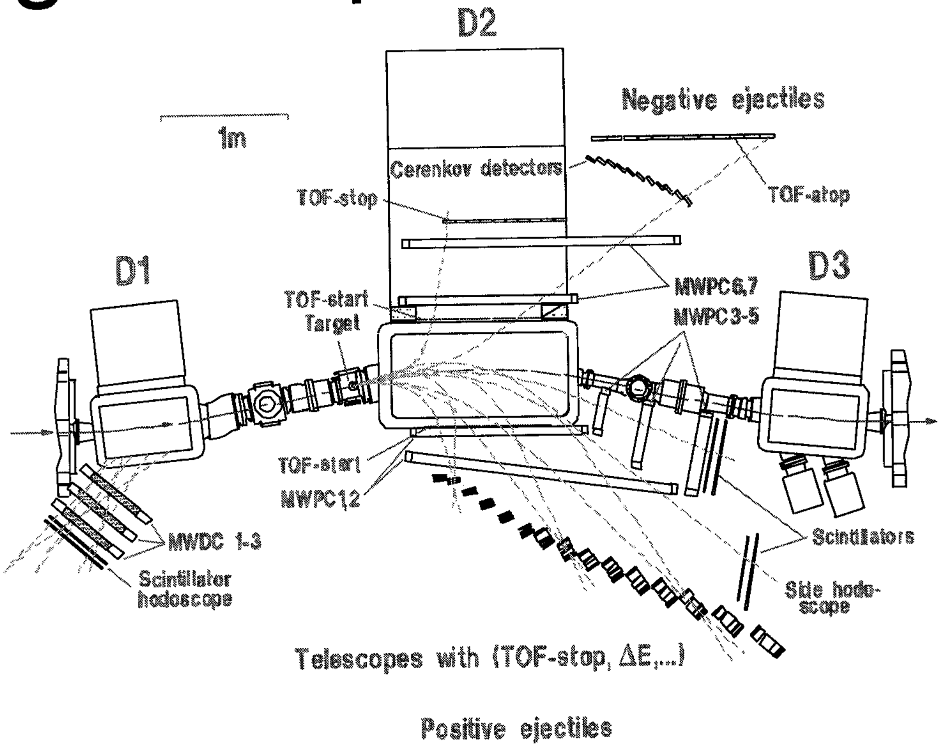

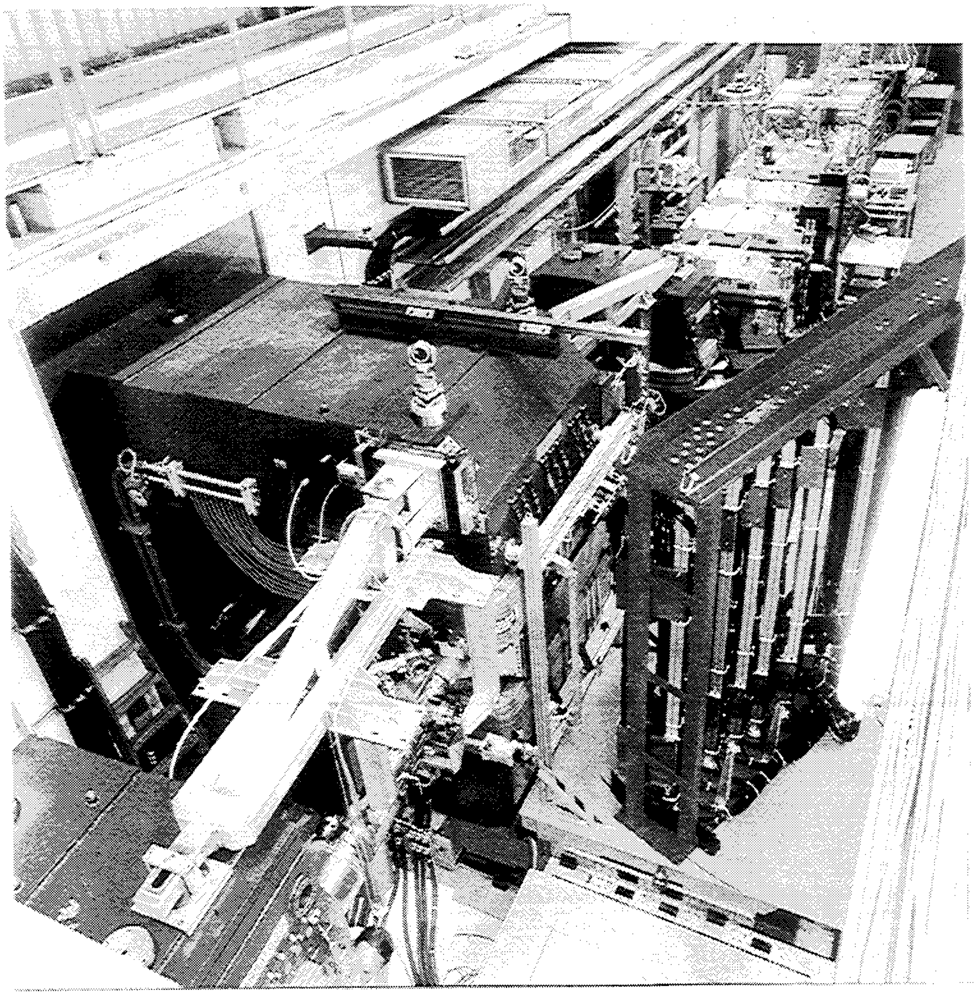

Nuclear Instruments and Methods in Physics Research A 462 (2001) 364–381

NUCLEAR
INSTRUMENTS
& METHODS
IN PHYSICS
RESEARCH
Section A

www.elsevier.nl/locate/nima

ANKE, a new facility for medium energy hadron physics at COSY-Jülich

S. Barsov[a], U. Bechstedt[b], W. Bothe[c], N. Bongers[b], G. Borchert[b], W. Borgs[b], W. Bräutigam[b], M. Büscher*[,b], W. Cassing[d], V. Chernyshev[e], B. Chiladze[f], J. Dietrich[b], M. Drochner[g], S. Dymov[b,h], W. Erven[g], R. Esser[b,i,1], A. Franzen[b], Ye. Golubeva[j], D. Gotta[b], T. Grande[b], D. Grzonka[b], A. Hardt[2,b], M. Hartmann[b], V. Hejny[b], L.v. Horn[b], L. Jarczyk[k], H. Junghans[b], A. Kacharava[f,h], B. Kamys[k], A. Khoukaz[l], T. Kirchner[m], F. Klehr[n], W. Klein[o], H.R. Koch[b], V.I. Komarov[h], L. Kondratyuk[e], V. Koptev[a], S. Kopyto[b], R. Krause[b], P. Kravtsov[a], V. Kruglov[h], P. Kulessa[b,k], A. Kulikov[h,p], N. Lang[l], N. Langenhagen[m], A. Lepges[b], J. Ley[i], R. Maier[b], S. Martin[b], G. Macharashvili[f,h], S. Merzliakov[h,p], K. Meyer[b], S. Mikirtychiants[a], H. Müller[m], P. Munhofen[b], A. Mussgiller[q], M. Nekipelov[a,b], V. Nelyubin[a], M. Nioradze[f], H. Ohm[b], A. Petrus[h], D. Prasuhn[b], B. Prietzschk[m], H.J. Probst[b], K. Pysz[r], F. Rathmann[s], B. Rimarzig[m], Z. Rudy[k], R. Santo[l], H. Paetz gen. Schieck[i], R. Schleichert[b], A. Schneider[b], Chr. Schneider[m], H. Schneider[b], U. Schwarz[t], H. Seyfarth[b], A. Sibirtsev[d], U. Sieling[g], K. Sistemich[b], A. Selikov[h], H. Stechemesser[n], H.J. Stein[b], A. Strzalkowski[k], K.-H. Watzlawik[b], P. Wüstner[g], S. Yashenko[h], B. Zalikhanov[h], N. Zhuravlev[h], K. Zwoll[g], I. Zychor[u], O.W. B. Schult[b], H. Ströher[b]

[a] *High Energy Physics Department, Petersburg Nuclear Physics Institute, 188350 Gatchina, Russia*
[b] *Institut für Kernphysik, Forschungszentrum Jülich, 52425 Jülich, Germany*
[c] *DESY, 22603 Hamburg, Germany*
[d] *Institut für Theoret. Physik, Justus-Liebig Universität Giessen, Heinrich-Buff Ring 16, 35392 Giessen, Germany*
[e] *Institute for Theoretical and Experimental Physics, Cheremushkinskaya 25, 117259 Moscow, Russia*
[f] *High Energy Physics Institute, Tbilisi State University, University Street 9, 380086 Tbilisi, Georgia*
[g] *Zentrallabor für Elektronik, Forschungszentrum Jülich, 52425 Jülich, Germany*
[h] *Laboratory of Nuclear Problems, Joint Institute for Nuclear Research, Dubna, 141980 Dubna, Russia*
[i] *Institut für Kernphysik, Universität zu Köln, Zülpicher Str. 77, 50937 Köln, Germany*
[j] *Institute for Nuclear Research, Russian Academy of Sciences, 117312 Moscow, Russia*
[k] *Institute of Physics, Jagellonian University, Reymonta 4, 30059 Cracow, Poland*
[l] *Institut für Kernphysik, Universität Münster, W.-Klemm-Street 9, 48149 Münster, Germany*
[m] *Institut für Hadronen- und Kernphysik, Forschungszentrum Rossendorf, 01474 Dresden, Germany*

---

*Corresponding author.

E-mail address: m.buescher@fz-juelich.de (M. Büscher).

[1] Now at BICRON, Vertriebs GmbH, 42929 Wermelskirchen, Germany.

[2] Now at FH Aachen, Abt. Jülich, Germany.

PII: S0168-9002(00)01147-5

ANKE beam times on K^+ production in nuclei

- pA → K^+ X, $T = 1.0 \ldots 2.3$ GeV, A = C, Cu, Au
- First set of 'serious' experiments after installation of ANKE (1998)
- Total beam time: 5 weeks (1999, 2000)

Goals:

=ANKE

- Facility which allows to detect (rare) K^+-mesons in a huge (p, π^+) background
- Measure K^+-production far below the free NN-threshold @ $T_{NN} = 1.58$ GeV
- Double differential cross sections down to $T = 1.0$ GeV

M. Nekipelov

- Information about cooperative effects in the target nucleus
- Reaction mechanisms (e.g. multi-step K^+-production) or high-momentum components of the NWF?

NIM A, accepted for publication

Identification of K$^+$-mesons from subthreshold pA collisions with ANKE at COSY-Jülich

↳ talk by M. Nekipelov

M. Büscher [a], H. Junghans [a], V. Koptev [b], M. Nekipelov [b],
K. Sistemich [a], H. Ströher [a], S. Barsov [b], G. Borchert [a],
W. Borgs [a], M. Debowski [c], W. Erven [d], R. Esser [e,f],
P. Fedorets [f], D. Gotta [a], M. Hartmann [a], V. Hejny [a],
A. Kacharava [g,h] H.R. Koch [a], V. Komarov [g], P. Kulessa [i],
A. Kulikov [g], S. Merzliakov [g], S. Mikirtychiants [b], H. Müller [c],
A. Mussgiller [a], R. Nellen [a], H. Ohm [a], A. Petrus [g],
F. Rathmann [a], Z. Rudy [i], R. Schleichert [a], Chr. Schneider [c],
O.W.B. Schult [a], H.J. Stein [a], I. Zychor [j]

[a] *Institut für Kernphysik, Forschungszentrum Jülich, 52425 Jülich, Germany*

[b] *High Energy Physics Department, Petersburg Nuclear Physics Institute, 188350 Gatchina, Russia*

[c] *Institut für Kern- und Hadronenphysik, Forschungszentrum Rossendorf, D-01474 Dresden*

[d] *Zentralinstitut für Elektronik, Forschungszentrum Jülich, 52425 Jülich, Germany*

[e] *Institut für Kernphysik, Universität zu Köln, Zülpicher Str. 77, 50937 Köln, Germany*

[f] *Institute for Theoretical and Experimental Physics, Cheremushkinskaya 25, 117259 Moscow, Russia*

[g] *Laboratory of Nuclear Problems, Joint Institute for Nuclear Research, 141980 Dubna, Russia*

[h] *High Energy Physics Institute, Tbilisi State University, University Street 9, 380086 Tbilisi, Georgia*

[i] *Institute of Physics, Jagellonian University, Reymonta 4,30059 Cracow, Poland*

[j] *The Andrzej Soltan Institute for Nuclear Studies, 05400 Swierk, Poland*

Abstract

The spectrometer ANKE has been put into operation at the accelerator COSY of the Forschungszentrum Jülich in spring 1998. An initial scientific goal is to study K$^+$-production in pA collisions at subthreshold energies far below the free NN-threshold at $T_p = 1.58$ GeV. This requires the identification of K$^+$-mesons in a background of pions and protons, about 10^6 times more intense. In this paper the

Deep subthreshold K^+ production

- complete momentum spectrum measured for the first time

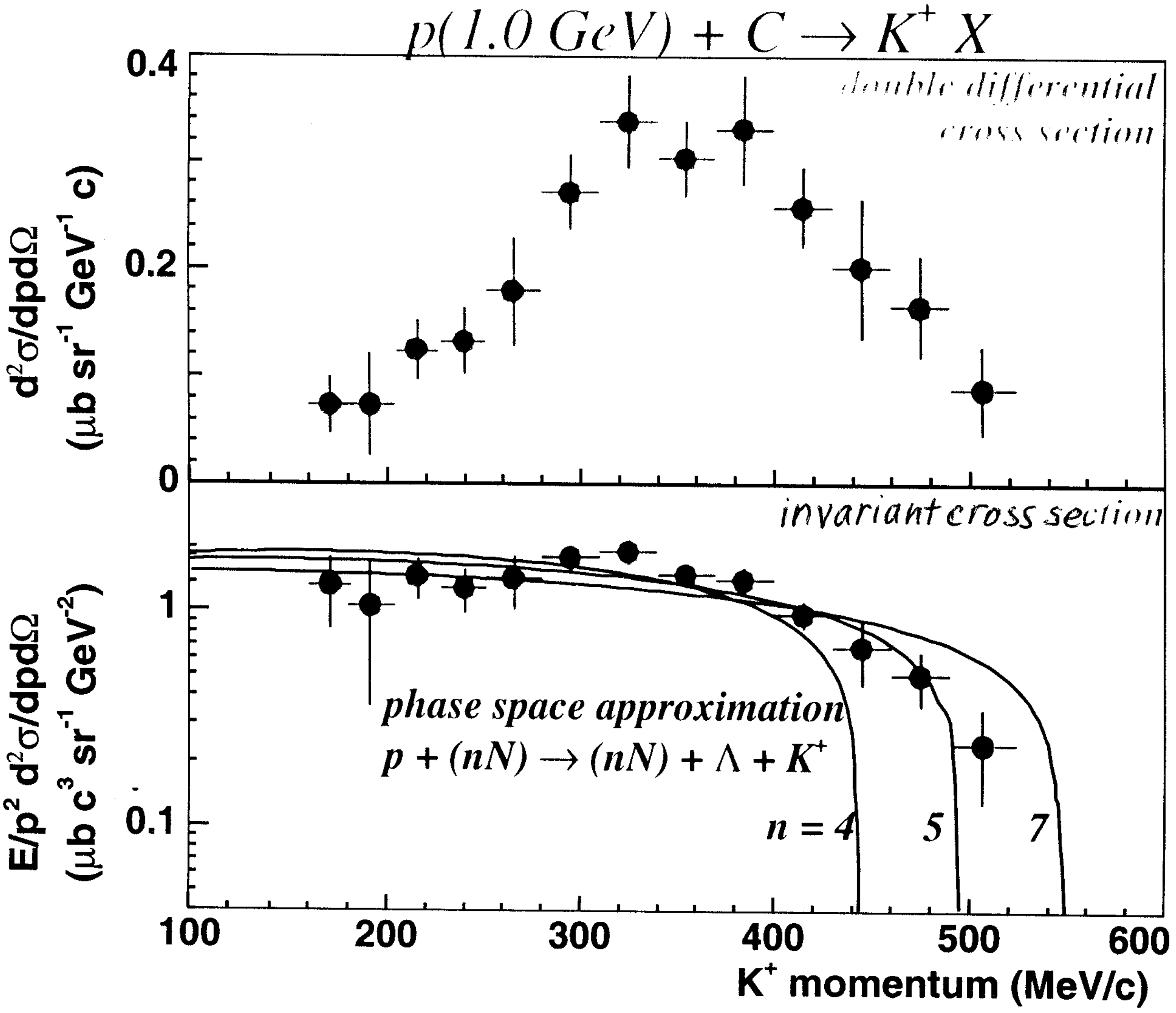

- *low-momentum* part of the spectrum:
  cannot be described by a thermal distribution, $\sigma \sim e^{-T/T_0}$
- *high-momentum* part of the spectrum:
  high collectivity of target nucleus

Forward K^+ Production in Subthreshold pA Collisions at 1.0 GeV

V. Koptev,[1] M. Büscher,[2] H. Junghans,[2] M. Nekipelov,[1,2] K. Sistemich,[2] H. Ströher,[2] V. Abaev,[1] H.-H. Adam,[3] R. Baldauf,[4] S. Barsov,[1] U. Bechstedt,[2] N. Bongers,[2] G. Borchert,[2] W. Borgs,[2] W. Bräutigam,[2] W. Cassing,[5] V. Chernyshev,[6] B. Chiladze,[7] M. Debowski,[8] J. Dietrich,[2] M. Drochner,[4] S. Dymov,[9] J. Ernst,[10] W. Erven,[4] R. Esser,[11,*] P. Fedorets,[6] A. Franzen,[2] D. Gotta,[2] T. Grande,[2] D. Grzonka,[2] G. Hansen,[12] M. Hartmann,[2] V. Hejny,[2] L. v. Horn,[2] L. Jarczyk,[13] A. Kacharava,[9] B. Kamys,[13] A. Khoukaz,[3] T. Kirchner,[8] S. Kistryn,[13] F. Klehr,[12] H. R. Koch,[2] V. Komarov,[9] S. Kopyto,[2] R. Krause,[2] P. Kravtsov,[1] V. Kruglov,[9] P. Kulessa,[2,13] A. Kulikov,[9,14] V. Kurbatov,[9] N. Lang,[3] N. Langenhagen,[8] I. Lehmann,[2] A. Lepges,[2] J. Ley,[11] B. Lorentz,[2] G. Macharashvili,[7,9] R. Maier,[2] S. Martin,[2] S. Merzliakov,[9] K. Meyer,[2] S. Mikirtychiants,[1] H. Müller,[8] P. Munhofen,[2] A. Mussgiller,[2] V. Nelyubin,[1] M. Nioradze,[7] H. Ohm,[2] A. Petrus,[9] D. Prasuhn,[2] B. Prietzschk,[8] H. J. Probst,[2] D. Protic,[2] K. Pysz,[15] F. Rathmann,[2] B. Rimarzig,[8] Z. Rudy,[13] R. Santo,[3] H. Paetz gen. Schieck,[11] R. Schleichert,[2] A. Schneider,[2] Chr. Schneider,[8] H. Schneider,[2] G. Schug,[2] O. W. B. Schult,[2] H. Seyfarth,[2] A. Sibirtsev,[2] J. Smyrski,[13] H. Stechemesser,[12] E. Steffens,[16] H. J. Stein,[2] A. Strzalkowski,[13] K.-H. Watzlawik,[2] C. Wilkin,[17] P. Wüstner,[4] S. Yashenko,[9] B. Zalikhanov,[9] N. Zhuravlev,[9] P. Zolnierczuk,[13] K. Zwoll,[4] and I. Zychor[18]

[1]*High Energy Physics Department, Petersburg Nuclear Physics Institute, 188350 Gatchina, Russia*
[2]*Institut für Kernphysik, Forschungszentrum Jülich, D-52425 Jülich, Germany*
[3]*Institut für Kernphysik, Universität Münster, W.-Klemm-Strasse 9, D-48149 Münster, Germany*
[4]*Zentralinstitut für Elektronik, Forschungszentrum Jülich, D-52425 Jülich, Germany*
[5]*Institut für Theoretische Physik, Universität Gießen, H.-Buff-Ring 16, D-35392 Gießen, Germany*
[6]*Institute for Theoretical and Experimental Physics, Cheremushkinskaya 25, 117259 Moscow, Russia*
[7]*High Energy Physics Institute, Tbilisi State University, University Street 9, 380086 Tbilisi, Georgia*
[8]*Institut für Kern- und Hadronenphysik, Forschungszentrum Rossendorf, D-01474 Dresden, Germany*
[9]*Laboratory of Nuclear Problems, Joint Institute for Nuclear Research, 141980 Dubna, Russia*
[10]*Institut für Strahlen- und Kernphysik, Universität Bonn, Nußallee 14, D-53115 Bonn, Germany*
[11]*Institut für Kernphysik, Universität zu Köln, Zülpicher Strasse 77, D-50937 Köln, Germany*
[12]*Zentralabteilung Technologie, Forschungszentrum Jülich, D-52425 Jülich, Germany*
[13]*Institute of Physics, Jagellonian University, Reymonta 4, 30059 Cracow, Poland*
[14]*Dubna Branch, Moscow State University, 141980 Dubna Moscow Region, Russia*
[15]*Institute of Nuclear Physics, Radzikowskiego 152, PL-31342, Cracow, Poland*
[16]*Physikalisches Institut II, Universität Erlangen-Nürnberg, Erwin-Rommel-Strasse 1, D-91058 Erlangen, Germany*
[17]*Physics Department, UCL, Gower Street, London WC1 6BT, United Kingdom*
[18]*The Andrzej Soltan Institute for Nuclear Studies, PL-05400 Swierk, Poland*

(Received 3 April 2001; published)

K^+-meson production in pA ($A = \mathrm{C, Cu, Au}$) collisions has been studied using the ANKE spectrometer at an internal target position of the COSY-Jülich accelerator. The complete momentum spectrum of kaons emitted at forward angles, $\vartheta \leq 12°$, has been measured for a beam energy of $T_p = 1.0$ GeV, far below the free NN threshold of 1.58 GeV. The spectrum does not follow a thermal distribution at low kaon momenta and the larger momenta reflect a high degree of collectivity in the target nucleus.

DOI:

PACS numbers: 25.40.Ve, 13.75.Cs, 29.40.-n

A central topic of hadron physics is the influence of the nuclear medium on elementary processes. This question can be studied by measuring the production of mesons in nuclei using projectiles with energies below the threshold for free NN collisions (so-called subthreshold production). These processes necessarily involve cooperative effects of the nucleons inside the target nucleus. The investigation of K^+ production is particularly well suited for this purpose since the meson is relatively heavy so that its production requires strong medium effects. Furthermore, the K^+ scatters little in nuclear matter so that its final-state interactions are expected to be small.

Proton-induced K^+ production at subthreshold energies has been studied at several accelerators. Total cross sections have been measured at the PNPI synchrocyclotron for targets between Be and Pb and projectile energies T_p from 0.8 to 1.0 GeV [1]. The results were discussed in terms of different models [1–5], in particular, of single- or two-step reactions involving the creation of an intermediate pion. It was concluded that additional experimental data were needed for an unambiguous determination of the reaction mechanism and the extraction of the information on nuclear-medium effects. Inclusive differential cross sections for pA interactions have been studied at BEVALAC [6], SATURNE [7], and CELSIUS [8]. Partial momentum spectra have been obtained at laboratory emission angles of 10°, 15°, 35°, 40°, 60°, 80°, and 90°, at projectile energies down to 1.2 GeV, and evidence for the dominance

0031-9007/01/()/(4)$15.00

ACC. CODE LD8049 AUTHOR koptev AIP ID 051127PRL

ANKE beam time on a_0^+ production

COSY proposal #55

- Jan./Feb. 2001, 2 weeks

Effective time ~ 5 days

- p(2.65 GeV) p → da_0^+

$$da_0^+ \to \pi^+\eta$$
$$da_0^+ \to K^+\bar{K}^0$$

Goals:

- measurement of a_0^+-production cross section
- determination of *B.R.*$(a_0^+ \to K^+\bar{K}^0/\pi^+\eta)$

Resume of first data analyses:

(V.Kleber, V.Koptev, M.Nekipelov)

- Goals can be achieved

Will be shown in a minute

- ANKE allows systematic studies of (neutral) scalar mesons

New proposal PAC 22

M.Büscher, 5/01

COSY working scheme 2001

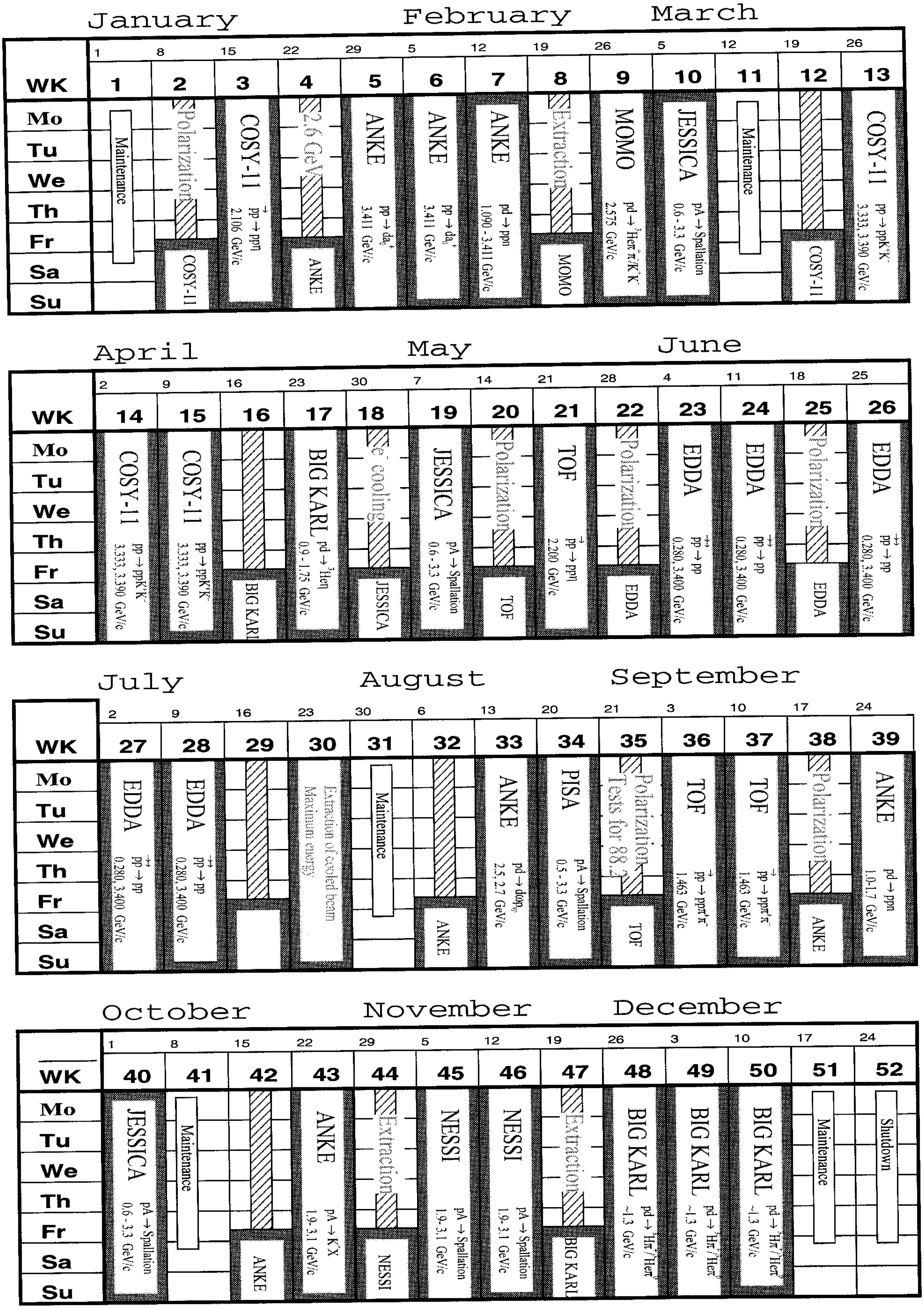

January February March

	1	8	15	22	29	5	12	19	26	5	12	19	26
WK	1	2	3	4	5	6	7	8	9	10	11	12	13
Mo Tu We Th Fr Sa Su	Maintenance	Polarization COSY-11	COSY-11 $\vec{p}p \to ppn$ 2.106 GeV/c	2.6 GeV ANKE	ANKE $pp \to da_0^+$ 3.411 GeV/c	ANKE $pp \to da_0^+$ 3.411 GeV/c	ANKE $pd \to ppn$ 1.090 - 3.411 GeV/c	Extraction MOMO	MOMO $pd \to {}^3He\pi^+\pi^-/K^+K^-$ 2.575 GeV/c	JESSICA $pA \to$ Spallation 0.6 - 3.3 GeV/c	Maintenance	COSY-11	COSY-11 $pp \to ppK^+K^-$ 3.333, 3.390 GeV/c

April May June

	2	9	16	23	30	7	14	21	28	4	11	18	25
WK	14	15	16	17	18	19	20	21	22	23	24	25	26
Mo Tu We Th Fr Sa Su	COSY-11 $pp \to ppK^+K^-$ 3.333, 3.390 GeV/c	COSY-11 $pp \to ppK^+K^-$ 3.333, 3.390 GeV/c	BIG KARL	BIG KARL $pd \to {}^3He\eta$ 0.9 - 1.75 GeV/c	e^- cooling JESSICA	JESSICA $pA \to$ Spallation 0.6 - 3.3 GeV/c	Polarization TOF	TOF $\vec{p}p \to ppn$ 2.200 GeV/c	Polarization EDDA	EDDA $\vec{p}\vec{p} \to pp$ 0.280, 3.400 GeV/c	EDDA $\vec{p}\vec{p} \to pp$ 0.280, 3.400 GeV/c	Polarization EDDA	EDDA $\vec{p}\vec{p} \to pp$ 0.280, 3.400 GeV/c

July August September

	2	9	16	23	30	6	13	20	21	3	10	17	24
WK	27	28	29	30	31	32	33	34	35	36	37	38	39
Mo Tu We Th Fr Sa Su	EDDA $\vec{p}\vec{p} \to pp$ 0.280, 3.400 GeV/c	EDDA $\vec{p}\vec{p} \to pp$ 0.280, 3.400 GeV/c		Extraction of cooled beam Maximum energy	Maintenance	ANKE	ANKE $pd \to dop_{sp}$ 2.5, 2.7 GeV/c	PISA $pA \to$ Spallation 0.5 - 3.3 GeV/c	Polarization Tests for 88.2 TOF	TOF $\vec{p}p \to pp\pi^+\pi^-$ 1.463 GeV/c	TOF $\vec{p}p \to pp\pi^+\pi^-$ 1.463 GeV/c	Polarization ANKE	ANKE $pd \to ppn$ 1.0-1.7 GeV/c

October November December

	1	8	15	22	29	5	12	19	26	3	10	17	24
WK	40	41	42	43	44	45	46	47	48	49	50	51	52
Mo Tu We Th Fr Sa Su	JESSICA $pA \to$ Spallation 0.6 - 3.3 GeV/c	Maintenance	ANKE	ANKE $pA \to K^+X$ 1.9-3.1 GeV/c	Extraction NESSI	NESSI $pA \to$ Spallation 1.9-3.1 GeV/c	NESSI $pA \to$ Spallation 1.9-3.1 GeV/c	Extraction BIG KARL	BIG KARL $pd \to {}^3H\pi^+/{}^3He\pi^0$ ~1.3 GeV/c	BIG KARL $pd \to {}^3H\pi^+/{}^3He\pi^0$ ~1.3 GeV/c	BIG KARL $pd \to {}^3H\pi^+/{}^3He\pi^0$ ~1.3 GeV/c	Maintenance	Shutdown

▩ User Operation ▨ Machine Development ☐ Maintenance

May 3, 2001
M. Büscher
m.buescher@fz-juelich.de

p(2.65 GeV)p → pK$^+$ X

- 'By product' of a_0^+ beam time
- Data allow to determine Λ/Σ ratio
- Higher resonances visible?

P. Kravchenko

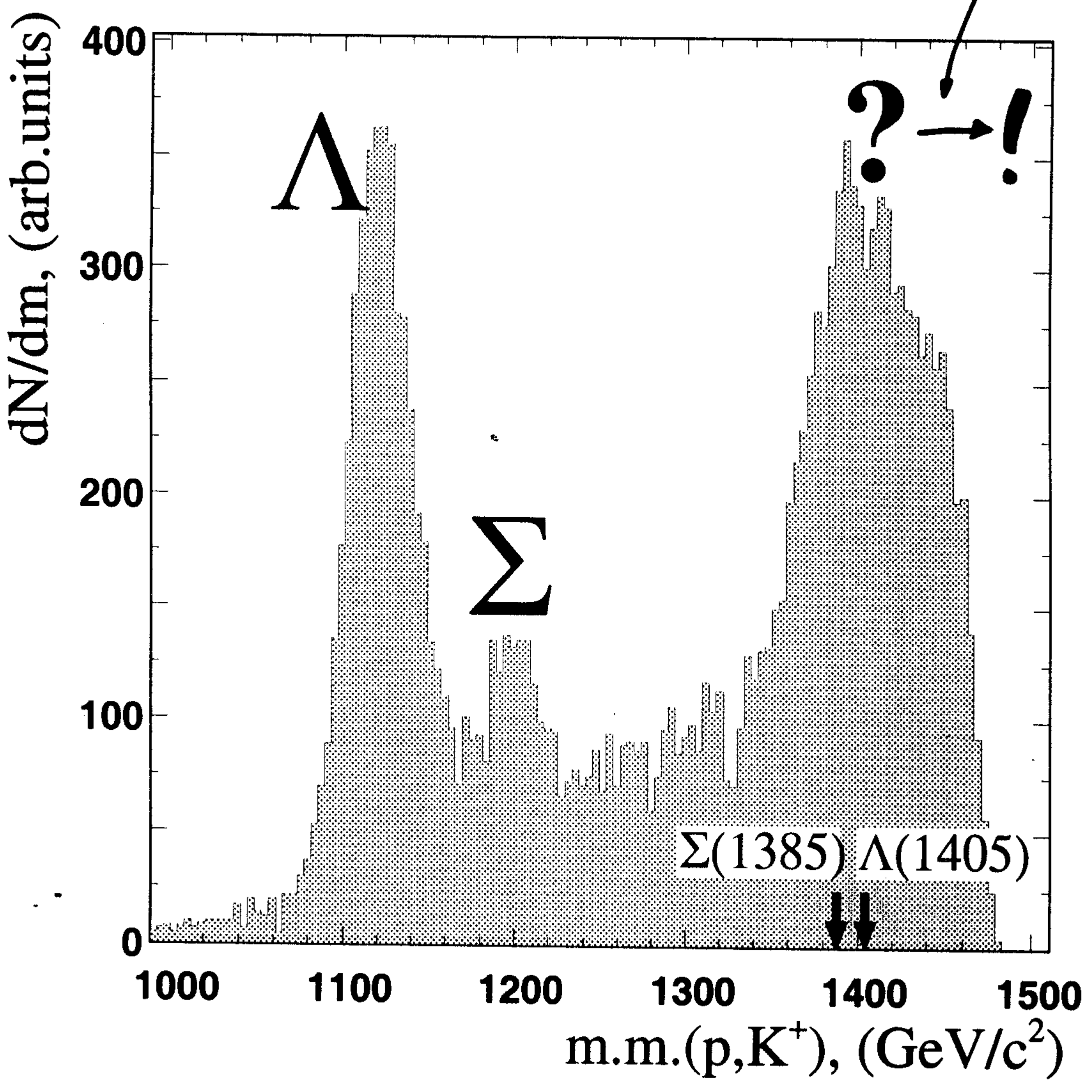

- Data of comparable quality for
  pn → nK$^+$ Λ/Σ
  are expected next year

Luminosities during ANKE experiments (A dependence)

R.Koch

Institut für Kernphysik
Forschungzentrum Jülich
52425 Jülich
Germany

The A-dependence of proton induced subthreshold K^+ -production was studied at ANKE in experiments with strip targets of C, Cu, and Au. It is expected that for targets of nuclear charge $Z \geq 6$ the lifetime of the circulating beam is limited by Cb-scattering. Scattering angles vary roughly with Z^2. Thus the luminostiy integrated over the beam life time should decrease with Z in the following way $LT \equiv \int Ldt \sim 1/Z^2$. However in the ANKE experiments a weaker dependence was observed: $LT \sim 1/Z^{1.2}$, suggesting that other particle loss mechanisms contribute. In order to accomplish optimal accelerator conditions in future K^+ and K^- experiments better understanding of energy loss in the target is needed. Rough estimation of LT can be obtained from integral formula, which yield the Gaussian distribution of multiple scattering through small angles and the mean energy loss (Bethe-Bloch). The calculation shows that for the relevant COSY ring parameters and for a particle momentum acceptance of $\Delta p/p \approx 0.3\%$ particle loss through energy degradation may occur for targets of $Z \geq 6$. Beam life times deduced from the integral formula alone may differ significantly from reality as effects of the tails of the probability distributions ($1/\theta^3$ for the scattering angle θ, $1/\Delta E^2$ for the energy losses ΔE) do not enter sufficiently. In particular the interaction of transversal and longitudinal phase spaces is missing. The existance of dispersion somewhere in the ring reduces the accepted transversal phase space. E.g. a beam momentum shift $\Delta p/p = 0.2\%$, a dispersion of D=20 m and a free beam tube diameter of 120 mm causes a shift of the beam axis of 40 mm, which reduces for the x-acceptance to 1/9 of the $\Delta p/p = 0$ value. More precise luminosities are obtained through MC simulations, in which the full probability distributions for energy loss and angular scattering for thin targets are reproduced. A C-program is now running, in which the same physical processes are modelled as in the old Fortran programs used in the early stage of COSY and ANKE for target beam interaction studies [1] [2]. Coulomb scattering is determined by the cross section

$$\sigma_{Cb} = 4\pi \left(\frac{Z1 * Z2 * e^2}{p * c * \beta * \alpha} \right)^2$$

with $Z1$, $Z2$: nuclear charge numbers, p: particle momentum, β: particle velocity, α: atomic screening angle. For MC-calculations random scattering angles can easily be deduced from a random number RN ($0 < RN \leq 1$) through $\theta = \alpha\sqrt{1/RN - 1}$ [3]. Energy loss is calculated using the Landaus distribution [4]. The long tail of the ΔE -distribution can easily be numerically computed after transformation to the distribution for $1/\Delta E$.

The calculations show, that for typical thin solid state targets (10 to 1000 $\mu g/cm^2$) LT is independent of target thickness and geometry. Therefore - for a certain target material and certain storage ring parameters - LT can be determined through MC calculations using any appropriate thin target. In the recent luminosity calculations the following parameters were used:

Beam kinetic energy: T = 1 GeV
Beta functions at target: $\beta_x = 4m$, $\beta_y = 5m$
Transversal acceptance of COSY: $A_x = 50$, $A_y = 16\ \pi * mm * mrad$
Figure of merit [1]: $FM = \frac{1}{\beta_x/A_x + \beta_y/A_y} = 2.5$ (resulting from values above)
Target thickness: $1mg/cm^2$
Injection: Transversal phase space filled up to ring acceptance
Acceleration: Tranversal beam emittance shrinks with 1/p
Momentum acceptance: $\Delta p/p$= 0.1 % and 0.3 % (assumed limits, the real value applicable for the ANKE experiments seems to be unknown.)

Compensation of mean energy loss in target: ON or OFF.
The ANKE experiments were made with a coasting beam. Thus energy loss was not compensated.

1	2	3	4	5	6	7
Targ.	Z	$\Delta p/p = 0.3\%$ dE compensation		nucl. react. probability $*100$	$\Delta p/p = 0.1\%$ no dE compens.	
		LT $/10^{20}/cm^2$	$LT * Z^2$ $/10^{24}/cm^2$		LT $/10^{20}/cm^2$	$LT * Z^{1.2}$ $/10^{20}/cm^2$
C	6	1130	4.1	2.4	270	2320
Al	13	260	4.4	1.0		
Cu	29	56	4.7	0.36	39	2220
Ag	47	25	5.5	0.23		
Au	79	9.8	6.1	0.12	8.4	1590

Tab. 1: Results of MC calculations: Integrated luminosities LT per circulating particle for the ring momentum acceptance $\Delta p/p = 0.3\%$ with compensation of the mean energy loss for each target crossing and for $\Delta p/p = 0.1\%$ without compensation of the mean energy loss. The nuclear reaction probability (column 5) is given for the 1st case (column 3). We see that for $Z \geq 6$ LT changes roughly as expected, if the mean energy loss in the target is compensated (column 4). If energy loss is not compensated (coasting beam) and if the momentum acceptance of the storage ring is low (0.1%) luminosities are strongly reduced for Z=6 targets (factor of 4) and slightly reduced for Z=29 targets (factor of 1.4, column 6). The luminosity obtained with a Au-target is only reduced by a factor of 1.16. The observed Z-dependance of LT can roughly be explained by a $Z^{-1.2}$ dependance (column 7). The precise value of the exponent was not determined, because it has no physics relevance. It depends of COSY beam optics which probably will differ in another beam experiment. The conclusion of the present study is, that for experiments with coasting beam energy loss in the target must be taken into account for targets of $Z \leq 29$. In future experiments energy loss compensation of the circulating beam should be applied.

References

[1] H.R.Koch, Reaction Rates in Internal Solid State Targets, Proc. 105th International WE-Heraeus-Seminar on Hadronic Processes at Small Angles in Storage Rings (1993) 67

[2] H.R.Koch, G.Riepe, A.Hamacher, J.Pfeiffer, O.W.B.Schult, A.Nakach, M.Olivier, A.Dewald, P.von Brentano, NIM A271 (1988) 375

[3] H.O.Meyer, NIM B10/11 (1985) 342

[4] L.Landau, Journal of Physics 8 (1944) 201

Luminosities at ANKE
A-dependence in the K^+-subthreshold experiments from MC simulations

R. Koch

Experiments with C, Cu, Au targets
Dominant process for beam losses:Cb-scattering ~ Z^2

Integral of the luminosity over the beam lifetime

$$LT \equiv \int Ldt \sim 1/Z^2$$

Observation: $LT \sim 1/Z^{1.2}$

For optimal conditions in future experiments K^+ and K^- in nuclei better understanding needed.

Question: Contribution of energy loss (~ Z) for C and Cu target.

Rough estimation of LT from integral formula (ref.: Review of Particle Physics)

- Gaussian distribution of multiple scattering through small angles
- Bethe-Bloch mean energy loss

Result for resonable target thickness and number of passages through the target:

Momentum acceptance <0.3 % and light targets:
Energy loss must be considered

Limitations of integral formula:

1. Multiple Cb-scattering:
- Gaussian shape, large angles suppressed
  Reality: $d\sigma/d\theta \sim 1/\theta^3$ for large angles ($d\theta$ cone shell element)
- Particle check inside or outside ring acceptance only once
  For angular scattering frequent checks are needed
  scattering angle is a vector, emittance may inrease or decrease
  Reality: circulating particle is checked by the walls of the beamline every revolution

2. Energy loss: mean energy loss is correct
- High energy tail is missing
  Reality: Landau distribution $d\sigma/dE \sim 1/E^2$
- Coupling transversal – longitudinal phase space is missing
  Energy loss causes reduction of maximum beam diameter or angular divergeance due to dispersion

1a

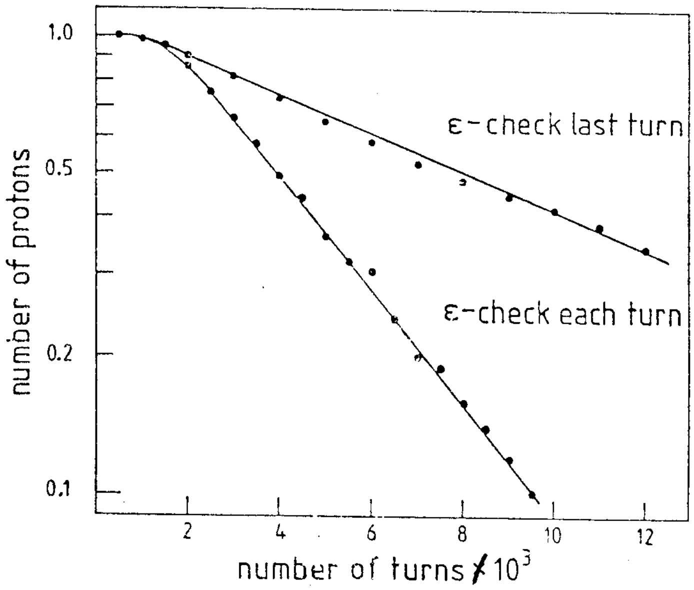

p(400 MeV) on Ni, 100 μg/c

$\beta_x = 8$ m $\beta_z = 2$ m

$A_x = 200$ $A_z = 50$ π mm mrad

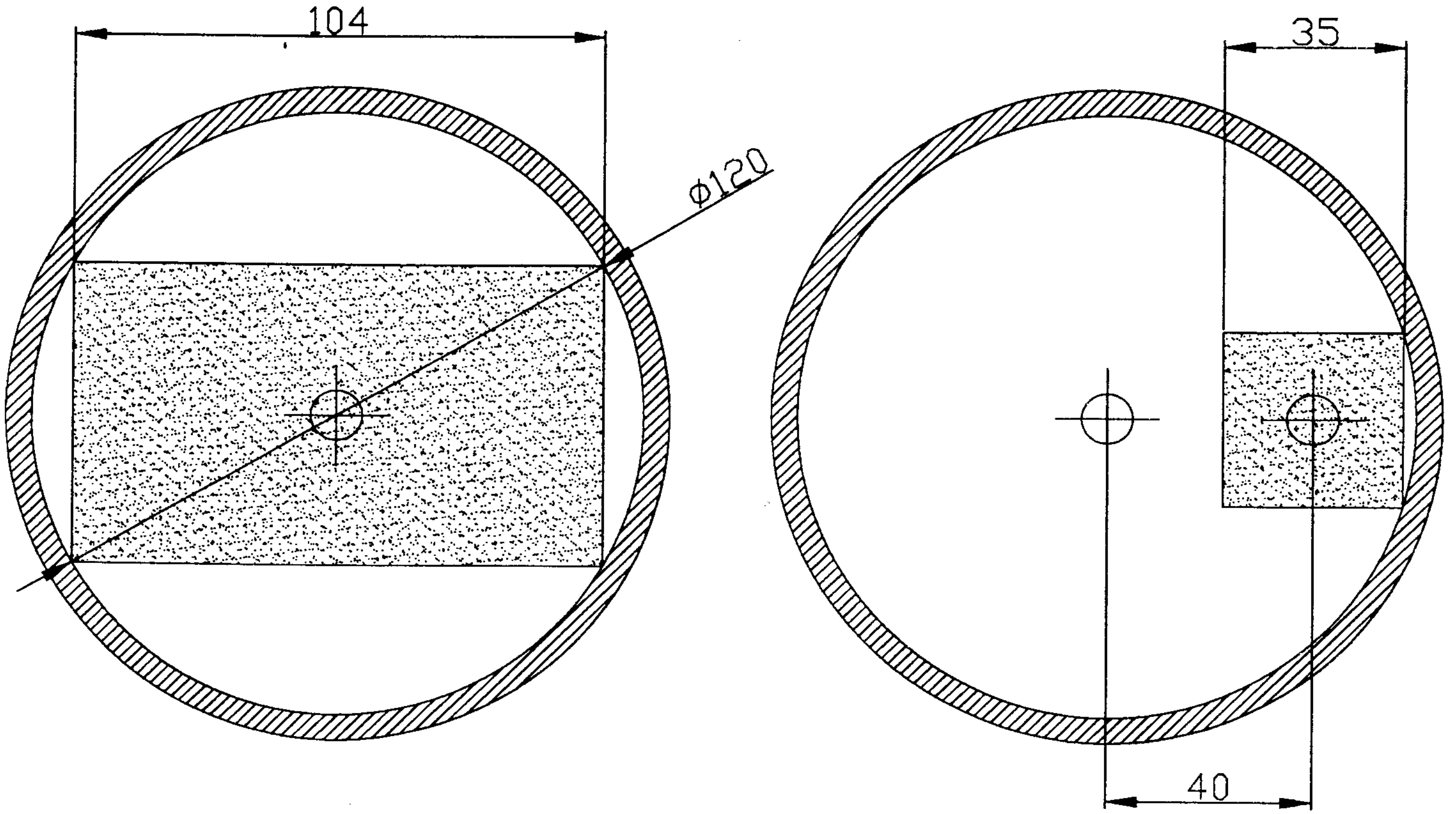

dp/p = 0

dp/p = 0.2%

Reduction of maximum beam dimension with momentum shift
dp/p = 0.002, dispersion D = 20 m.
Resulting shift of beam axis: dp/p*D = 40 mm
Resulting change of x-emittance: 1 to 0.11

More precise calculation of luminosities:

MC simulations, single energy loss and angular scattering processes, using realistic probability distributions for thin targets, including the tails .
C-program running, same physical processes as in the old Fortran programs, used in the early stage of COSY and ANKE for target beam interaction studies.
Result:

For thin solid state targets:
the luminosity integrated over the beam lifetime
is independent of target thickness and geometry

Integrated luminosity per particle:
$LT = \int Ldt = t * npas$ t = target thickness, atoms / cm^2
npas = number target passages per particle

Limitation through angular scattering:

$\varepsilon\_max = \Delta\varepsilon\_mean * t * npas$

$\Delta\varepsilon\_mean$ = mean emittance growth per target passage and unit thickness
function of z, Z, p, FM of storage ring

$LT = \varepsilon\_max / \Delta\varepsilon\_mean$

Limitation through energy loss:

$\Delta E\_max = dE/dx * t * npas$
$LT = \Delta E\_max / dE/dx$

Consequence:
LT for a certain material determined through MC calculation using a thin target of any appropriate thickness

Basic relation:
Cb-potential with electronic screening:

$$V(r) = \frac{z Z \cdot e^2}{r} \cdot e^{-r/a}$$

atomic radius $a = 0.468 \cdot 10^{-8} Z^{-1/3}$

$$\frac{d\sigma}{d\theta} = 8\pi \left(\frac{z Z \cdot e^2}{p \cdot \beta \cdot c} \right)^2 \cdot \frac{\theta}{(\theta^2 + \alpha^2)^2}$$

screening angle $\alpha = \frac{1.13}{137} \cdot Z^{1/3} \cdot \frac{m_e \cdot c}{p}$

Ref.: W.T.Scott, Rev. Mod. Phys. 35(1963)231
J.D.Jackson, Classical Electrodynamics
Tschalär NIM B5(1984) 455

$\theta \gg \alpha$: $d\sigma / d\theta \sim Z^2$ dominant process for emittance growth

$\theta \ll \alpha$: $d\sigma / d\theta \sim Z^2/Z^{4/3} = Z^{2/3}$

Computation method:

$$\sigma_{cb} = 4\pi \left(\frac{z Z e^2}{p \cdot c \cdot \beta \cdot \alpha} \right)^2$$

$$\Theta = \alpha \sqrt{\frac{1}{rn} - 1} \qquad 0 < rn < 1$$

Energy loss:

- Probability density for loss ΔE from original Landau distribution (L.Landau, J.Physics VIII (1944) 201)
- Transformation ΔE → 1/ΔE to eliminate the long high energy tail
- Approximation by polygon of equal area elements
- Random number → 1/ΔE
- Backsubstitution → ΔE

Parameters used for MC calculations:

Beam energy: T = 1 GeV

Beta functions at rarget:
β_x=4m
β_y=5m

Transversal acceptance of COSY:
A_x=50π*mm*mrad
A_y=16π*mm*mrad

Figure of merit: $FM=1/(\beta_x/A_x + \beta_y/A_y)=2.5$

Target thickness: 1mg/cm^2

Injection: Transversal phase space filled up to ring acceptance
Acceleration: Beam emittance shrinks with 1/p
Momentum acceptance: $\Delta p/p$ = 0.1% or = 0.3%

Compensation of mean energy loss in target:

ON or OFF

Experiments : acceleration cavity off
no compensation of mean
energy loss

Target	Z	LT $cm^2/10^{**}20$ dp/p=0.3% with dE compens.	LT * Z^2 $cm^2/10^{**}24$ dp/p=0.3% with dE compens.	nucl. react. probability /100	LT $cm^2/10^{**}20$ dp/p=0.1% without dE compens.	LT * $Z^{1.2}$ $cm^2/10^{**}20$ dp/p=0.1% without dE compens.
C	6	1130	4.1	2.4	270	2320
Al	13	260	4.4	1.0		
Cu	29	56	4.7	0.36	39	2220
Ag	47	25	5.5	0.23		
Au	79	9.8	6.1	0.12	8.4	1590

Tab. 1: Integrated luminosities LT per circulating particle for the ring momentum acceptance dp/p=0.3% with compensation of the mean energy loss for each target crossing and for dp/p=0.1% without compensation of the mean energy loss. The nuclear reaction probability is given for the 1st case (column 3).

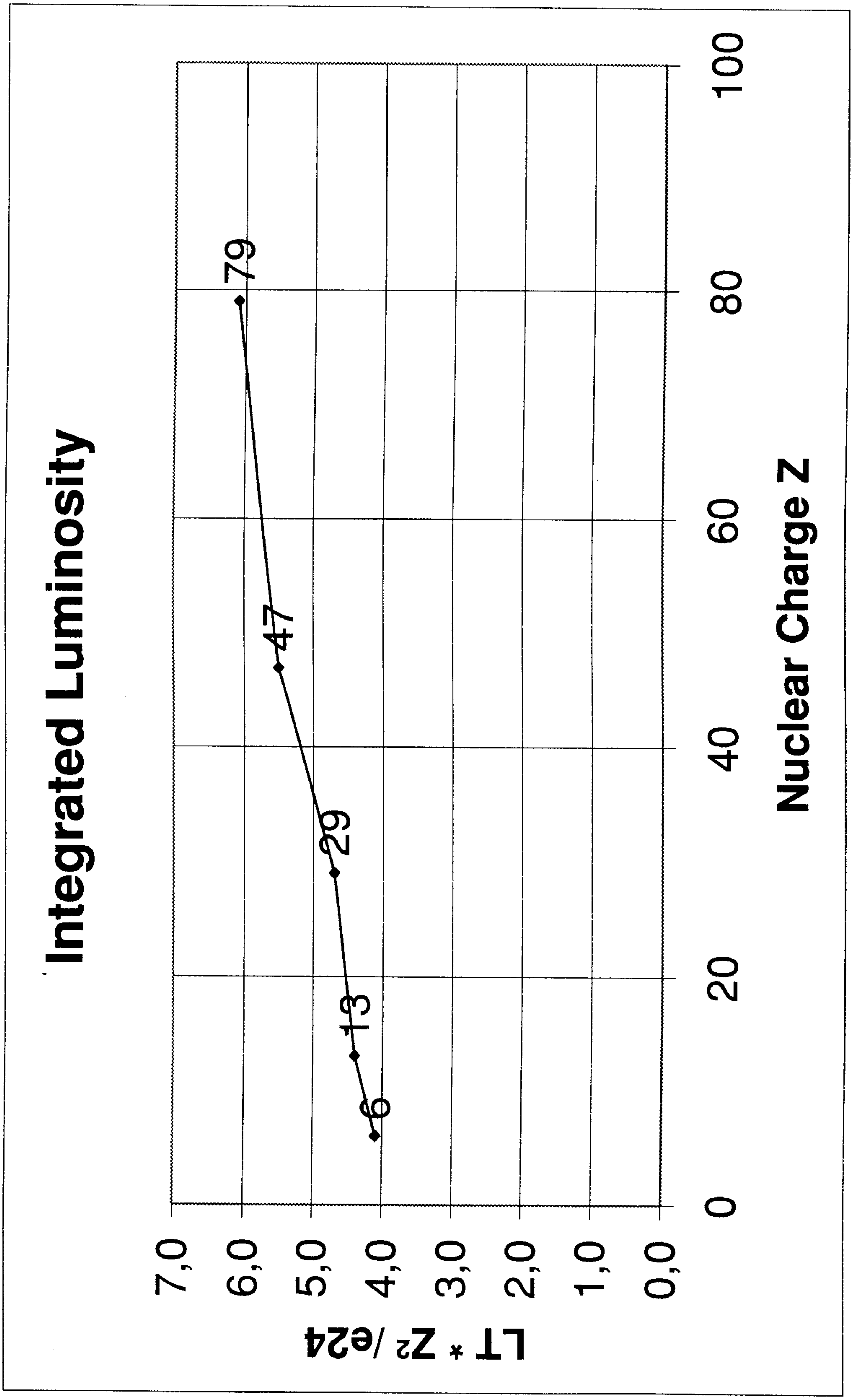
Integrated Luminosity
LT * Z² /e24
7,0
6,0
5,0
4,0
3,0
2,0
1,0
0,0
0
20
40
60
80
100
Nuclear Charge Z
6
13
29
47
79

Conclusions:

- The observed A-dependence of the integrated luminosities is explained through
  small angle scattering
  AND
  energy loss in the targets C and Cu.
  The HF-cavity was not active during the irradiation phase.

Future experiments:

- For Au target compensation of energy loss has only minor effect
- For the lighter targets HF should be on, if the highest luminosity is aimed at. This entails special COSY operation for energies which require the shift of the γ-transition and restauration of high transversal ring acceptance

Investigation of K^+ production in proton-nucleus collisions with ANKE

M.Nekipelov

Institut für Kernphysik
Forschungzentrum Jülich
52425 Jülich
Germany

One of the primary goals of ANKE was to investigate K^+-meson production in proton-nucleus collisions below and above the free nucleon-nucleon threshold at 1.58 GeV. Inclusive momentum spectra of kaons emitted at forward angles (less than 12 degrees) have been measured for C, Cu and Au strip targets in a proton energy range T_p=1.0...2.3 GeV. Double differential cross sections were obtained by a normalization to known pion-production cross sections measured at similar kinematical conditions [1,2].

The main experimental challenge was that at low energies the background (of mostly pions and protons) is approximately factor of 10^6 more intense than the signal (kaons). The detection system of ANKE allows to suppress this huge background and to detect rare K^+-mesons in the momentum range p$\approx$200...500 MeV/c. Combining hardware and software criteria such as time-of-flight, information from the wire chambers and delayed veto requirement gives us a unique possibility to identify K^+-mesons. Details about the data analysis can be found in [3]. At the lowest incident beam energy of 1.0 GeV a complete kaon-momentum spectrum was measured for the first time [4]. We also expect a wide momentum coverage at 1.2 GeV during beam-time scheduled in late fall 2001.

To compare the cross sections measured at ANKE with other data we have chosen the single point on the momentum spectrum, namely 500 MeV/c. Assumptions about the angular dependence of the cross sections and about the target-mass dependence allowed us to make an extrapolation of the results to same conditions. One can see, that all the points on the energy dependence of the cross section can be connected with a smooth curve.

An analysis of the cross sections as well as their target-mass dependence does not give an unambiguous conclusion about the underlying reaction mechanisms. Therefore, it was proposed to investigate the production K^+ mesons correlated with protons and deuterons from 1-step or 2-step production mechanisms. K^+d final state can only be observed in case of the 2-step reaction, while K^+p comes both from the 2-step and direct production mechanisms. In the latter case an analysis of more than 2 correlated particles may provide a recognition of the πN or pN channels.

The possibility of a correlation experiment was tested during the last ANKE beam-time devoted to a_0^+ production (2.65 GeV). Additional measurements at lower energy (1.2 GeV) should give us an answer whether we can directly measure the contributions of different mechanisms.

[1] J. Papp *et al.*, *Phys.Rev.Lett.* **34**, 601(1975).
[2] V. V. Abaev *et al.*, *J.Phys.* **G14**, 903(1988).
[3] M. Büscher *et al.*, *NIM A*, accepted for publication.
[4] V. Koptev *et al.*, *Phys.Rev.Lett.* **87**, 022301(2001).

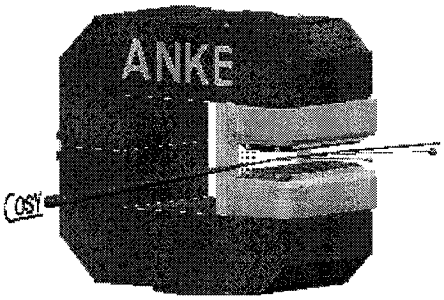

Investigation of K^+ production in proton-nucleus collisions with ANKE

M.Nekipelov for the ANKE Collaboration

- $pA \rightarrow K^+ X$, $T = 1.0 \ldots 2.3$ GeV, A = C, Cu, Au

Goals:

- Facility (ANKE) which allows to detect (rare) K^+-mesons in a huge (p, π^+) background
- Measure K^+-production far below the free NN-threshold @ $T_{NN} = 1.58$ GeV
- Double differential cross sections down to $T = 1.0$ GeV
- Reaction mechanisms (e.g. multi-step K^+-production) or high-momentum components of the NWF?

How to extract the K^+ cross sections

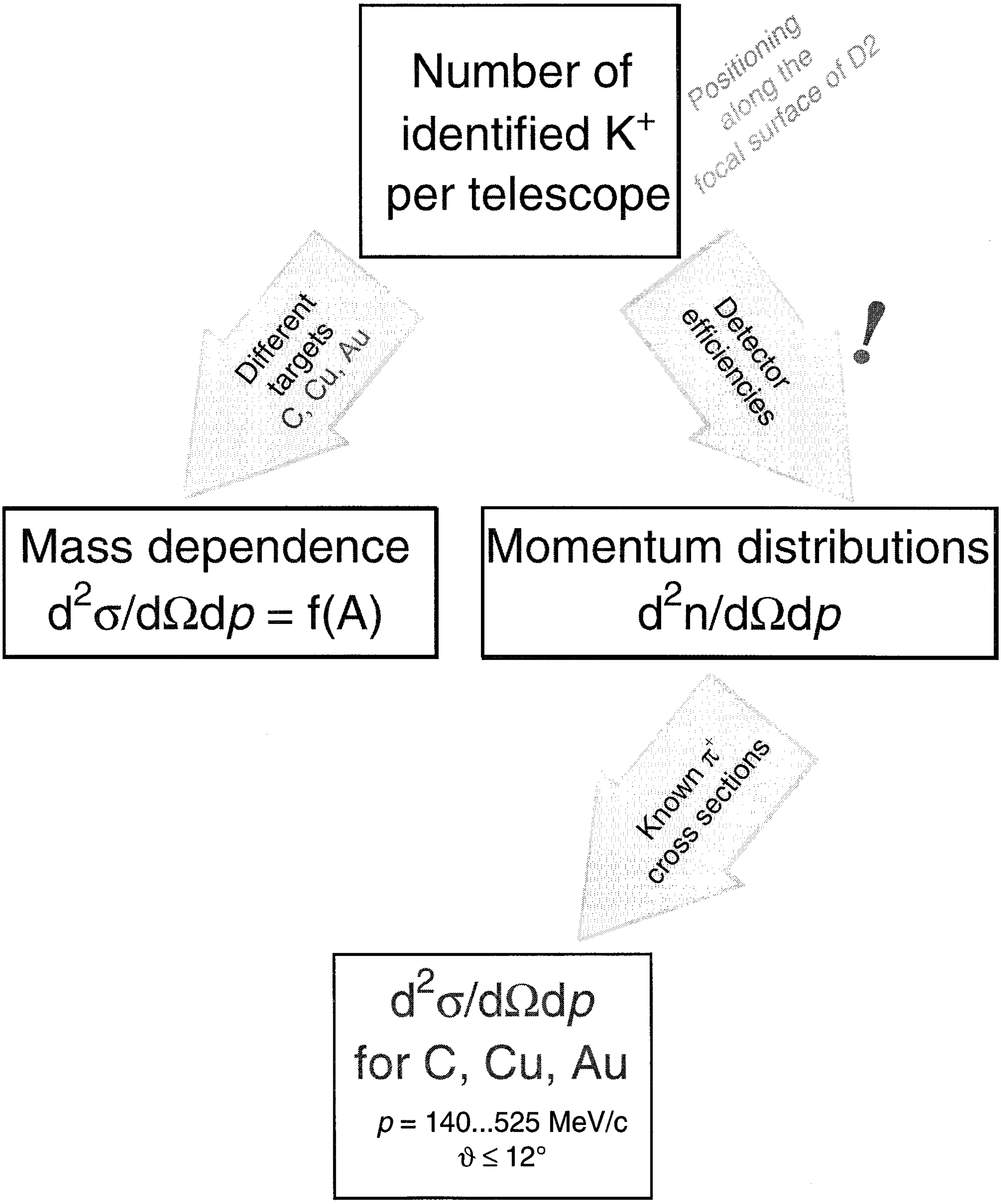

Number of identified K^+ per telescope

Positioning along the focal surface of D2

Different targets C, Cu, Au

Detector efficiencies

!

Mass dependence $d^2\sigma/d\Omega dp = f(A)$

Momentum distributions $d^2n/d\Omega dp$

Known π^+ cross sections

$d^2\sigma/d\Omega dp$

for C, Cu, Au

$p = 140...525$ MeV/c

$\vartheta \leq 12°$

ANKE Spectrometer

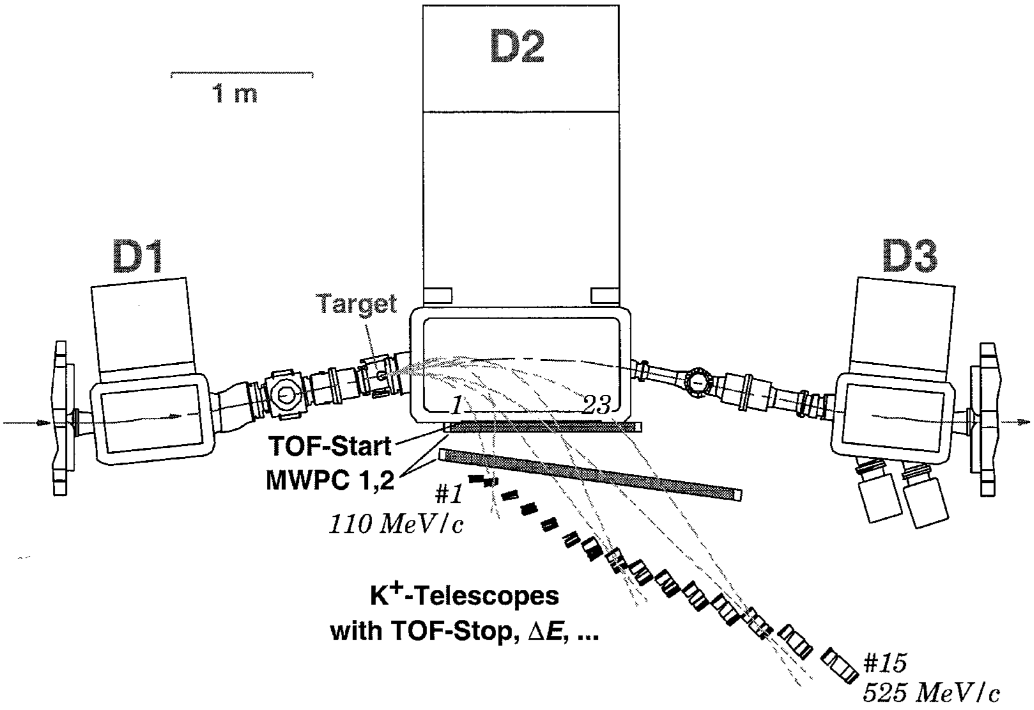

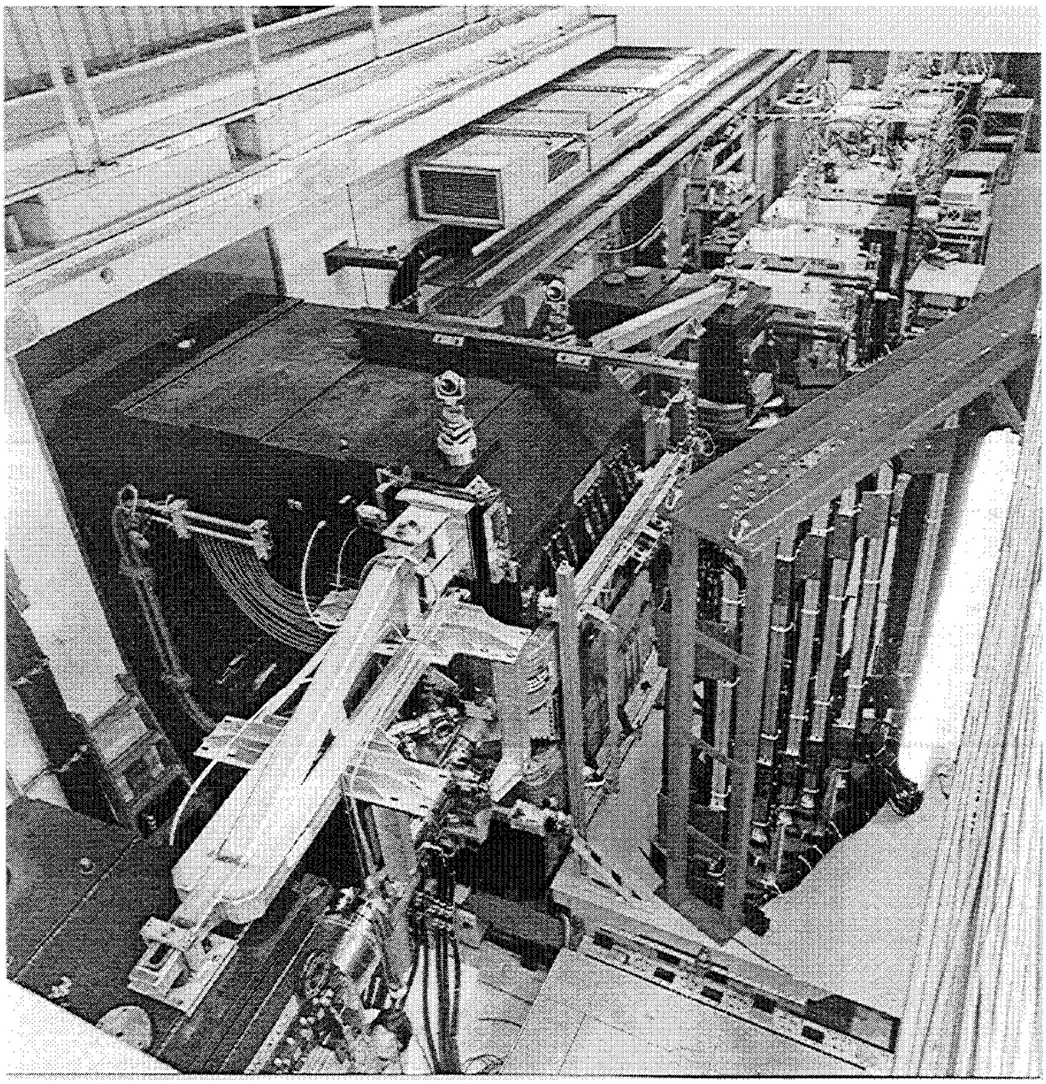

K^+ identification: TOF

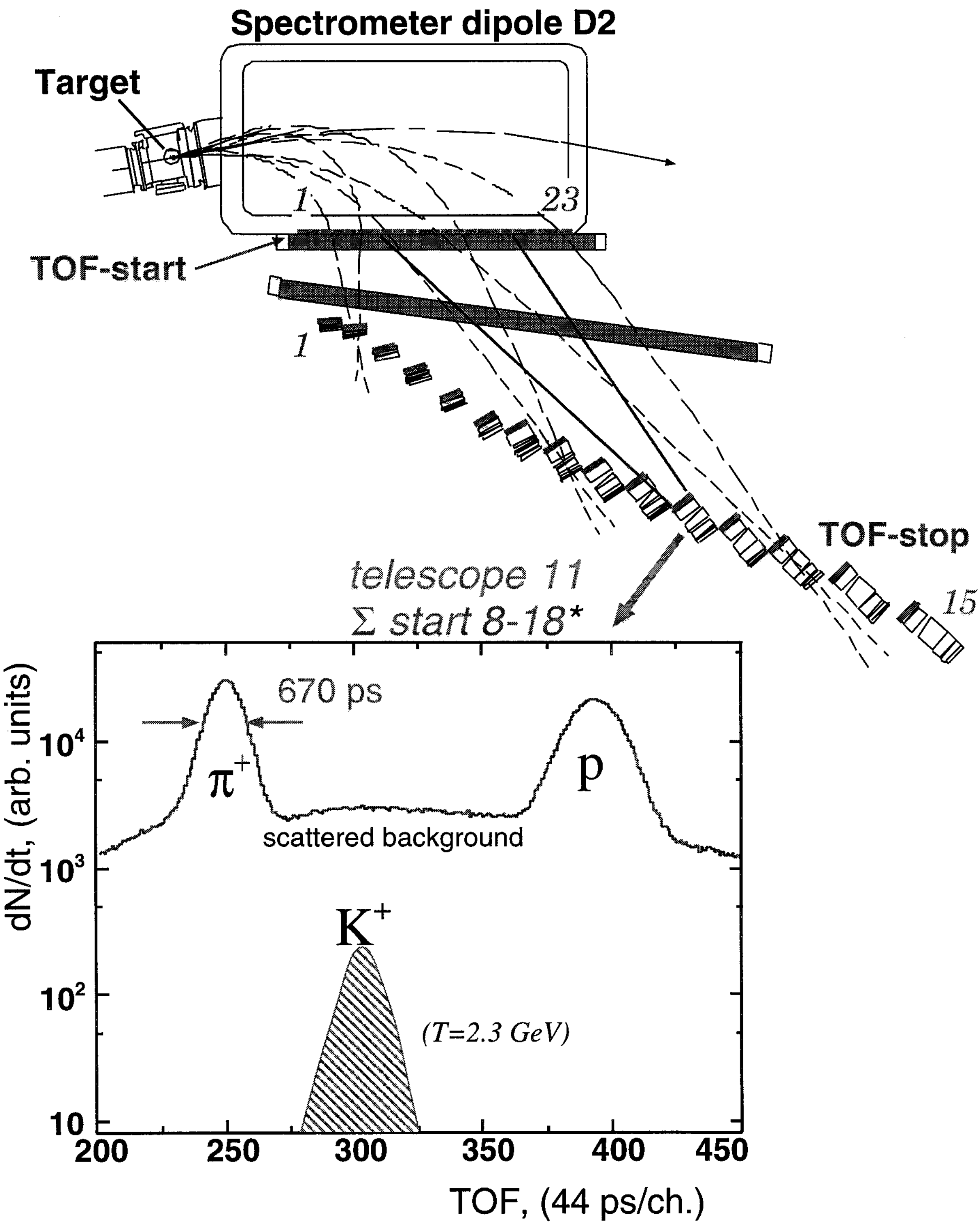

* Selection of valid start-stop combinations by fast on-line trigger

K^+ *identification: MWPC's*

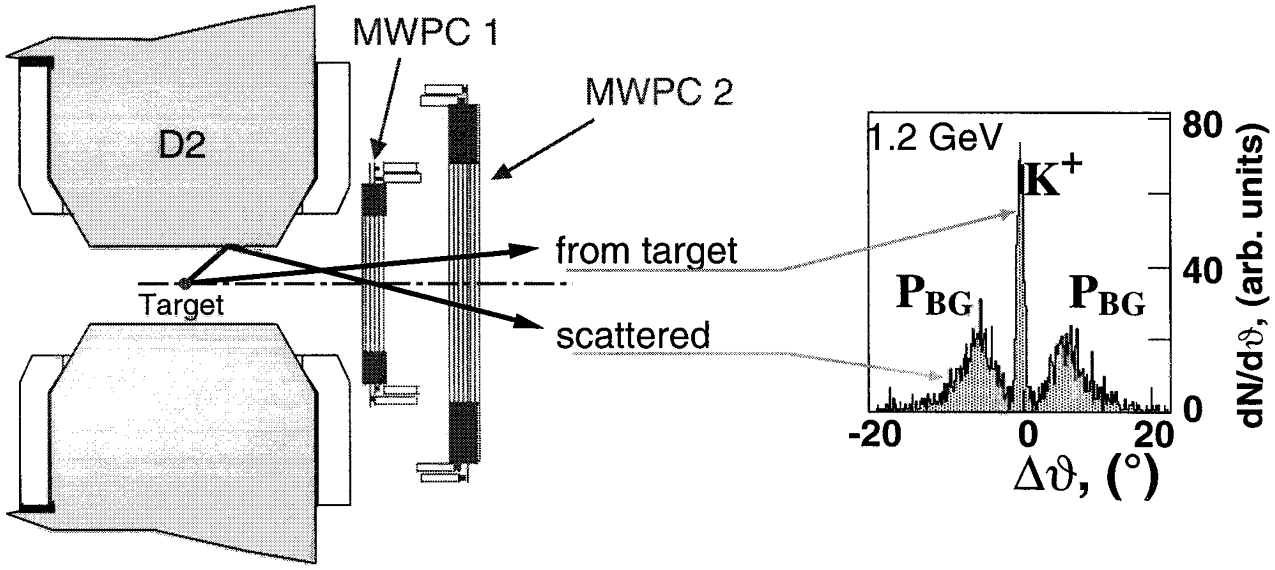

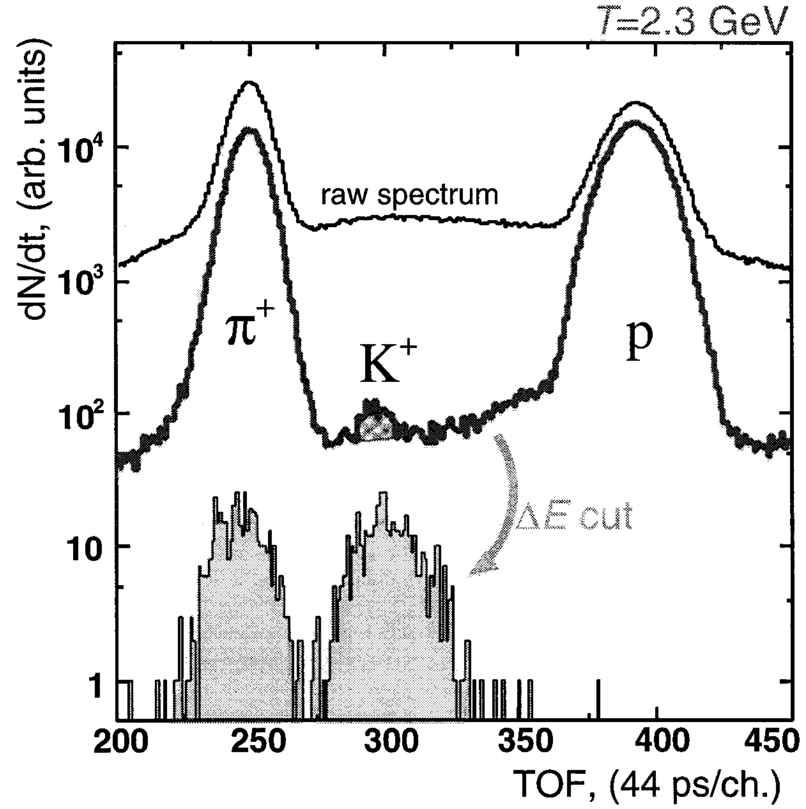

K^+ *identification:*

Range telescopes

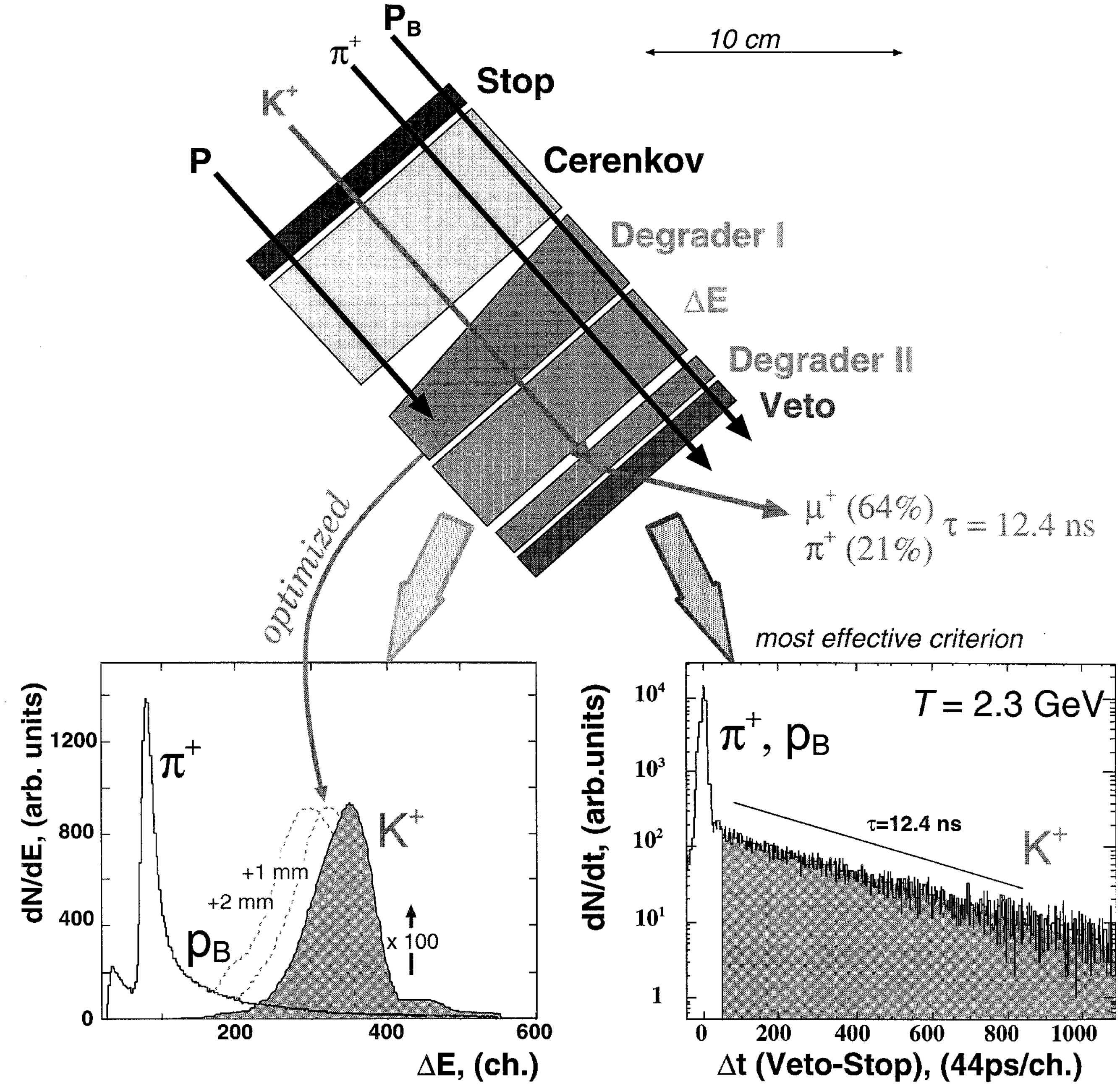

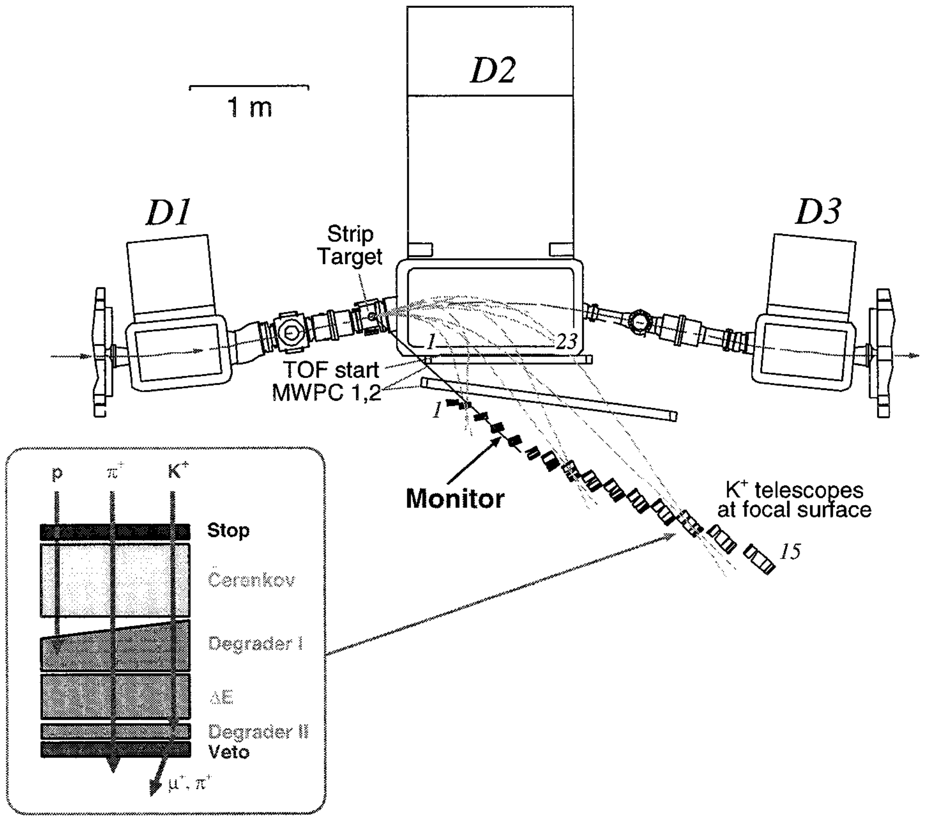

Kaon selection criteria:

	ε_K	background reduction
TOF(start − stop) = ±0.65ns	0.98 − 0.99	20
Vertical angle smearing = ±1.5°		40
Energy losses in start and stop		2
Energy losses in ΔE − counters	0.5 − 0.7	6 − 10
Kaon decay products in veto: delay > 2.5ns	0.2 − 0.3	> 1000

Relative monitoring ± 2%

Normalization to $pA \to \pi^+ \ldots$ (±10%):

$$\frac{\mathrm{d}^2\sigma_\mathrm{K}}{\mathrm{d}\Omega\mathrm{d}p} = \frac{\mathrm{d}^2\sigma_\pi}{\mathrm{d}\Omega\mathrm{d}p} \cdot \frac{\varepsilon^\pi_\mathrm{decay}}{\varepsilon^\mathrm{K}_\mathrm{decay}} \cdot \frac{N_\mathrm{K}}{N_\pi} \cdot \frac{M_\pi}{M_\mathrm{K}} \cdot \frac{\varepsilon_\pi}{\varepsilon_K}$$

Calibration of the telescopes *(T=2.3 GeV)*

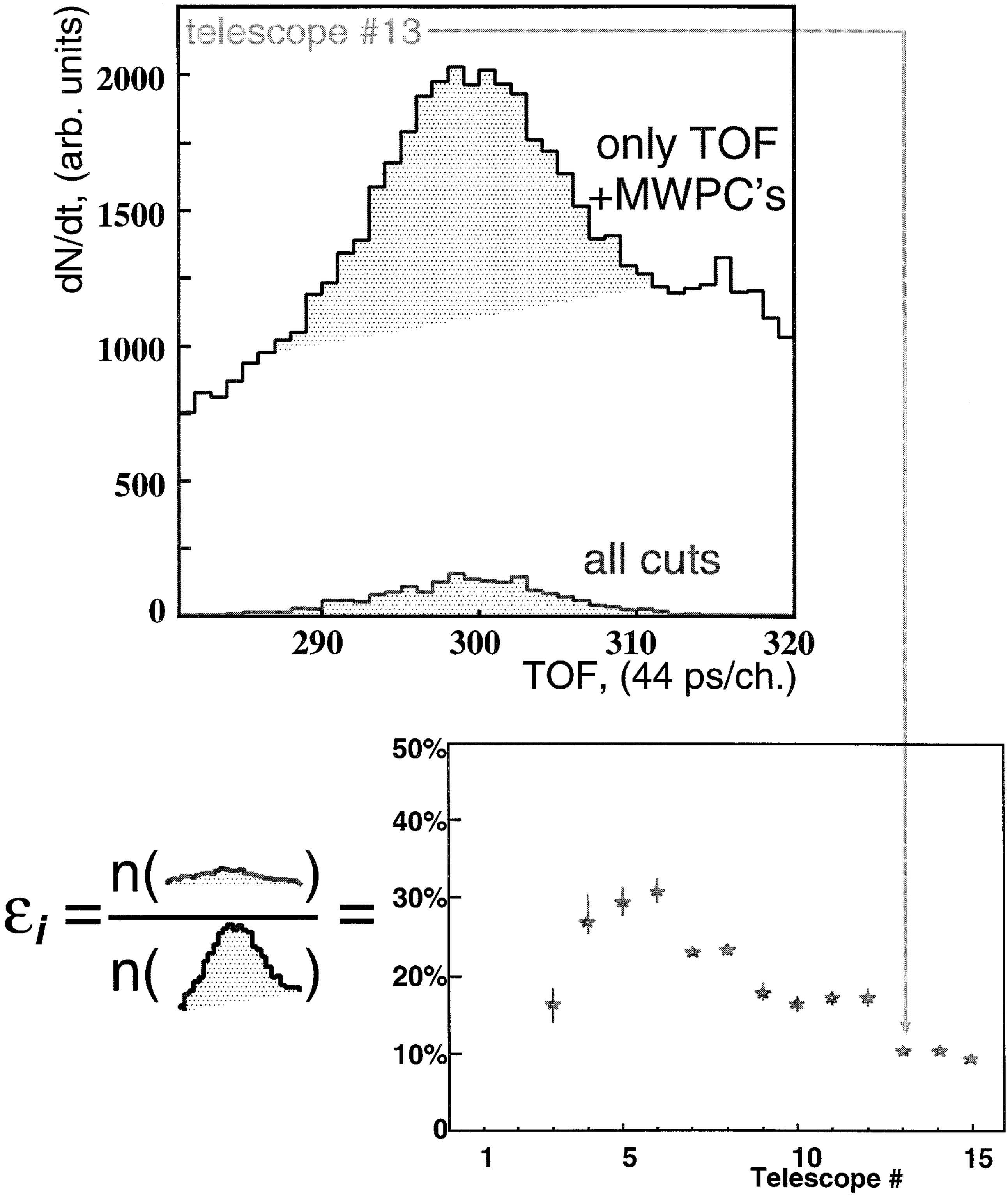

K^+-production cross sections

$pC \rightarrow K^+ X, \quad \vartheta_K < 12°$

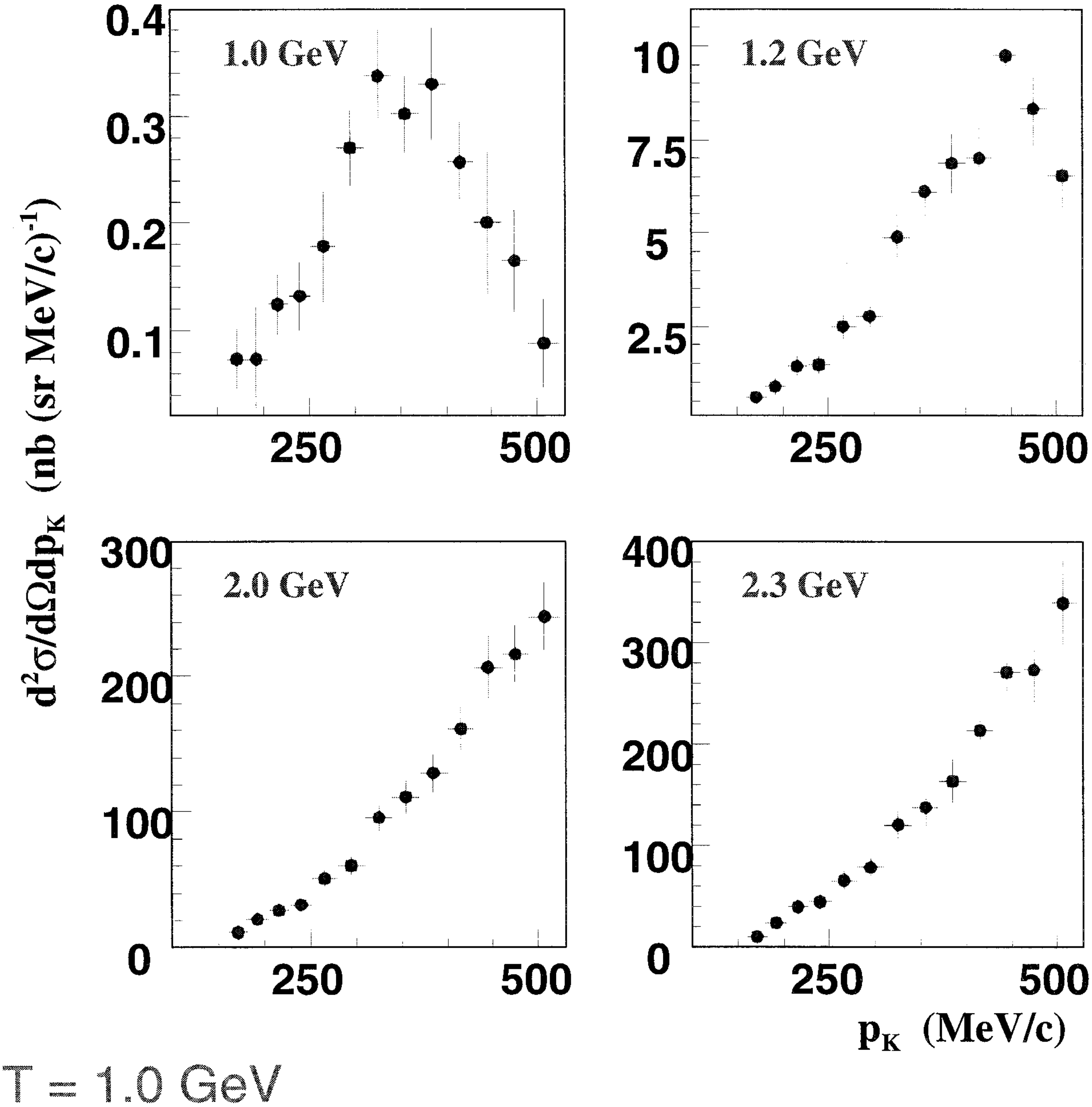

- T = 1.0 GeV

  First differential spectra, 'full' momentum coverage

- T ≥ 1.2 GeV

  Measurements up to p_k ~ 1000 MeV/c in fall 2001

K^+-production: comparison with other data

Kaons with 500 MeV/c

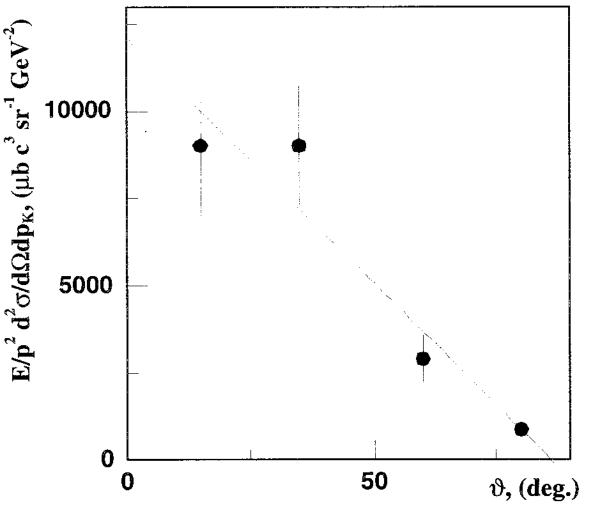

Schnetzer et al., p(2.1 GeV) Pb → K^+ X

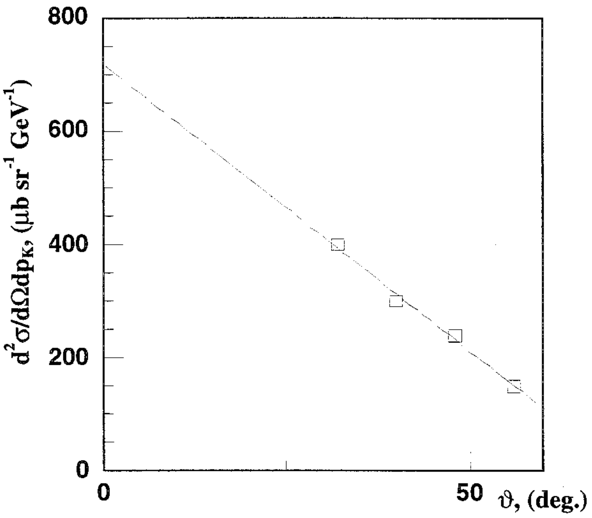

KAOS, p(3.5 GeV) C → K^+ X

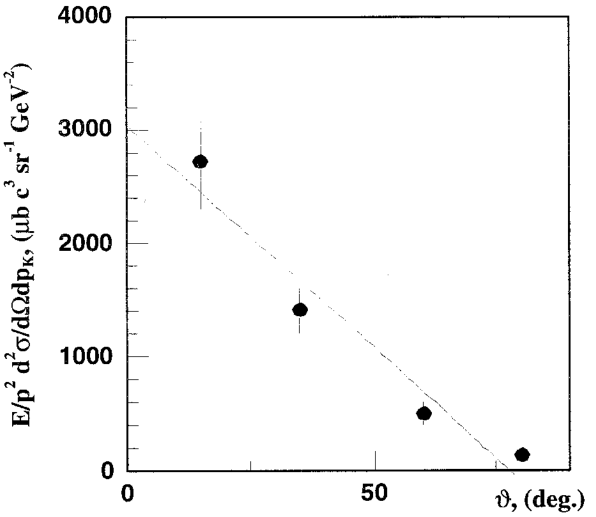

Schnetzer et al., p(2.1 GeV) NaF → K^+ X

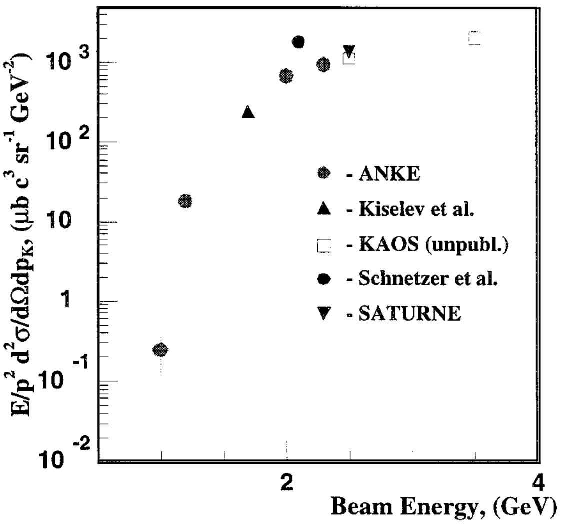

Energy dependence, pC → K^+ X, ϑ=0°

$d^2\sigma / d\Omega dp\ (K^+)$

N = number of identified K^+/π^+

$$\frac{d^2\sigma}{d\Omega dp}(K^+) = \underset{\text{known}}{\frac{d^2\sigma}{d\Omega dp}(\pi^+)} \cdot \underset{\text{detektor efficiencies}}{\frac{\varepsilon_\pi}{\varepsilon_K}} \underset{\text{decay in flight}}{\frac{(1-w_{\pi\to\dots})}{(1-w_{K\to\dots})}} \underset{\text{luminosities}}{\frac{L_\pi}{L_K}} \quad \frac{N_K}{N_\pi}$$

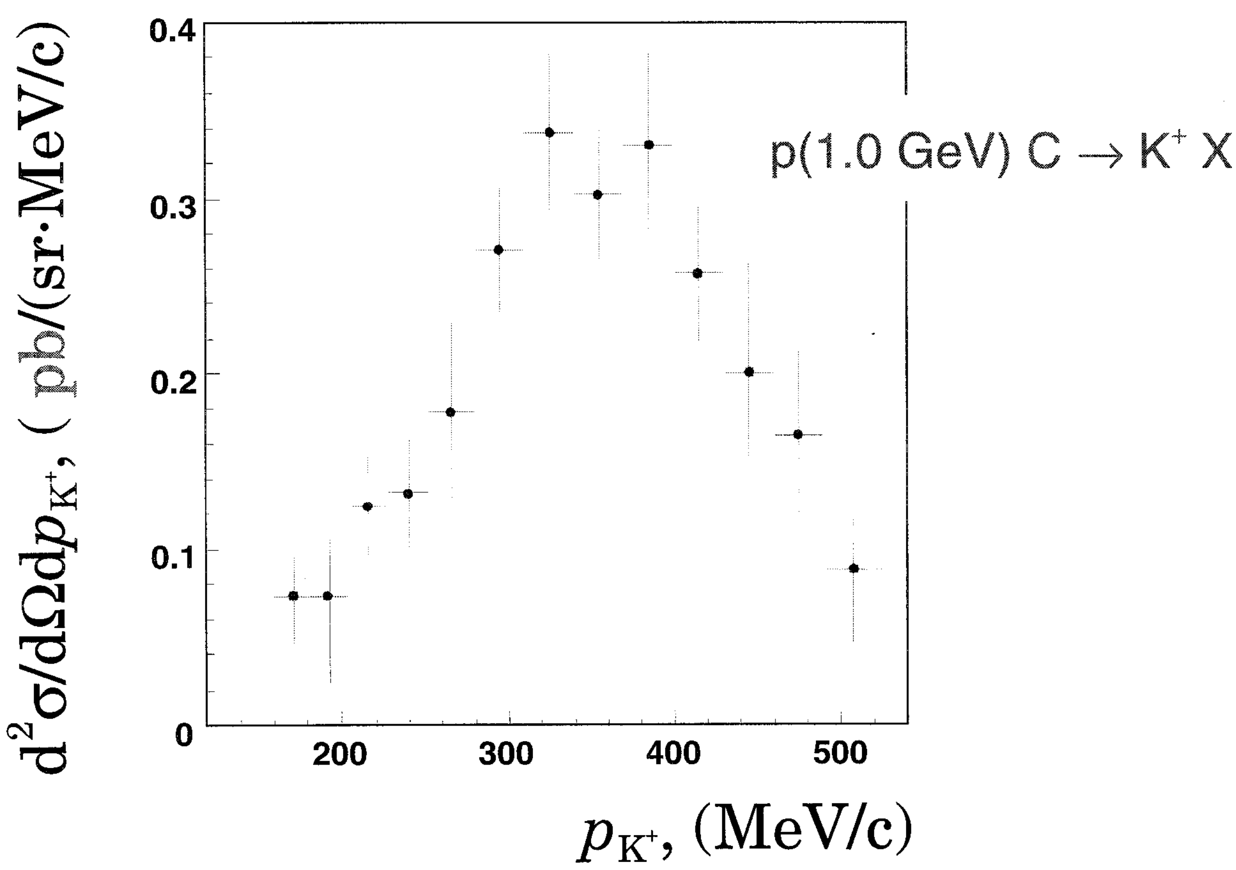

- *Full momentum spektra!*
- *Target mass: A=12...197*
- *Beam energy: T=1.0...2.3 GeV*

Model calculations !?

K^+-production - theoretical interpretation

- Different approaches:
    H.Müller (FZ Rossendorf): ROC model
    (Improvement after including high momentum components)
    W.Cassing (Giessen), Z.Rudy (Cracow): CBUU model
    J.Aichelin (SUBATEC Nantes): IQMD model
    A.Sibirtsev (FZ Jülich): Folding model
    E.Ya.Paryev (INR Moscow): Folding model

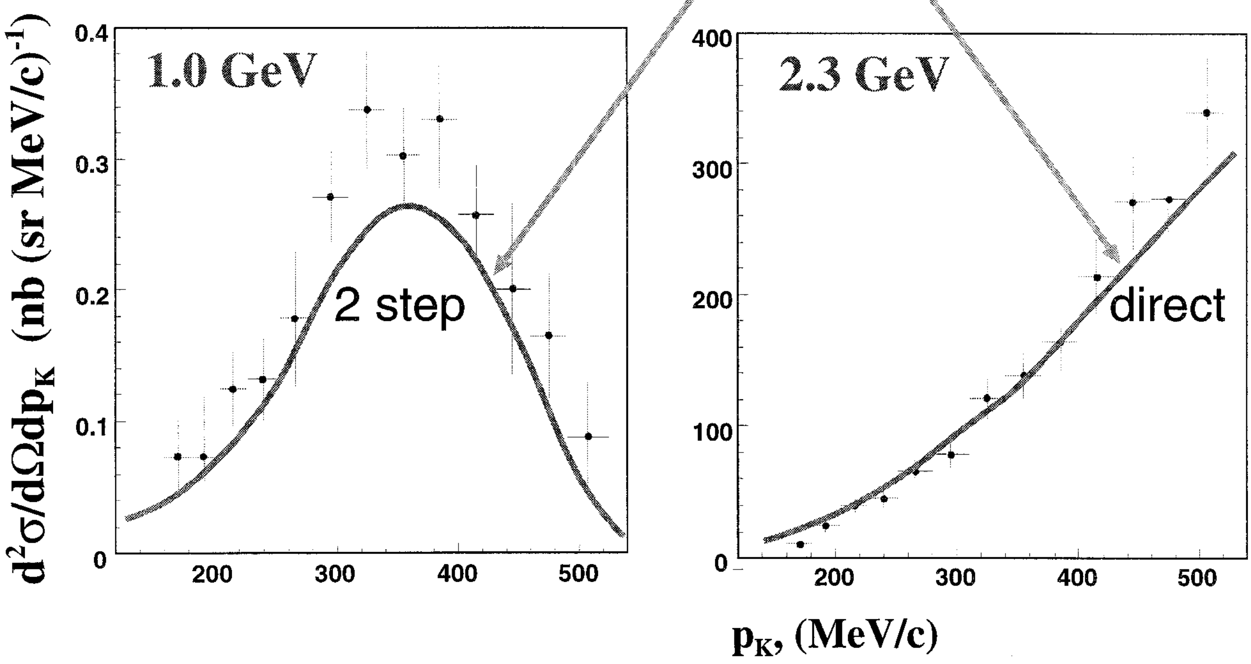

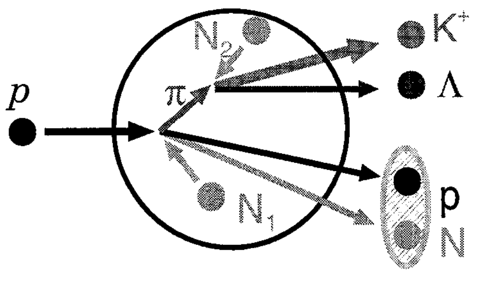

2 step → $\sigma \propto A$

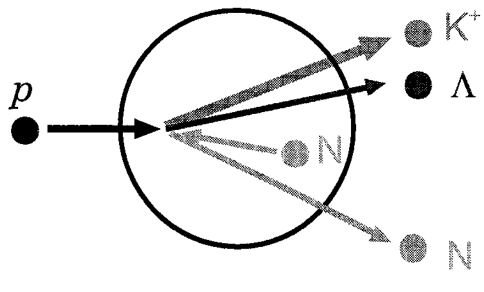

Direct → $\sigma \propto A^{2/3}$

K^+-production: target-mass dependence

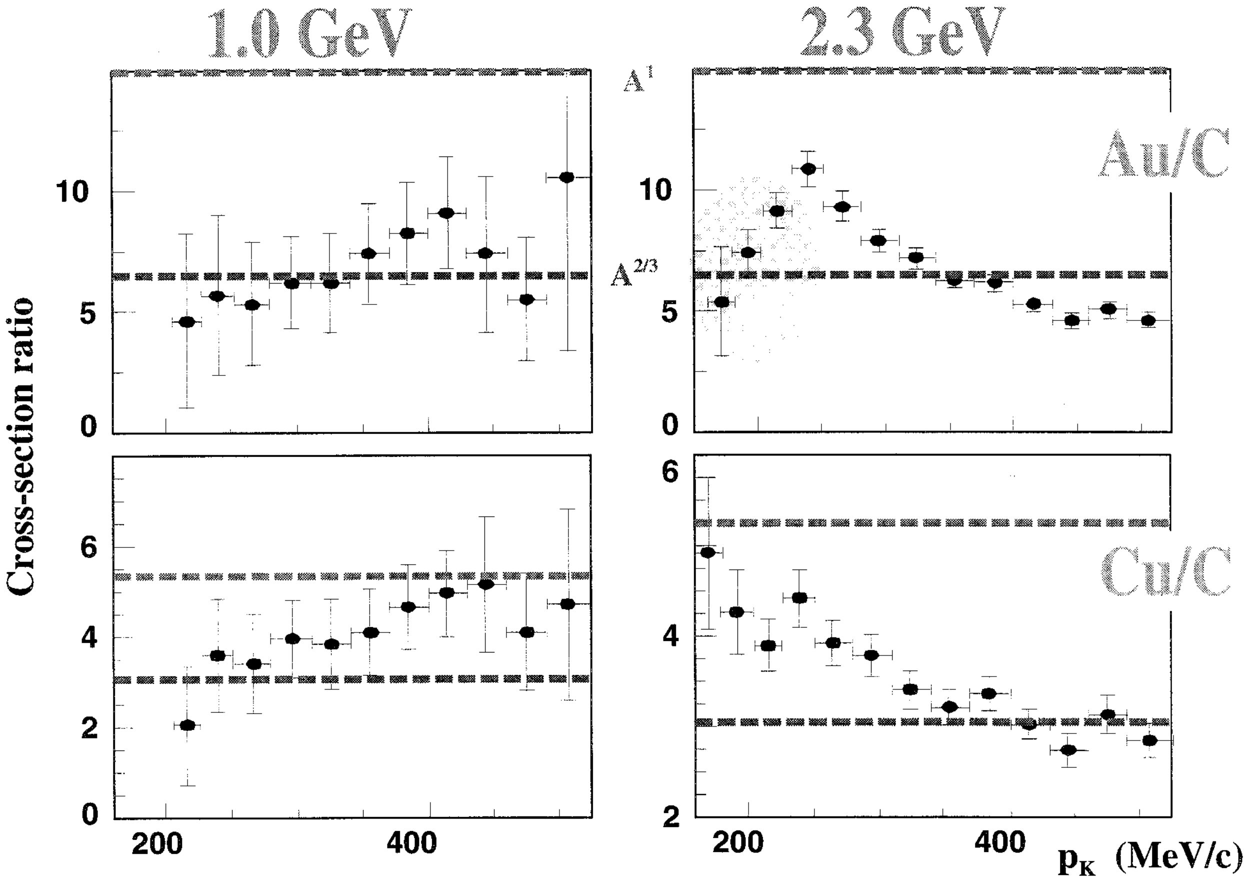

A-dependence cannot be explained in this simple picture:

2 step → $\sigma \propto A$

Direct → $\sigma \propto A^{2/3}$

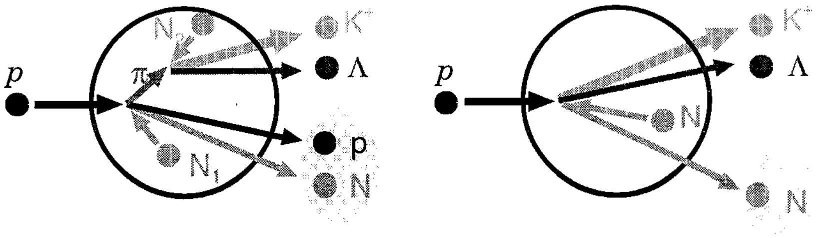

→ **More data in fall 2001**

- **Measurements with heavy targets**
- **K^+p, K^+d coincidences**

Set-up in 2001

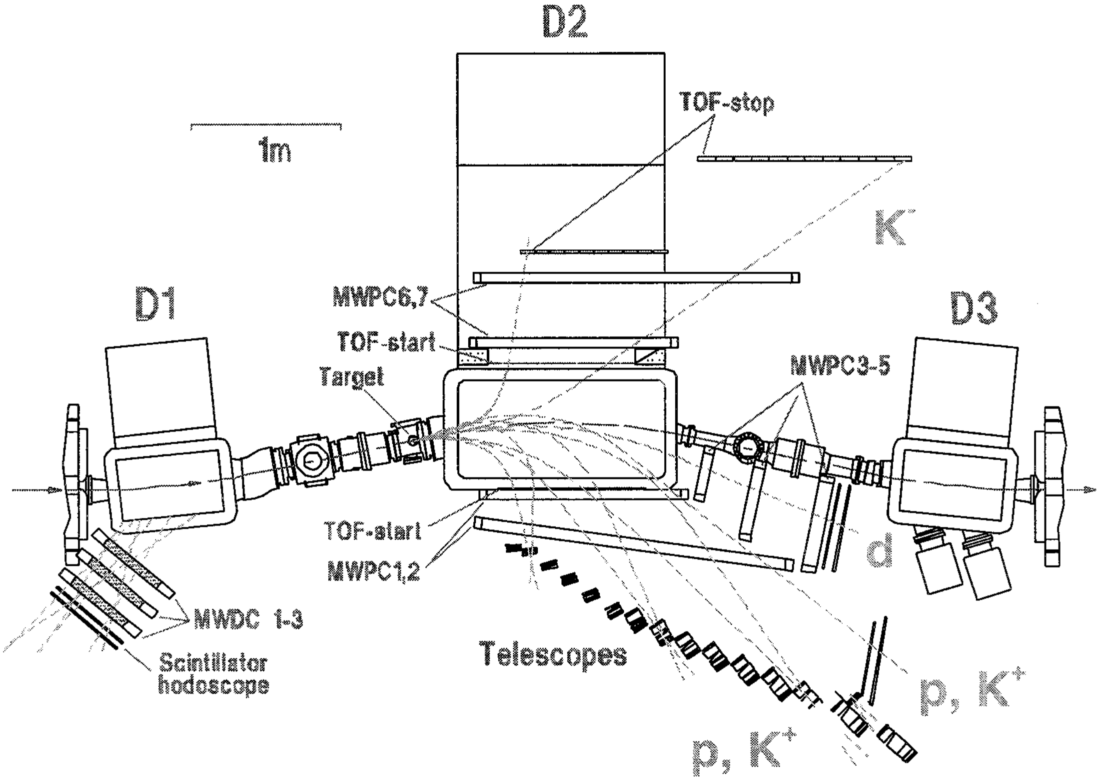

Deuteron identification

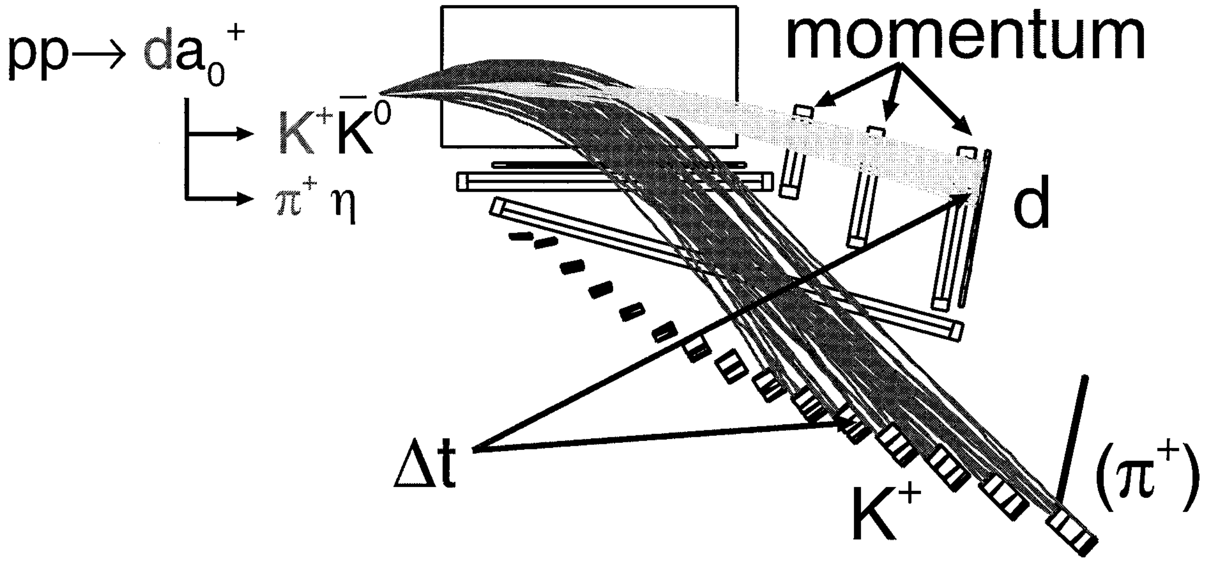

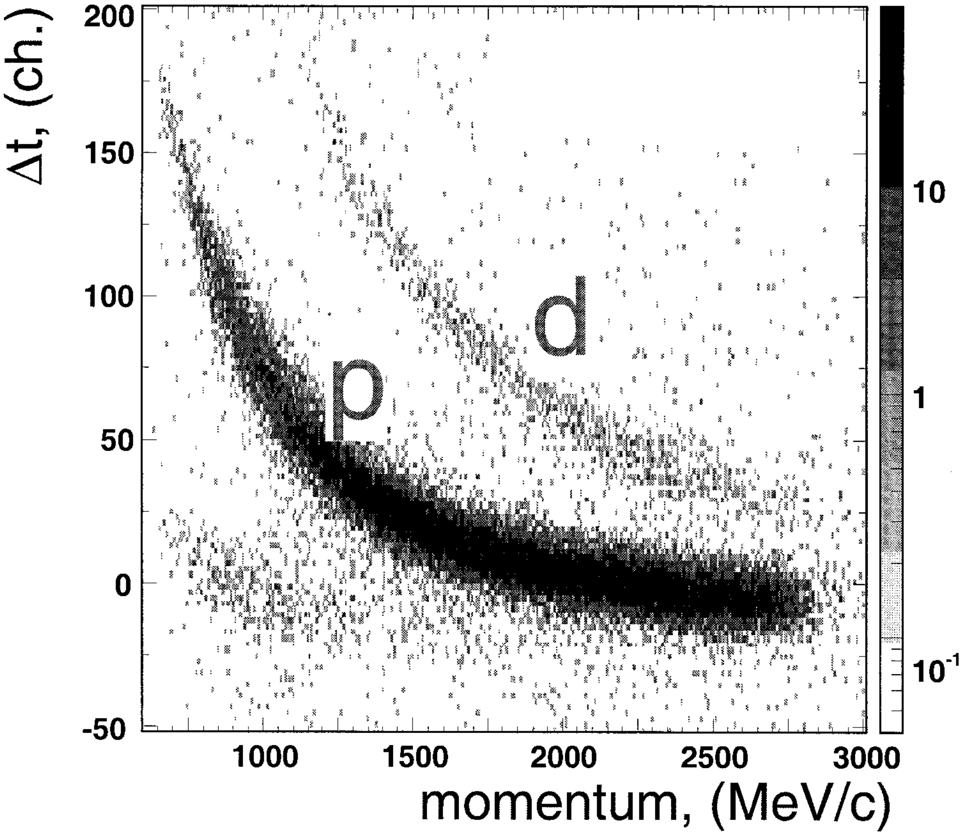

→ unambiguous identification of
$pp \rightarrow dK^+(\pi^+)\,X$ events

$p(2.65\ \text{GeV})p \rightarrow pK^+ X$

- 'By product' of a_0^+ beam time
- Data allow to determine Λ/Σ ratio
- Higher resonances visible?

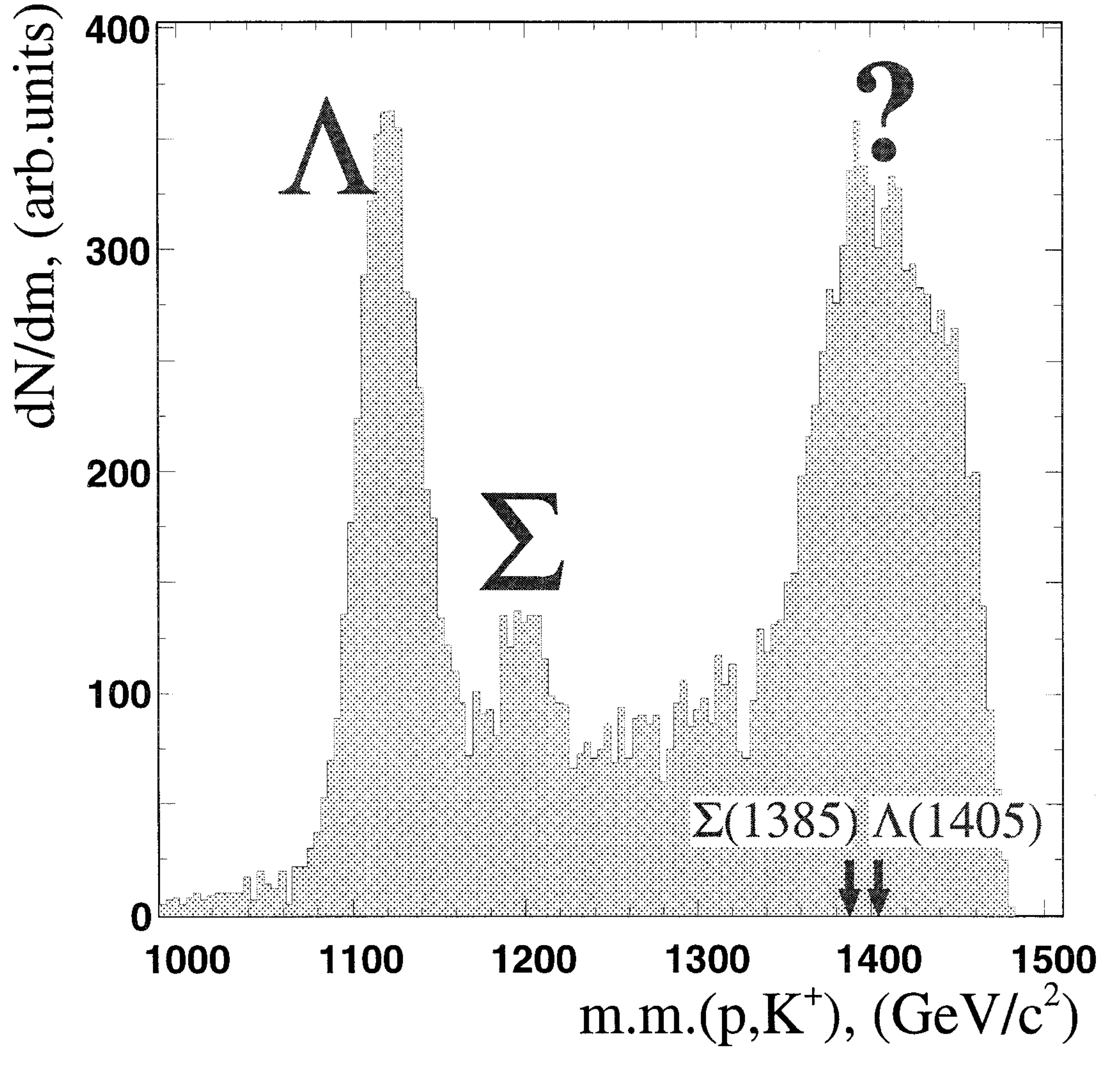

- Data of comparable quality for $pn \rightarrow nK^+ \Lambda/\Sigma$ are expected next year

Summary

- Double differential cross sections at *T* = 1.0 ... 2.3 GeV
- Measurements with C, Cu, Au targets
  -> mass dependence of the cross sections
- Comparison with diferent models is started
- A possibility of the correlation experiment is proved
  -> direct measurement of 1-step and 2-step mechanism contributions

K^+ production: Systematics of existing data

M.Büscher, A.Sibirtsev

Institut für Kernphysik
Forschungzentrum Jülich
52425 Jülich
Germany

One of the most important problems in experimental study of interactions of hadrons with nuclei has been the questions how this interaction proceeds with formation of particles in the nucleus and to what extend this process differs from the interaction between the hadron and a free nucleon.

The measure of this difference is given by the target-mass (A)-dependence of the particle production. It is expected that the A-dependence in hadron-nucleus interactions is dominated by the production mechanism. Such expectations indeed stimulate detailed studies of the A-dependence at different beam energies and for different projectiles and produced particles.

There is now a large set of experimental data on the A-dependence, mostly at incident proton energies above 12 GeV. It is well known that experimental results on differential cross sections can be well described as

$$\frac{d^2\sigma}{dTd\omega} \propto A^{\alpha}, \tag{1}$$

where the exponent α ranges from 0.3 to 0.7 depending on the projectile particle and its kinetic energy.

In this study we report on a systematical analysis of the A-dependence of K^+-meson production in proton-nucleus collisions at beam energies below 3 GeV.

In the second part of this work, the existing data on K^+ production are analyzed as a function of the four-momentum transfer t between the beam proton and the produced kaon. It is shown that at negative values of t all data scale like exp $(const. \cdot t)$ as suggested by Regge phenomenology. Only the spectra obtained at ANKE cover the region of positive t and the invariant cross section strongly decrease when approaching the kinematical limit at $t \sim 0.14$ GeV^2, corresponding to the formation of Λ-Hypernuclei.

Phenomenological analysis of K^+-meson production in proton-nucleus collisions

Target-mass dependence

- The target mass dependence for K^+-meson production can be factorized in terms of the A-dependence of the production process and A-dependence of the K^+ propagation in nuclei
- Due to the strangeness conservation K^+-mesons are not absorbed in nuclear matter
- Because of the large mean free path $\lambda \simeq 5$ fm the elastic scatterings of kaons are almost negligible
- Therefore K^+-mesons are almost not distorted in nuclear matter
- The A-dependence for K^+-meson production is given by the kaon production mechanism.
- However, there are no results from a systematical analysis of the target mass dependence of K^+-meson production in $p{+}A$ collisions

Systematical analysis of the A-dependence of K^+ meson production in p+A collisions.

- Let us to describe the data on the total or differential K^+-meson production cross section as

$$\frac{d^2\sigma}{dp_K d\Omega_K} = const \times A^{\alpha}, \tag{1}$$

- and to evaluate the slope α as a function of the beam energy T_p, kaon momentum p_K and kaon production angle θ_K.
- Obviously, the function

$$\alpha(T_p, p_K, \theta_K) \tag{2}$$

contains information about the K^+-meson production mechanism, which might be different at beam energies above and below T_p=1.58 GeV given as a threshold for kaon production in p+N→$N + \Lambda$+K^+ reaction in free space.

PNPI data

V.P. Koptev et al., JETP **67**, (1988) 2177.

Total K^+-meson production cross sections in proton-nucleus collisions at beam energies $0.842 \leq T_p \leq 0.99$ for Be, C, Cu, Sn and Pb target was measured at the Petersburg Nuclear Physics Institute.

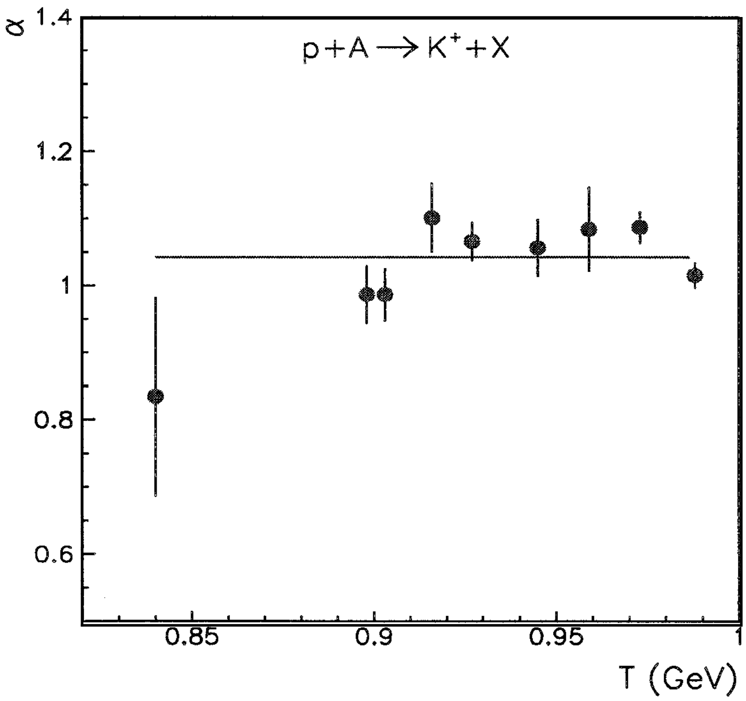

The dependence of the slope α on the beam energy T_p evaluated from the PNPI data. The solid line indicates the fit by α=1.04±0.01.

LBL data

S. Schnetzer et al., Phys. Rev. C **40**, (1989) 640.

K^+-meson production at emission angles θ_K=15^0, 35^0, 60^0 and 80^0 induced by 2.1 GeV protons on NaF and Pb has been studied at Lawrence Berkeley Laboratory.

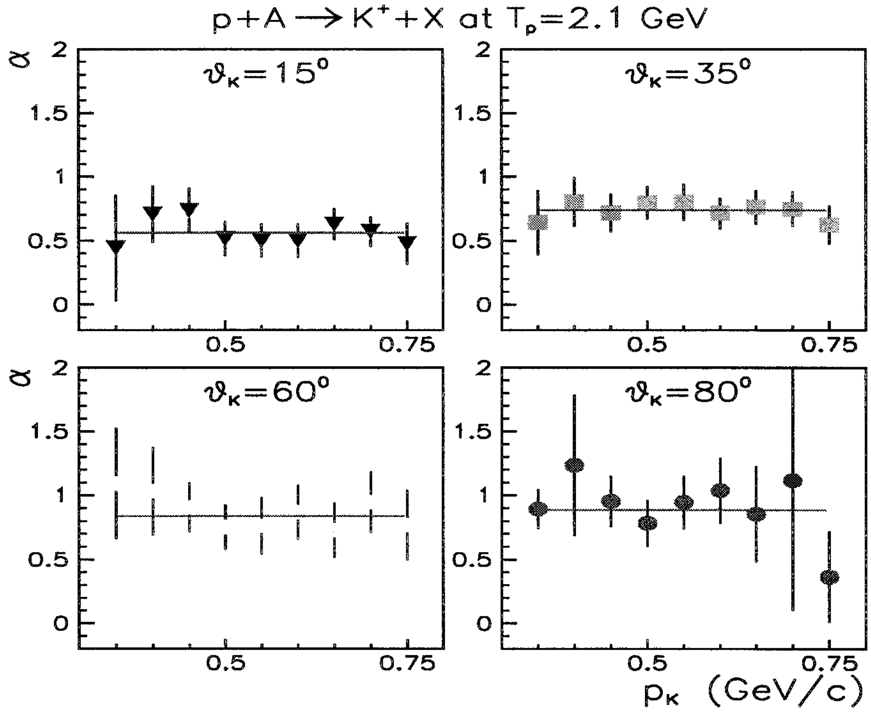

The slope α as a function of laboratory K^+-meson momentum evaluated from the LBL data. The solid lines shows the fit by a constant values α

θ_K=15^o, α=0.56±0.05; θ_K=35^o, α=0.74±0.05

θ_K=60^o, α=0.84±0.08; θ_K=80^o, α=0.88 ± 0.08

SATURNE data

M. Debowski et al., Z. Phys. A **356**, (1996) 313.

Double differential cross sections for K^+-meson production in $p+C$ collisions at T_p=1.2, 1.5 and 2.5 GeV and in $p+Pb$ collisions at T_p=1.2 and 1.5 GeV at the production angle $\theta_K=40^0$ have been measured at SATURNE.

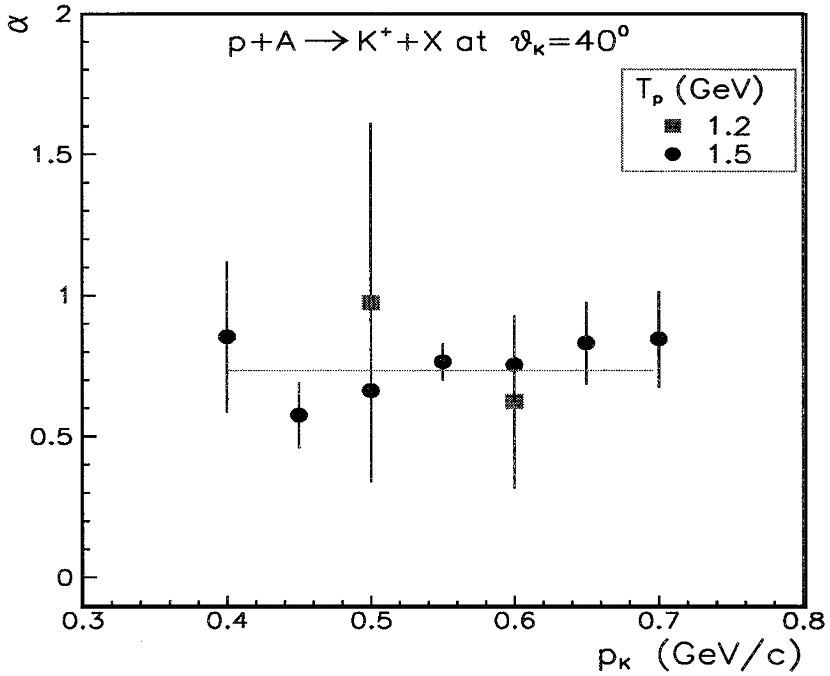

The dependence of the slope α on the K^+-meson momentum p_K evaluated from the SATURNE data. The different symbols corresponds to different beam energies T_p. The solid line shows the fit by $\alpha=0.73\pm0.04$.

ITEP data

A.V. Akindinov et al., JETP Lett. **72**, (2000) 100.

The production of K^+-meson with a momentum of p_K=1.28 GeV/c at an angle θ_K=10.5^o in proton-nucleus collisions for *Be*, *Al*, *Cu* and *Ta* targets at proton beam energies 1.65$\leq T_p \leq$2.91 GeV were measured at the Institute of Experimental and Theoretical Physics.

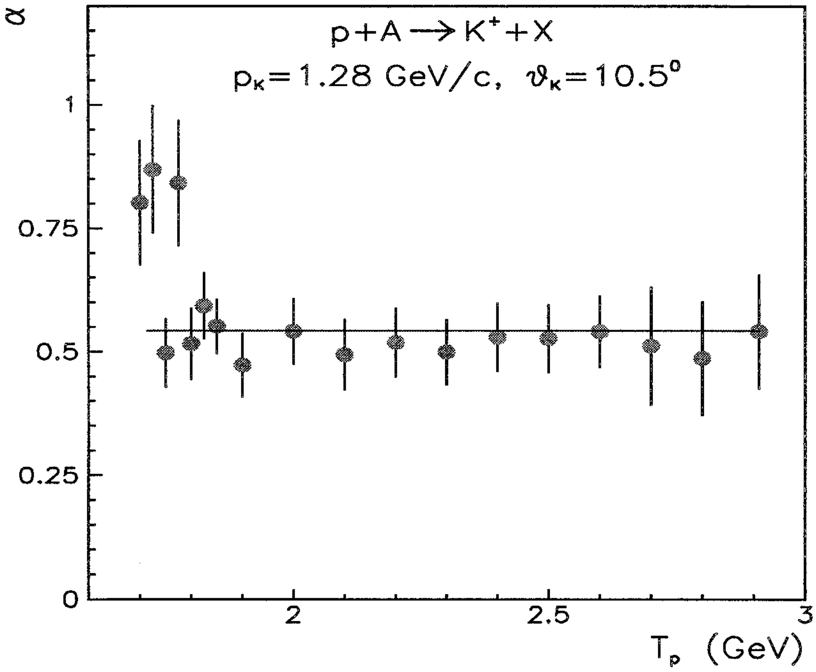

The slope α as a function of the proton beam energy T_p evaluated from the ITEP data. The line shows the fit by a constant value α=0.54±0.02.

ANKE-COSY data

The double differential cross section of K^+-meson production at emission angles $0 \leq \theta_K \leq 12^o$ induced by T_p=1 GeV protons on C, Cu and Au targets has been recently studied by ANKE at COSY.

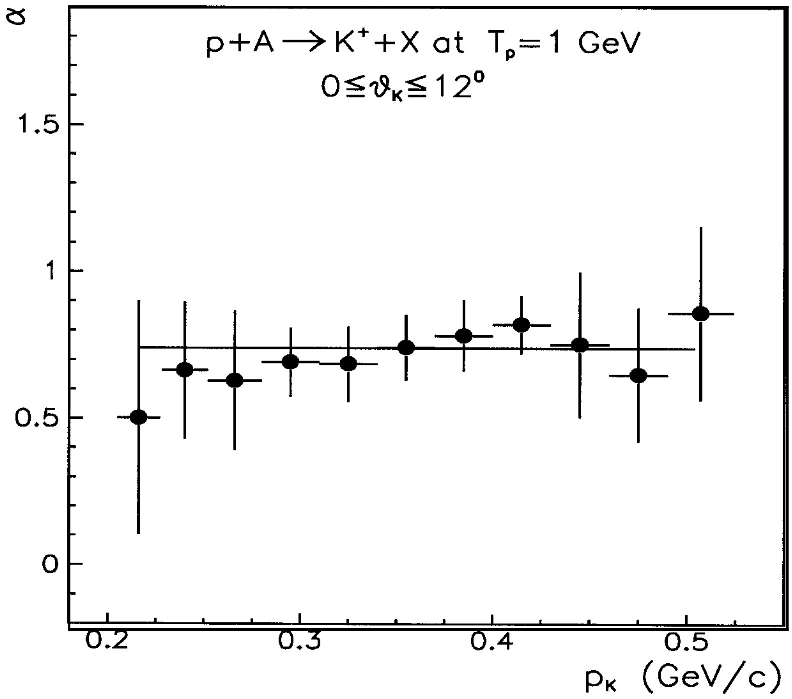

The dependence of the slope α on the K^+-meson momentum p_K evaluated from the ANKE-COSY data. The solid line shows the fit by constant value α=0.74±0.07.

Final results

T_p (GeV)	p_K (GeV/c)	θ_K (deg.)	α	Ref.
0.842–0.99	*total*	*total*	1.04±0.01	PNPI
2.1	0.35–0.75	15	0.56±0.05	LBL
2.1	0.35–0.75	35	0.74±0.05	LBL
2.1	0.35–0.75	60	0.84±0.08	LBL
2.1	0.35–0.75	80	0.88±0.08	LBL
1.2	0.5–0.7	40	0.69±0.3	SATURNE
1.5	0.5–0.7	40	0.73±0.04	SATURNE
1.7–2.91	1.28	10.5	0.54±0.02	ITEP
1.0	0.171–0.507	0–12	0.74±0.075	COSY

- The data on K^+-meson production available at $1.2 \leq T_p \leq 2.9$ GeV can be reasonably described by an A^α dependence with α varying between 0.54±0.02 and 0.88±0.08, providing an average value $< \alpha >=$ 0.71±0.08
- The ANKE data indicate α=0.74±0.05 at proton beam energy T_p=1.0 GeV.
- There is overall disagreement with PNPI data, which , however, were collected at $0.842 \leq T_p \leq 0.99$ GeV and integrated over available K^+-meson momenta p_K and emission angles θ_K.

A-dependence for direct $p{+}N{\rightarrow}Y{+}N{+}K^+$ process

In leading order, the A dependence for direct kaon production in collisions of the beam proton with a single target nucleon is given by the inelasticity of the $p{+}A$ interaction. This also holds for the production of others mesons, since the summation over all possible mesonic inelastic $p{+}A$ reaction channels is proportional to the total inelastic $p{+}A$ cross section.

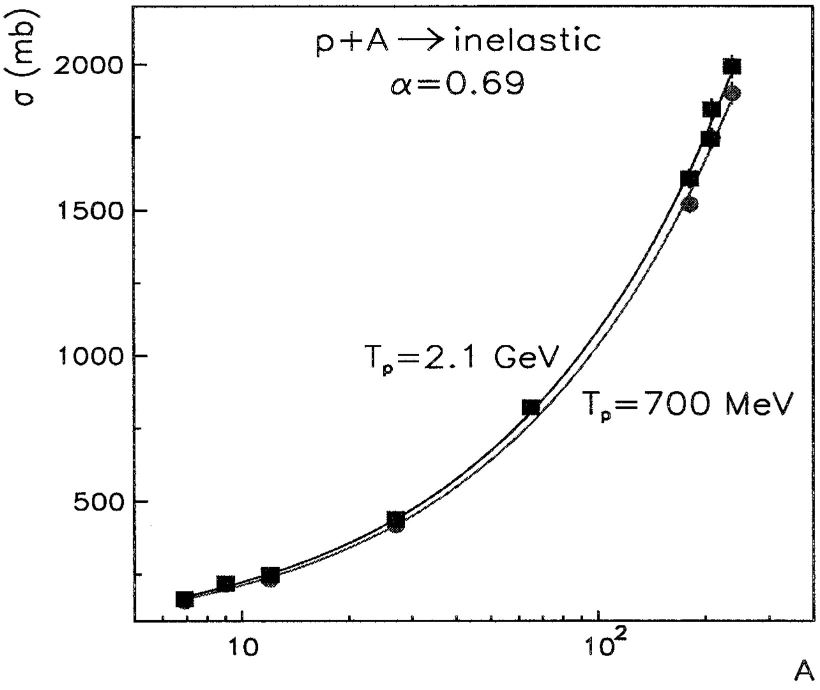

The A-dependence of $p{+}A$ inelastic cross sections. The solid line shows the fit by A^α with slope α=0.69±0.01.

Summary

- The PNPI data on total K^+-meson production cross section at proton beam energies T_p from 842 MeV to 990 MeV indicate strong $\simeq A^1$ dependence. Such dependence might be interpreted as a volume effect due to the interaction involving effectively all nucleons of the target. It can be the two-step reaction mechanism as well as others few or many body processes.
- The LBL, SATURNE and ITEP data on differential K^+-meson production cross section available at different kaon emission angles θ_K and kaon momenta p_K and at proton beam energies from 1.2 GeV to 2.91 GeV can be well described by an $\simeq A^{0.7}$ dependence. Similar dependence is expected from the direct K^+ production mechanism
- This discrepancy might be addressed to the different beam energies studied at PNPI from one side and LBL, SATURNE and ITEP experiments from other. To resolve this diadem the K^+-meson production in p+A collisions has been studied by ANKE at COSY.

However

- New ANKE measurements on K^+-meson production in $p+A$ collisions at T_p=1 GeV show an $\simeq A^{0.7}$ dependence.
- There is an additional reason for the observed discrepancy due to the different kinematics of the PNPI and ANKE measurements. PNPI experiment was devoted to the measurements on the total K^+-meson production cross section, while ANKE measured the forward kaon production at $0 \leq \theta_K \leq 12^0$. ANKE measurement corresponds to $\simeq$10% of the total kaon production cross section available from PNPI data.
- We may address the discrepancy to the strong variation of the A-dependence with the kaon emission angle at beam energies below 1 GeV.
- However, the available data on kaon production at $1.2 \leq T_p \leq 2.9$ GeV show weak dependence of the exponent α on the K^+-meson production angle θ_K.
- Furthermore, all available data indicate that A-dependence does not variate with the kaon momenta p_K.

K^+*-production: systematics of existing data*

Problem:
different data were obtained at
different kinematical conditions
(beam energies, K^+ emission angles, momenta)
→ how can they be compared???

Regge approach:

$$A(s, t, m_X^2) \propto f\,(t, m_X^2)\ \exp\{\ \gamma(t)\ \ln s\ \}$$

linear t dependence →

$$E\ d^3\sigma/d^3p \propto \exp(const.\ \cdot \underset{\uparrow}{t})$$

t = four-momentum transfer between beam proton and K^+*-meson*

K^+-production: systematics of existing data

Data:

Schnetzer et al., LBL; T = 2.1 GeV

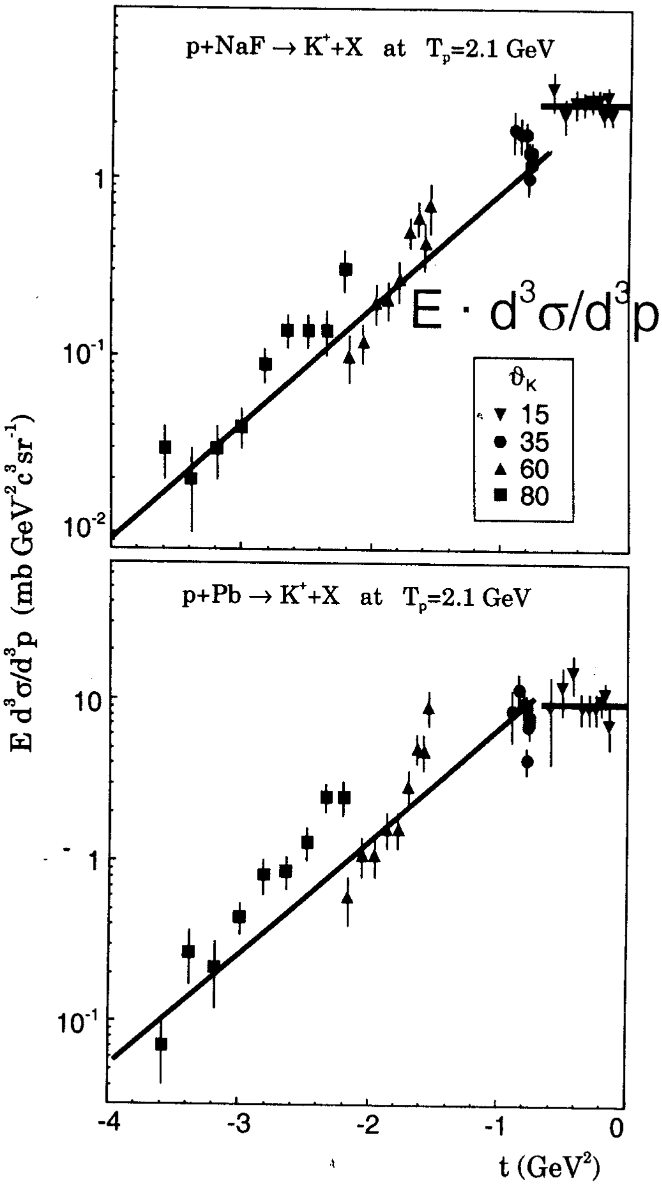

$$E \cdot d^3\sigma/d^3p = c_0 \cdot \exp(b_0 \cdot t)$$

$\Longrightarrow$ *Regge approach works at 'high' energies above threshold*

M.Büscher, 6/01

K^+-production: systematics of existing data

Data:

Debowski et al., SATURNE;
T = 1.2 ... 2.5 GeV

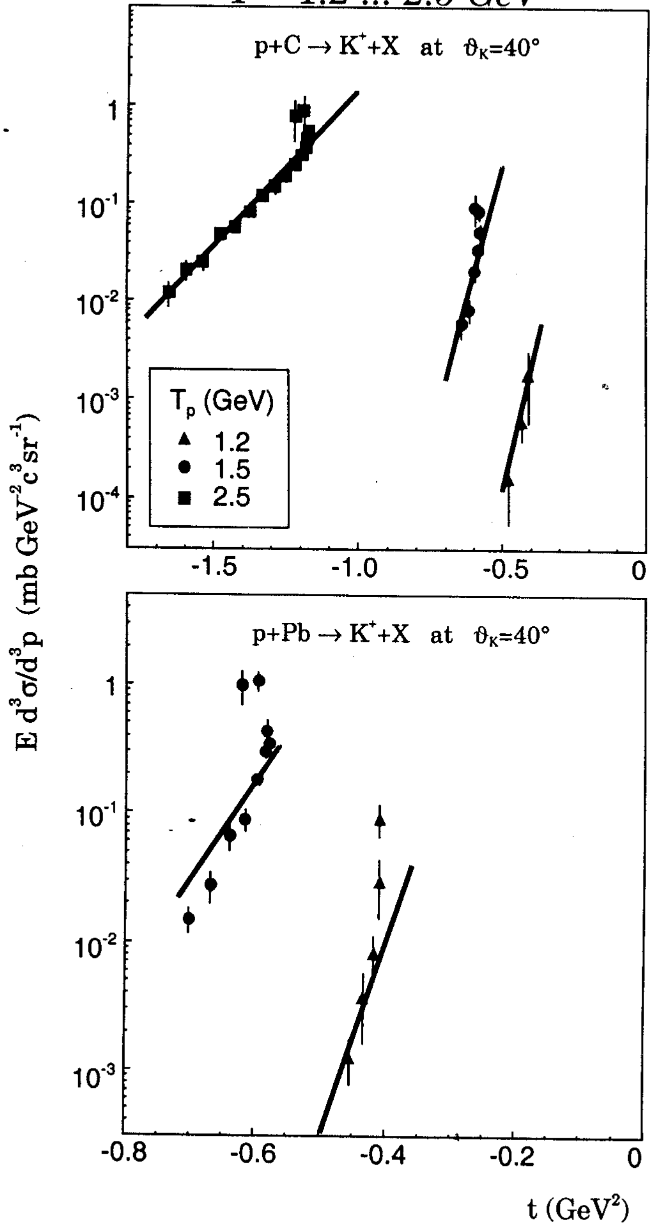

Badala et al., CELSIUS;
T = 1.2 GeV

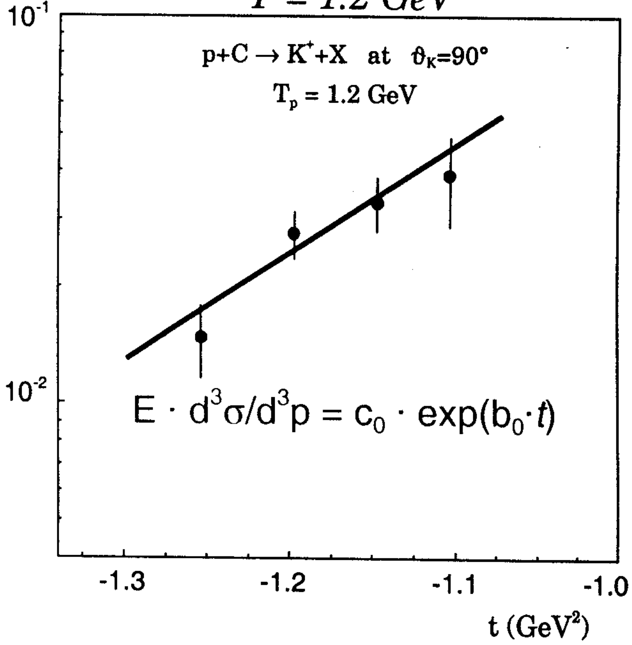

$\Longrightarrow$

Regge approach works even at energies below the NN threshold

K^+-production: systematics of existing data

Data Kiselev et al., ITEP; T = 1.7 ... 2.91 GeV

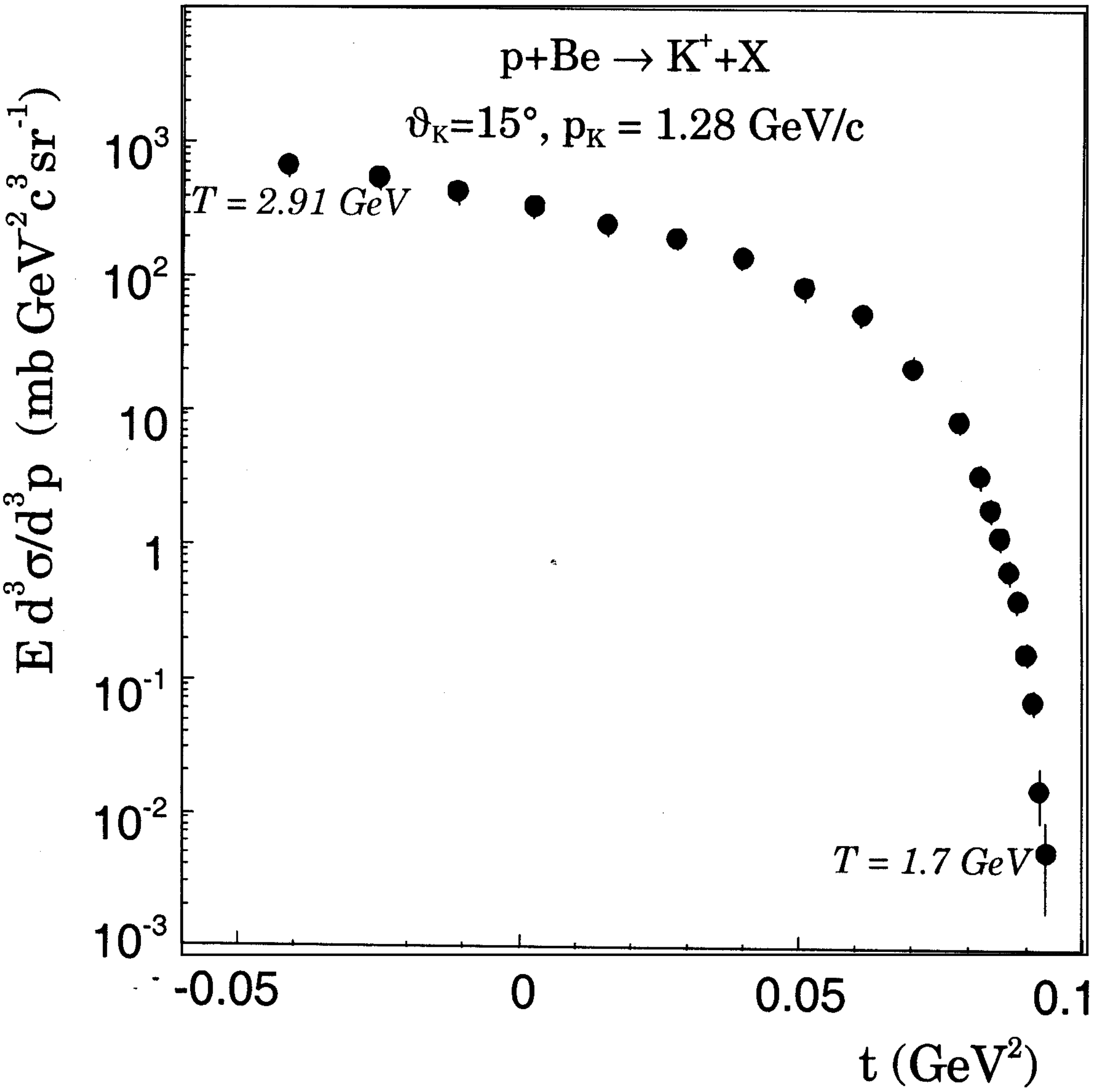

Data cover region of **positive** *t*

But:

t dependence governed by *T* dependence

M.Büscher, 6/01

K^+-production: systematics of existing data

Data: ANKE; T = 1.0 GeV

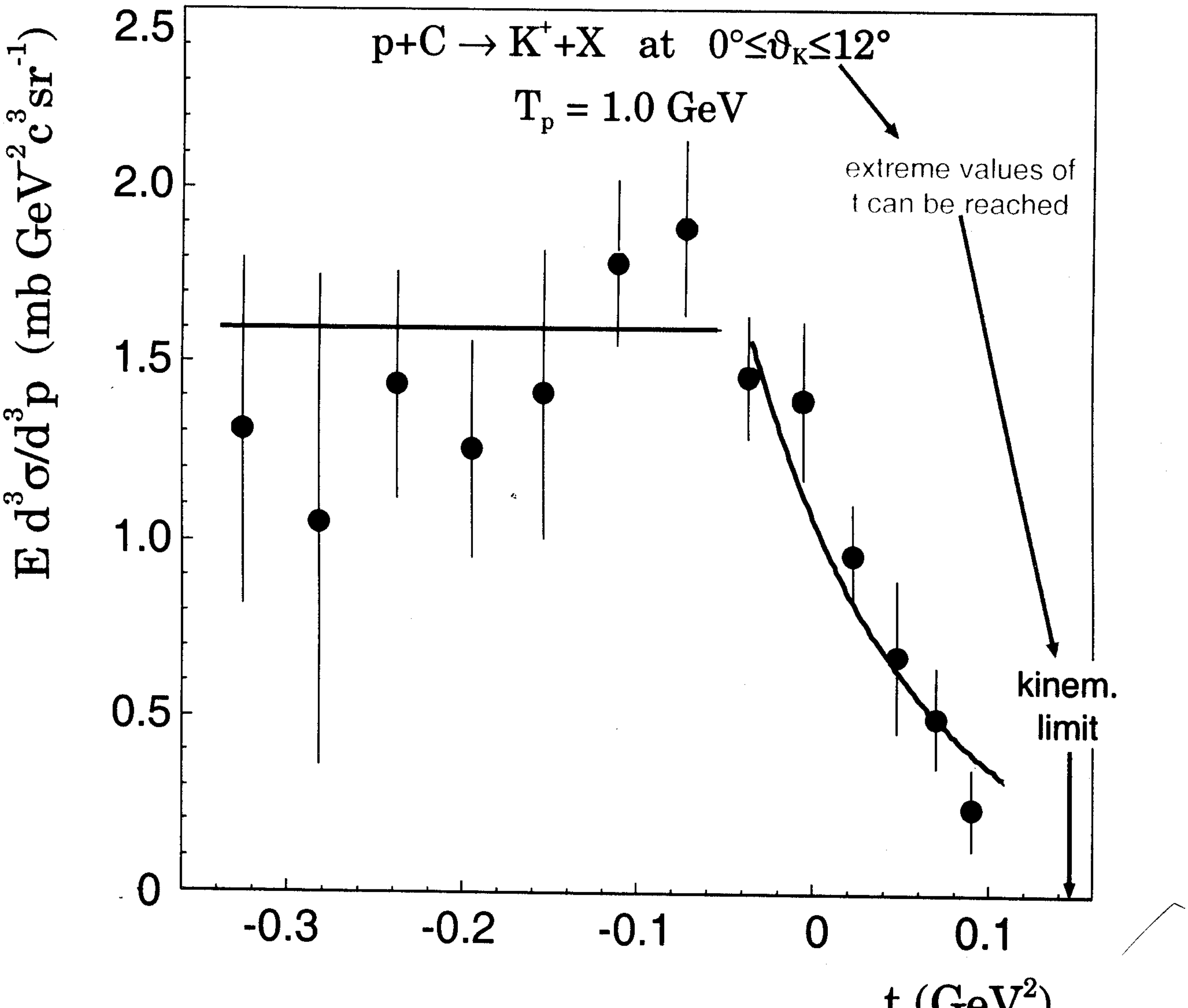

Interpretation of positive *t* ?
Further data at
larger beam energies and forward angles

M.Büscher, 6/01

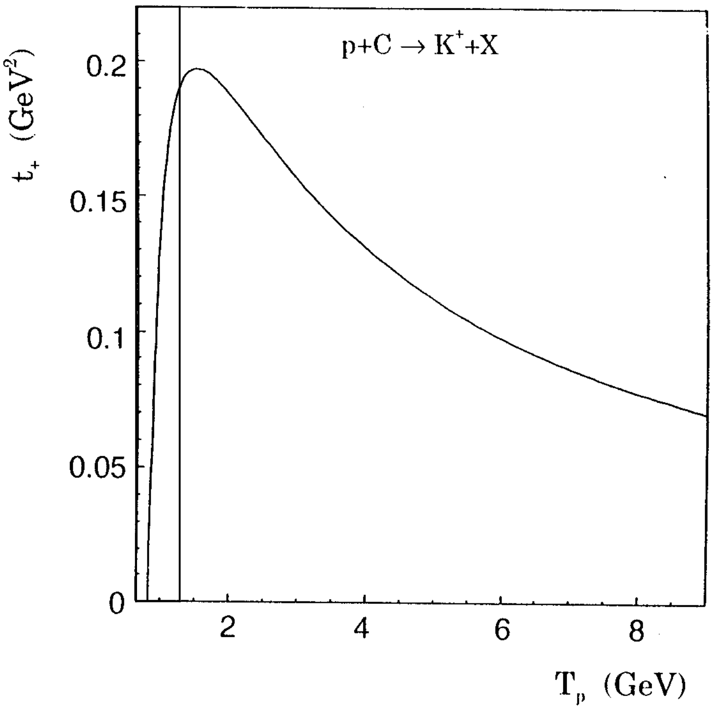
p+C → K⁺+X
t₊ (GeV²)
0.2
0.15
0.1
0.05
0
2
4
6
8
Tₚ (GeV)

Experiments on strangeness production in pp and pA interactions at ANKE (Results of CBUU calculations)

Z.Rudy

M. Smoluchowski Institute of Physics
Jagellonian University
PL-30059 Cracow
Poland

The production and propagation of strangeness in proton–induced reactions is a highly non–equilibrated transport process. Here, an impinging proton penetrates through a bulky volume of target; binary nucleon–nucleon collisions may lead to creation of e.g. K^+ mesons in a associated strangeness production. A microscopic model approach is indispensable that allows to treat final-state interaction to a good accuracy. For this purpose the coupled channel Boltzmann–Uehling–Uhlenbeck model (CBUU) has been used. In order to compensate for the low statistics in the strangeness channels especially close to threshold a perturbative treatment of particle production and propagation had been used. On the following transparencies:

1. (very) short summary of model details (transport equation and solving method via test particles approach) is given;
2. CBUU calculations have been performed and compared with:
   - inclusive K^+ data taken from the literature[1].
   - recently measured by ANKE collaboration [2] inclusive K^+ data, for p+A entrance channel, for $T_p = 1.0, 1.2, 2.0, 2.3$ GeV, for A={Au, Cu, C}

From the shape of presented theoretical distributions one comes to the conclusion that it is desirable to extend experimental measurements of kaons to kaon momenta at least 1 GeV/c. (This goal will require operation of D2 magnet [3] in 1.6 Tesla regime and inclusion of Forward Detector information in Event Builder during data taking.) Concerning the comparison of the experimental (ANKE) data and CBUU model predictions, one concludes that the shapes of momentum distributions are very similar but they differ significantly in magnitude. The reasons of the discrepancy is under investigation.

References

[1] Schnetzer, S. et al., Phys. Rev. **C40**, 640 (1989); Debowski, M. et. al., Z. Phys. **A356**, 313 (1996)

[2] http://www.fz-juelich.de/ikp/anke

[3] S. Barsov et al., **NIM A462/3**, 364 (2001)

W. Cassing, B. Kamys, Z. Rudy

Giessen, Kraków

CBUU model

(Coupled-Channels-Boltzmann-Uhling-Uhlenbeck
transport equation)

describes the propagation and mutual interactions of nucleons, delta's, N* resonances, mesons...

Transport approach

The coupled channel Boltzmann–Uhling-Uhlenbeck CBUU model

Separate phase-space distributions $f_N, f_\pi, f_\Delta, f_\eta$, and f_{N^*} describes the propagation and mutual interactions of nucleons, delta's, N* resonances, π and η mesons.

$$
\begin{aligned}
&\{\frac{\partial}{\partial t} + \frac{\mathbf{p}_{N1}}{m_{N1}}\frac{\partial}{\partial \mathbf{r}} - \frac{\partial}{\partial \mathbf{r}} U_{N1}(\mathbf{r},t)\frac{\partial}{\partial \mathbf{p}_{\mathrm{N1}}}\} f_{N1}(\mathbf{r},\mathbf{p}_{\mathrm{N1}},t) = \\
&\quad \frac{4}{(2\pi)^3}\int\int d^3p_2\; d^3p'_{N1}\int d\Omega\; |v_{N1N}|\frac{d\sigma_{N1N}}{d\Omega}(\sqrt{s})\delta^3(\mathbf{p}_{\mathrm{N1}}+\mathbf{p}_2-\mathbf{p}'_{\mathrm{N1}}-\mathbf{p}_4) \\
&\quad [f_{N1}(\mathbf{r},\mathbf{p}'_{N1},t)f_N(\mathbf{r},\mathbf{p}_4,t)(1-f_{N1}(\mathbf{r},\mathbf{p}_{N1},t))(1-f_N(\mathbf{r},\mathbf{p}_2,t)) \\
&\quad -f_{N1}(\mathbf{r},\mathbf{p}_{N1},t)f_N(\mathbf{r},\mathbf{p}_2,t)(1-f_{N1}(\mathbf{r},\mathbf{p}'_{N1},t))(1-f_N(\mathbf{r},\mathbf{p}_4,t))]
\end{aligned}
$$

$$
\begin{aligned}
&+\sum_{\tau_1\;\tau_2}\frac{4}{(2\pi)^6}\int\int d^3p_1 d^3p_2\; |v_{NN}|\frac{E_{N1'}}{E_{N1}}\frac{d\sigma_{NN\to N1+X}}{d^3p_N1'}(\sqrt{s})f_N(\mathbf{r},\mathbf{p}_1,t)f_N(\mathbf{r},\mathbf{p}_2,t) \\
&+\sum_{\tau_\pi\;\tau_2}\frac{2}{(2\pi)^6}\int\int d^3p_\pi d^3p_2\; |v_{\pi N}|\frac{E_{N1'}}{E_{N1}}\frac{d\sigma_{\pi N\to N1+X}}{d^3p_N1'}(\sqrt{s})f_\pi(\mathbf{r},\mathbf{p}_\pi,t)f_N(\mathbf{r},\mathbf{p}_2,t) \quad ,
\end{aligned}
$$

v_{N1N}, v_{NN}, and $v_{\pi N}$ are the relative velocities of the colliding N1-nucleon, nucleon-nucleon and pion-nucleon pairs.

Time dependent mean-field potential $U_{N1}(\mathbf{r})$ parameterized as a function of the nuclear density

The essence of the test particle method: represent the one-body phase-space distribution by discretized test particles The test particles propagate between collisions according to classical Hamilton equations of motion,

$$\dot{\mathbf{p}}_i = -\nabla_r U(r_i) \quad , \qquad \dot{\mathbf{r}}_i = \mathbf{p}_i/\sqrt{m^2+p^2} \quad . \tag{1}$$

Density distribution in coordinate space $\mathbf{r}_g$,

$$\rho(\mathbf{r}_g) = \frac{1}{N}\sum_{i=1}^{NA}\frac{1}{(2\pi\Delta^2)^{3/2}}exp(\frac{-(\mathbf{r}_g-\mathbf{r}_i)^2}{2\Delta^2} \quad , \tag{2}$$

N – the number of test particles per nucleon

The phase-space distribution f(**r**; **p**; t) is calculated from positions and momenta of the particles:

$$f(\mathbf{r},\mathbf{p},t)) = \frac{6}{N}\frac{1}{N}\sum_{\mathbf{r}_g}\int d^3p \sum_{j=1}^{NA}\Theta(q_0 - \mid \mathbf{p}_j - \mathbf{p} \mid)(2\pi\Delta^2)^{-3/2} exp(\frac{-(\mathbf{r}_g - \mathbf{r}_j)^2}{2\Delta^2}) \quad (3)$$

$$(4)$$

$$|\mathbf{r}_i - \mathbf{R}| \geq R_A + 2fm, \quad (5)$$

where $R_A = 1.2fm\ A_t^{1/3}$ denotes the radius of the target

$N_p(t)$ – number of particles emitted

One is able to evaluate then the fragment's average mass number, its excitation energy, three-momentum and angular momentum by exploring the conservation of total energy, mass number, momentum and angular momentum:

$$\begin{aligned} < E^* > (t) &= E_{tot} - \sum_{j=1}^{N_p(t)} \sqrt{p_j^2 + M_j^2} - M_{res} - E_{coul} \\ < A_F > (t) &= A_t - N_p(t), \\ < \mathbf{p} > (t) &= \mathbf{P}_{tot} - \sum_{j=1}^{N_p(t)} \mathbf{p}_j(t), \\ < \mathbf{L} > (t) &= \mathbf{L}_{tot} - \sum_{j=1}^{N_p(t)} \mathbf{r}_j(t) \times \mathbf{p}_j(t). \end{aligned} \quad (6)$$

In equation M_{res} denotes the mass of the 'residual nucleus', E_{coul} stands for the Coulomb energy between the emitted particles and the 'residual nucleus'

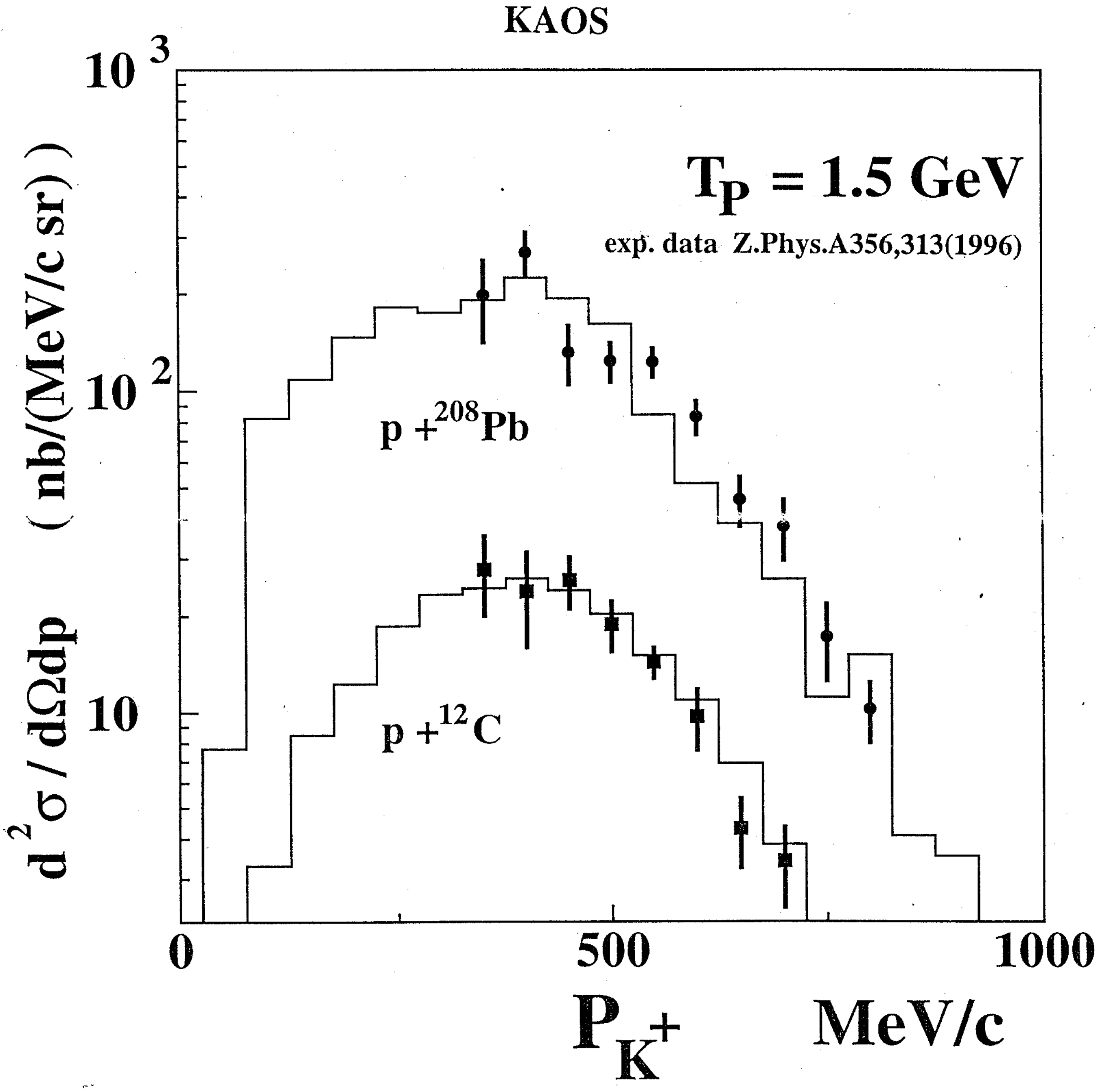
KAOS
10 3
10 2
10
d 2σ / dΩdp (nb/(MeV/c sr))
T_P = 1.5 GeV
exp. data Z.Phys.A356,313(1996)
p +208Pb
p +12C
0
500
1000
P_K+ MeV/c

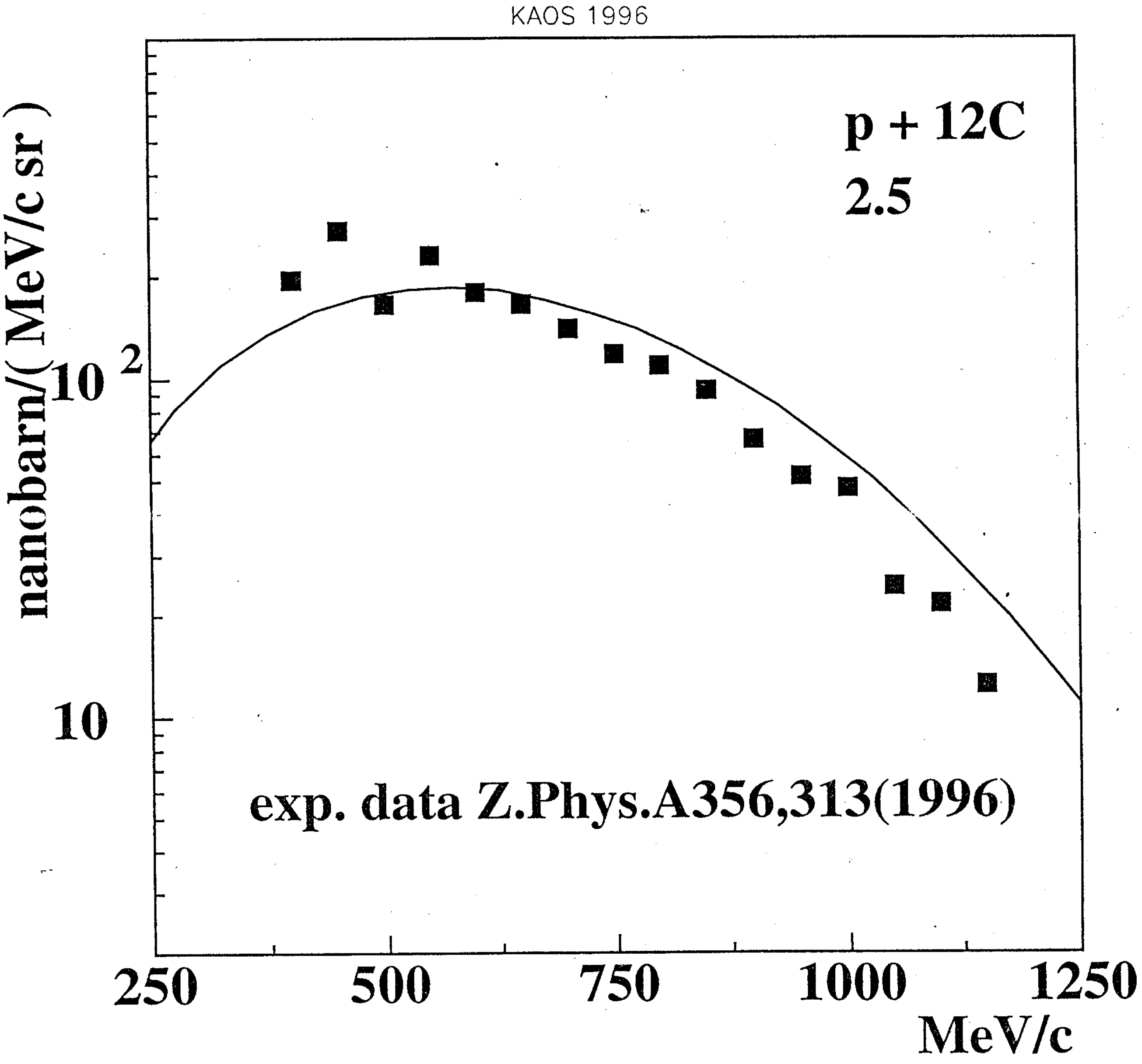
KAOS 1996
nanobarn/(MeV/c sr)
10 2
10
p + 12C
2.5
exp. data Z.Phys.A356,313(1996)
250
500
750
1000
1250
MeV/c

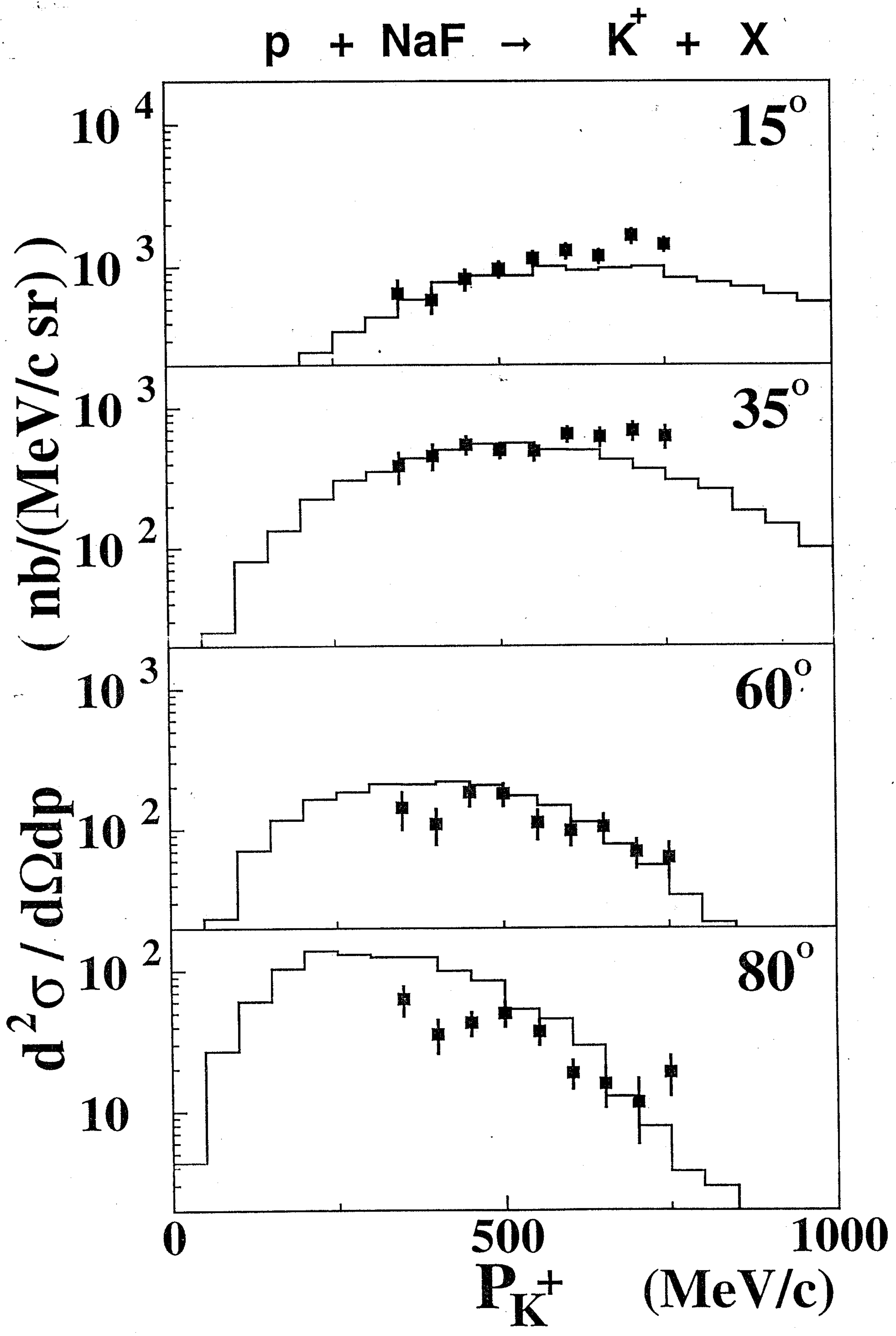

T_p = 2.1 GeV *Schnetzer et al., Phys.Rev.C40,640(1989)*

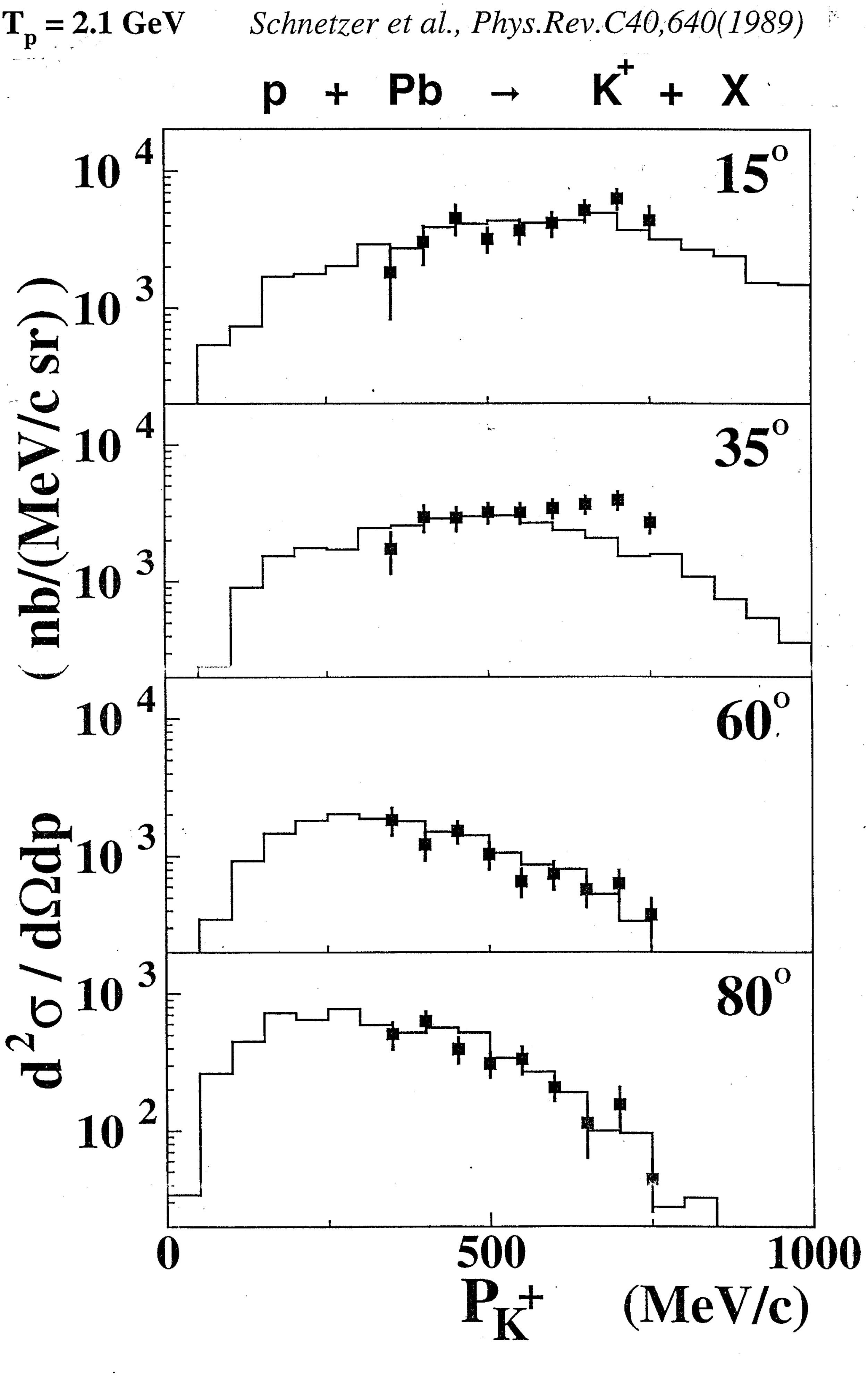
T_p = 2.1 GeV
Schnetzer et al., Phys.Rev.C40,640(1989)
p + Pb → K^+ + X
15°
35°
60°
80°
10^4
10^3
10^2
$d^2\sigma$ / dΩdp (nb/(MeV/c sr))
0
500
1000
P_{K^+} (MeV/c)

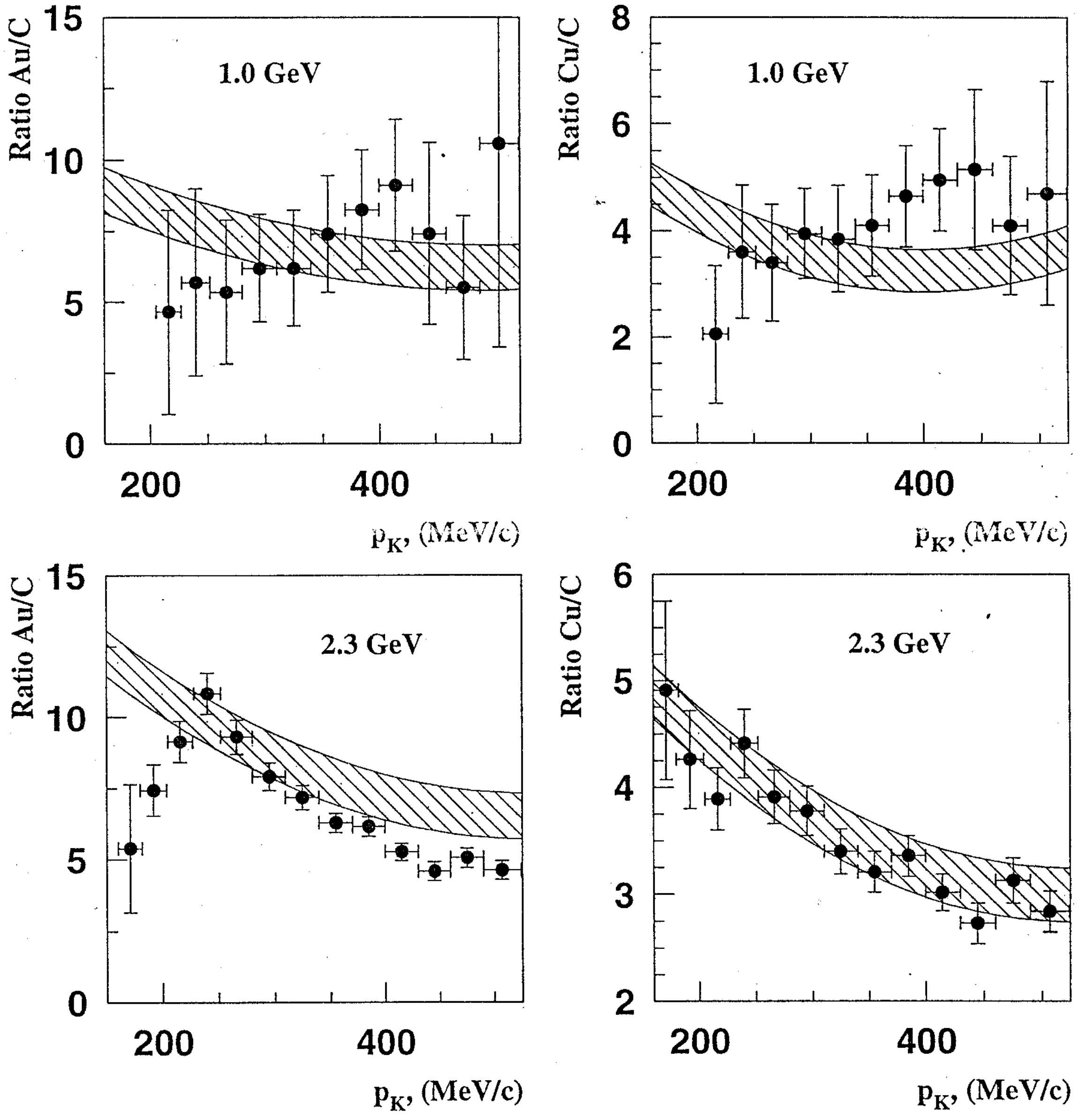
Ratio Au/C
1.0 GeV
15
10
5
0
200
400
p_K, (MeV/c)
Ratio Cu/C
1.0 GeV
8
6
4
2
0
200
400
p_K, (MeV/c)
Ratio Au/C
2.3 GeV
15
10
5
0
200
400
p_K, (MeV/c)
Ratio Cu/C
2.3 GeV
6
5
4
3
2
200
400
p_K, (MeV/c)

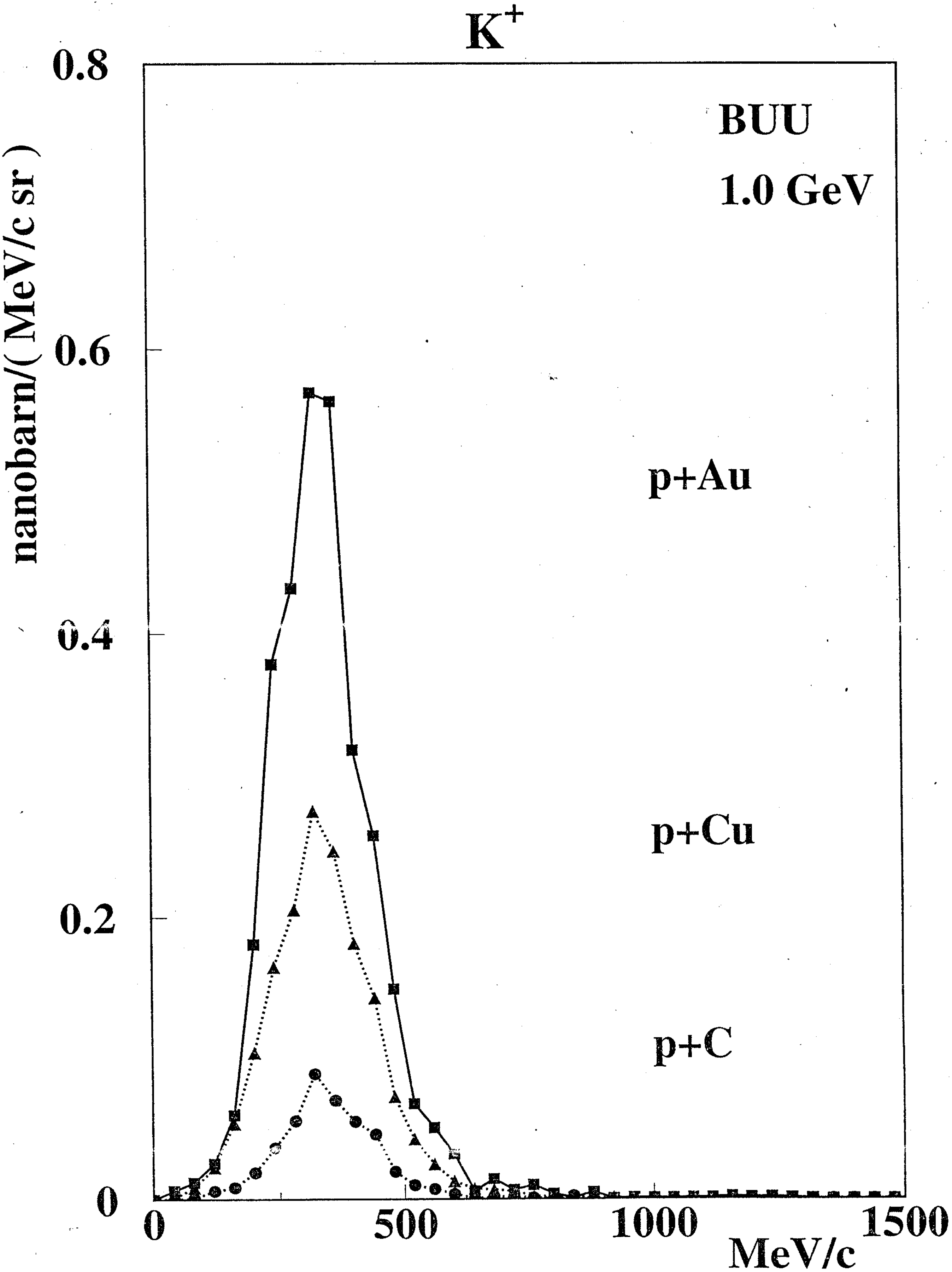
K$^+$
BUU
1.0 GeV
p+Au
p+Cu
p+C
nanobarn/(MeV/c sr)
0.8
0.6
0.4
0.2
0
0
500
1000
1500
MeV/c

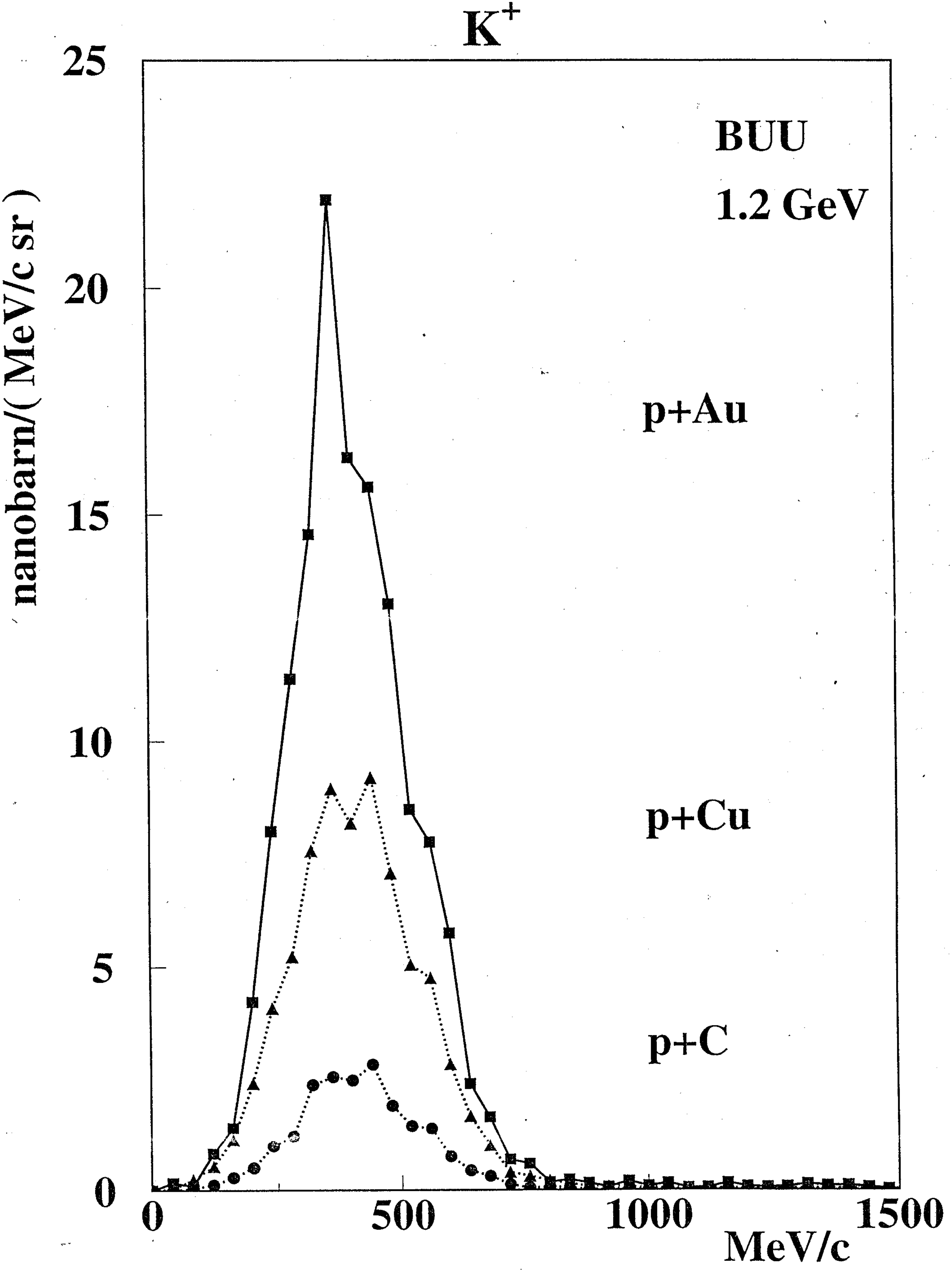
K$^+$
BUU
1.2 GeV
p+Au
p+Cu
p+C
nanobarn/(MeV/c sr)
25
20
15
10
5
0
0
500
1000
1500
MeV/c

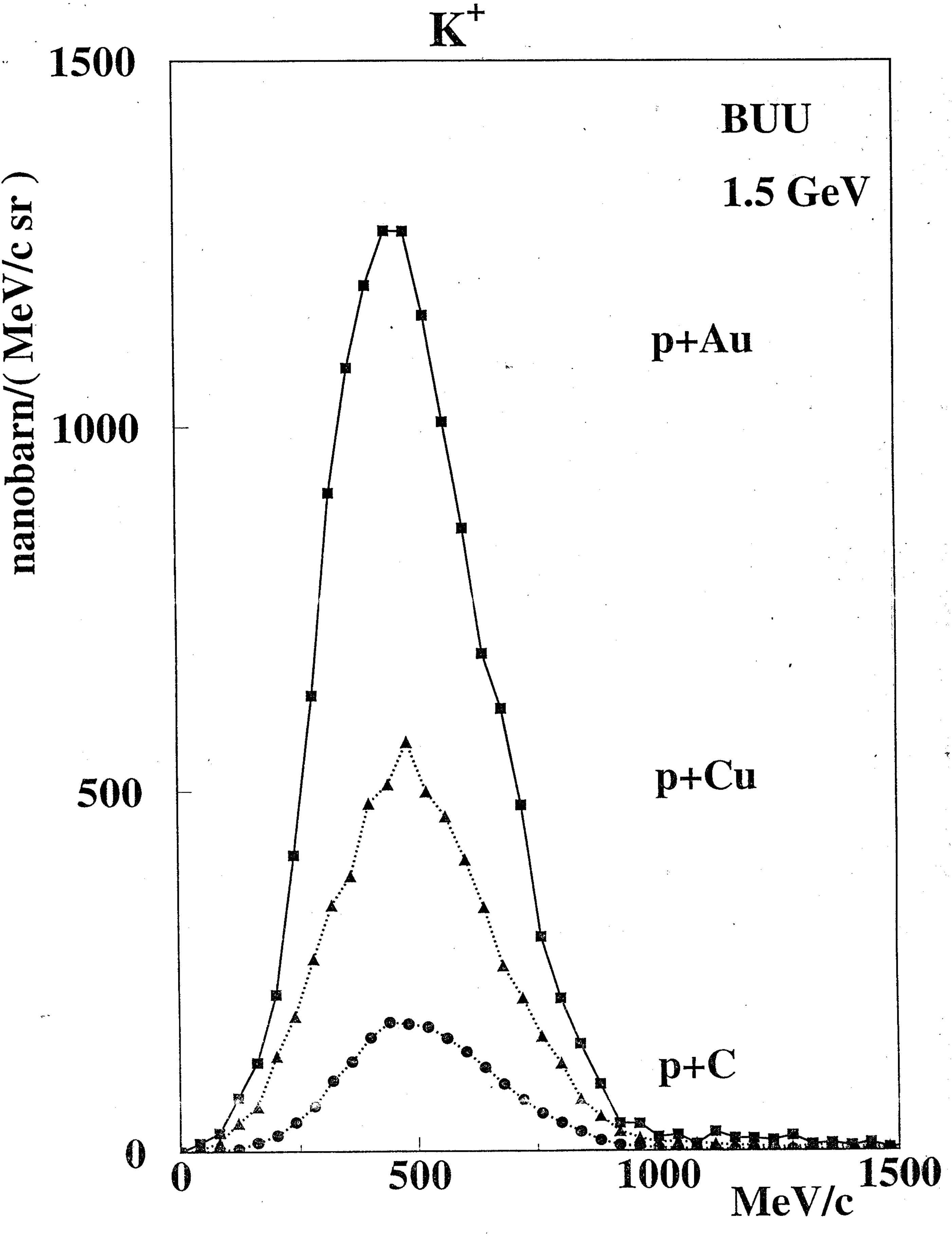
K$^+$
BUU
1.5 GeV
p+Au
p+Cu
p+C
nanobarn/(MeV/c sr)
1500
1000
500
0
0
500
1000
1500
MeV/c

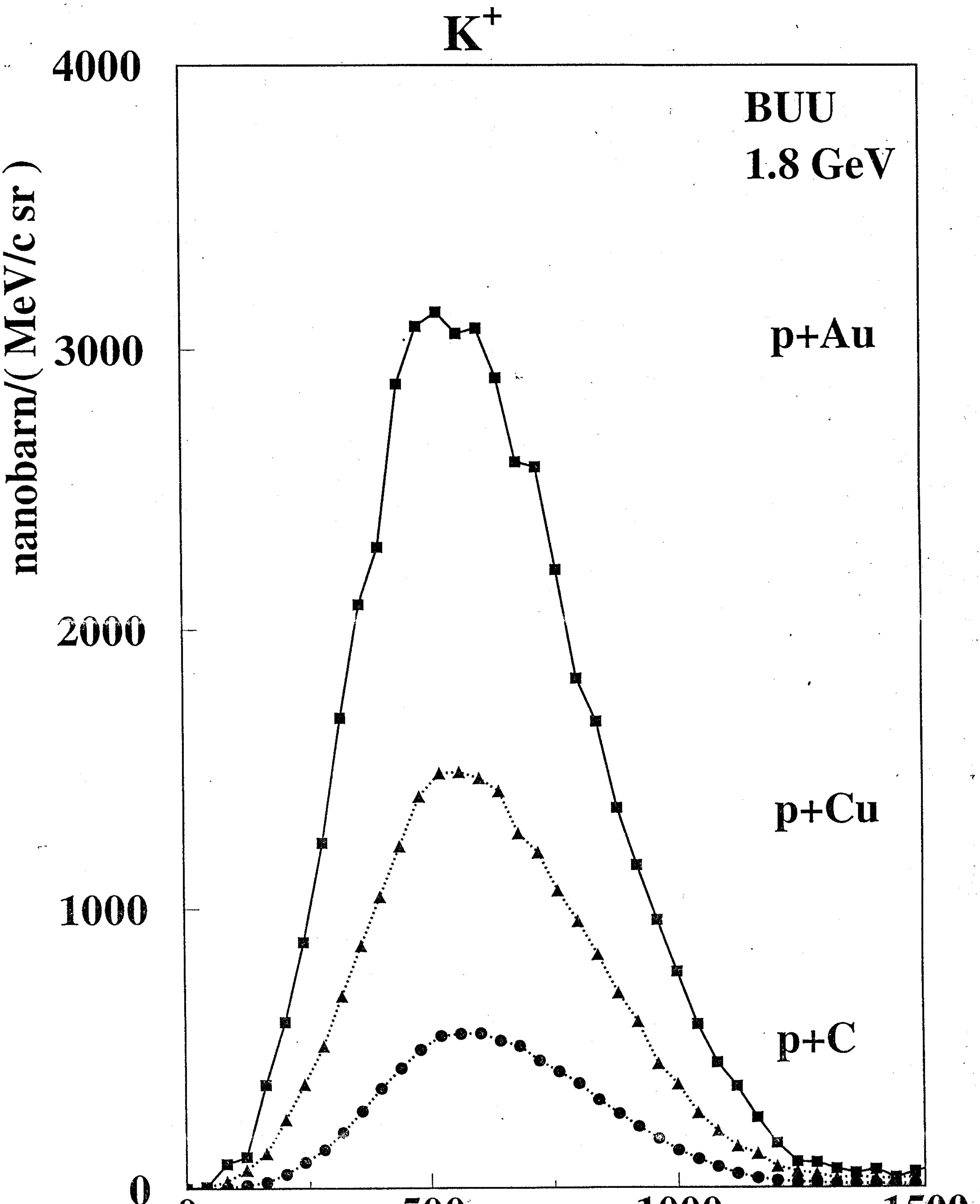
K$^+$
BUU
1.8 GeV
p+Au
p+Cu
p+C
nanobarn/(MeV/c sr)
4000
3000
2000
1000
0
0
500
1000
1500
MeV/c

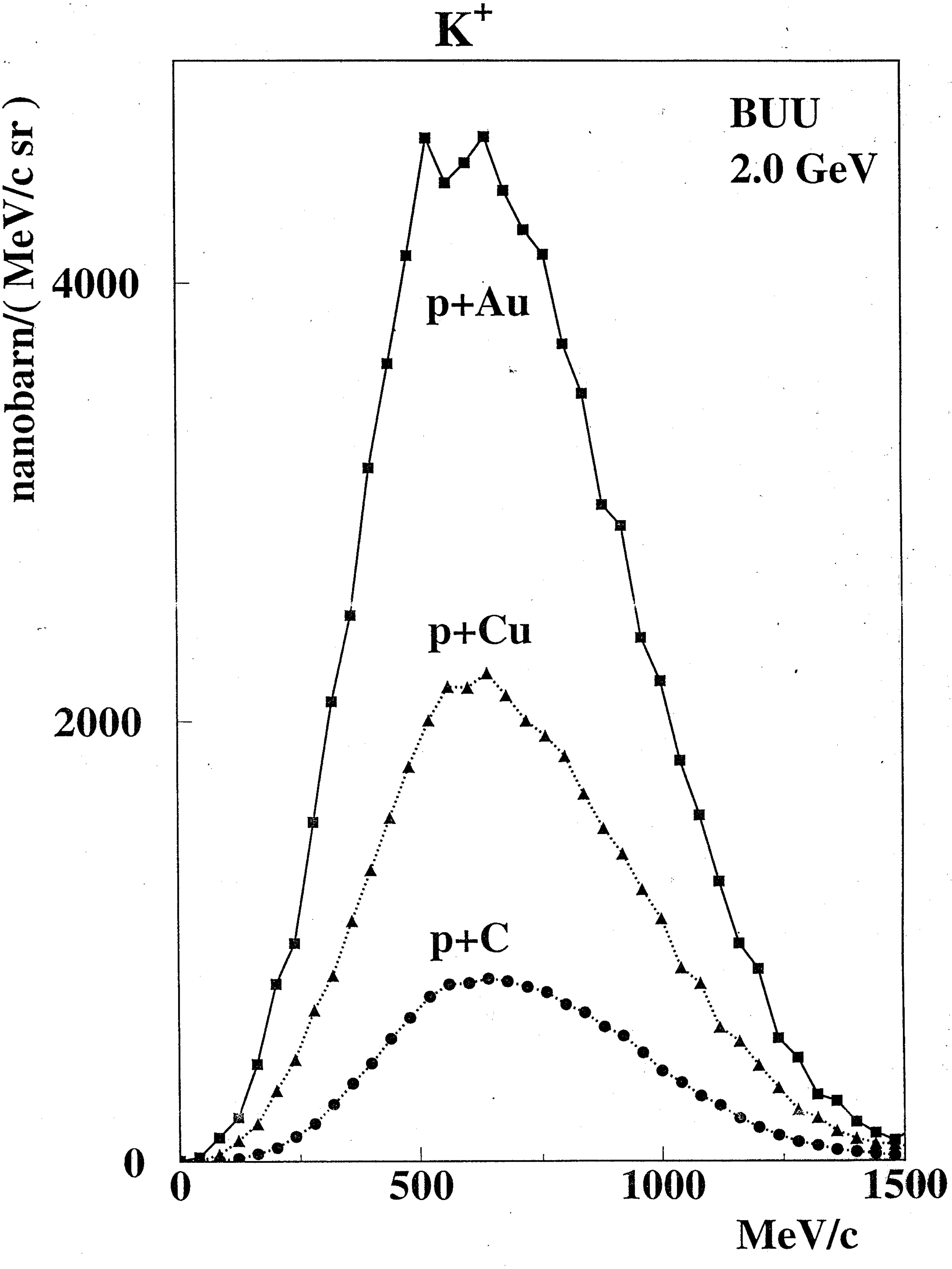
K$^+$
BUU
2.0 GeV
p+Au
p+Cu
p+C
nanobarn/(MeV/c sr)
4000
2000
0
0
500
1000
1500
MeV/c

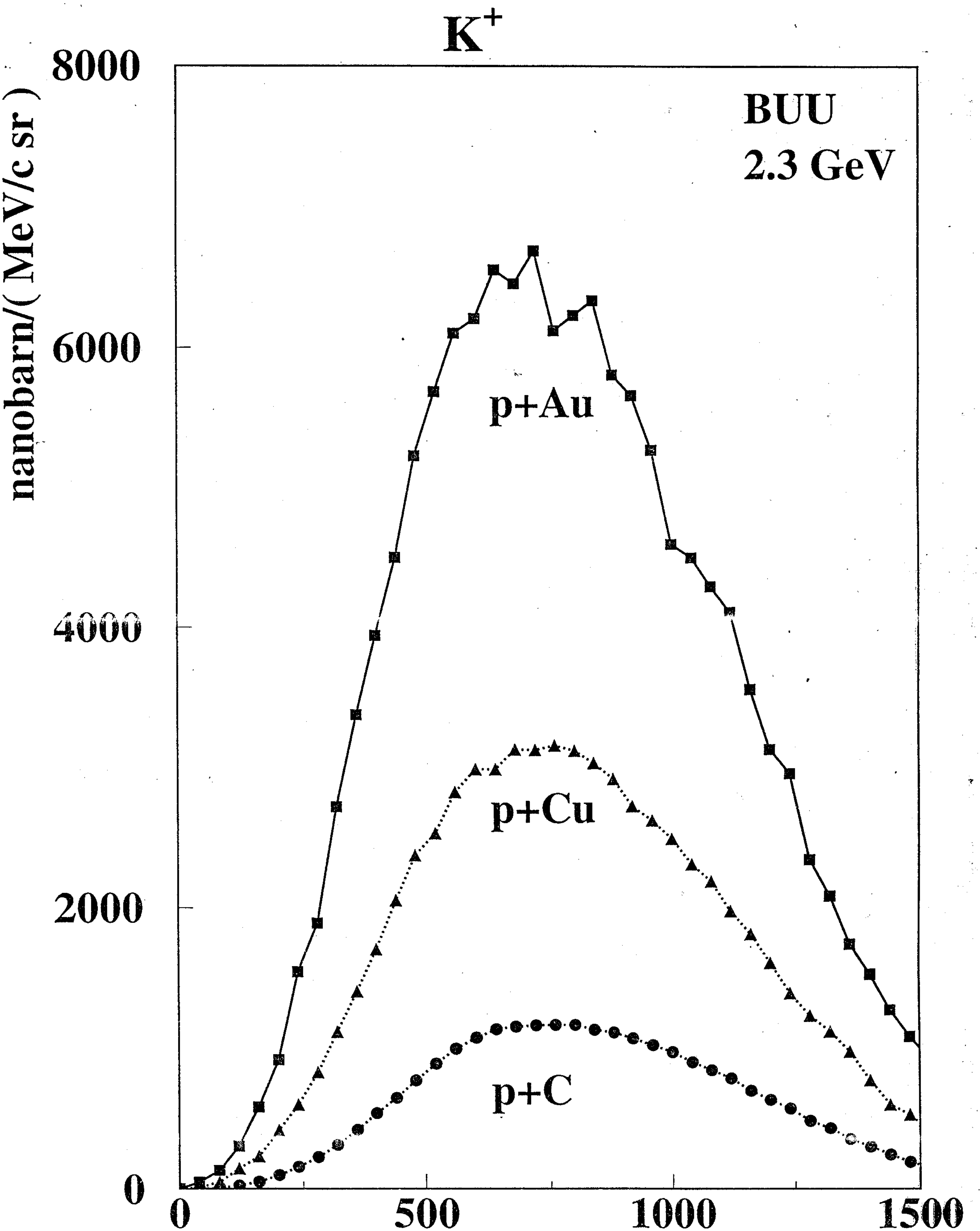
K$^+$
BUU
2.3 GeV
nanobarn/(MeV/c sr)
8000
6000
4000
2000
0
0
500
1000
1500
MeV/c
p+Au
p+Cu
p+C

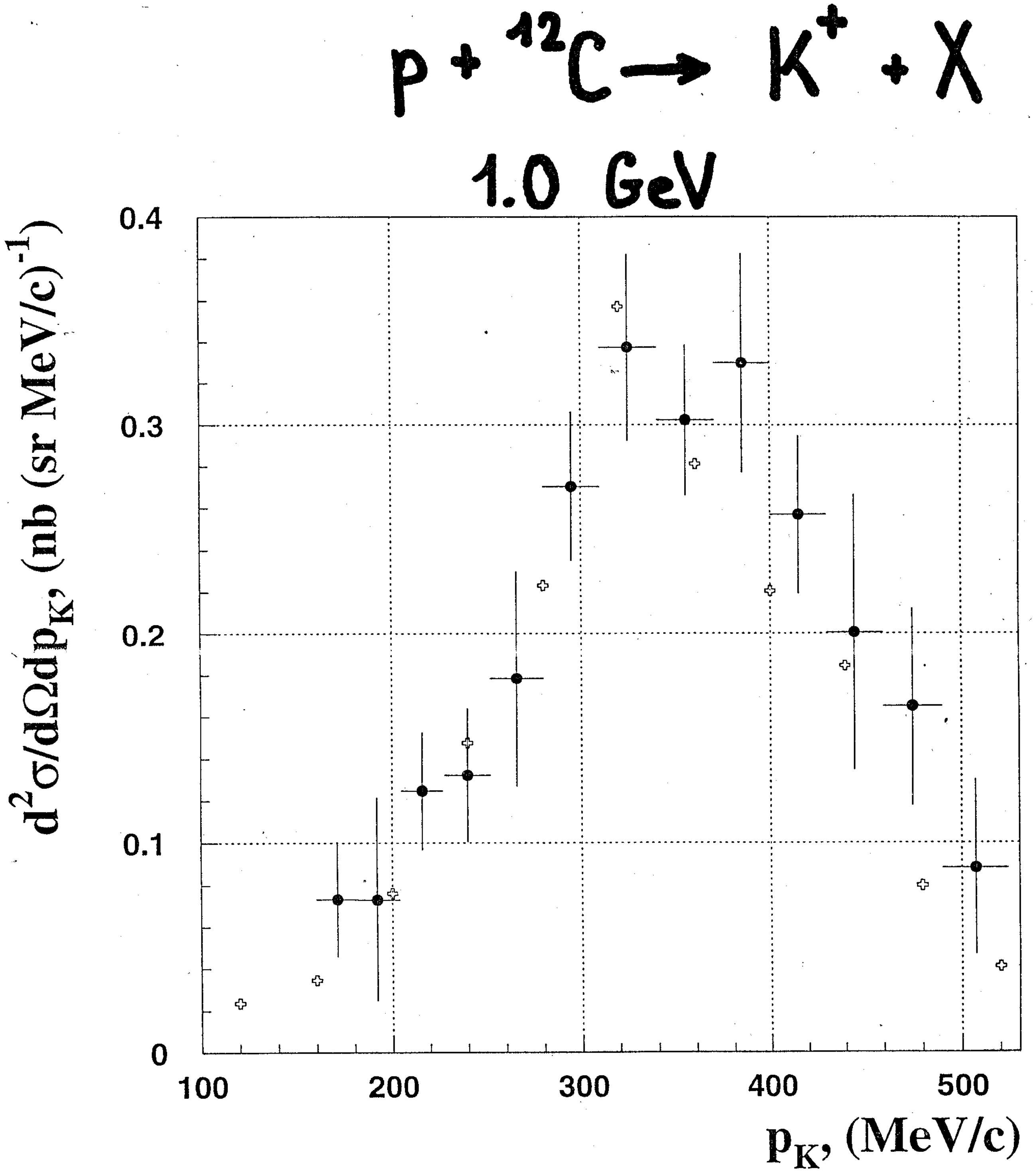

theory multiplied by 4

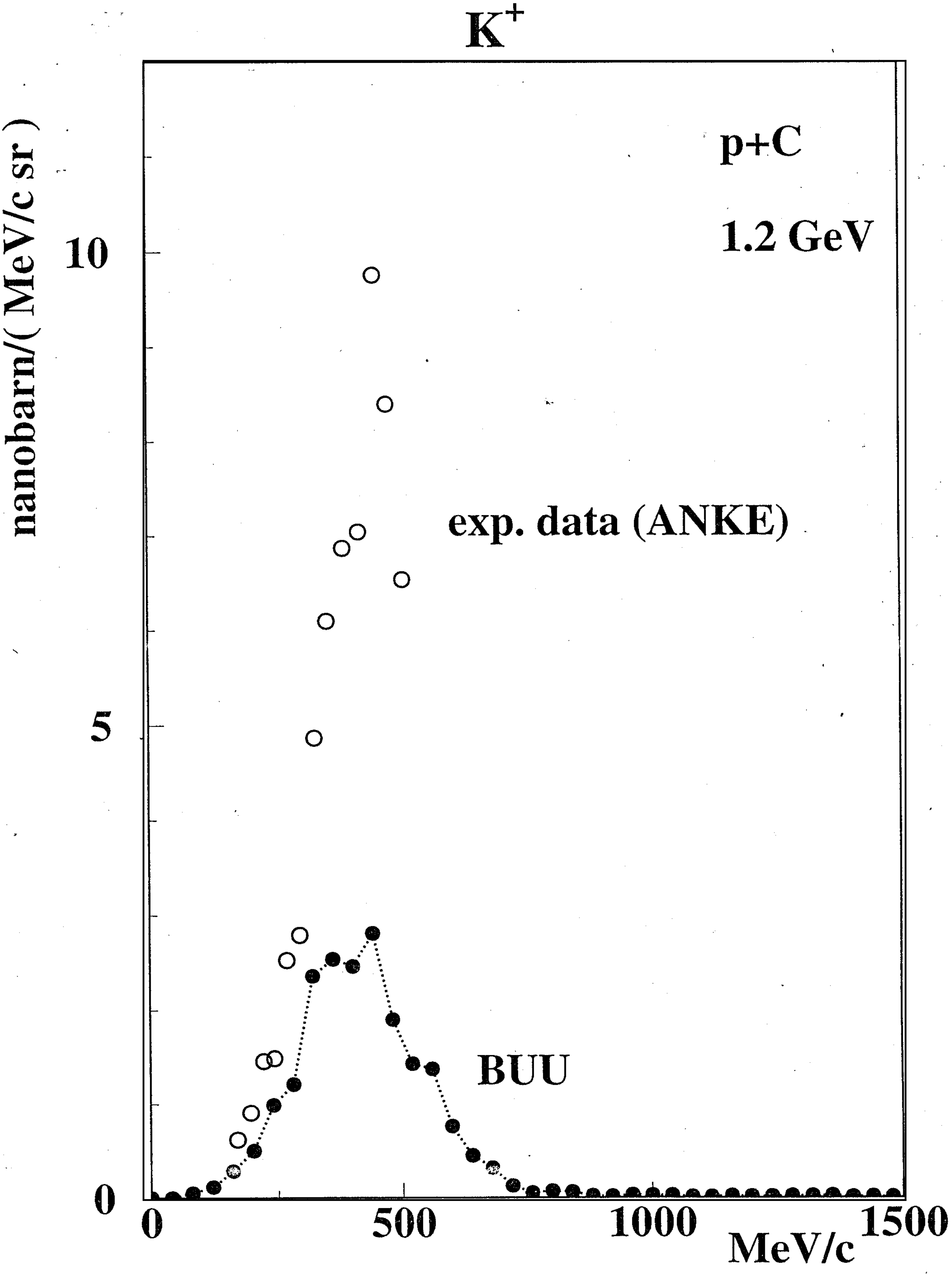
K+
p+C
1.2 GeV
exp. data (ANKE)
BUU
nanobarn/(MeV/c sr)
0
5
10
0
500
1000
1500
MeV/c

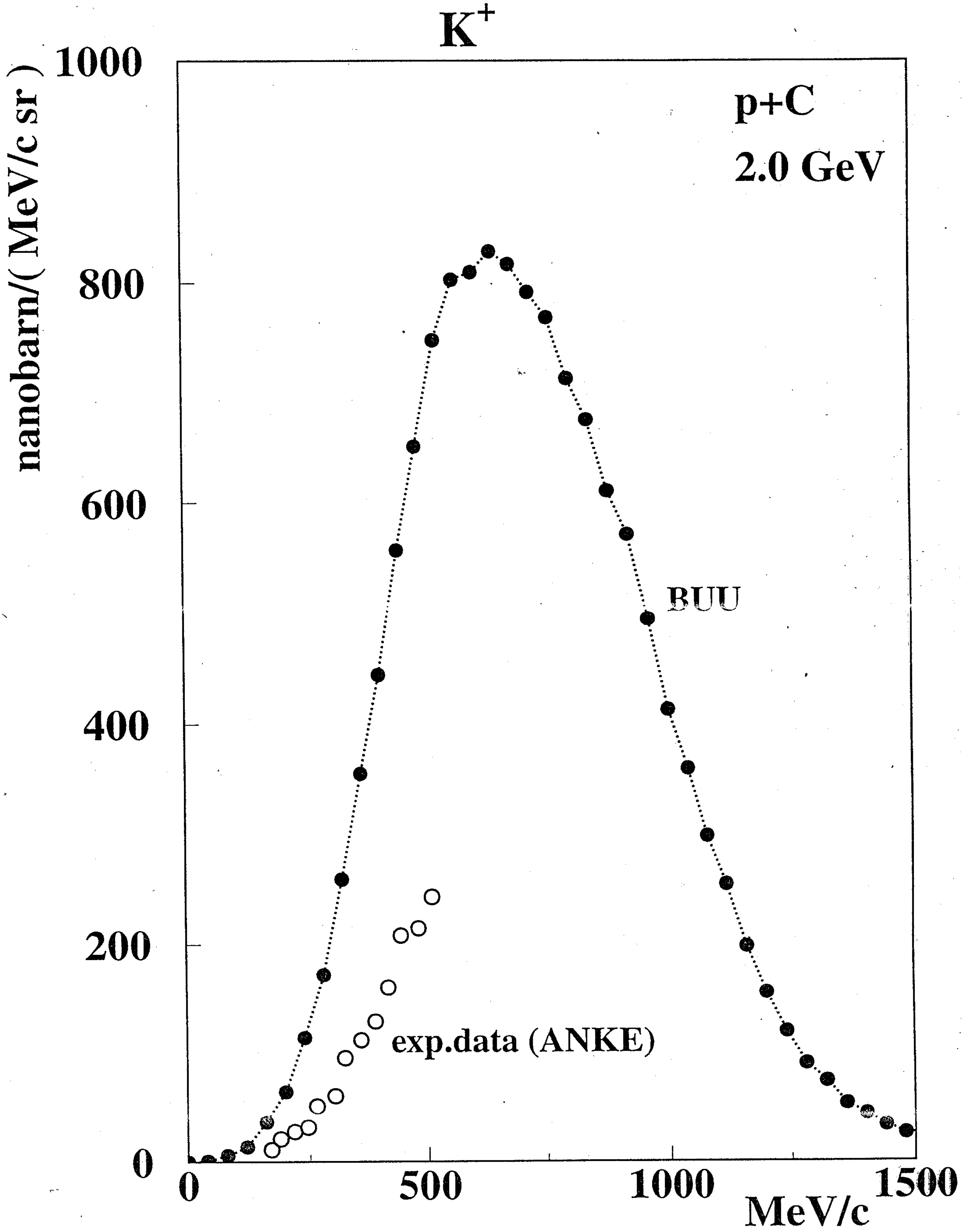
K+
p+C
2.0 GeV
BUU
exp.data (ANKE)
nanobarn/(MeV/c sr)
1000
800
600
400
200
0
0
500
1000
1500
MeV/c

$p + {}^{12}C \rightarrow K^{+} + X$

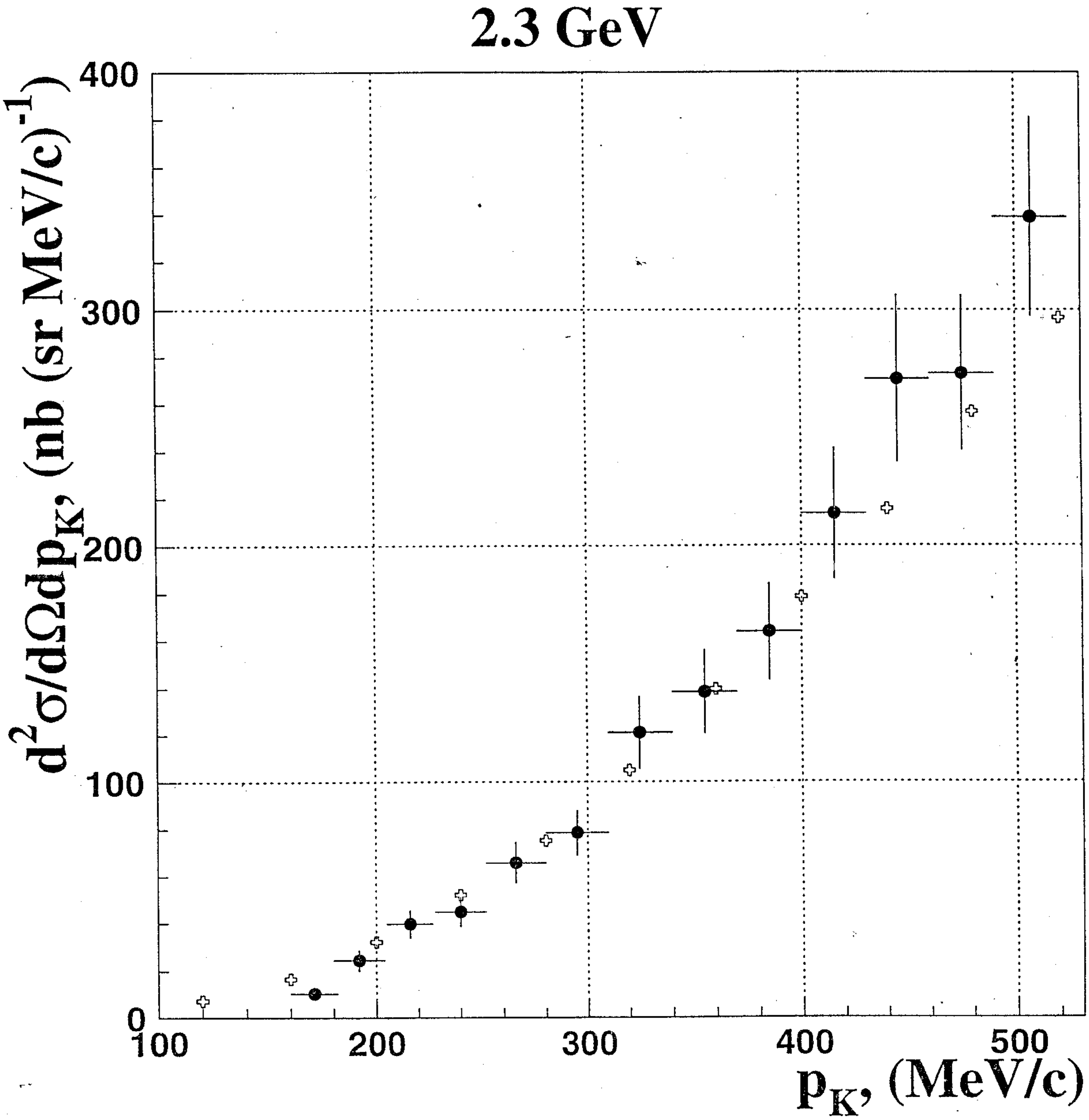

theory divided by 3

The cross section is thus given by

$$\frac{d^2\sigma^K}{d\Omega dp} = \frac{d^2\sigma^\pi}{d\Omega dp}\frac{N^K_{\mathrm{tel}(i)}}{N^\pi_{\mathrm{stop}(i)}}\frac{M^\pi}{M^K}\frac{1}{\epsilon},$$

$$\epsilon = \frac{\epsilon^K_{\mathrm{tel}(i)}\epsilon^K_{\mathrm{MWPC}(i)}\epsilon^K_{\mathrm{decay}}}{\epsilon^\pi_{\mathrm{stop}(i)}\epsilon^\pi_{\mathrm{MWPC}(i)}\epsilon^\pi_{\mathrm{decay}}},$$

Summary

BU$\boxed{\text{U}}$ model

K^+ data (KAOS, Schnetzer)

K^+ data of ANKE
1.0 GeV
1.2 GeV
1.5 GeV
1.8 GeV
2.0 GeV
2.3 GeV

Subthreshold and near threshold K^+–meson production on light nuclei by protons

E.Ya.Paryev

Institute for Nuclear Reasearch
Russian Academy of Sciences
117312 Moscow
Russia

The inclusive K^+-meson production in proton-nucleus collisions in the near threshold and subthreshold energy regimes is analyzed with respect to the one-step ($pN \to K^+YN$, $Y = \Lambda, \Sigma$) and two-step ($pN \to NN\pi$, $\pi N \to K^+Y$) incoherent production processes on the basis of an appropriate folding model, which takes properly into account the struck target nucleon removal energy and momentum distribution (nucleon spectral function), novel elementary cross sections for proton-nucleon reaction channel close to threshold as well as nuclear mean-field potential effects on the one-step and two-step creation process. A detailed comparison of the model calculations of the K^+ total and differential cross sections for the reactions $p +^9 Be$ and $p +^{12} C$ with the existing experimental data is given.

The available now experimental data on subthreshold K^+ production in proton-nucleus collisions

1) Total K^+ production cross sections in pA-reactions,
$T_0 = 800 - 1000$ MeV, $(pC \to K^+X)$
Koptev V. P., et al., ZhETF, 94 (1988) 1.

---

2) Differential K^+ production cross sections in pA-collisions,
$pC \to K^+X$, $\theta^{lab}_{K^+} = 40^\circ$, $T_0 = 1.2$, 1.5, 2.5 GeV
$pPb \to K^+X$, $\theta^{lab}_{K^+} = 40^\circ$, $T_0 = 1.2$, 1.5 GeV $\to \sigma^{tot}_{K^+}$
Debowski M., et al., Z. Phys. A 356 (1996) 313.

---

3) Differential K^+ production cross sections:
$pC \to K^+X$, $\theta^{lab}_{K^+} = 90^\circ$, $T_0 = 1.2$ GeV $\Rightarrow \sigma^{tot}_{K^+}$
Badala A., et al., Phys. Rev. Lett. 80 (1998) 4863.

---

4) Excitation functions for K^+ production in pA-reactions
A = Be, Al, Cu, Ta; $p_{K^+} = 1.28$ GeV/c, $\theta^{lab}_{K^+} = 10.5^\circ$
Akindinov A., Chumakov M., Kiselev Yu., et al.,
Preprint ITEP 37-99, 1999.

---

5) Differential K^+ production cross sections:
$pC \to K^+X$, $\theta^{lab}_{K^+} = 0^\circ$, $T_0 = 1.0$, 1.2, 2.0, 2.3 GeV; ANKE collaboration.

1) S.V. Efremov, E.Ya. Paryev: Eur. Phys. J A 1 (1998) 99.

2) E.Ya. Paryev: Eur. Phys. J A 5 (1999) 307.

1. Direct K^+ Production Processes

1.1 Kaon Production Cross Section

3.0 GeV

Since we are interested in a few GeV region (up to ~~2.5~~ GeV), we have taken into account the following elementary processes which have the lowest free production thresholds:

(1) $$p + N \to K^+ + \Lambda + N,$$ (1.5

(2) $$p + N \to K^+ + \Sigma + N.$$ (1.7

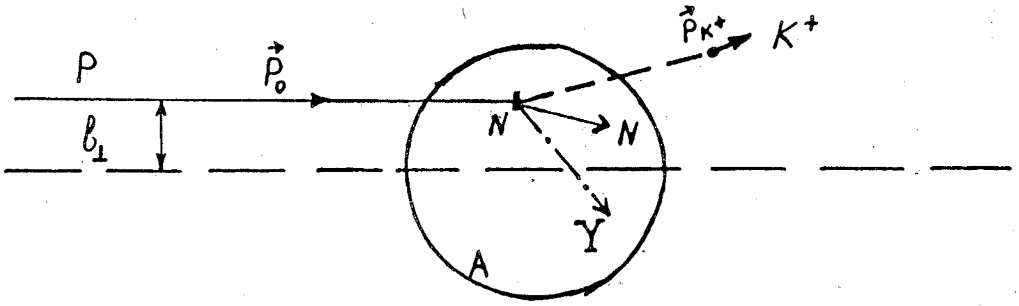

Following the predictions of the effective chiral Lagrangian approach by Kaplan and Nelson [17], we assume that the mass of the produced kaon is not changed in the nuclear medium. $\Longrightarrow$ $E_{K^+} = \sqrt{p_{K^+}^2 + m_K^2}$, m_K is the rest mass of a kaon in free spa

(3)

The effective masses m_h^* of other final hadrons (nucleon and hyperon) participating in the K^+ production processes (1), (2), are defined by the following dispersion relation:

(4) $$E_h^2 = p_h^2 + m_h^{*2} \approx (\sqrt{p_h^2 + (m_h + U_s^h)^2} + U_v^h)^2.$$

m_h^* include the effective scalar mean-field potentials U_{eff}^h, needed for our calculations:

(5) $$m_h^* = m_h + U_{eff}^h.$$

the average kinetic energies $\leq 0.1\ GeV$ for the outgoing nucleon and hyperon

$\Downarrow$

Lee, C.H., *Phys. Lett.* **412B**, 235 (1997) $\longrightarrow$ $U_{eff}^N = -34\ MeV$.

$$U_{eff}^\Lambda = -30\ MeV,\ U_{eff}^\Sigma = -26\ MeV$$

Using (3)–(5), this leads to the following expression for the in medium reaction thresholds:

$$\sqrt{s_{th}^*} = m_K + m_Y^* + m_N^* = \sqrt{s_{th}} + U_{eff}^Y + U_{eff}^N.$$

where $\sqrt{s_{th}} = m_K + m_Y + m_N$ are the threshold energies in free space

N : $$E_t = M_A - \sqrt{(-p_t)^2 + (M_A - m_N + E)^2},$$

p: $$E_0' = E_0 - \frac{\Delta p^2}{2M_A}.$$ $$\Delta p = \frac{E_0}{p_0} V_0,$$

$$p_0' = p_0 - \Delta p.$$

$$V_0 \approx 40\ MeV$$

1. Direct K^+ Production Processes

1.1 Kaon Production Cross Section

Since we are interested in a few GeV region (up to 2.5 GeV), we have taken into account the following elementary processes which have the lowest free production thresholds:

(1) $$p + N \to K^+ + \Lambda + N, \qquad (1.58\,\mathrm{GeV})$$

(2) $$p + N \to K^+ + \Sigma + N. \qquad (1.78\,\mathrm{GeV})$$

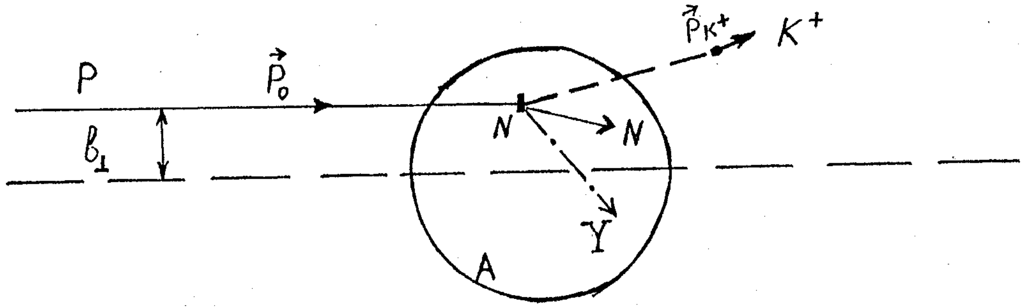

Then we can represent the invariant inclusive cross section of K^+ production on nuclei by the initial proton with momentum $\vec{p}_0$ as follows:

$$E_{K^+}\frac{d\sigma^{(prim)}_{pA\to K^+X}(\mathbf{p}_0)}{d\mathbf{p}_{K^+}} = I_V[A]\times \tag{3}$$

$$\left\{\left\langle E_{K^+}\frac{d\sigma_{pN\to K^+\Lambda N}(\mathbf{p}_0,\mathbf{p}_{K^+})}{d\mathbf{p}_{K^+}}\right\rangle + \left\langle E_{K^+}\frac{d\sigma_{pN\to K^+\Sigma N}(\mathbf{p}_0,\mathbf{p}_{K^+})}{d\mathbf{p}_{K^+}}\right\rangle\right\},$$

where

$$I_V[A] = A\int \rho(\mathbf{r})d\mathbf{r}\exp\left[-\mu(p_0)\int\limits_{-\infty}^{0}\rho(\mathbf{r}+x\mathbf{\Omega}_0)dx\right], \tag{4}$$

$$\mu(p_0) = \sigma^{in}_{pp}(p_0)Z + \sigma^{in}_{pn}(p_0)N; \tag{5}$$

$$\left\langle E_{K^+}\frac{d\sigma_{pN\to K^+YN}(\mathbf{p}_0,\mathbf{p}_{K^+})}{d\mathbf{p}_{K^+}}\right\rangle = \int\int P(\mathbf{p}_t,E)d\mathbf{p}_t dE\times \tag{6}$$

$$\left[E_{K^+}\frac{d\sigma_{pN\to K^+YN}(\sqrt{s},\mathbf{p}_{K^+})}{d\mathbf{p}_{K^+}}\right].$$

$\lambda_{K^+} \approx 7$ fm ; $R_{C^{12}} = 2.8$ fm , $R_{Cu^{64}} \simeq 4.8$ fm , $R_{Au^{197}} \simeq 7.0$ fm.

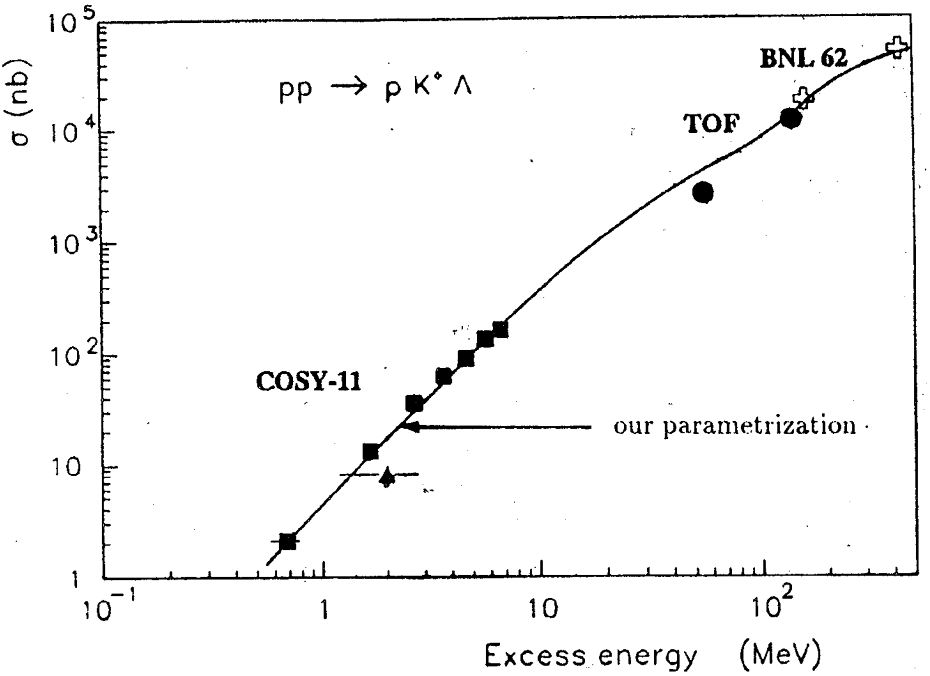

Fig.1. The total cross section for $pp \to K^{+} \Lambda p$ reaction as a function of an excess energy $(\sqrt{s} - \sqrt{s_{th}})$.

Oelert, W.: *LANL Preprint* Nucl–ex/9803004 (1998);

$$\sigma_{pp\to K^+YN}(\sqrt{s}, \sqrt{s_{th}}) = \frac{A_Y (s - s_{th})^2}{4m_p^2 + B_Y(s - s_{th})^2} +$$

$$+C_Y(s - s_{th})^2[0.5 - (s - s_{th})/GeV^2]^{2.328}\Theta[0.5 - (s - s_{th})/GeV^2]/(4m_p^2),$$

where $\Theta(x) = (x + |x|)/2|x|$ and the constants A_Y, B_Y, C_Y and s_{th} are given in Table 1.

Table 1. Parameters in the approximation of the partial cross sections for the production of K^+ mesons in *pp*–collisions

Reaction	A_Y,$\mu b \cdot GeV^{-2}$	B_Y, GeV^{-2}	C_Y,$\mu b \cdot GeV^{-2}$	s_{th},GeV^2
$p + p \to K^+ + \Lambda + p$	122.943	2.015	2515.56	6.490
$p + p \to K^+ + \Sigma + N$	104.026	1.006	0.	6.880

2. Two–Step K^+ Production Processes

2.1 Kaon Production Cross Section

Kinematical considerations show that in the bombarding energy range of our interest ($\leq 2.5\ GeV$) the following two–step production processes may not only contribute to the K^+ production in pA interactions but even dominate at subthreshold energies ($\leq 1.5\ GeV$):

$\mathcal{E}_N \approx 0.1\,GeV$

$U_{eff}^N = -34\,MeV$ $\Rightarrow$

$$p + N_1 \to N + N + \pi, \qquad (22)$$

$$p + N_1 \to N + N + 2\pi. \qquad (23)$$

m_N^*

$$\Downarrow$$

$U_{eff}^Y \Rightarrow$

$$\pi + N_2 \to K^+ + \Lambda, \qquad (24)$$

$$\pi + N_2 \to K^+ + \Sigma. \qquad (25)$$

m_Y^*

(free production thresholds, respectively, are 0.76 and 0.89 GeV)

$$E_{K^+}\frac{d\sigma^{(sec)}_{pA\to K^+X}(\vec{p}_0)}{d\vec{p}_{K^+}} = \sum_{i,j=0,1} E_{K^+}\frac{d\sigma^{(sec)}_{ij}(\vec{p}_0)}{d\vec{p}_{K^+}}, \qquad (26)$$

where

$$E_{K^+}\frac{d\sigma^{(sec)}_{ij}(\vec{p}_0)}{d\vec{p}_{K^+}} = \sum_{\pi=\pi^+,\pi^0,\pi^-} \int\int P_i(\vec{p}_t, E)\,d\vec{p}_t\,dE \times \qquad (27)$$

$$\times \int\limits_{p_\pi^{abs}}^{p_\pi^{max}(\vec{p}_t,E)} p_\pi^2 dp_\pi \int\limits_{4\pi} d\vec{\Omega}_\pi I_V[A, \sigma^{in}_{pN}(p_0), \sigma^{tot}_{\pi N}(p_\pi), \vartheta_\pi]\frac{d\sigma_{pN\to\pi X}(\sqrt{s}, \vec{p}_\pi)}{d\vec{p}_\pi}\times$$

$$\times \int\int P_j(\vec{p'}_t, E')\,d\vec{p'}_t\,dE' \left[E_{K^+}\frac{d\sigma_{\pi N\to K^+X}(\sqrt{s_1}, \vec{p}_{K^+})}{d\vec{p}_{K^+}}\right]$$

and

$$I_V[A, \sigma^{in}_{pN}(p_0), \sigma^{tot}_{\pi N}(p_\pi), \vartheta_\pi] = A^2 \int\int d\vec{r}\,d\vec{r}_1 \Theta(x_\parallel)\delta^{(2)}(\vec{x}_\perp)\rho(\vec{r})\rho(\vec{r}_1)\times \qquad (28)$$

$$\times \exp\left[-\mu(p_0)\int\limits_{-\infty}^{0} \rho(\vec{r}_1 + x'\vec{\Omega}_0)dx' - \mu(p_\pi)\int\limits_{0}^{x_\parallel} \rho(\vec{r}_1 + x'\vec{\Omega}_\pi)dx'\right].$$

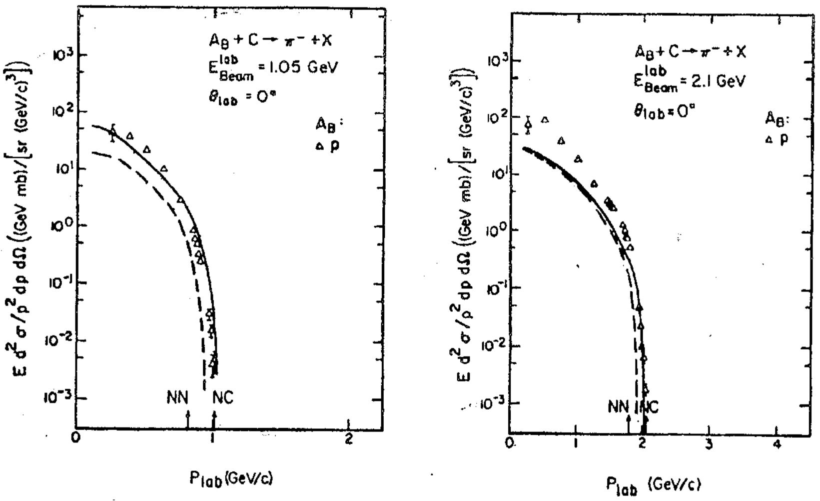

Fig.2. Lorentz invariant negative pion inclusive cross sections versus the (lab) momentum at 0° for 1.05 (left) and 2.1 *GeV* (right) protons interacting with a carbon target.

The experimental data (open triangles) are from [*].

[*]. Moeller, E., Anderson, L., Brückner, W., Nagamiya, S., Nissen-Meyer, S., Schroeder, L., Shapiro, G., Steiner, H.: *Phys. Rev.* **C28**, 1246 (1983).

The curves are calculation: ——— $U^N_{eff} = -34\ MeV$: $m^*_N = m_N + U^N_{eff}$

— — — — — — $U^N_{eff} = 0$: $m^*_N = m_N$

$P + N_1 \to N + N + \pi$,

$P + N_1 \to N + N + 2\pi$.

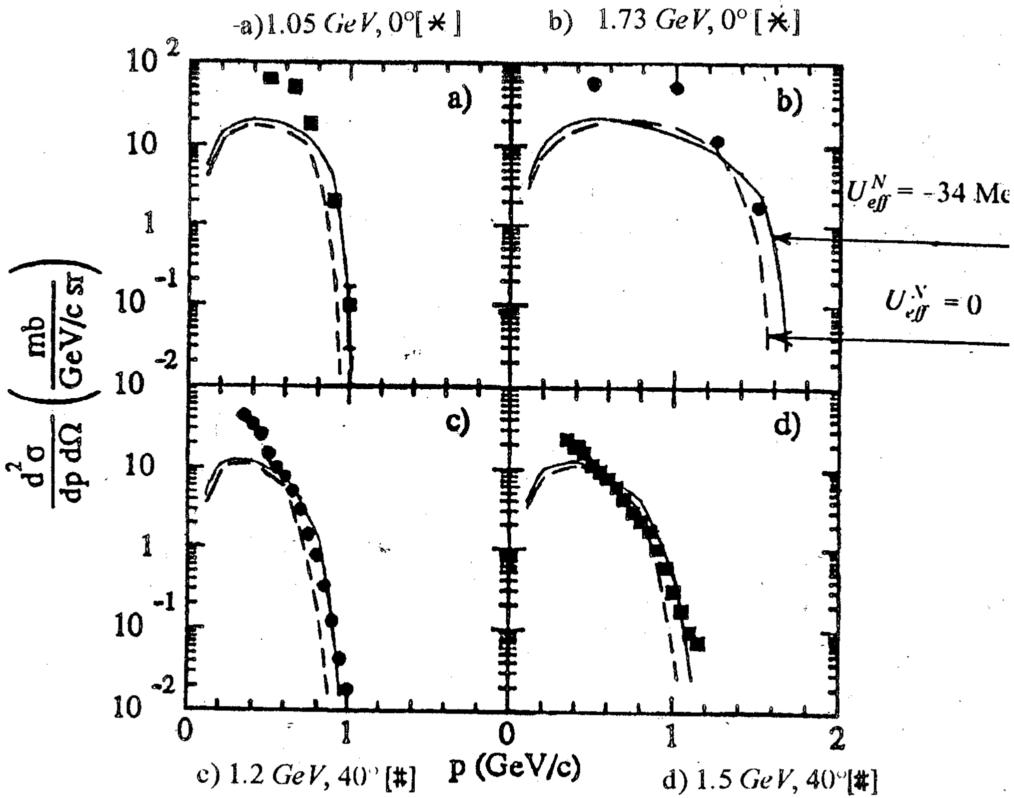

-a) 1.05 GeV, 0°[*] b) 1.73 GeV, 0° [*]

c) 1.2 GeV, 40° [#] d) 1.5 GeV, 40°[#]

Fig.3. Measured and calculated positive pion production cross sections in pC collisions at different bombarding energies and outgoing laboratory angles.

*. Papp, J., Jaros, J., Schroeder, L., Staples, J., Steiner, H., Wagner, A., Wiss, J.: *Phys. Rev. Lett.* **34**, 601 (1975); *Phys. Rev. Lett.* **34**, 991 (1975)

#. Debowski, M., Barth, R., Boivin, M., Le Bornec, Y., Cieslak, M., Comets, M.P., Courtat, P., Gacougnolle, R., Grosse, E., Kirchner, T., Martin, J.M., Miskowiec, D., Müntz, C., Schwab, E., Senger, P., Sturm, C., Tatischeff, B., Wagner, A., Walus, W., Willis, N., Wurzinger, R., Yonnet, J., Zghiche, A.: *Z. Phys.* **A356**, 313 (1996)

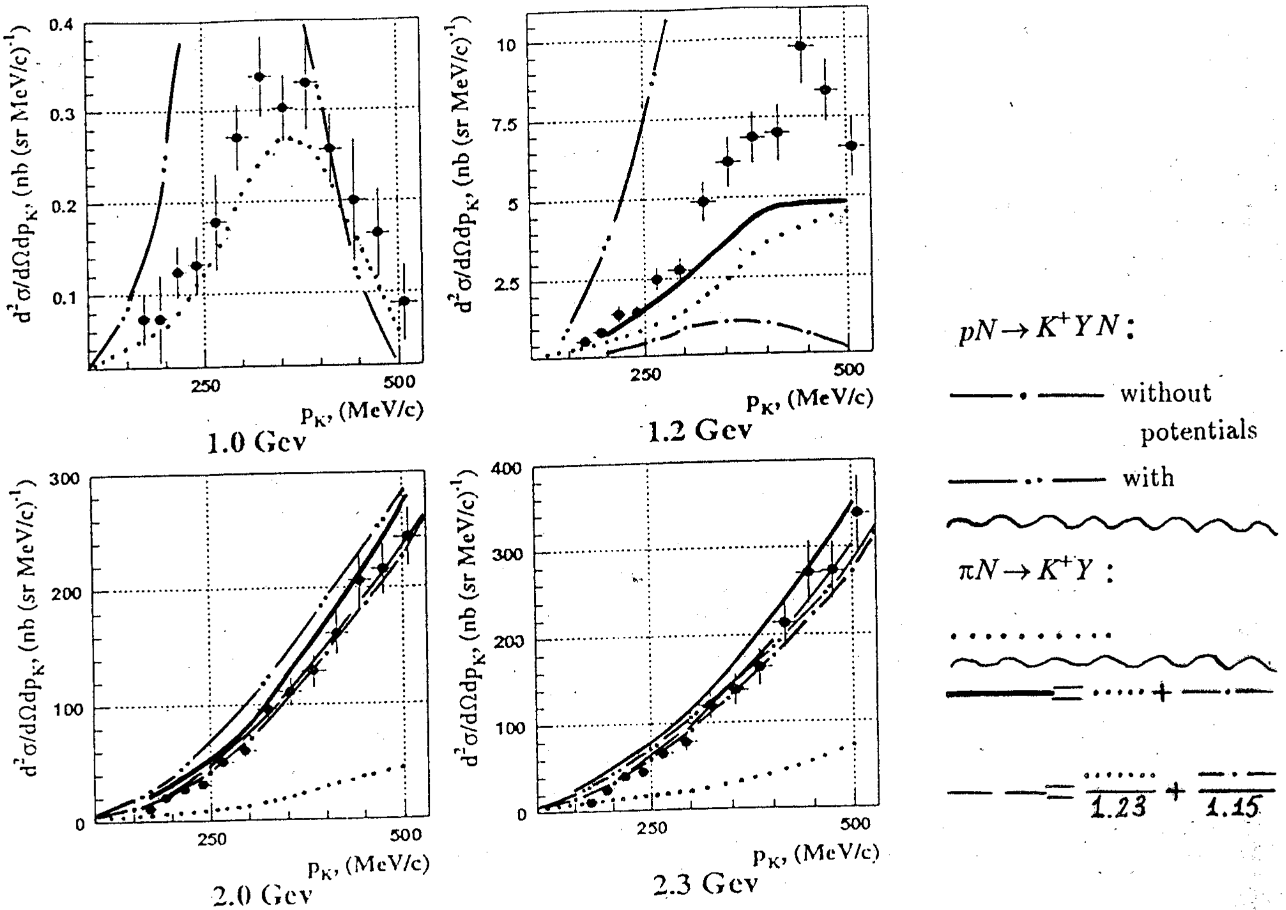

Figure 1: Double differential K^+-production cross section for the reaction $p + {}^{12}C \rightarrow K^+(\vartheta \leq 12°)X$ as a function of the K^+-momentum.

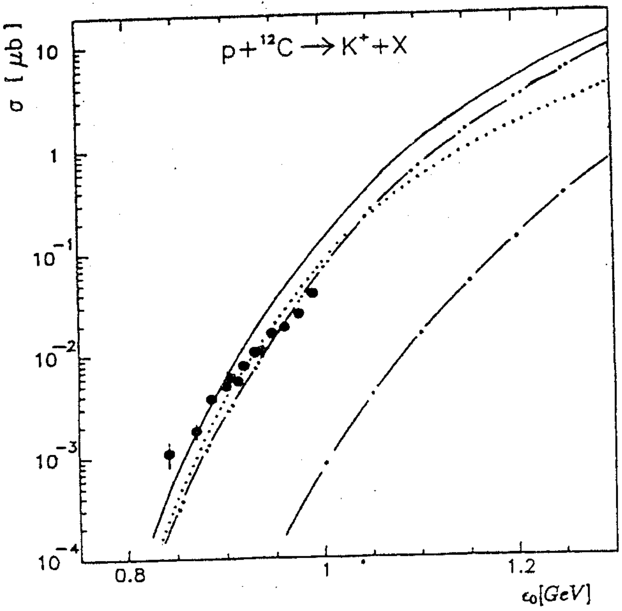

Fig. 9. The total cross sections for K^+ production in $p + C^{12}$ reactions as functions of the laboratory energy of the proton. The experimental data (full dots) are from [1]. The curves are calculation. The dashed lines with one and two dots are calculations for primary production processes (1), (2) with the total nucleon spectral function at $V_0 = 0$, $U^N_{eff} = 0$, $U^\Lambda_{eff} = 0$, $U^\Sigma_{eff} = 0$ and $V_0 = 40\ MeV$, $U^N_{eff} = -34\ MeV$, $U^\Lambda_{eff} = -30\ MeV$, $U^\Sigma_{eff} = -26\ MeV$, respectively. The dotted line is calculations for the secondary production process (22) with Λ particle in the final state at $V_0 = 40\ MeV$, $U^N_{eff} = -34\ MeV$, $U^\Lambda_{eff} = 0$, respectively. The thin solid line is the sum of the dashed line with two dots and dotted line

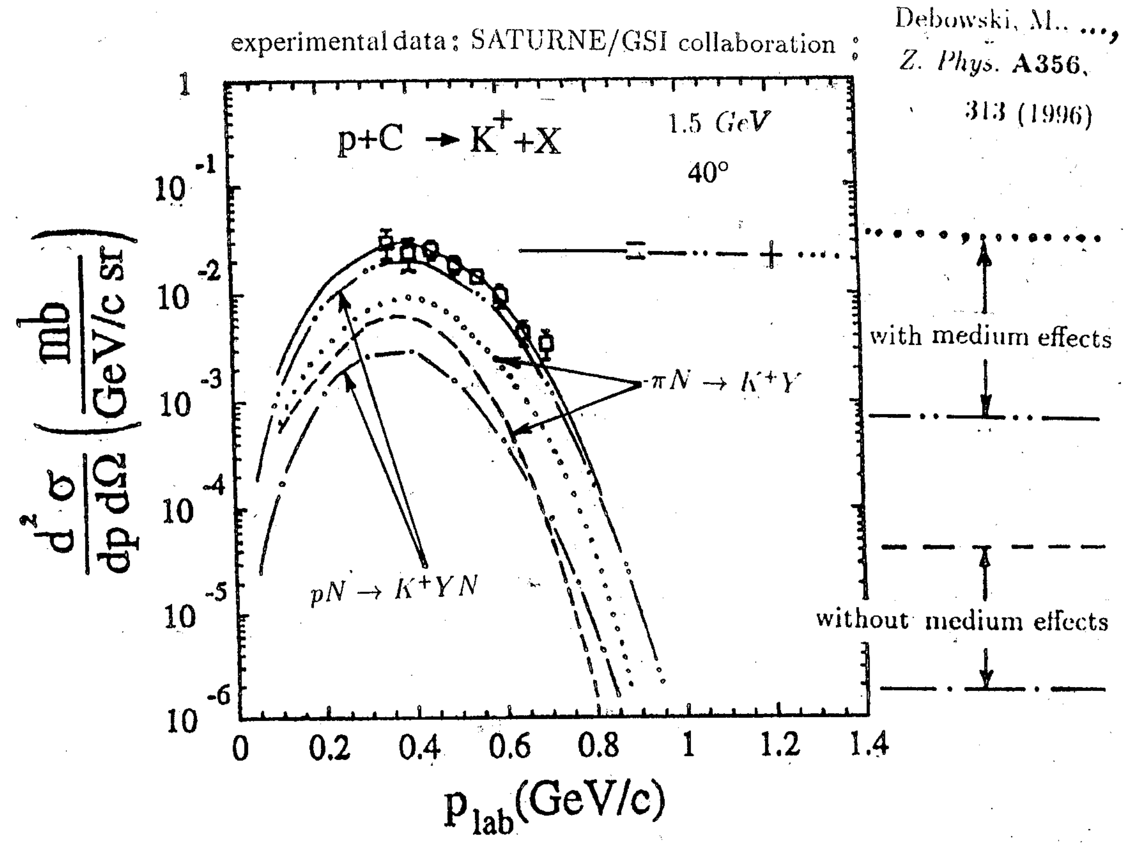

Fig.6. Double differential cross sections for the production of K^+ mesons at an angle of 40° in the interaction of 1.5 *GeV* protons with the C^{12} nuclei as functions of kaon momentum.

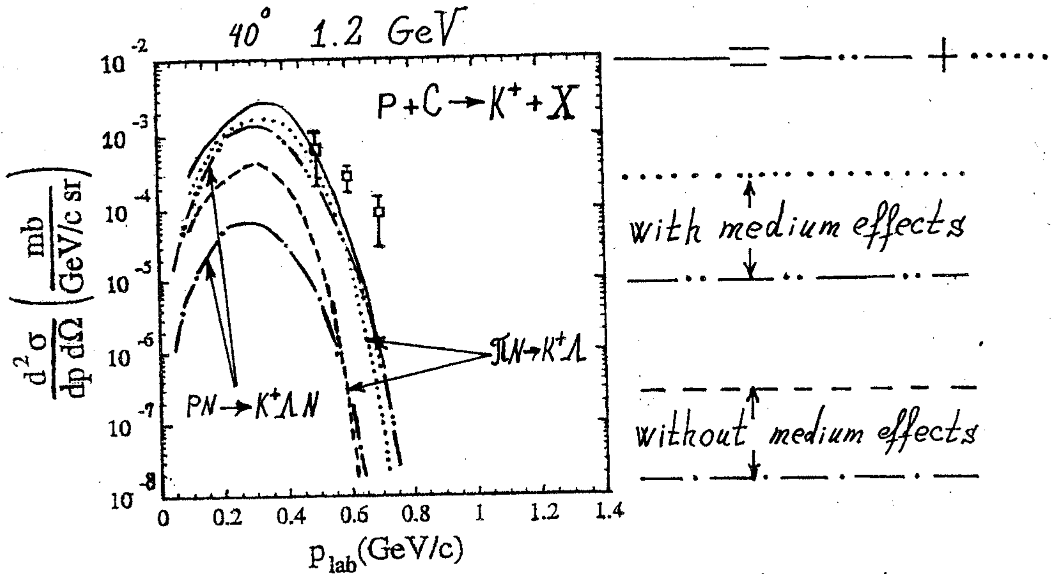

Fig. 5. Double differential cross sections for the production of K^+ mesons at an angle of 40^0 in the interaction of 1.2 *GeV* protons with the C^{12} nuclei as functions of kaon momentum.

Data points:
M. Debowski et. al.:
Z. Phys A356(1996)313.

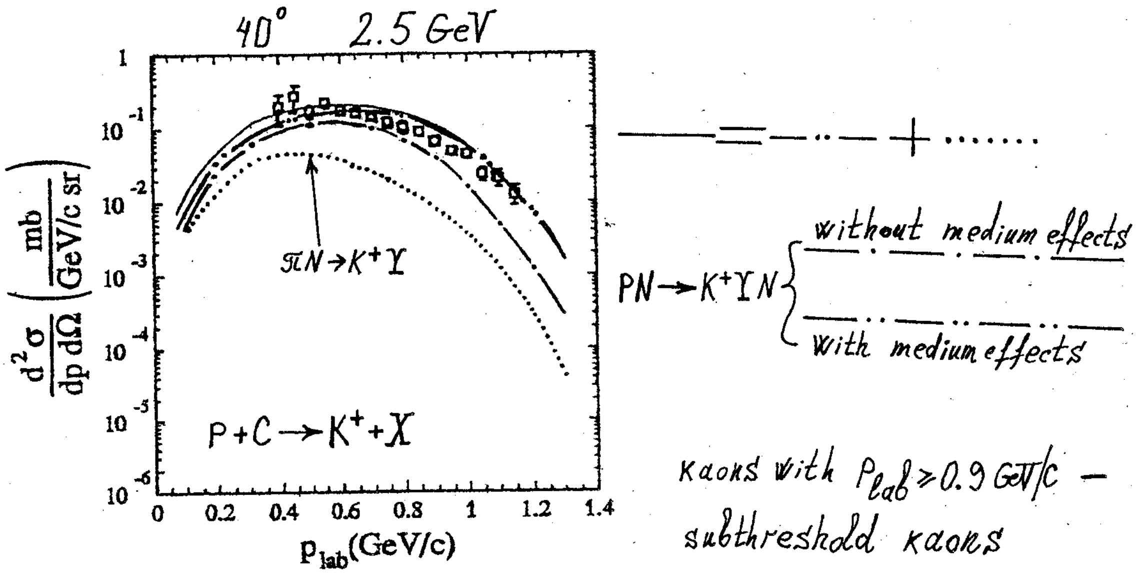

Kaons with $P_{lab} \geq 0.9$ GeV/c – subthreshold kaons

Fig. 7. Double differential cross sections for the production of K^+ mesons at an angle of 40^0 in the interaction of 2.5 *GeV* protons with the C^{12} nuclei as functions of kaon momentum.

Data Points: M. Debowski et al.,
Z. Phys. A 356 (1996) 313.

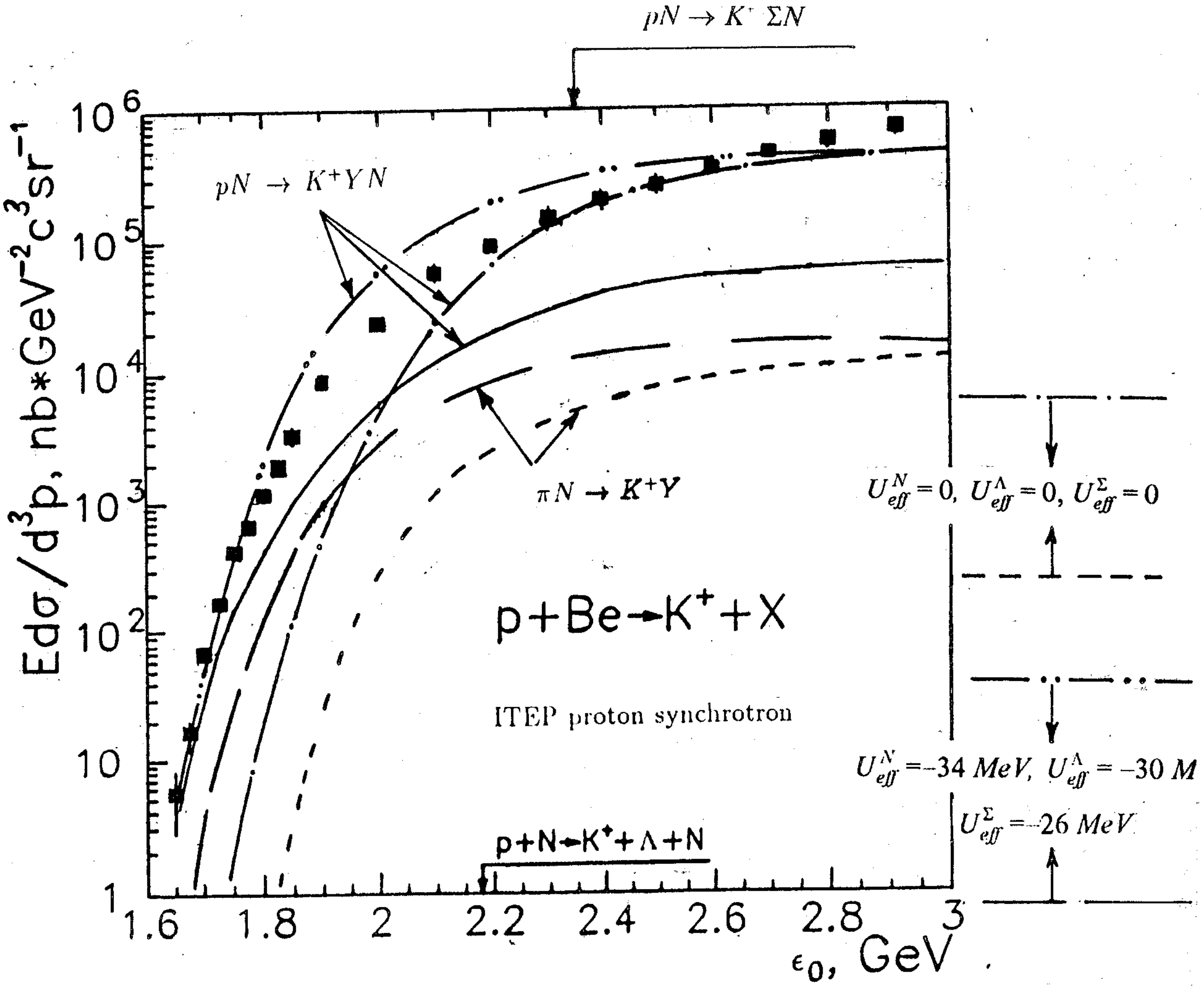

Fig.4. Lorentz invariant cross sections for the production of K^+ mesons with momentum of 1.28 *GeV/c* at the lab angle of 10.5° in $p + Be^9$ reactions as functions of the laboratory energy of the proton. The experimental data (full squares) are from [*].

*, Akindinov, A.V., Chumakov, M.M., Kiselev, Yu.T., Martemyanov, A.N.; *APH N.S., Heavy Ion Physics* **4**, 325 (1996)

——— denotes the same as —··— but it is supposed that:

$$P(p_t, E) \Rightarrow P_1(p_t, E)$$

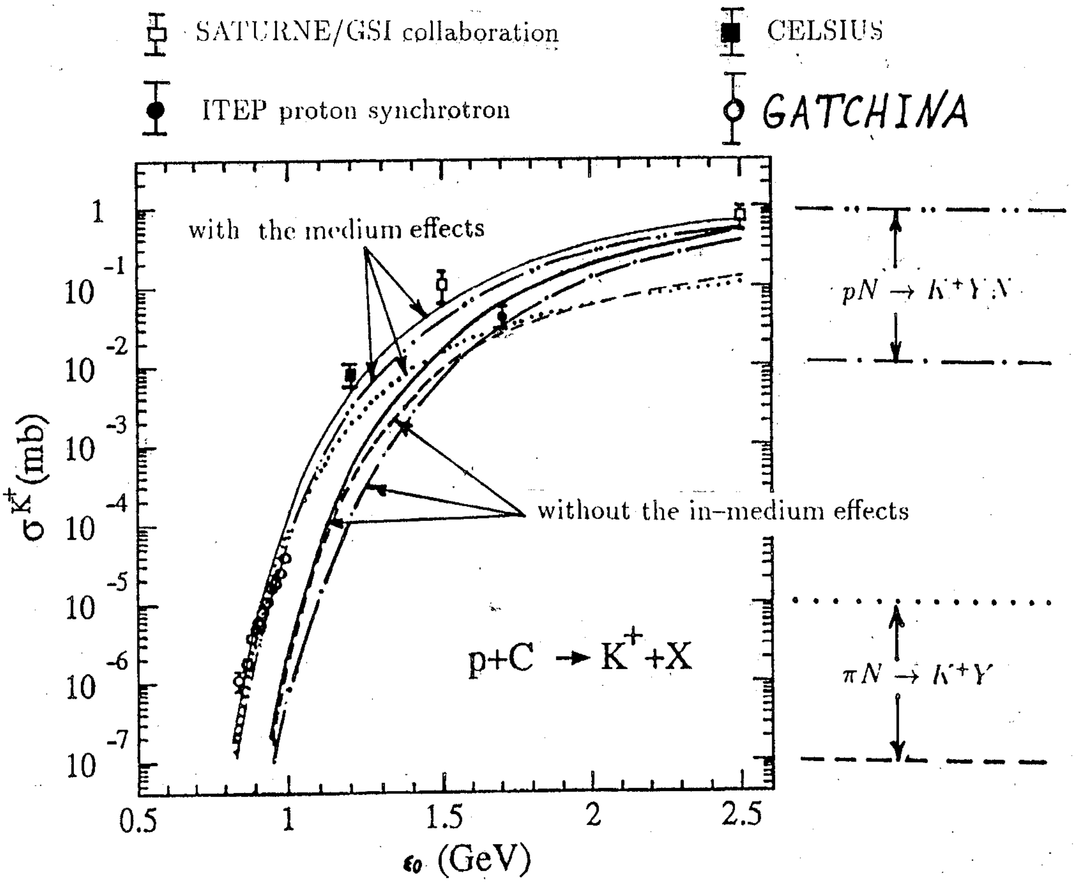

Fig.10. The total cross sections for K^+ production in $p + C^{12}$ reactions as functions of the laboratory energy of the proton.

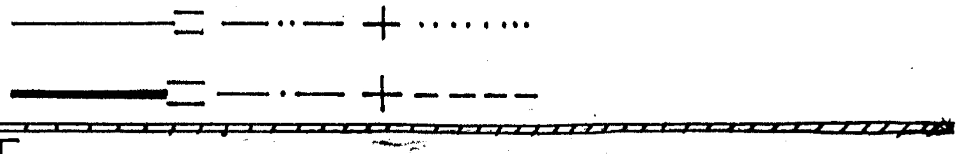

☐ Debowski, M.,..., *Z. Phys.* **A356**, 313 (1996)

● Kiselev, Yu.T., Sheinkman, V.A.: Private communication

○ Koptev et al.: *ZhETF.* **94**, 1 (1988)

■ Badala, A.,..., Phys. Rev. Lett. 80, 4863(1998)

Summary

1). The data on K^+ production on light nuclei (C, Be) at energies $T_0 \approx 1.0 \div 1.5$ GeV and lab. angles $\theta_{K^+}^{lab} \approx 30 \div 40^\circ$ are needed (from ANKE Collaboration) both to reliably test the spectral function approach presented here and to deeply elucidate the underlying mechanism of subthreshold kaon production.

2). The data on excitation functions for "hard" K^+ production ($P_{K^+}^{lab} \approx 1$ GeV/c, $\theta_{K^+}^{lab} \approx 0^\circ$) are needed as well for the same purpose.

Systematical theoretical analysis of K^+–meson production in proton–nucleus collisions at energies below 3 GeV

A.Sibirtsev

Institut für Kernphysik
Forschungzentrum Jülich
52425 Jülich
Germany

The description of particle production in hadron-nucleus collision should be considered relative to an energy scale given by the binding energy of the target nuclei. The impulse approximation is an appropriate basis when the projectile energy is much higher than the binding energy and the target nucleons can be taken as free particles.

However, at low bombarding energies the nuclear structure might play an essential role in the production process. When the bombarding energies are below the reaction threshold in free space the production process proceeds according to the total energy available from the target. The reaction mechanism can no longer be considered as an interaction of the projectile with a quasi-free target nucleons, but instead as an interaction with the whole nucleus, which might be approximated by the sum over the interactions with one nucleon (single scattering approximation), two nucleons (two-nucleon current) and further many-body collisions.

In momentum space these many-body effects can be interpreted in terms of high momentum components of the nuclear wave function. These high momentum components of the nuclear wave function can be reasonably well described by short range two-nucleon correlations. In this sense the contribution from the high momentum components to particle production can be considered as a reaction mechanism due to the two-nucleon current.

We study the K^+-meson production from nuclei at energies below 3 GeV. We consider both direct strangeness production mechanism due to the collision of incident proton with target nucleons and two step production mechanism with intermediate pions. The elementary $pN \to K^+\Lambda N$ production amplitude is reasonably well fixed by recent experimental results from COSY. The elementary $pN \to \pi N$ and $\pi N \to K^+\Lambda$ amplitudes are as well known from available data.

Since K^+-mesons only weakly interact with the nuclear medium due to the strangeness conservation, the information about the production mechanism does not get distorted significantly. This is essential in evaluation of strangeness production mechanism from the data.

Systematical Theoretical Analysis of K^+-meson production in proton-nucleus collisions at energies below 3 GeV

A. Sibirtsev
IKP, Forschungszentrum Jülich

- There are a variety of models for strangeness production in proton-nucleus and heavy ion collisions. These models are based on a quite different theoretical assumptions about the reaction dynamics and underlying strangeness production mechanisms.
- Most of the model calculations are able to reproduce the data on total K^+-meson production cross section in p+A collisions at proton beam energies from 840 to 990 MeV.
- It might be that the data on total K^+-meson production cross section are not sensitive to the dynamics of strangeness production.
- It might be possible, that more differential data can be more selective to the underlying theory
- However, there are no results from a systematical theoretical analysis of strangeness production in p+A collisions available from any of the known models.

Folding model

- In terms of the multiple scattering theory the kaon production in p+A collisions can be described as an incoherent sum of the two-body interactions.
- In nuclear matter the incident proton interacts with the target nucleon, which has a certain internal momentum q_T and total energy E_T.
- The joint probability to pickup a target nucleon with the momentum q_T and total energy E_T is given by nuclear spectral function. Note that in nuclei

$$E_T \neq \sqrt{q_T^2 + m_N^2}. \tag{1}$$

- The amplitude of the meson production in the interaction of the incident proton with the target nucleon can be evaluated from the data available in free space. The K^+-meson production involves the data on:
- $p+N \rightarrow N + Y+K^+$ reaction in free space, with N denoting proton or neutron, and Y being Λ or Σ-hyperon.
- $p+N \rightarrow \pi+X$ and $\pi+N \rightarrow Y+K^+$ reactions.
- Details are given in A. Sibirtsev, W. Cassing and U. Mosel, Z. Phys. A 358 (1997) 357.

Systematical analysis of K^+ meson production in $p+A$ collisions within the Folding Model. SATURNE data

K^+-meson production at emission angle θ_K=40^0 in $p+C$ and $p+Pb$ collisions at T_p=1.2 GeV. M. Debowski et al., Z. Phys. A **356**, (1996) 313.

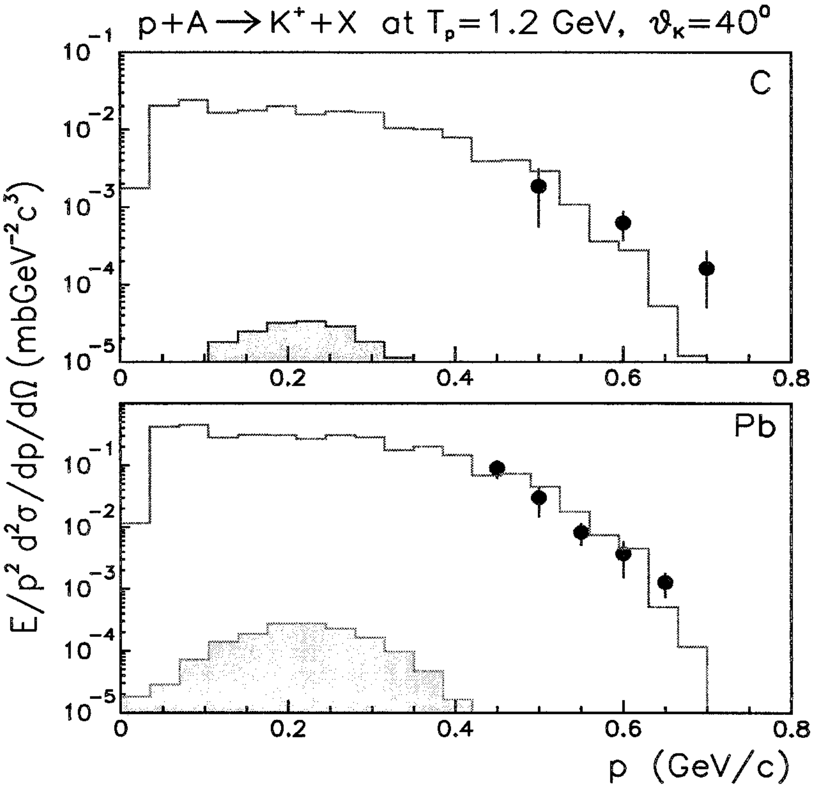

The histograms indicates the FM calculations. The hatched histograms show the contribution only from the direct production mechanism.

Systematical analysis of K^+ meson production in p+A collisions within the Folding Model. SATURNE data

K^+-meson production in p+C and p+Pb collisions at T_p=1.5 GeV at the emission angle θ_K=40^0. M. Debowski et al., Z. Phys. A **356**, (1996) 313.

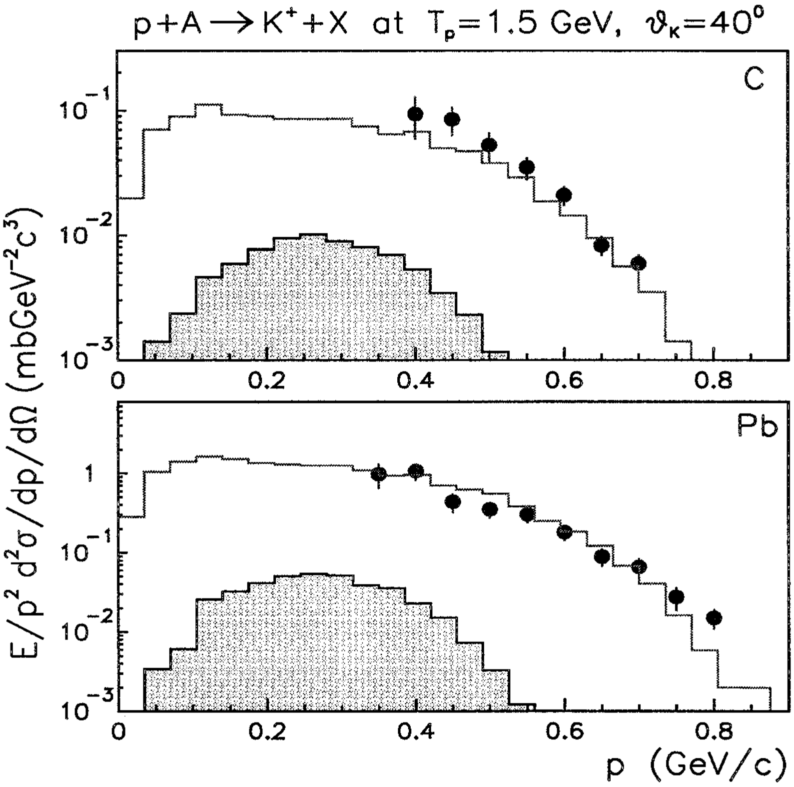

The histograms indicates the FM calculations. The hatched histograms show the contribution only from the direct production mechanism.

Systematical analysis of K^+ meson production in p+A collisions within the Folding Model. SATURNE data

K^+-meson production at θ_K=40^0 in p+C collisions at T_p=2.5 GeV. Data published in M. Debowski et al., Z. Phys. A **356**, (1996) 313.

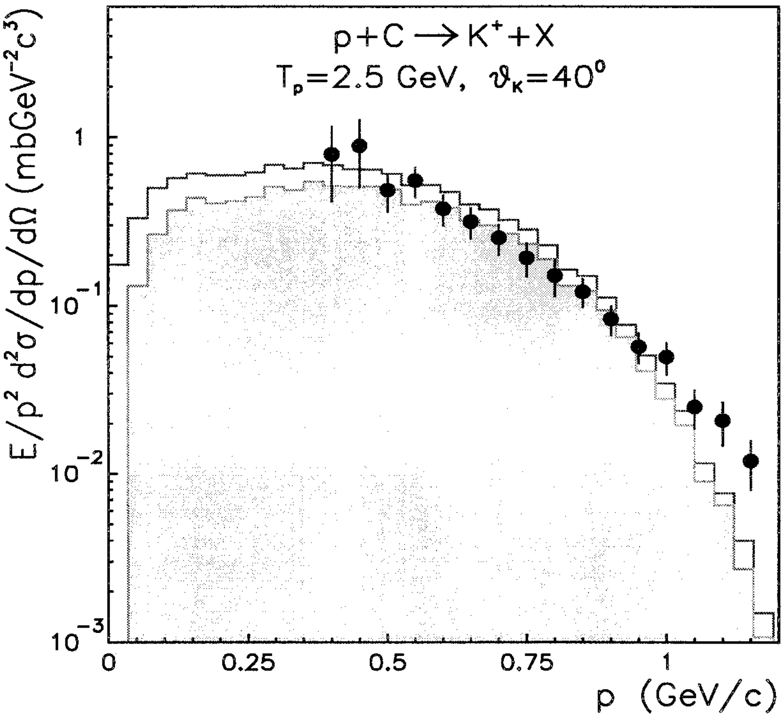

The histograms indicates the FM calculations. The hatched histograms show the contribution only from the direct production mechanism.

Systematical analysis of K^+ meson production in $p{+}A$ collisions within the Folding Model. LBL data

K^+-meson production at emission angles θ_K=15^0, 35^0, 60^0 and 80^0 induced by 2.1 GeV protons on *Pb*. S. Schnetzer et al., Phys. Rev. C **40**, (1989) 640.

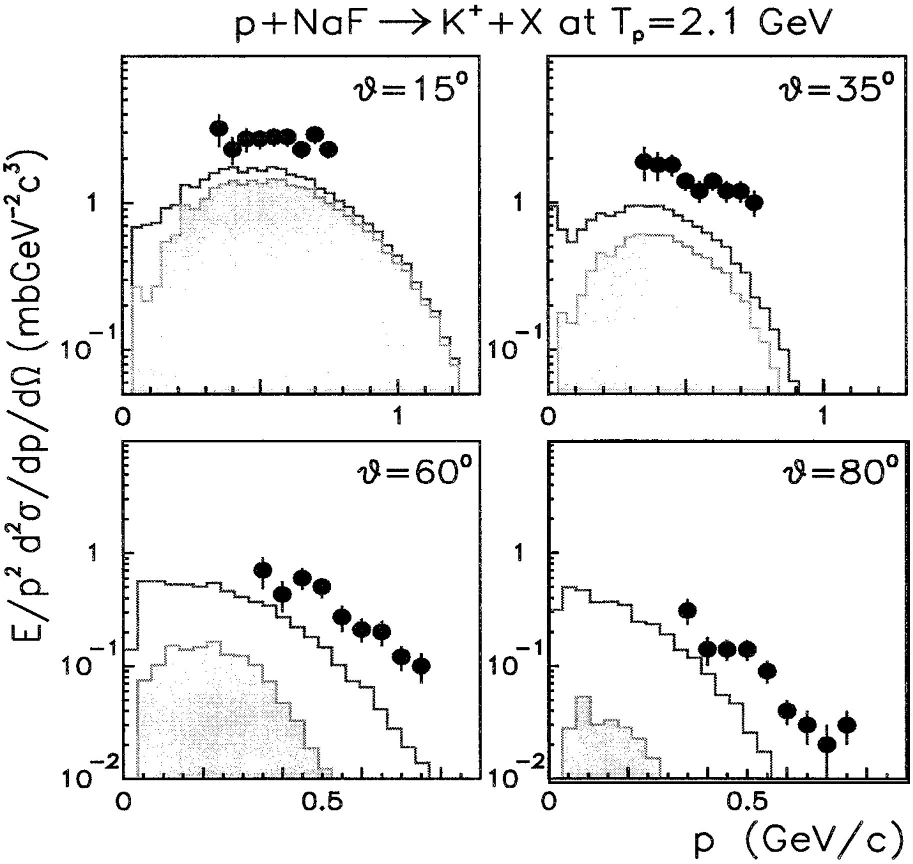

The histograms indicates the FM calculations. The hatched histograms show the contribution only from the direct production mechanism.

Systematical analysis of K^+ meson production in p+A collisions within the Folding Model. LBL data

K^+-meson production at emission angles θ_K=15^0, 35^0, 60^0 and 80^0 induced by 2.1 GeV protons on NaF. S. Schnetzer et al., Phys. Rev. C **40**, (1989) 640.

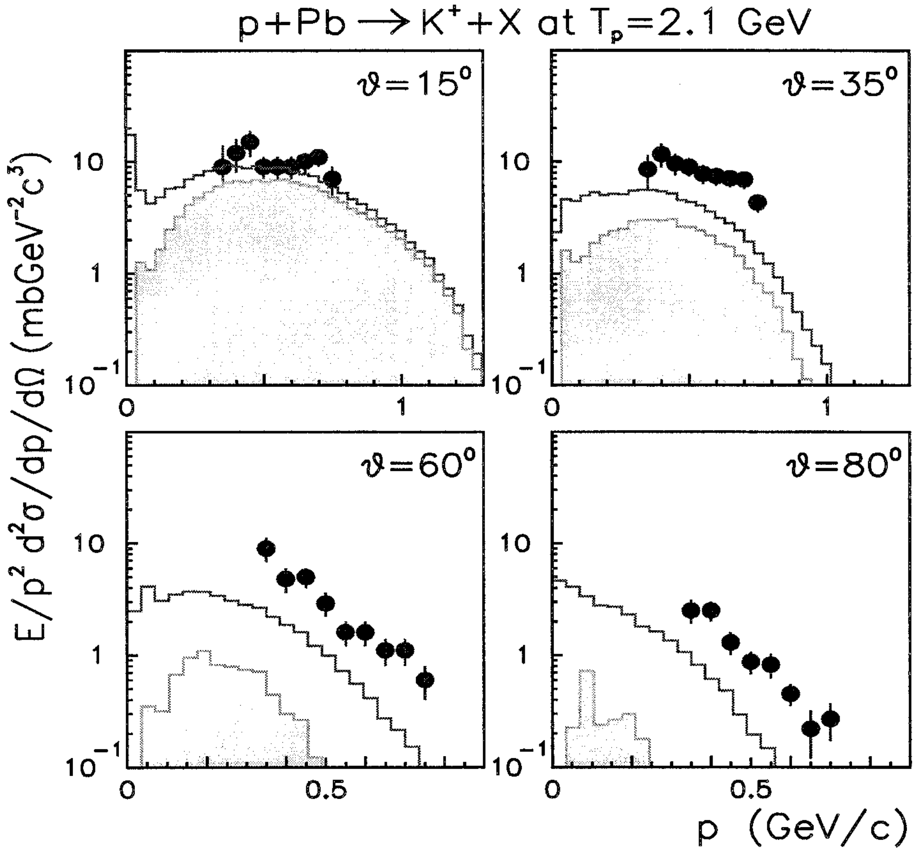

The histograms indicates the FM calculations. The hatched histograms show the contribution only from the direct production mechanism.

Systematical analysis of K^+ meson production in p+A collisions within the Folding Model. CELSIUS data

K^+-meson production at emission angle θ_K=90^0 induced by 1.2 GeV protons on C target. A. Badala et al., Phys. Rev. Lett. **80**, (1998) 4863.

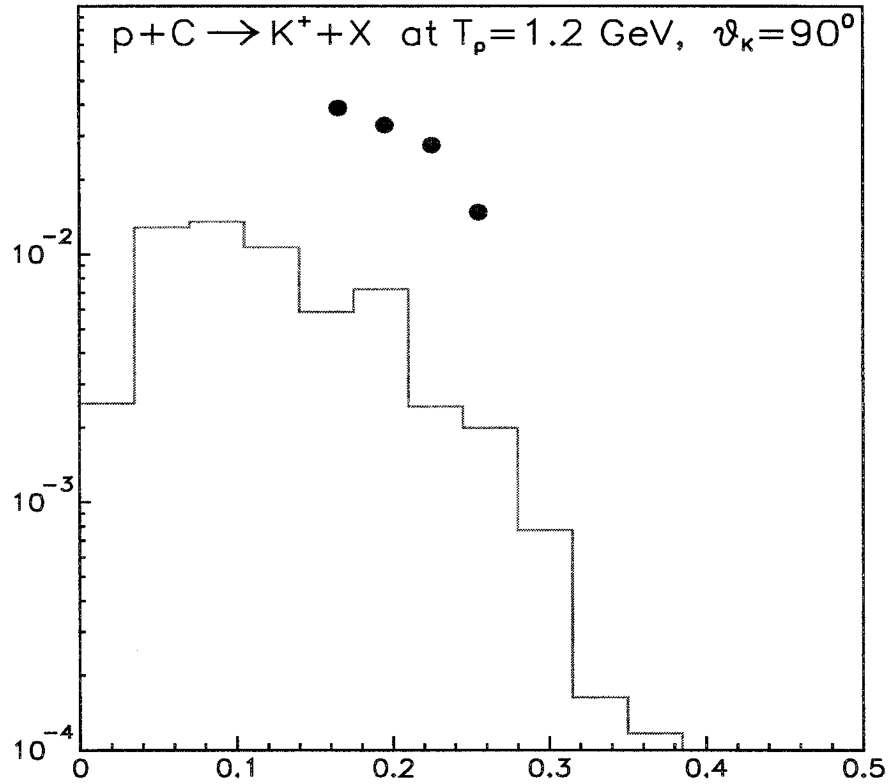

The histograms indicates the results from FM calculations.

Systematical analysis of K^+ meson production in $p+A$ collisions within the Folding Model. ANKE-COSY data

K^+-meson production at emission angles $0 \leq \theta_K \leq 12^o$ induced by T_p=1 GeV protons on C, Cu and Au targets has been recently studied by ANKE at COSY.

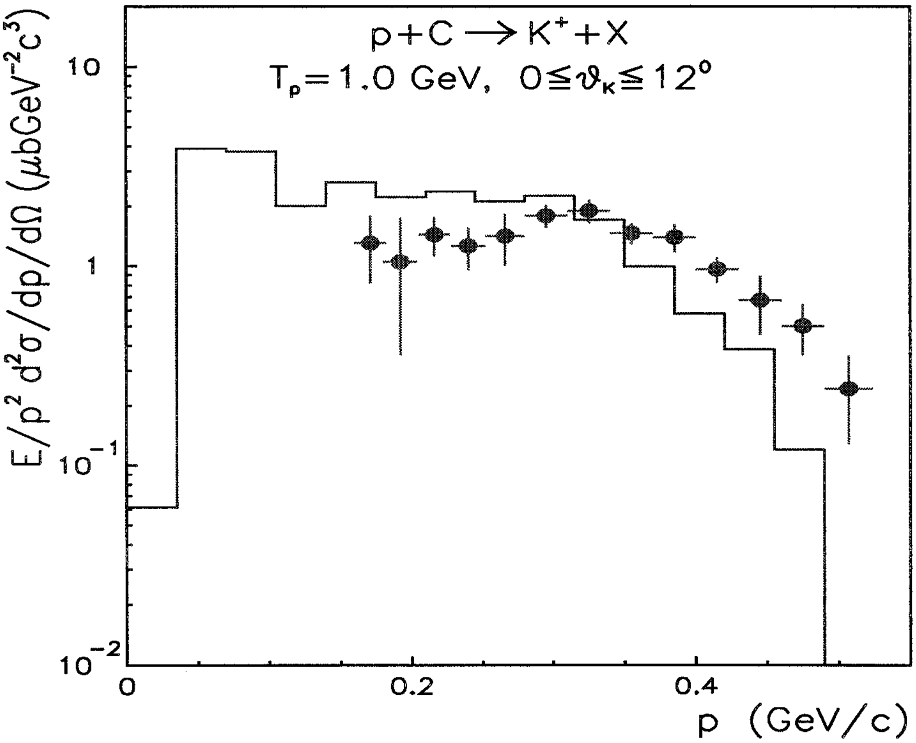

The histogram indicates the result from FM calculations.

Summary

- The SATURNE and ANKE data on differential K^+-meson production cross section available at proton beam energies T_p from 1.0 GeV to 2.5 GeV can be well described by the Folding Model calculations.

- The folding model calculations could not reproduce the large part of the LBL data at proton beam energy of 2.1 GeV. The FM calculations substantially underestimates data especially at large kaon production angles.

- The FM calculations could not describe the CELSIUS data at T_p=1.2 GeV and kaon emission angle θ_K=90^0.

- The partial discrepancy between the FM calculations and the data might indicate the physics beyond that incorporated by the model.

- Obviously, there are needs for more data at the beam energy range from 1.0 to 2.5 GeV in order to clarify the situation.

K^+-meson production in proton-nucleus interactions near threshold

H.Müller
(presented by M.Büscher)

Institut für Kern- und Hadronenphysik
Forschungszentrum Rossendorf
01314 Dresden
Germany

In the ROC model a nuclear reaction is described on the basis of the participant-spectator picture. Each interaction of the incident proton with the target nucleus (AZ) consisting of A nucleons and Z protons is characterized by the number a of target nucleons and z of target protons involved in the reaction. The cross sections σ_{az} for the interaction of the projectile with (az) target nucleons are calculated on the basis of a probabilistic interpretation of the Glauber theory [2]. A multi-step picture is proposed to describe the interaction process, where a group of (az) participating target nucleons is treated as a single entity. In the first step translational energy is converted into internal excitation energy of subsystems emerging from the projectile-participant interaction and of the residual nucleus containing $A - a$ nucleons and $Z - z$ protons.

The excited subsystems contain the valence quarks of the participants and additional quark-antiquark pairs created during the collision. In the second stage of the reaction all quarks recombine randomly to baryons and mesons in accordance with the rules of quark statistics [3]. Primarily produced resonances decay further into stable hadrons. The structure of the residual nucleus is disturbed by the primary projectile-participant reactions as well as by secondary interactions of the outgoing particles with the nuclear environment. Thus, the residual nucleus becomes excited too, and may break into several fragments. During the second stage of the reaction all channels α_{az} are populated, which are allowed by quantum number conservation. By introducing the relative probability $\mathrm{d}W_{az}(s;\alpha_{az})$ of populating the channel α_{az} the differential cross section is calculated as an incoherent sum

$$\mathrm{d}\sigma(s) = \sum_{a=1}^{A} \sum_{z=max(0,a-Z)}^{min(a,Z)} \sigma_{az} \sum_{\alpha_{az}} \mathrm{d}W_{az}(s;\alpha_{az}) \tag{1}$$

with s denoting the square of the CM energy of the projectile-target system. The cross sections σ_{az} depend on the nucleon density in the target nucleus and on the elementary NN cross section σ_{NN}. For details concerning the calculation of σ_{az} the reader is referred to [4]. The quantities

$$\mathrm{d}W_{az}(s;\alpha_{az}) \propto \mathrm{d}L_n(s;\alpha_{az})A^2(\alpha_{az}) \tag{2}$$

describe the collision dynamics, the relative probabilities of the various channels and the distribution of the final particles in phase-space. They are given by the Lorentz-invariant phase-space factor $\mathrm{d}L_n(s;\alpha_{az})$ of the n primarily produced final particles times the square of the empirical reaction matrix element $A^2(\alpha_{az})$.

The matrix element is split into factors describing the relative momentum distribution between the residual nucleus and the participants, the interaction of the projectile with the participants and the excitation and subsequent decay of the various subsystems.

The ROC model aims at a simultaneous description of both hadronic *and* nuclear reactions. For the present investigation the same parameter values are taken as in a recent paper about particle production in pp interactions up to ISR energies [1]. In case of nuclear interactions some of the parameter values depend on the number of participants in a similar way as described in [5]. The treatment of the residual nucleus is discussed in [4].

The ROC model is implemented as a Monte-Carlo generator which samples complete events from which nearly all kinds of measurable quantities can be deduced and compared with experimental results. As an example in fig. "Papp" the production of pions and protons in pA interactions at various energies is considered. The overall agreement between data and calculations is quite satisfactory. In case of K^+ production the resulting picture is rather controversial. While the LBL data (fig. "LBL") are strongly underestimated we observe in case of the ANKE data (fig. "ANKE") a much too high calculated cross section, except the high-momentum part at 1.0 GeV, which is again underestimated. Only for the SPESIII data (fig. "SPES3") a satisfactory agreement between data and calculations could be achieved. It should be stressed, however, that the data are measured under quite different kinematical conditions. Therefore, a direct comparison of the data is difficult. Further considerations are necessary in order to understand the observed discrepancies. Possible improvements are a more refined treatment of the residual nucleus and the inclusion of a high-momentum component in the internal momentum distribution of the nucleus.

References

[1] H. Müller. Eur. Phys. J. C **18**, 563 (2001)

[2] R. J. Glauber, J. Mathiae. Nucl. Phys. B **21**, 135 (1970)

[3] V. V. Anisovich, V. M. Shekhter. Nucl. Phys. B **55**, 455 (1973)

[4] H. Müller, K. Sistemich. Z. Phys. A **344**, 197 (1992)

[5] H. Müller. Z. Phys. A **353**, 103 (1995)

Data : ANKE

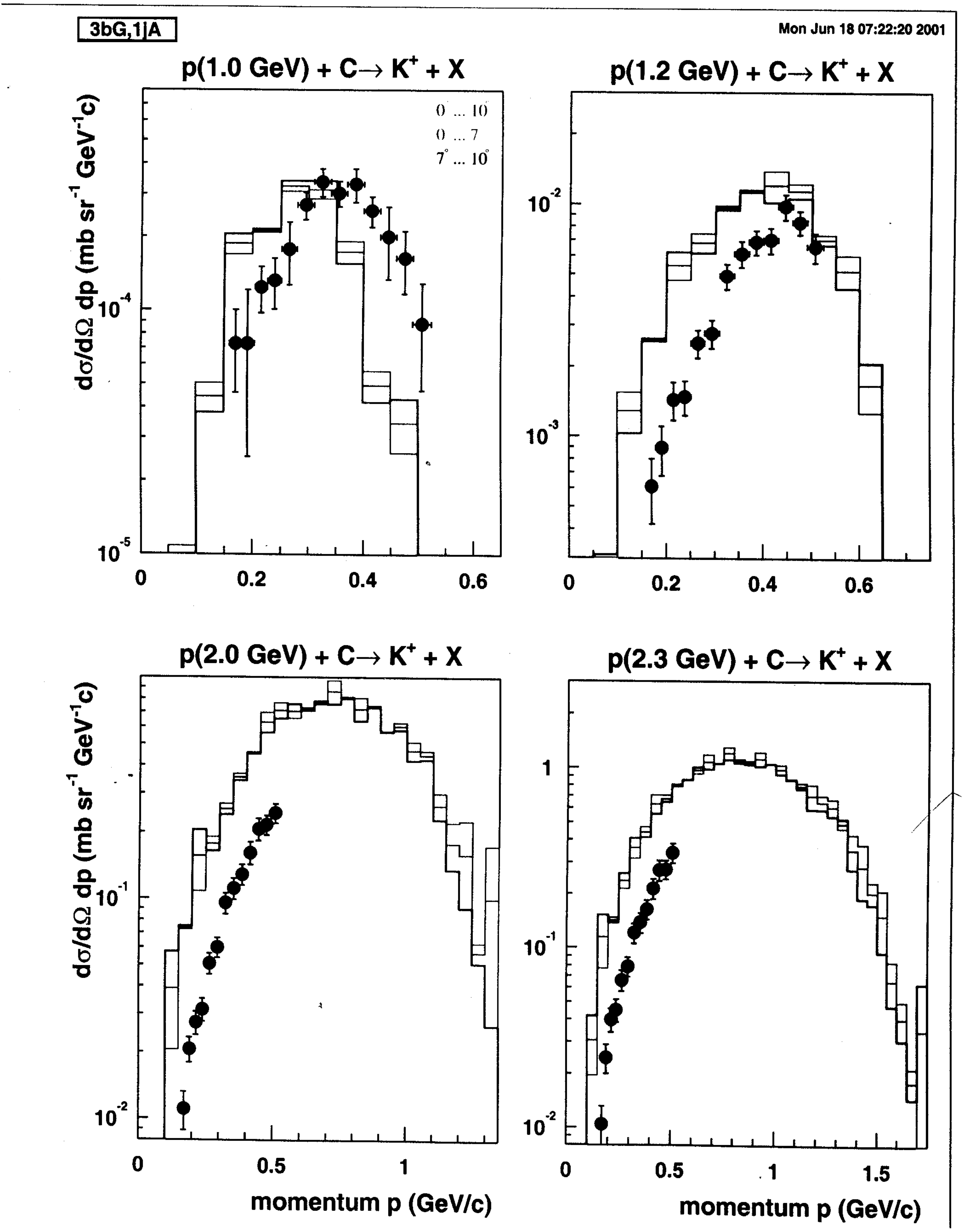
3bG,1|A
Mon Jun 18 07:22:20 2001
p(1.0 GeV) + C→ K⁺ + X
p(1.2 GeV) + C→ K⁺ + X
p(2.0 GeV) + C→ K⁺ + X
p(2.3 GeV) + C→ K⁺ + X
0° ... 10°
0 ... 7
7° ... 10°
dσ/dΩ dp (mb sr⁻¹ GeV⁻¹c)
10⁻⁵
10⁻⁴
10⁻³
10⁻²
10⁻¹
1
0
0.2
0.4
0.6
0.5
1
1.5
momentum p (GeV/c)

Data : ANKE , 1.0 GeV

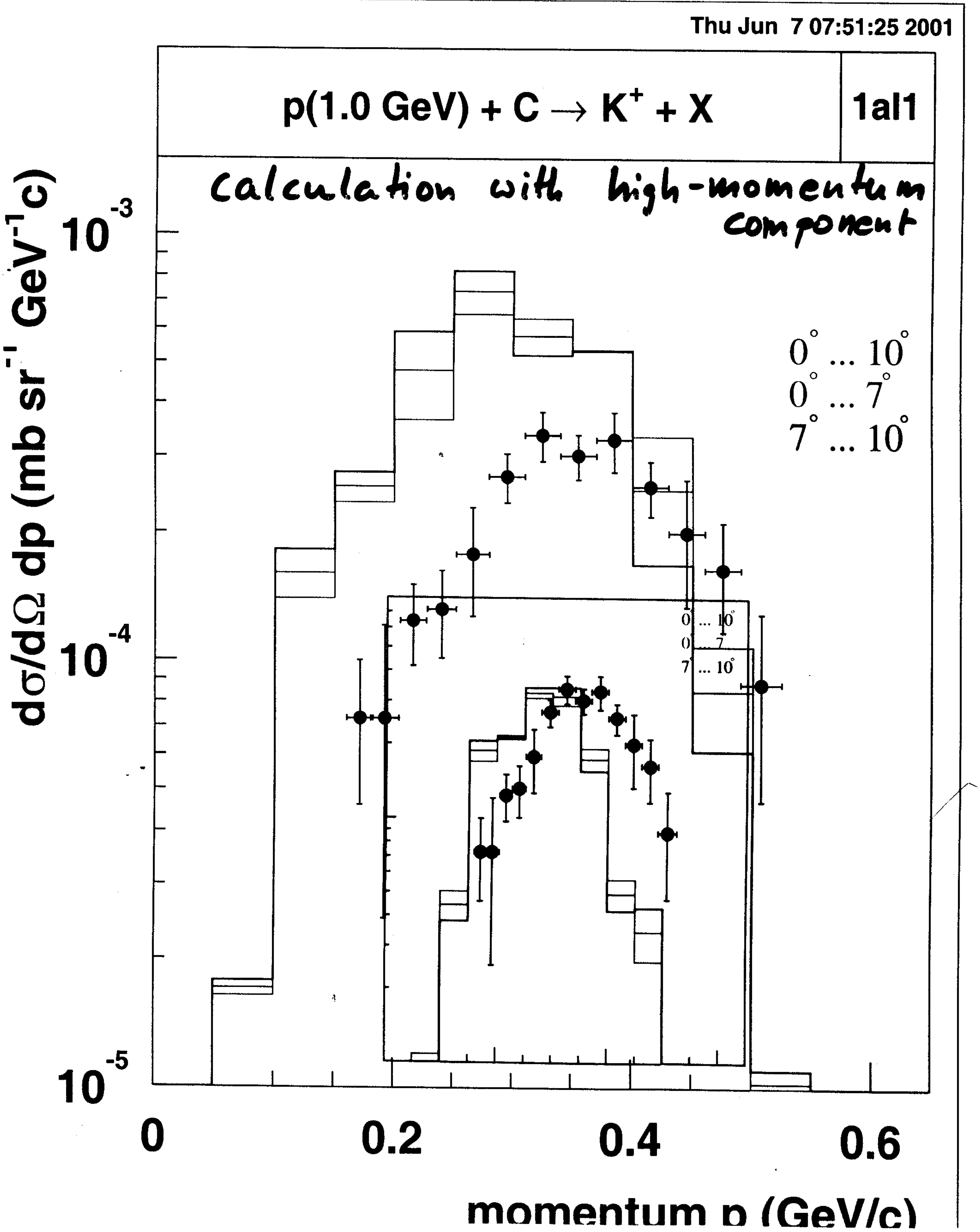

Thu Jun 7 07:51:25 2001

Calculation with high-momentum component

Data : Papp et al. (used for normalization of ANKE data)

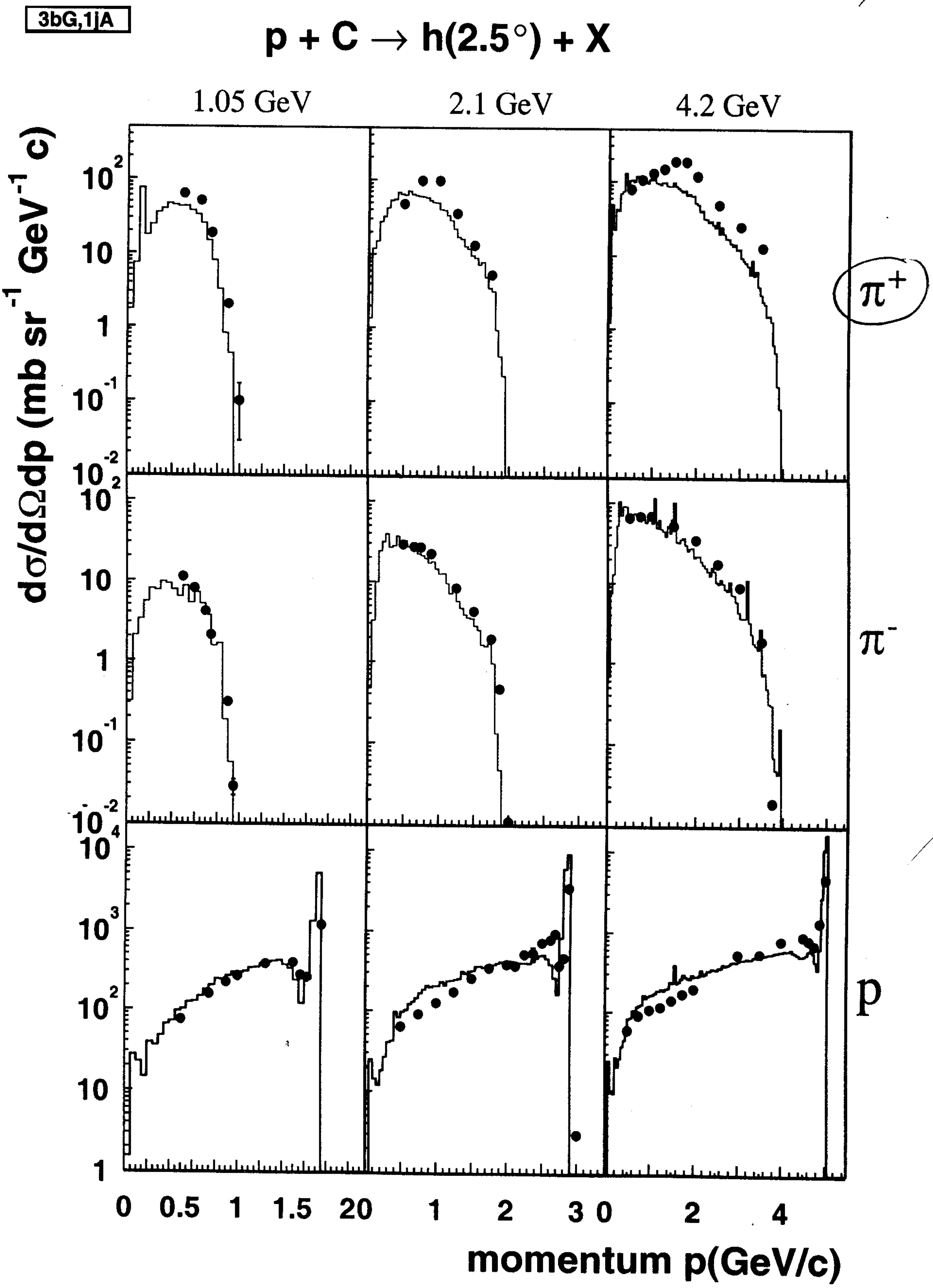

Data : Schnetzer et al., LBL

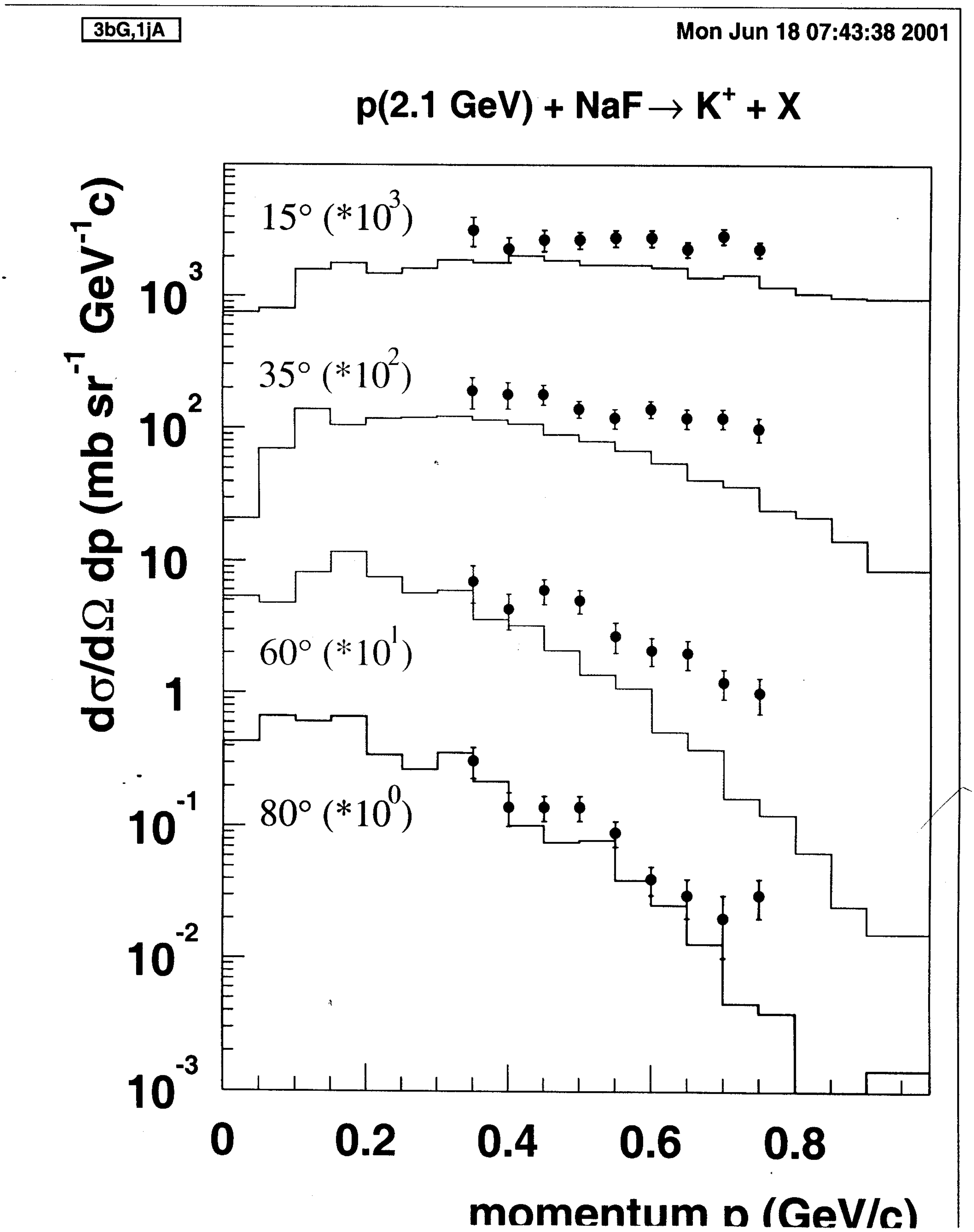

Data: Debowski et al., SATURNE

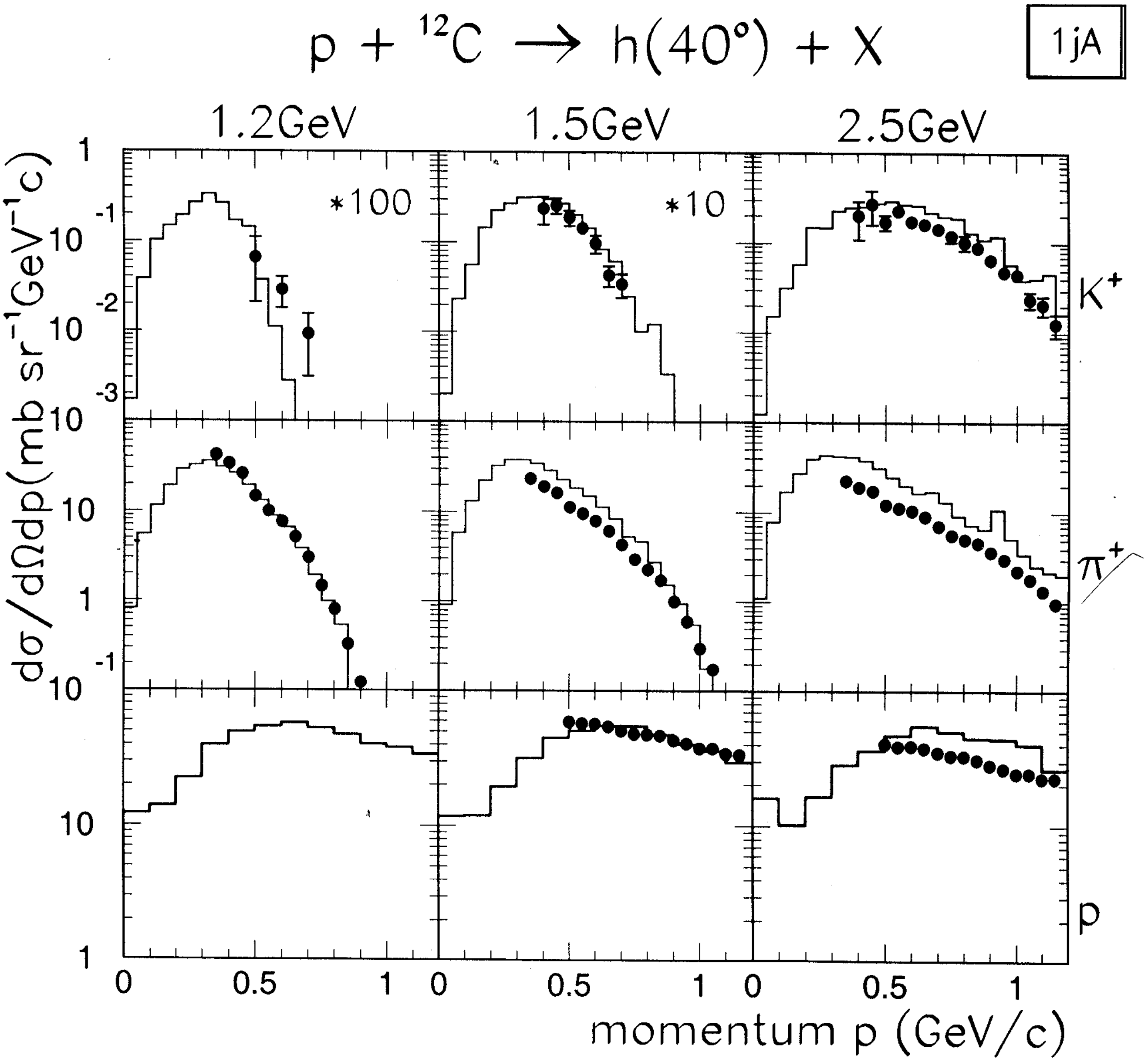

K^+-production: comparison with other data

Kaons with 500 MeV/c (545 MeV/c)

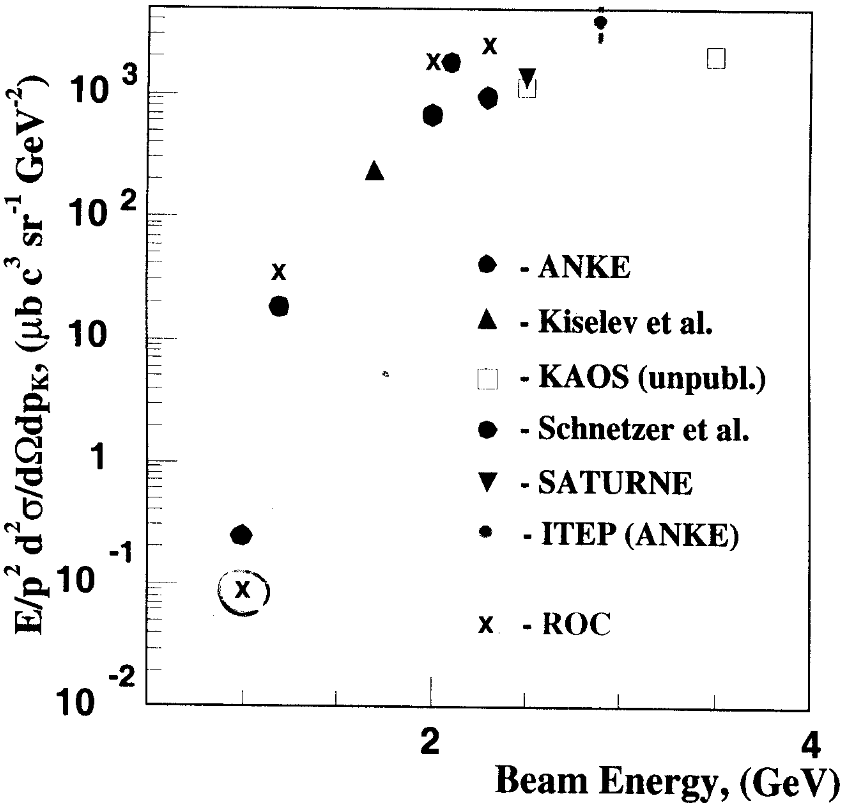

Energy dependence, pC → K^+ X, ϑ=0°

(x) - total cross section ~factor 3 too LARGE

M.Büscher, 5/01

What have we learned about K^+-production in nuclei?

W.Cassing

Institut für Theoretische Physik
D-35392 Giessen
Germany

The ANKE Collaboration has presented a systematic set of differential K^+ spectra at this workshop that ranges in bombarding energy from 1.0 – 2.3 GeV for light targets such as ^{12}C up to heavy targets as ^{197}Au. The data from V. Koptev on total cross sections below 1 GeV (taken more than a decade ago) show a scaling in mass of exponent $\alpha \approx 1$ which lead to the early suggestion, that a two-step mechanism ($pN \to \pi NN, \pi N' \to K^+Y$) might be responsible for the surprisingly large cross sections seen experimentally. This exponent, however, is not observed in the differential data of ANKE at 1.0 GeV taken in the forward direction. A. Sibirtsev has demonstrated within the folding model - employing one-step and two-step production mechanisms as well as realistic spectral functions for the targets - that the existing data on K^+ production for pA reactions can approximately be described in this 'almost parameter free' model. An exception seem to be the BEVALAC data at 2.1 GeV which appear too high by about a factor of 2 especially in forward direction as well as data taken at large angles. Such calculations show the dominance of the two-step mechanism for low bombarding energies and the leading one-step mechanism at high energy. But, do we really understand the ANKE data within this framework?
E. Paryev, furthermore, has demonstrated within his folding model that attractive nucleon potentials are necessary to properly describe the high momentum pion spectra and the K^+ yield at high laboratory momentum (from ITEP), where the one-step mechanism seems to play the major role. But what about the momentum-dependence of the nucleon potentials in the entrance and exit channels? These potentials shift the relative position of the spectra in momentum and also the total cross section as a function of bombarding energy quite substantially. We recall that the nucleon optical potential changes from roughly -60 MeV at zero momentum to $\approx$ 40 MeV at p = 2 GeV/c. Thus, depending on the nucleon final state momentum, a variation in the differential K^+ yield should be substantial. So far, no selfconsistent calculations are available that include our present knowledge about the nucleon and kaon potentials in a satisfactory manner.
The rather involved transport calculations presented by Z. Rudy so far did not incorporate these potentials, however, the latter are implemented in the transport code and have been tested in nucleus-nucleus collisions some time ago. From the results shown we learn that elastic K^+N rescattering plays an important role especially for heavy targets and large scattering angles. This leads to the suggestion that the A-dependence of the kaon yield in the narrow ANKE acceptance at forward angles does not allow to determine the reaction mechanism from the α parameter alone. Simply due to the phase-space of one-step and two-step reactions the relative fraction of kaons from one-step processes seen by ANKE in forward direction is much larger than the fraction of kaons from the two-step reaction mechanism. Though the K^+ spectral shape of the transport calculation is well in line with the experimental observations, the integrated cross sections differ up to a factor of 3. Is this indicative for some new physics or does it merely reflect normalization errors (both in theory and/or experiment)?
The calculations within the statistical ROC collision model presented by M. Büscher (performed by H. Müller) discard any dynamical effects and incorporate multi-nucleon collision processes. Is the mechanism of kaon production merely a statistical process? Here the ANKE data at 1.0 GeV give a preliminary answer; the spectrum peaks at somewhat higher momenta than expected in the ROC model. Since the shift of the K^+ peak to lower momentum – relative to the one-step kinematics – is an indication of beginning thermalization, this observation by ANKE clearly rules out thermal models as adequate descriptions of the data seen.

Apart from the models presented here, that involve essentially on-shell dynamics between subsequent reactions, one has to worry about off-shell effects due to the large width of the nucleon spectral function in the medium ($\sim 40-80$ MeV) and the width of the in-medium K^+ ($\sim 20-40$ MeV) according to dispersion relations. In the context of nucleus-nucleus collisions such off-shell effects indeed were found to be large in subthreshold particle production since a nucleon (or kaon) can be populated with a much lower invariant mass M' in the medium. The probability for such phenomena is directly proportional to the hadron spectral function. The propagation to the vacuum then proceeds (via energy conservation) by a compensation of invariant mass squared $\Delta M^2 = M_v^2 - M'^2$ with the momentum squared $\Delta p^2 = p'^2 - p_v^2$. Do we have the same sensitivity in pA reactions?
In summarizing, there are presently more open questions than answers and a lot of theoretical work has to be done to clarify the situation. Especially data from ANKE up to 1 GeV/c of momentum at different bombarding energies will provide unique constraints on the theoretical approaches, that have to enter a new stage of sophistication by now.

Nearest future plans for the subthreshold K^+ production

V.Koptev

High Energy Physics Department
Petersburg Nuclear Physics Institute
188350 Gatchina
Russia

At the last PAC, 2 weeks were requested for

Energy	D2 mode	targets	item	time
2.3 GeV	1.3 T	C, Ag, Au	A-dependence at low kaon momentum, angular dependence within 0-12 deg	3 days
2.3 GeV	1.6 T	C	fine tuning of degraders, wide momentum range (150-1000 MeV) measurements	2 days
1.5 GeV	1.6 T	C, Au	measurements in the near threshold region	3 days
1.2 GeV	1.6 T	C, Au	A-dependence, test K^+p, K^+d correlation measurements to estimate an accidental background	6 days

Only 1 week was approved by PAC which means that we must simplify the program. We can have only 1 or maximum 2 changes of beam-ANKE conditions.

Priority number 1 is or to check the obtained unexpected A dependence at low kaon momenta and to have high statistics for the $(0\text{-}12)^o$ angular dependence of the cross sections at 2.3 GeV. Since in any case we have problems for telescope 1 it is proposed to do all the measurements in only one D2 mode, (1.6 T mode) with delayed veto in the on-line trigger.

We shall try to do fine tuning of degraders during ANKE machine development.

Priority number 2 is to measure a wider kaon spectrum ($\leq$ 650 MeV/c) at 1.2 GeV at least from one target: Carbon.

Priority number 3 is to start K^+p, K^+d correlation measurement as a test to understand possible accidental background. So happened that we have never switched on the forward detector for the strip-target and know nothing about it's possibilities at these experimental conditions.

For the correlation measurement at 1.2 GeV we need SW calibration with the pp $\rightarrow$ dπ^+ reaction with the deflection angle 10.6^o and at energies of 700 MeV or 800 MeV with a CH_2 target.

It is proposed to do these measurements during one night of the ANKE machine development time.

The lowest priority is 1 or 2 days measurements with a carbon target either at 2.3 GeV in a wide momentum range or at 1.5 GeV (close to the kaon production threshold of 1.58 GeV).

The choice of the energy and the real possibility of these low priority measurements will depend on the results of theoretical analysis and how successful we are in the beginning of the beam time in autumn 2001.

The final goal of the subthreshold kaon production measurements are the K^+p, K^+d correlations at 1.0 GeV. For these measurements we need 4 weeks. It is intended to prepare the proposal and the beam–time request in spring 2002. It strongly depends on the results of the measurements at 1.2 GeV where we must spend not less than 4 days of measurements. For K^+d, K^+p correlation measurements it is necessary to have full ANKE system working including the forward and the negatively charged particle detectors.

Measurements of forward protons and π^- in correlation with kaons will permit us to reconstruct the $\Lambda(1116)$ and from effective $(K^+\Lambda)$ mass measurement we can also make a conclusion whether they are originated from πn or pN interactions. Therefore, this possible beamtime can take place in the late autumn 2002 or spring 2003.

K^+K^- correlations at ANKE. The new detector system for measurements of negatively charged ejectiles

M. Hartmann

Institut für Kernphysik
Forschungzentrum Jülich
52425 Jülich
Germany

The accepted ANKE experiment "Subthreshold K^- production" [1] requires the measurement of K^- mesons. A detector system similar to that used for measurement of positively charged ejectiles [2] is constructed [3] and the first steps to build up the detector elements have been done. It will be placed inside the return yoke of the C-shaped D2 dipole (magnetic field 0 to $\approx$ 200 mT) and partly outside the magnet (Fig. ANKE detector layout). At the maximum field of D2 (1.6 T) negatively charged ejectiles can be measured in the momentum range from $\approx$ 120 to $\approx$ 1000 MeV/c. The horizontal and vertical angular acceptances are roughly: α_{hor}=$\pm 12^o$; α_{ver}=$\pm 8^o$ at 200 MeV/c and α_{hor}=-2^o to 12^o, α_{ver}=$\pm 5^o$ at 1000 MeV/c [Fig. ANKE detector layout].

With such a detector setup also negatively charged pions can be detected. Thus in combination with the positive detector systems additional reactions can be investigated at ANKE. For the investigation of the reactions pn$\rightarrow$ a_0^0d (K^+K^-) and pn$\rightarrow$ f_0d (K^+K^-,$\pi^+\pi^-$) [4][5] already 3 weeks of beamtime are approved at COSY. Parasitically one can study the production of ϕ–mesons on the neutron. For the investigation of heavy hyperons the new detector group is also very useful; e.g. the nature of the $\Lambda(1405)$ resonance can be studied in pp$\rightarrow\Lambda(1405)K^+$p or in pd$\rightarrow\Lambda(1405)K^+$d [6].

In addition to the elementary reaction also p+nucleus reactions can be studied at ANKE to investigate so called medium effects. Interesting candidates are K^+K^-–correlations – respectively the ϕ–meson [7] – or $\pi^+\pi^-$–correlations [8]. In this context the mass modification of the K^-–meson is assumed to explain the high K^-/K^+–ratio in comparison to the K^-/K^+–ratio in elementary production [9][10]. Experiments which investigate density effects of the isoscalar state of two strongly interacting pions – the f_0(400-1200) – have been done at CHAOS (TRIUMF) [8] and at Crystall Ball (AGS) and are also subject of measurements with the TAPS detector system.

The transparencies discuss mainly only the in–medium modifications of the ϕ–meson. But also an absolute measurement of pp$\rightarrow$ppϕ at ANKE appears promising. The theoretical interpretation [11] of the existing experimental ω and ϕ data in p+p reaction shows potentially that only the ϕ data point from the DISTO collaboration [12] deviate to some extend from the OZI rule. DISTO measured the ϕ production at T_p=2.85 GeV (Q$\approx$82MeV) COSY-11 measured pp$\rightarrow$ppK^+K^- at Q=17 MeV (T_p=2.547 GeV) [13]. At this energy K^+K^- production via the ϕ–meson is forbidden. The threshold for ϕ production is at T_p=2.593 GeV, which is between the energy of the COSY 11 and DISTO measurements. A measurement of ϕ–meson production slightly above threshold at T$\approx$2.65 GeV is therefore reasonable since information about ϕ production close to threshold as well as about K^+K^- through the resonances a_0/f_0 can be obtained. The maximum beam energy at COSY of around 2.65 GeV corresponds for the ϕ–meson to an excess energy of 18.6 MeV. In the range of this Q value experimental data points for the ω production from DISTO and SPESIII [14] exists so that it would be adequate to measure at ANKE only the ϕ production.

The A–dependence measurements of ϕ–production can help to understand the interaction ($\sigma_{\phi N}$) and decay (Γ_ϕ, m_ϕ) of the ϕ–meson in nuclear matter. Various theoretical publications predict – already for normal nuclear density – a shift of the pole mass up to a value of 40 MeV [15][16] as well as an increasing of the free width from Γ_ϕ = 4.4 MeV up to 22 - 45 MeV [16][17]. For the A dependence exists the following theoretical prediction: $\sigma(A) \sim \sigma(1)^\alpha$, $\alpha = 0.66 \pm 0.03$ [18].

For ϕ production in the p+nucleon reaction at threshold the K^- momenta range from 403 to 795 MeV/c. If the ϕ–meson or K^+K^-–pairs are produced in p+nucleus reactions

www.pn.scphys.kyoyo-u.ac.jp/ enyo/e325/phi.root.ps.Z).
[8] F. Bonutti, Phys. Rev. C60 (1999) 018201: "pp pairs in nuclei and the σ meson".
[9] A. Sibirtsev, W. Cassing, Nuc. Phys. A641 (1998) p. 476.
[10] E. Ya. Paryev, Eur. Phys. J (2000) p. 521.
[11] A. Sibirtsev, W. Cassing, Eur. Phys. J A7 (2000) p. 407.: "On the current status of OZI violation in πN and pp reactions".
[12] F. Balestra et al. Phys. Rev. C63 (2001) 024004: "ϕ and ω production in pp reaction at plab=3.67 GeV/c".
[13] C. Quentmeier et al. Phys. Lett. B, in print.
[14] F. Hibon et al. Phys. Rev. Lett. 83 (1999) p. 492.
[15] T. Hatsuda and S. H. Lee, Phys. Rev. C46 (1992) R24.
[16] F. Klingl, T. Waas, W. Weise, Phys. Lett. B43 (1998) p. 245.
[17] E. Oset and A. Ramos, Nucl. Phy. A679 (2001) p. 616.
[18] M. Binkley et al. Phys. Rev. Lett. 37 (1976) p. 571.

K^+K^- correlation at ANKE and a new detector system for measurement of negatively charged ejectiles

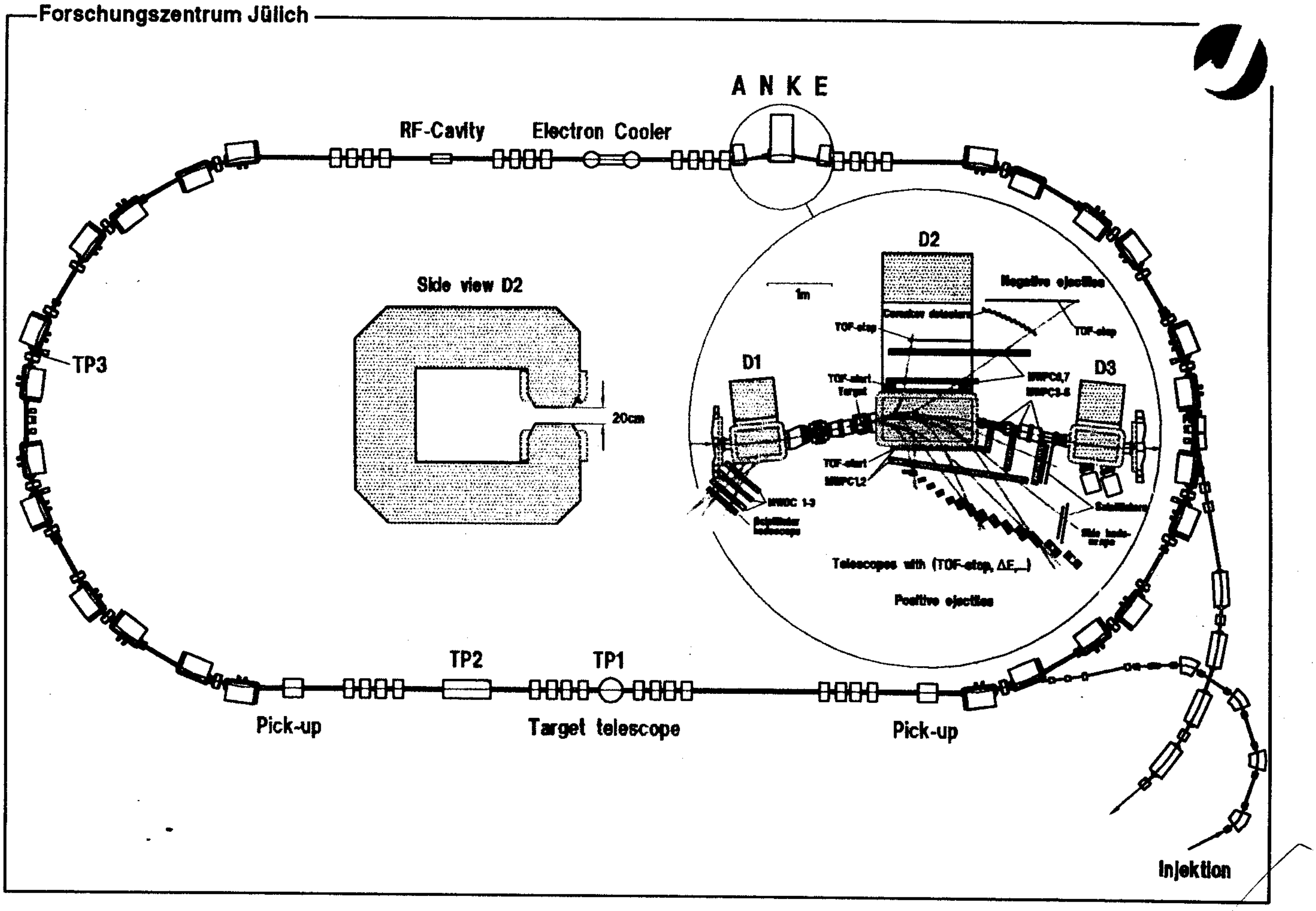

M.Hartmann@FZ-Juelich.de
for the ANKE collaboration

K^+K^- ($\pi^+\pi^-$) Correlations

pp,pn (elementary)

$pp \rightarrow a_0^+d$ (beamtime 02/2001)	K^+d
$pn \rightarrow a_0^0d$	K^+K^-d
$pn \rightarrow f_0d$	K^+K^-d, $\pi^+\pi^-d$
$pn \rightarrow \phi d$	K^+K^-d

pA (in nucleus)

(i) ϕ production ⇒ interaction ($\sigma_{\phi N}$) and decay (Γ,m_ϕ) of ϕ mesons in nuclear matter

(ii) K^- production ⇒ K^- yield and absorption, mass modification (K^- potential)

(iii) $\pi^+\pi^-$ correlation ⇒ spectra of invariant mass (f_0(400-1200)?)

in-medium effects

more π^-

$pp \rightarrow K^+p\Lambda(1405)$	$\Lambda(1405) \rightarrow \Sigma^+\pi^-$, ($\Lambda(1115) \rightarrow p\pi^-$)
$pd \rightarrow dN^{+*}$	$d = \|pn\rangle + \|NN^*\rangle$
$pd \rightarrow (pp)N^{0*}$	$N^{0*} \rightarrow p\pi^-$ (300-400 MeV/c)
$\omega \rightarrow \pi^0\gamma$ (8.5%)	η, ω Produktion
$\omega \rightarrow \pi^+\pi^-\pi^0$ (88.8%)	

Interaction of ϕ mesons in nuclear matter ($\sigma_{\phi N}$)

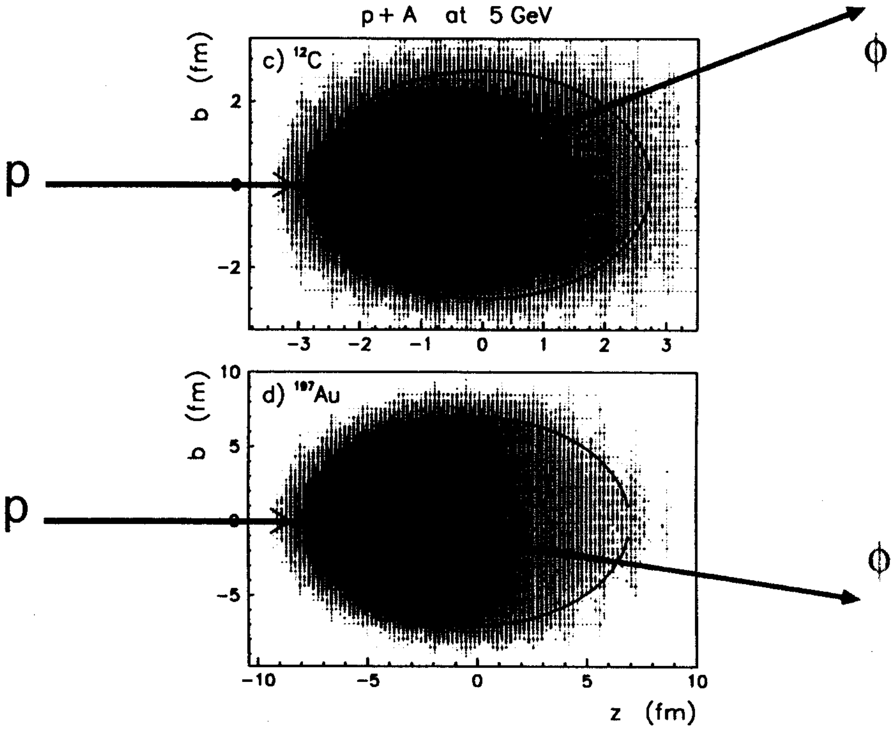

$$\sigma_{\phi,\text{production}}\,(A) \otimes \sigma_{\phi,\text{absorption}}\,(A)$$

simple estimation: $N_{\phi} \sim \exp^{-(L/\lambda_0)} \sim \exp^{-(L\cdot\rho\sigma_{\phi N})}$

reliable estimation: $\boxed{\text{Glauber Model, Cascade Model, ROC, BUU, ...}}$ $\Rightarrow \lambda_0 \Rightarrow \sigma_{\phi N}$

other observables: $\sigma_{\phi N}(p_{\phi})$,
spectra of invariant mass (K^+K^-)
peak width and shift

18.06.01 zweig

Φ properties in nuclear matter (theoretical predictions)

dense matter (ρ≠0)

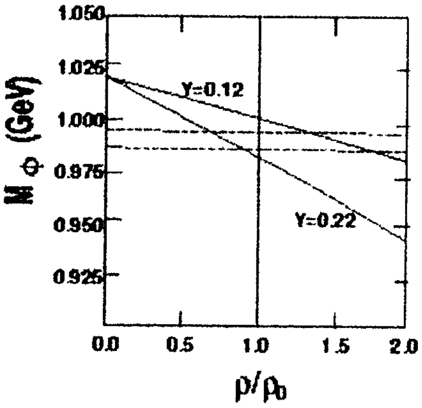

Figure 1. Hatsuda and Lee's predictions for the density dependence of the mass of ϕ meson. Dashed lines are the threshold of the $K\bar{K}$ channels. The two solid lines represent the range of the strange-quark condensate expected from the experimental observation ($Y=2\langle s\bar{s}\rangle/(\langle u\bar{u}\rangle+\langle d\bar{d}\rangle)$).

hot matter (T≠0)

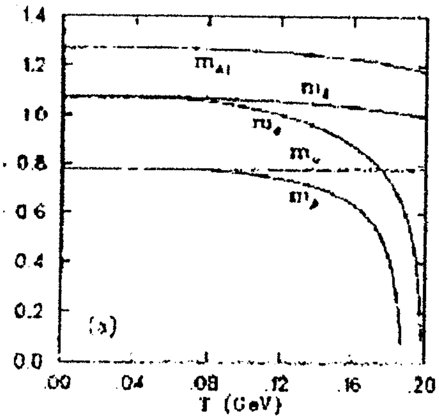

$$M^* \sim \langle q\bar{q}\rangle^{1/3} \sim \left(1-\frac{T^2}{T_c^2}\right)^{1/6}$$

$$\sim 1-\left(\frac{T}{T_c}\right)^2$$

Φ at rest in ρ_0	Δm_ϕ	Γ_ϕ [MeV]
T. Hatsuda and S.H. Lee, Phys. Rev. C46 (1992) R24.	20 - 40	--
F. Klingl, T. Waas, W. Weise, Phys. Let. B43 (1998) 245.	20 - 40	45
E. Oset and A. Ramos, Nucl. Phy. A679 (2001) 616.	< 10	22

M. Binkley et al.,
Phys. Rev. Lett. 37 (1976) 571.

$\sigma(A) \sim \sigma(1) x A^{\alpha}$, $\underline{\alpha = 0.66 \pm 0.03}$

Nuclear production of Φ meson at KEK (KEK-PS E325) (Tsukuba) *(exp. data, preliminary !!)*

Table 1
Experiments to study nuclear density effect on vector mesons

place	channel	status	Ref.
KEK(Tanashi)-ES	$\gamma + A \rightarrow \rho + X$ $(\rho \rightarrow \pi^+\pi^-)$	Published	[3]
KEK-PS	$p + A \rightarrow \phi + X(\phi \rightarrow K^+K^-/e^+e^-)$	Running (this work)	[4]
SPring-8	$\gamma + A \rightarrow \phi + X$ $(\phi \rightarrow K^+K^-)$	Ready to run	[5]
GSI/HADES	$\pi + A \rightarrow \omega + X$ $(\omega \rightarrow e^+e^-)$	Preparation	[6]
GSI/FRS	$d + A \rightarrow ^3He + A^*(\text{bound})$	Ready to run	[7]

$pA \rightarrow \phi X$, $T_p = 12$ GeV

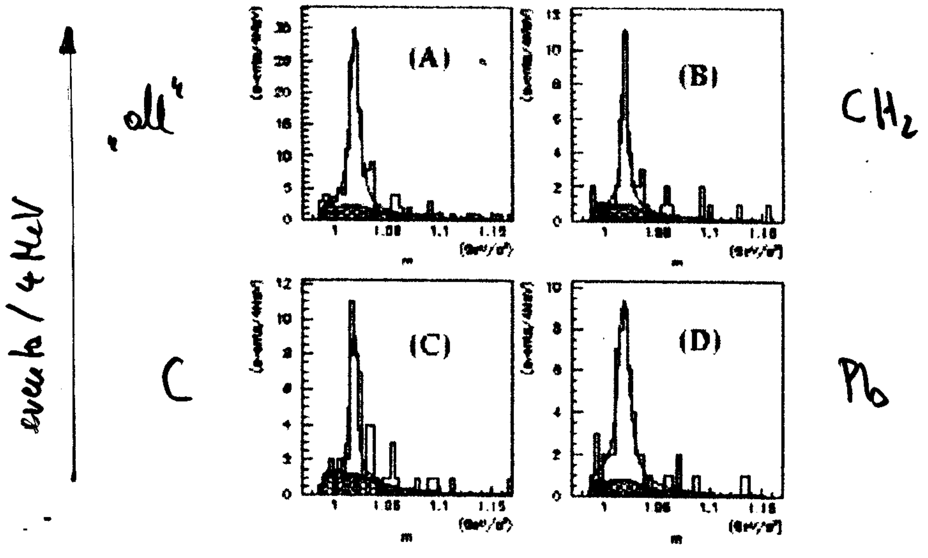

Figure 6. The invariant K^+K^- spectra. In (A) we include all the three targets. The spectra (B),(C) and (D) are corresponding to polyethylene, carbon and lead targets respectively. The hatched areas are the backgrounds evaluated by the event-mixing method.

Nuclear production of Φ meson at KEK (KEK-PS E325) (exp. data, preliminary !!)

Δm_ϕ ->

Γ_ϕ ->

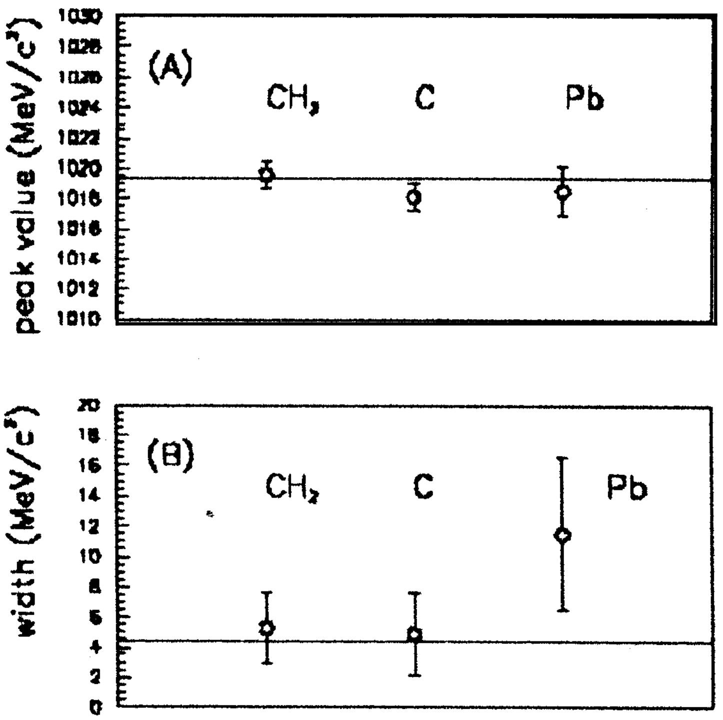

Figure 7. The resonance position (A) and width (B) of the observed ϕ mesons. The line is drawn at the values in free space.

The resonance position obtained by the present work are consistent with the known value of 1019.4 MeV/c^2. The widths of Φ meson from polyethelene and the carbon target are also consistent with the natural width of Φ meson. For the lead target case, the width looks larger but the present statistical significanse is not enough to conclude the difference.

phi decay probability inside of nuclei

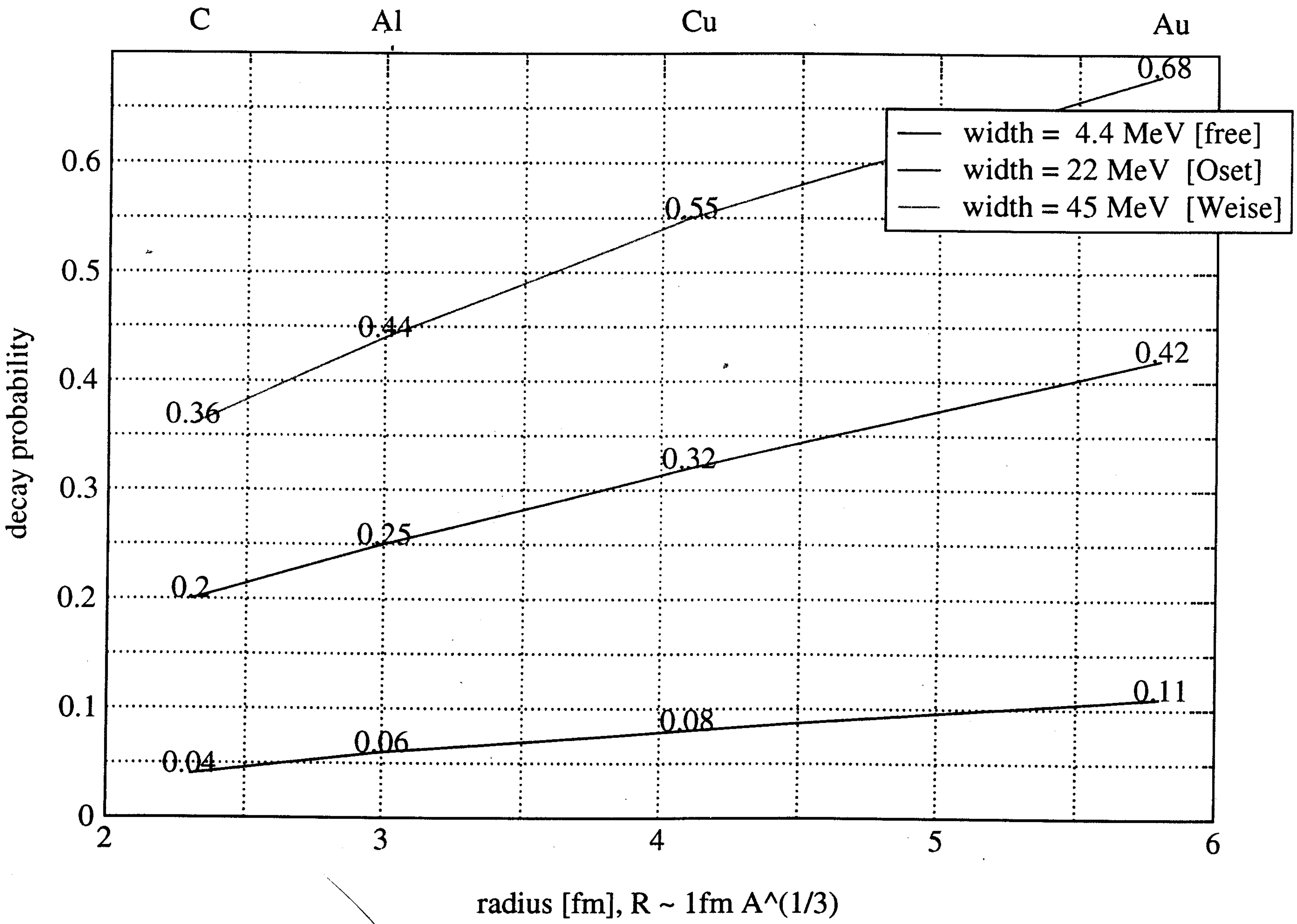

Sat Jun 16 13:31:14 2001

Nuclear production of Φ meson at KEK (KEK-PS E325) (exp. data, preliminary !!)

$$\sigma(A) = \sigma(A{=}1) \times A^{\alpha}$$

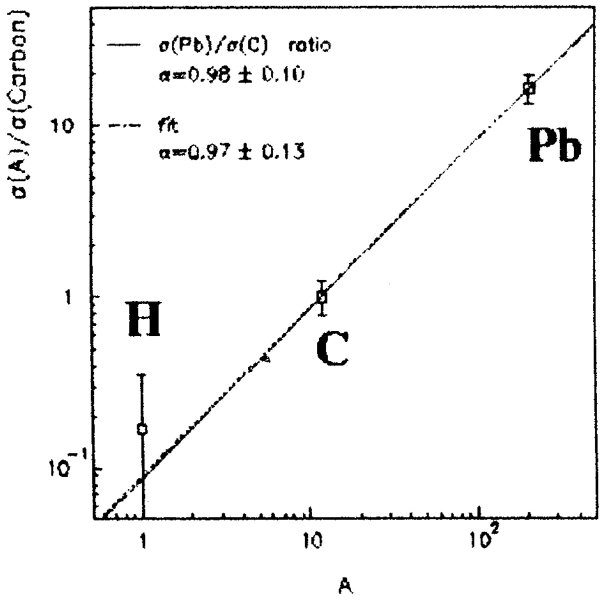

$\alpha \approx 1$

Figure 8. Mass number dependence of the cross section. The solid line is obtained by the ratio of the lead to the carbon data. The dashed line is the best fit over the three points. The data point for hydrogen is obtained by the CH_2-C subtraction.

Table 2
Comparison of the α parameters and the kinematic regions.

	$\sqrt{s}$ (GeV)	α	p_T (GeV/c)	x_F
12GeV $p + Pb/C$(present work)	5.1	0.98±0.10	0.4< p_T <1.5	-0.8< x_F <0.3 ←
120GeV/c $p + Ta/Be$[10]	15.1	0.86±0.02	0< p_T <1	0< x_F <0.3
100GeV/c $p + Be/p$[10]	14.2	0.96±0.04	0< p_T <1	0.11< x_F <0.24
70GeV $n + A$ [11]	11.6	0.81±0.06	0< p_T <1	0< x_F

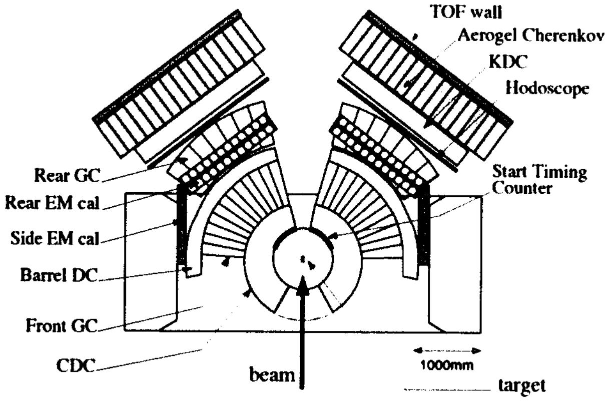

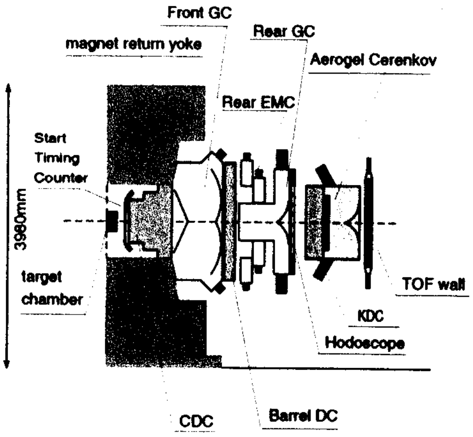

Figure 3. Top view of the E325 setup

Figure 4. Side view of the E325 setup

points are more than 20 mm apart from the target. The clear resonance peak of Λ shows the mass resolution of 2.2 MeV/c^2.

By rescaling this mass resolution by taking account of the differences in the Coulomb scattering effects and in the momentum distributions of protons, pions, and kaons, we evaluated the mass resolution of the $\phi \rightarrow K^+K^-$ invariant mass to be 1.2 MeV/c^2, which is good enough for the present analysis. The peak value of the Gaussian fit is 1115.11 MeV/c^2, which is consistent with the mass of Λ in the literature[12], 1115.68 MeV/c^2.

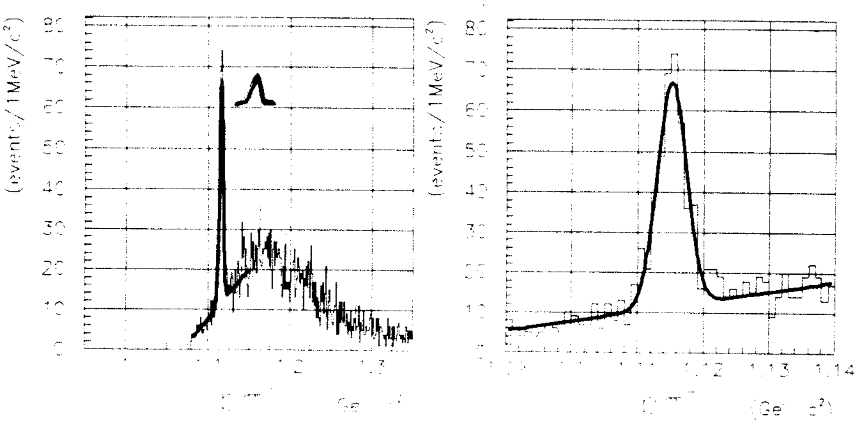

Figure 5. The pπ^- invariant mass spectra. The line is the best fit result of a Gaussian with a linear background. Λ is seen at 1115.11 MeV/c^2 with a resolution of 2.2 MeV/c^2.

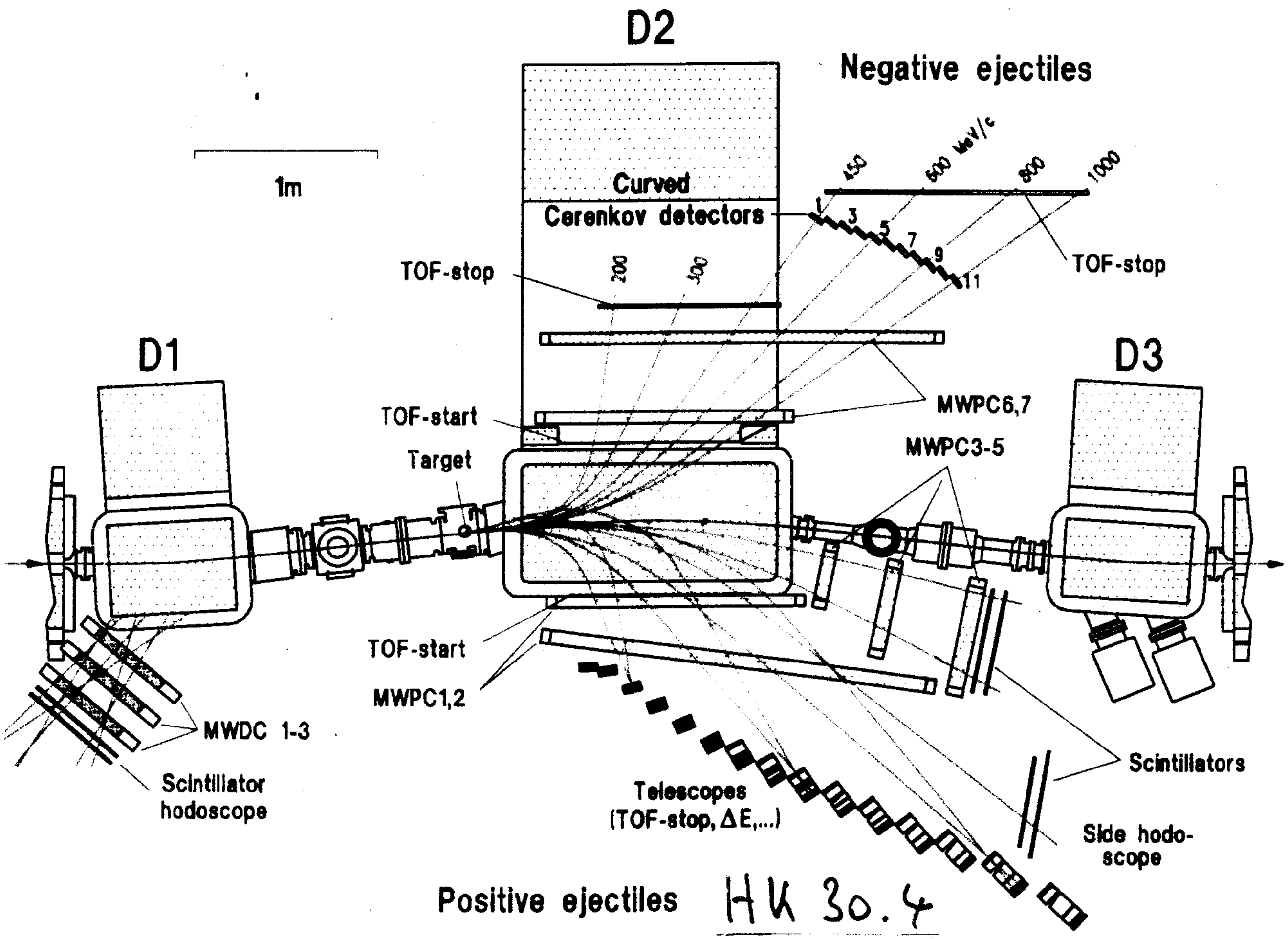

HK 30.4

K⁻ horizontal and vertical angular acceptances are roughly:

a_{hor}=±12°; a_{ver}=±8° at 200 MeV/c and

a_{hor}=-2°, a_{ver}=±5° at 1000 MeV/c

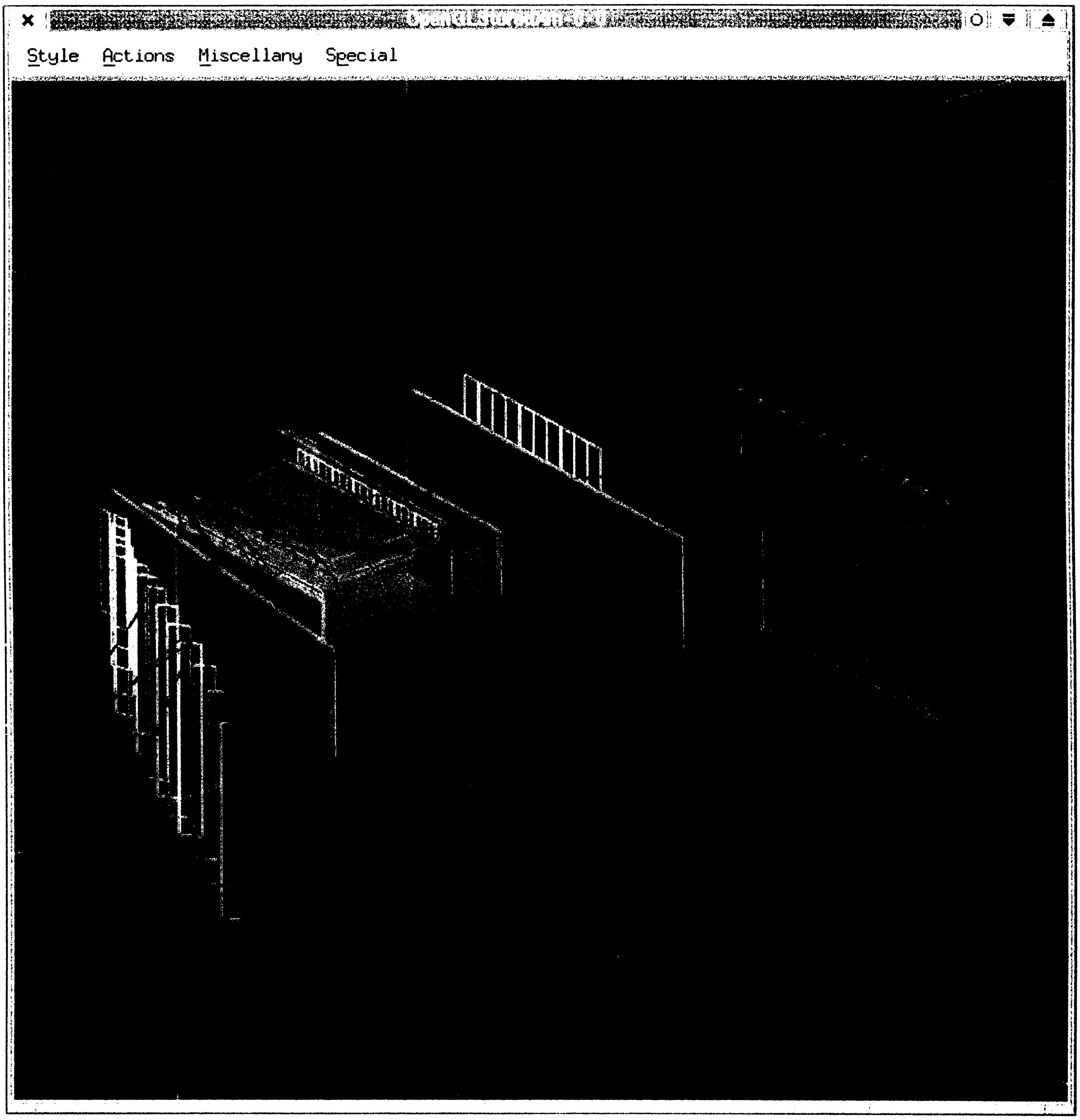
Style
Actions
Miscellany
Special

18.06.01 zweig

ROC: $pC \to K^+ K^- X$, $T=2.5\ GeV$

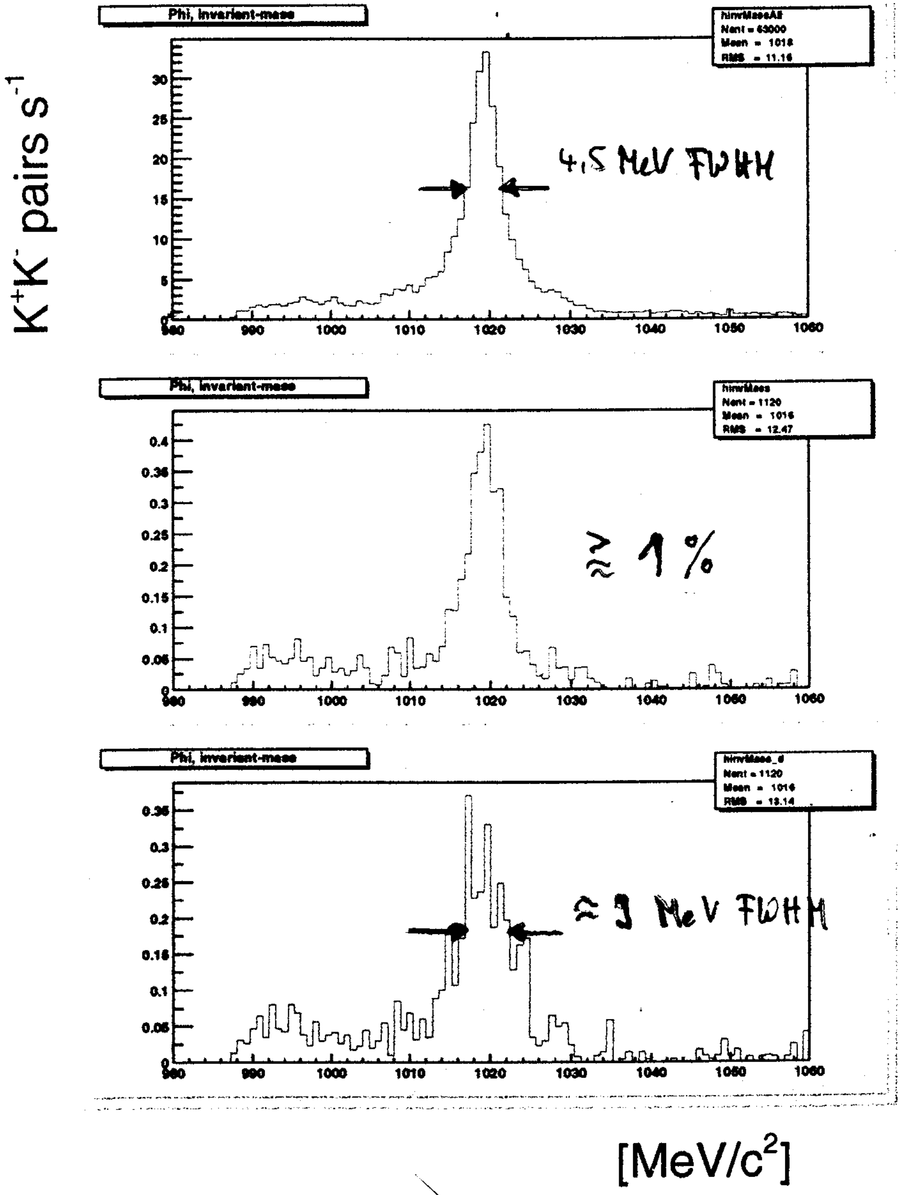

<- spectra of invariant mass (K^+K^-)

$L = 1x10^{32}cm^{-2}s^{-1}$

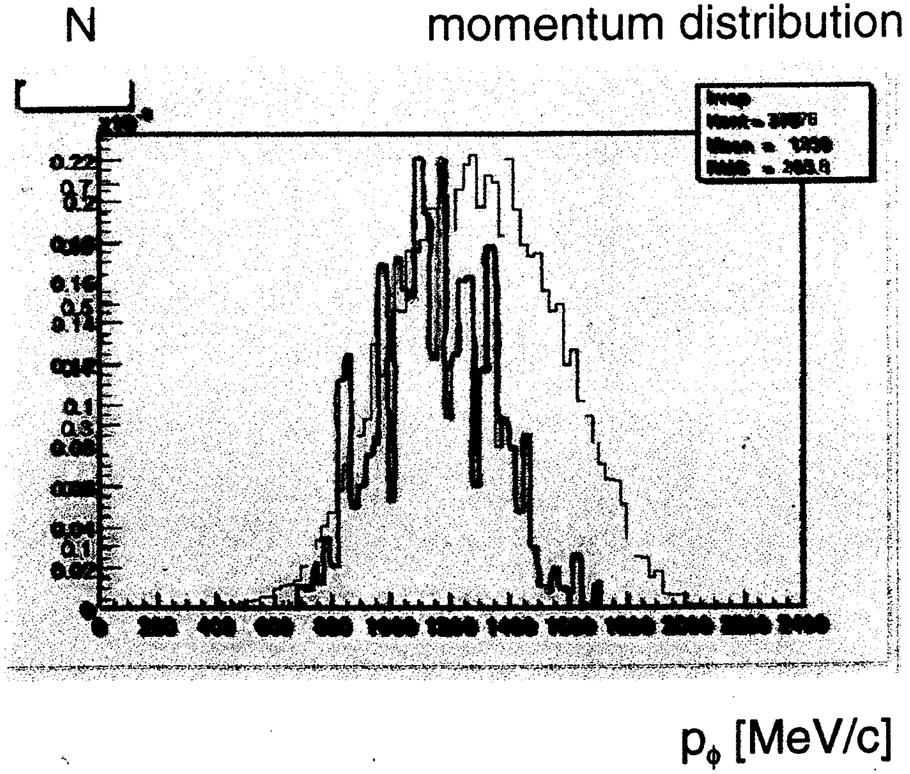

exp. data: pA → K^-X

1) ITEP, Y. Kiselev (preliminary!)

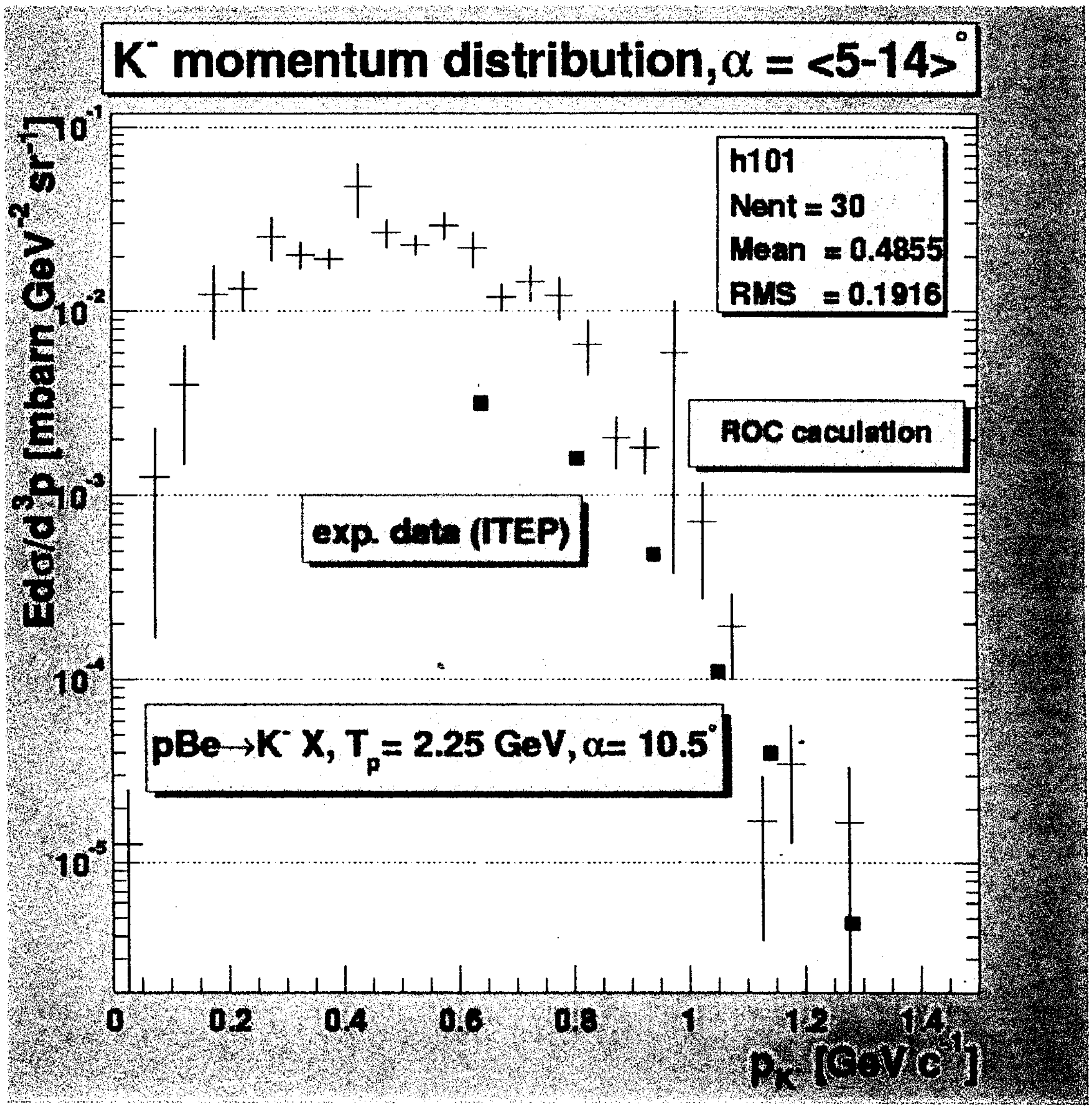

2) GSI, W. Scheinast (FZ-Rossendorf) (preliminary!)

pAu |
p=0,64 GeV/c
T=2,5 GeV
α=40°

→ pBe | ≈ 2-4 μb/(GeV^2sr)
p=0,64 GeV/c
T=2,5 GeV
α=10°

pC |
p=0,64 GeV/c
T=3,5 GeV
α=40°

rate estimation: $pC \rightarrow K^{+}K^{-}X$, T=2.5 GeV

$L = 1\cdot10^{+32}cm^{-2}s^{-1}$

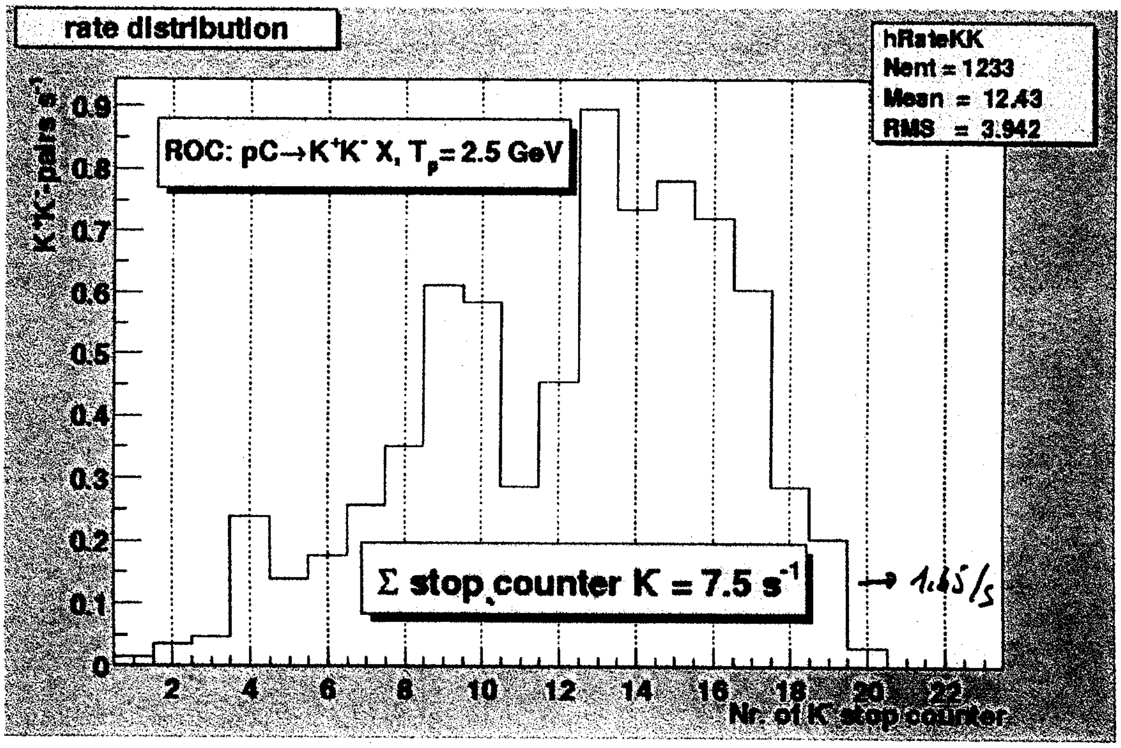

Σ pos. START: ~ $3\cdot10^{+5}$ s^{-1} (≈ π+/π-)

Σ neg. START: ~ $1\cdot10^{+5}$ s^{-1}

coincidence window: 50 ns

⇒ Triggerrate: 30.000 s^{-1}

⇒ Triggerrate: 3.000 s^{-1}

50% deadtime of DAQ & 50% K^{+} detection efficiency

⇒ 1500 $K^{+}K^{-}$pairs per hour

A. Sibirtsev, W. Cassing, Eur. Phys. J. A7 (2000) 407
On the current status of OZI violation in πN and pp reactions.

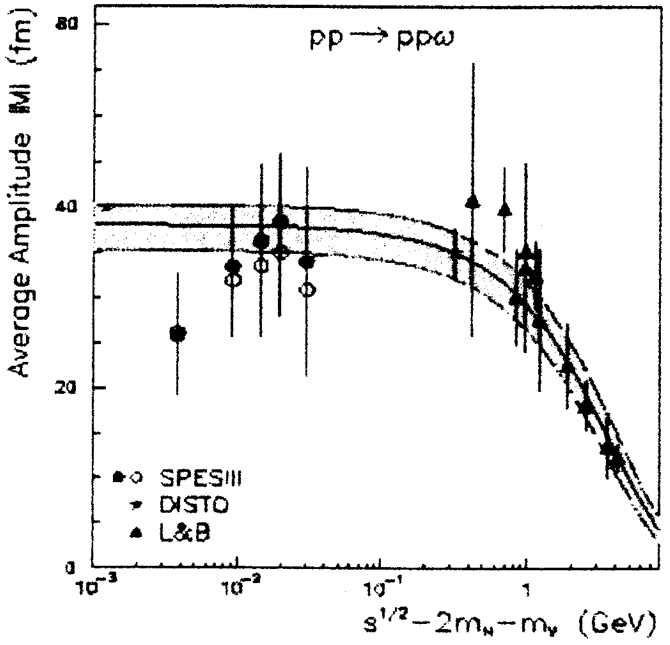

Fig. 5. The average amplitude $|M|$ for the $pp \to pp\omega$ reaction as a function of the excess energy ϵ. The circles show the SPES-III [15] data evaluated with the FSI model from [16] (open circles) and from [17] (full circles). The triangles indicate the data from [7]; the star is our extrapolation for the DISTO experiment. The solid line shows the parameterization (3) while the dashed area indicates the related uncertainty

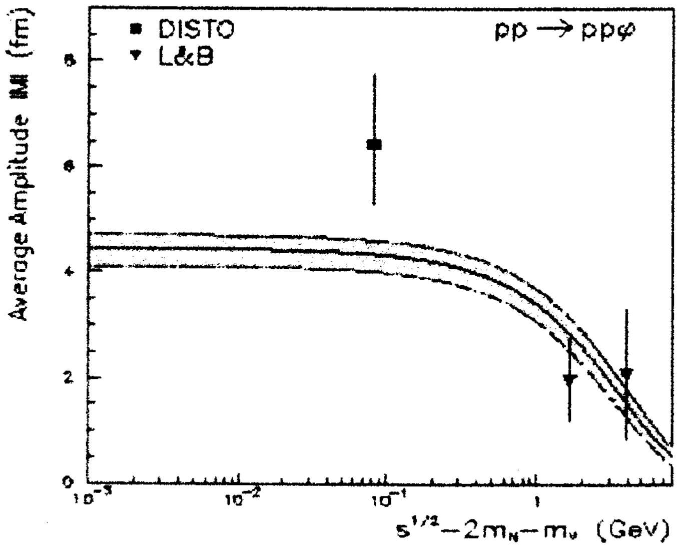

Fig. 7. The average amplitude $|M|$ for the $pp \to pp\phi$ reaction as a function of the excess energy ϵ. The solid line shows the approximation (3) for the $pp \to pp\omega$ amplitude divided by the factor 8.5, while the dashed area is the uncertainty of the approximation with respect to the $pp \to \omega pp$ data.

A. Sibirtsev, W. Cassing, Eur. Phys. J. A7 (2000) 407
On the current status of OZI violation in πN and pp reactions.

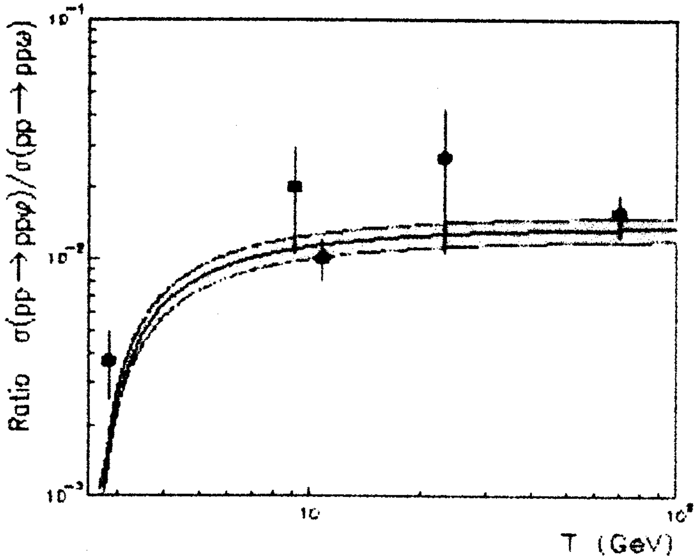

Fig. 8. The ratio of the $pp \to pp\phi$ and $pp \to pp\omega$ cross sections as a function of the beam energy T. Experimental data are taken from [7, 8, 19, 20]. The solid line shows the result calculated with the energy independent ratio $|M_\omega|/|M_\phi|=8.3$, while the dashed area indicates the parent standard deviation.

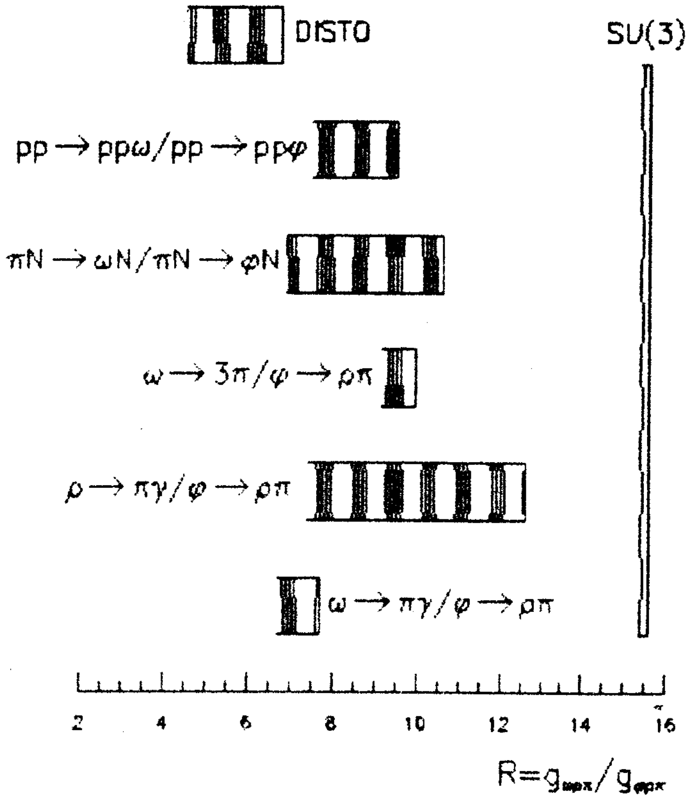

Fig. 10. The ratio of the $\omega\rho\pi$ and $\phi\rho\pi$ coupling constants evaluated from different sources of experimental data in comparison to the SU(3) prediction for $\Theta_V = 39^0$.

19.06.01 zweig

summing-up

- preparation of a ϕ-proposal for the next PAC meeting (nov. 2001)

- beamtime request's for the highest possible COSY energie:

  (i) pp -> ppϕ , H_2-target (incl. detector commissioning) roughly one - two weeks

  (ii) pA -> ϕX , several solid targets (C, Al, Cu, Au) roughly one - two weeks

of
course
every
contribution
is
welcome !

Status of a_0^+ studies with ANKE

V.Kleber

Institut für Kernphysik
Forschungzentrum Jülich
52425 Jülich
Germany

Until now no satisfying interpretation of scalar mesons could be found. With the beam time in January/February this year we want to shed more light on the scalar meson a_0^+. The goals of this beam time are the measurement of the a_0^+ production cross section and the determination of the branching ratio $a_0^+ \rightarrow (\pi^+\eta)/(K^+\overline{\mathrm{K}}^0)$.
In the analysis the reaction is identified in three steps. First a π^+/K^+ is identified in the side detection system. Criteria are time of flight (TOF), vertical angle (to identify particles from the target) and energy loss in the counters (mostly needed for K^+ identification). As the second step deuterons are selected via their TOF and as the last step the missing masses m(pp,dπ/K) and m(pp,d) are calculated to identify the reaction.
In the Kaon decay channel the missing $\overline{\mathrm{K}}^0$ can clearly be identified in the missing mass spectrum m(pp,dK$^+$) with a FWHM of 16 MeV. The m(pp,d) distribution shows a peak at the mass of the a_0^+. By all these criteria the reaction $pp \rightarrow dK^+\overline{\mathrm{K}}^0$ can be identified unambiguously. Nevertheless these criteria do not help to make a statement about resonant and non-resonant contributions.
According to the model of V.Grishina et al. [1] the non-resonant contribution should be negligible. Furthermore, applying the model on COSY 11 and DISTO data for the reaction $pp \rightarrow ppK^+K^-$ [2] assuming all events stem from non-resonant production, taking into account our excess energy, the fusion probability of two protons into a deuteron and a 3-body phase space (d$K^+\overline{\mathrm{K}}^0$) instead of four ($ppK^+K^-$) gives a very low contribution of non-resonant reactions $pp \rightarrow dK^+\overline{\mathrm{K}}^0$. Assuming all COSY 11 and DISTO events to be resonant ($pp \rightarrow ppa_0^0 \rightarrow ppK^+K^-$) gives a cross section for our reaction which is consistent with our present estimation.
V.E.Tarasov made calculations for the missing mass distribution m(pp,d) assuming resonant and non-resonant production. The χ^2-test gives no unique preference to either resonant or non-resonant distribution but rather shows that it is not possible to distinguish resonant or non-resonant production by just looking at the missing mass distribution. The distribution is not yet corrected for efficiency or acceptance but it is not expected that this will help to distinguish resonant and non-resonant production.
For the $\pi\eta$ channel the reaction cannot be identified as easily as in the $K^+\overline{\mathrm{K}}^0$ channel. The m(pp,dπ) distribution shows an enhancement at the η mass which is still broad. In the m(pp,d) distribution a shoulder at the mass of the a_0^+ can be seen. For this channel additional criteria have to be found in order to suppress non-resonant background and events from other channels than $pp \rightarrow d\pi^+\eta$.
With the present result on the $K^+\overline{\mathrm{K}}^0$ channel a preliminary estimate of the a_0^+ production cross section has been done assuming all events to be resonant. The analysis of the luminosity is still going on and shows large discrepancies at this stage. If $L = 1.0 * 10^{31} s^{-1} cm^{-2}$ is assumed then our estimate of the a_0^+ production cross section is 0.62 μbarn with unknown error yet. The value is consistent with the model of V.Grishina et al. [1] and the estimation from COSY 11 and DISTO data [2].
For a more exact determination it is necessary to know the efficiencies of the individual counters in more detail. The efficiency of the cut on energy loss in the ΔE counter of a telescope is determined by the ratio of K^+ events after and before the cut. This efficiency has been determined for telescopes 11-15. It shows a decreasing tendency with increasing K^+ momentum. Moreover for each telescope it is decreasing with decreasing hit angle.
The efficiency of the track reconstruction and the forward chambers has been studied for different telescope and forward counter combinations and different valid start coun-

ters. For each telescope and forward counter combination it seems to be constant (not depending on the K^+ hit angle on the telescope). The efficiency is slightly increasing with decreasing forward momentum but seems to be independent on the angular distribution of the forward particle.
Summarizing one can say that the reaction channels $pp \to dK^+\overline{\mathrm{K}}^0/d\pi^+\eta$ can be identified. It seems that we see a_0^+ production but this still needs more investigations and the data analysis still is in progress.

[1] V.Yu.Grishina et al., EPJ A9, 277, 2000; nucl-th/0007074
[2] preliminary report of the COSY 11 collaboration, nucl-ex/0109001

ANKE Workshop on
Strangeness Production
in pp and pA Interactions at ANKE
June 21-25, 2001
PNPI, Gatchina

Status on a_0^+ with ANKE

Vera Kleber
IKP
FZ Julich

Properties of the $a_0(980)$

Review of Particle Physics, European Physical Journal C3, 1 (1998)
(Status of April 2000)

$a_0(980)$ $I^G (J^{PC}) = 1^- (0^{++})$

... the interpretation of the scalar mesons is a long standing puzzle ...

The $f_0(980)$ and $a_0(980)$ are often interpreted as being multiquark states (JAFFE 77) or $K\bar{K}$ bound states (WEINSTEIN 90) ...

More detailed models exist, which include more theoretical input at least phenomenologically. One such unitarized quark model with coupled channels can understand ... light scalars as ... unitarized manifestations of bare quark model $\bar{q}q$ states ...

To reveal its true coupling constants a coupled channel model ... must be applied.

$a_0(980)$ MASS

VALUE (MeV)
984.7±1.3 OUR AVERAGE

$a_0(980)$ WIDTH

VALUE (MeV)	
50 to 100 OUR ESTIMATE	Width determination very model dependent. Peak width is about 60 MeV, but decay width can be much larger.

Benefits from Measurement with ANKE

a_0(980) DECAY MODES

	Mode	Fraction (Γ_i/Γ)
Γ_1	$\eta\pi$	dominant
Γ_2	KK	seen
Γ_3	$\rho\pi$	
Γ_4	$\gamma\gamma$	seen
Γ_5	e^+e^-	

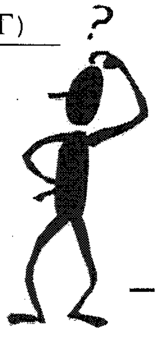

$R = g_{KK}/g_{\pi\eta} = 0.9 \ldots 2.05$ (depending on fit)

Existing data $R = g_{KK}/g_{\pi\eta}$:

$g_{\pi\eta} =$

- E852 (BNL): - $m(a_0^+) = 998.3 \pm 4.0$ MeV/c^2 — 0.122 ± 0.008
  - $\pi\eta$ channel only — 0.324 ± 0.015
- Crystal Barrel: - $m(a_0^+) = 984.45 \pm 1.23 \pm 0.34$ MeV/c^2
  - mass resolution Δm only ~ 27 MeV/c^2
  - contaminations from heavier resonances
  - KK and $\pi\eta$ channels in different data sets

ANKE:

- high mass resolution: $\Delta m \sim 10$ MeV/c^2
  (→ Forward detectors)
- simultaneous measurement of two decay channels

$p(2.65\ \mathrm{GeV})\ p \to d\ a_0^+$

$\hookrightarrow \pi^+\ \eta$

$\hookrightarrow K^+\ \bar{K}^0$

approved proposal #55
(PAC 14)

ANKE Beam Time on a_0^+ Production

Experiment:

* 2 weeks in January/February 2001

* $p\ (2.65\ \text{GeV}) + p \rightarrow d + a_0^+$

$\rightarrow \pi^+ + \eta$

$\rightarrow K^+ + \overline{K}^0$

Goals:

* determination of the branching ratio

$a_0^+ \rightarrow (\pi^+ + \eta)/(K^+ + \overline{K}^0)$

* measurement of the a_0^+ production cross section

Data Analysis Strategy

$$\begin{tikzcd} & d + \pi^+ + \eta \\ p + p \rightarrow d + a_0^+ \arrow[ur] \arrow[dr] & \\ & d + K^+ + \overline{K}^0 \end{tikzcd}$$

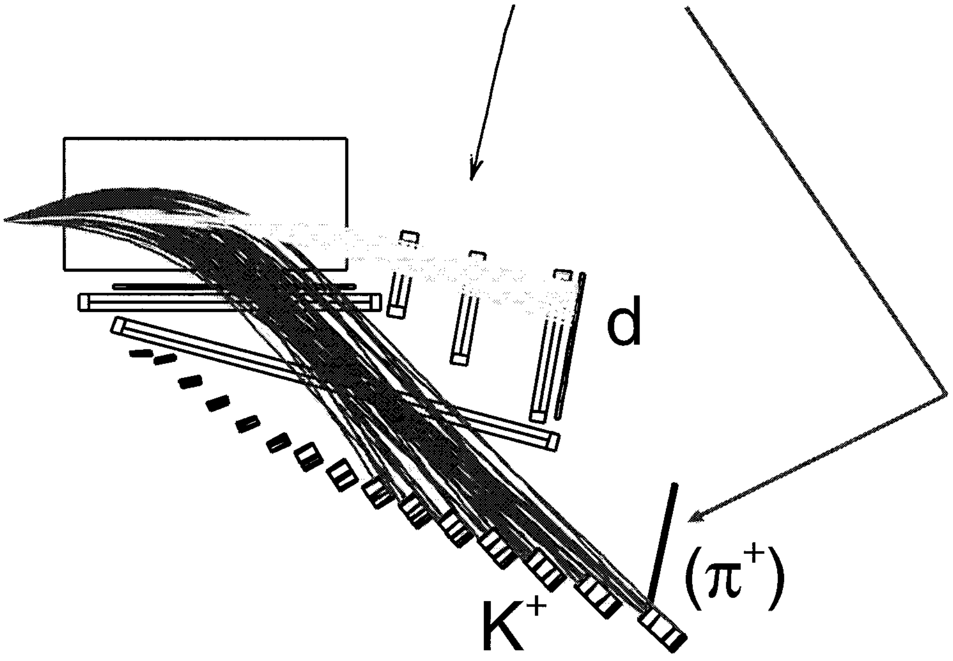

strategy:

1. π^+/ K^+ in SD
2. d by TOF (forward-side)
3. a_0^+ by missing mass
   + others ?

Identification of K$^+$/π$^+$ (Side Detection System)

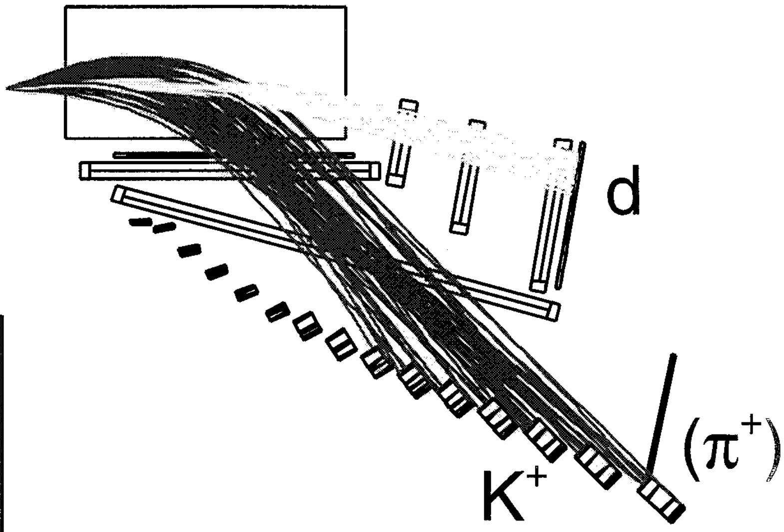

K$^+$/π$^+$ selected by:

- * vertical angle

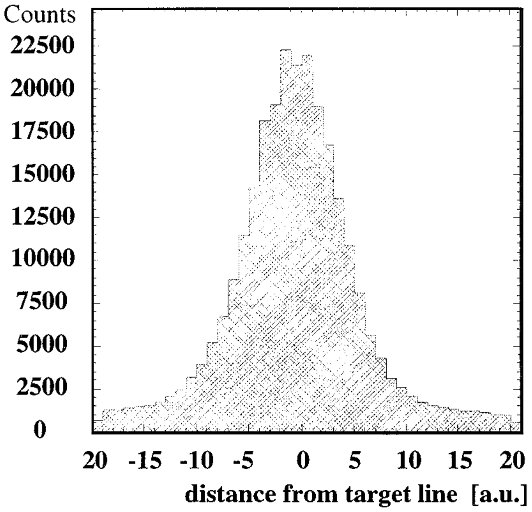

- * TOF

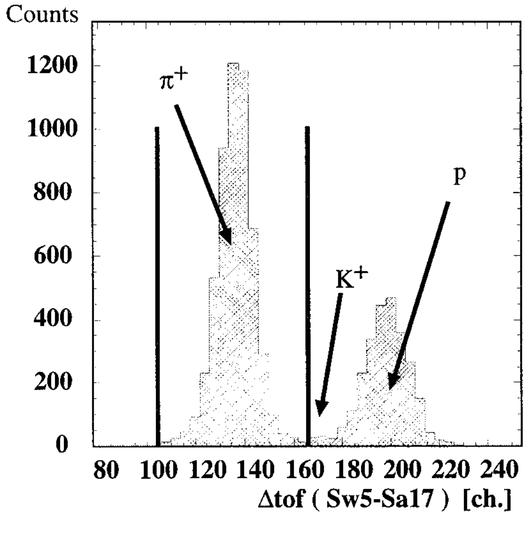

- * energy loss of K$^+$ (π$^+$)

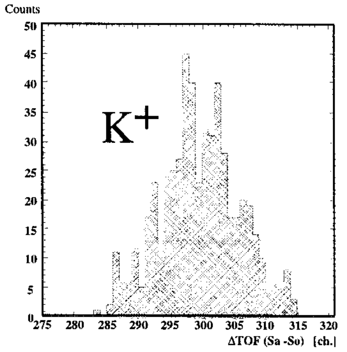

Deuteron Identification (FD Detection System)

$pp \rightarrow a_0^+$

$\rightarrow K^+\overline{K}^0$

$\rightarrow \pi^+ \eta$

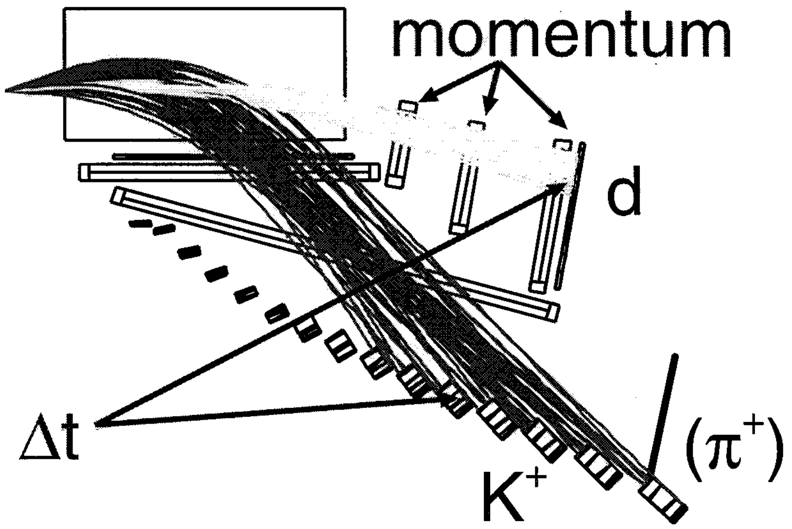

TOF versus momentum distribution

(for a π^+ in the sidewall and a particle in the FD detection system)

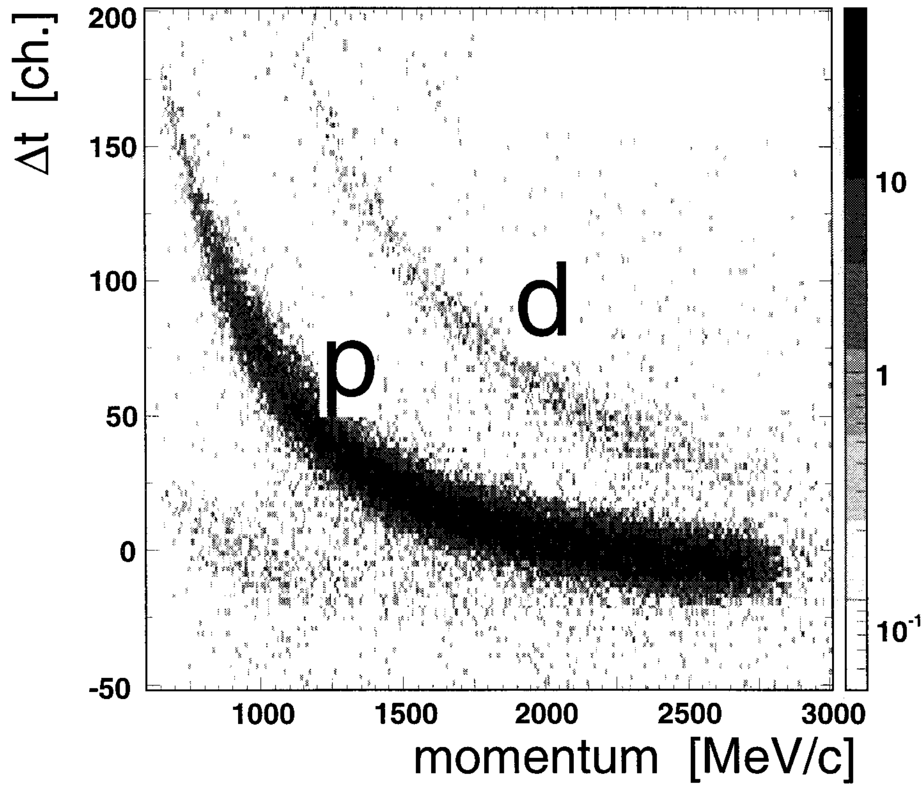

→ unambiguous identification of

$pp \rightarrow dK^+/\pi^+ X$ events

a_0 by Missing Mass

$$p + p \rightarrow d + a_0^+ \rightarrow d + K^+ + \overline{K}^0$$

(software) conditions:

very preliminary missing mass distributions!!!

- * K^+ in telescopes 11-15
  - * particle in FW 1-4
    - * cut on momentum (1650 - 2650 MeV)
      - * cut on ΔTOF (→ d in FW)

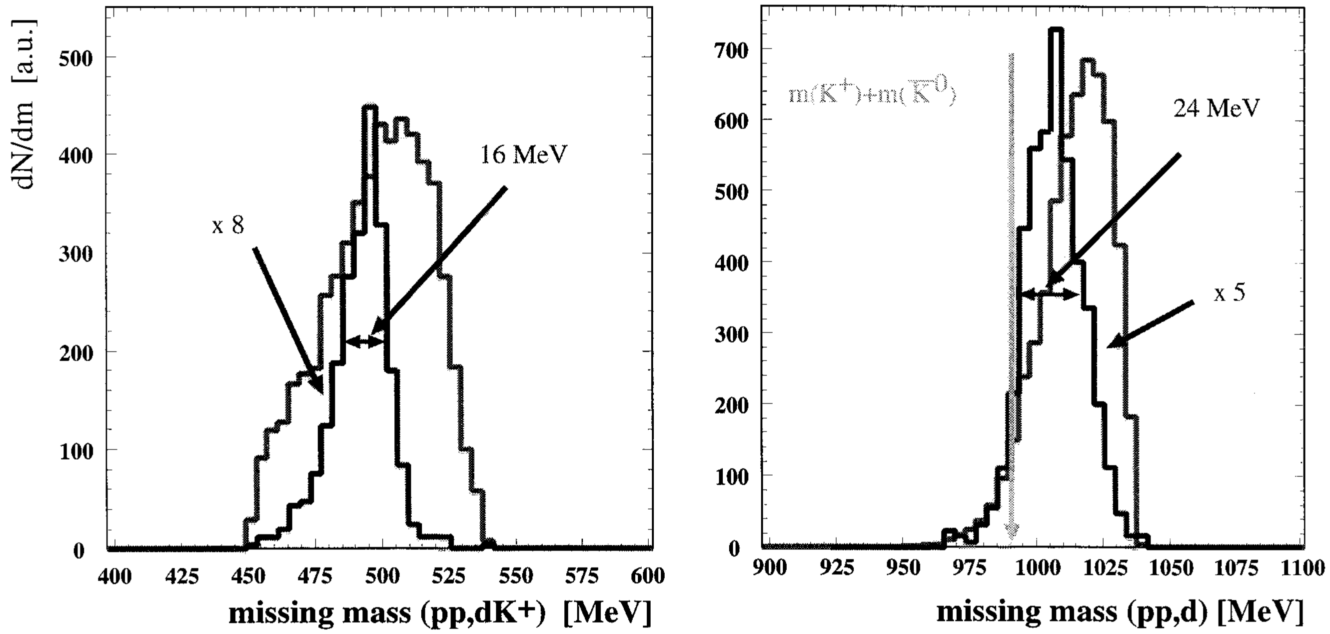

Nonresonant background? ⟶ expected to be small

- * from model (V.Grishina et al.)
- * from comparison with $pp \rightarrow ppK^+K^-$ from COSY11, DISTO

$p + p \rightarrow p + p + K^+ + K^-$

43 PS

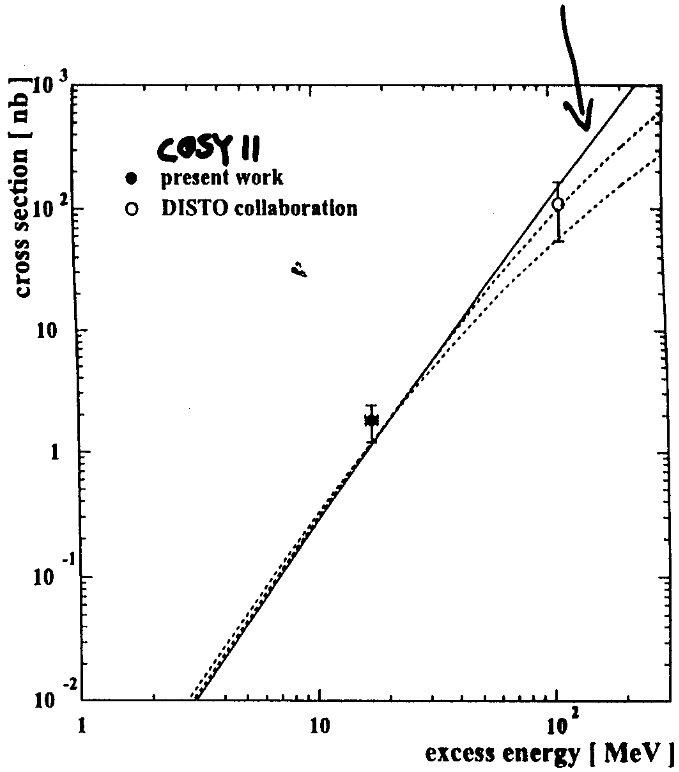

Figure 8: Total cross sections for the free K^+K^- pair production in proton-proton collisions. The lines indicate fits to the data according to the non-resonant four-body phase space expectations (solid line) and three-body phase space calculations for the resonant K^+K^- production via the f_0 (dashed lines), including the pp FSI and the Coulomb interaction. The effect of the large uncertainty about the width of the $f_0(980)$ resonance ($\Gamma = 40$ - 100 MeV [5]) is indicated by the dashed area.

V.E. Tarasov (ITEP)

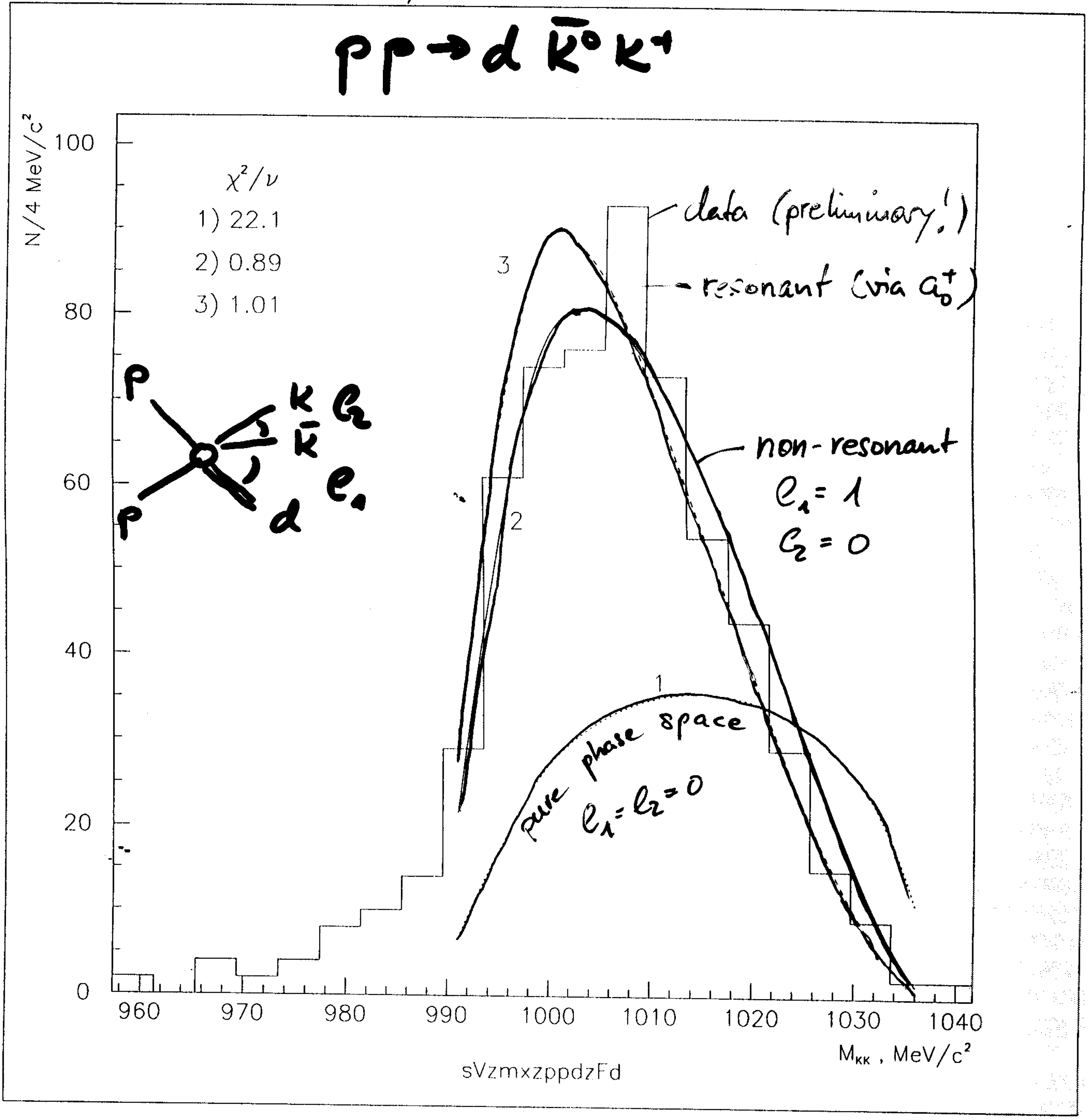

Fig. 1

V.E. Tarasov (ITEP)

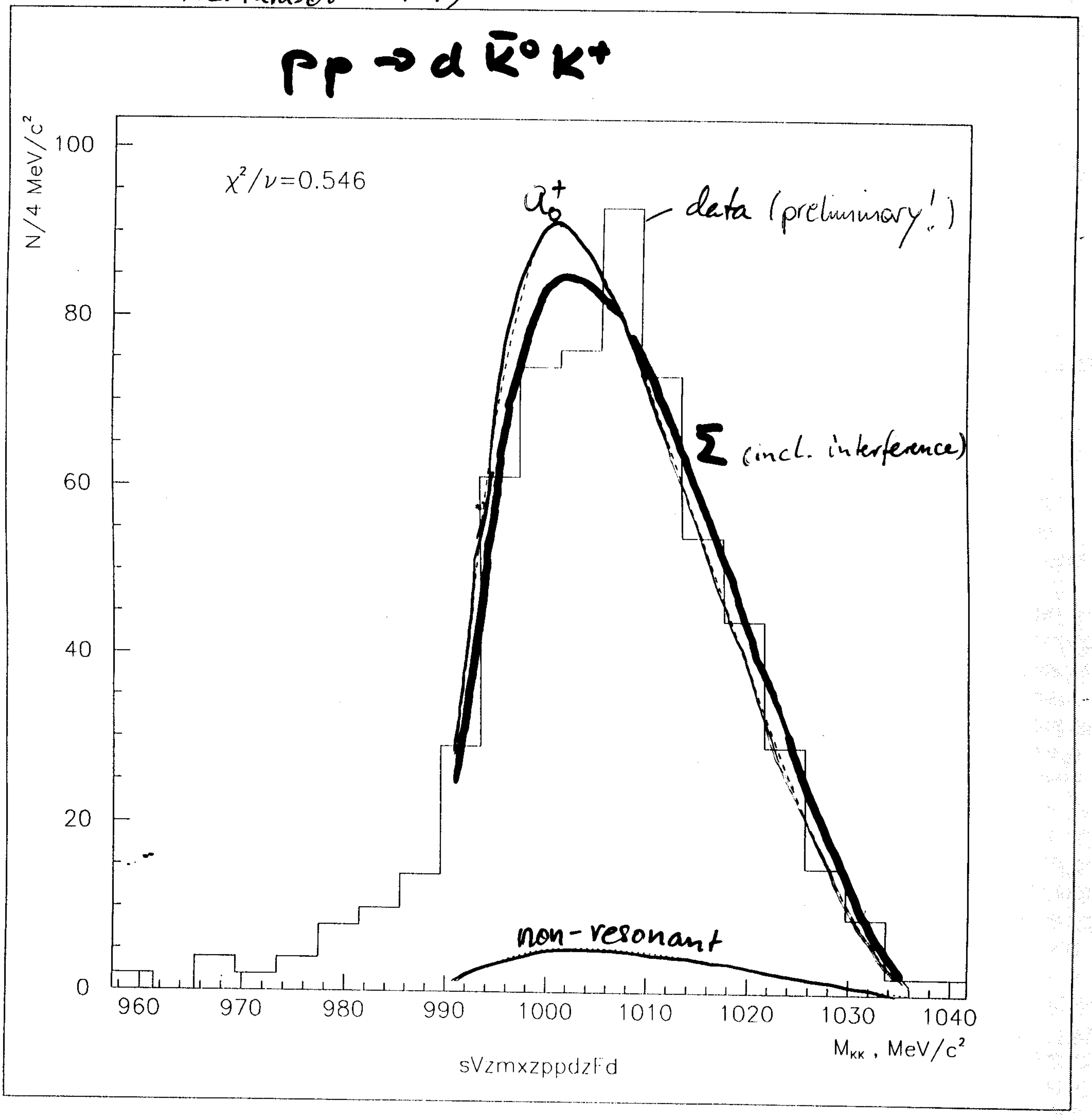

Fig. 2

V.E. Tarasov (ITEP)

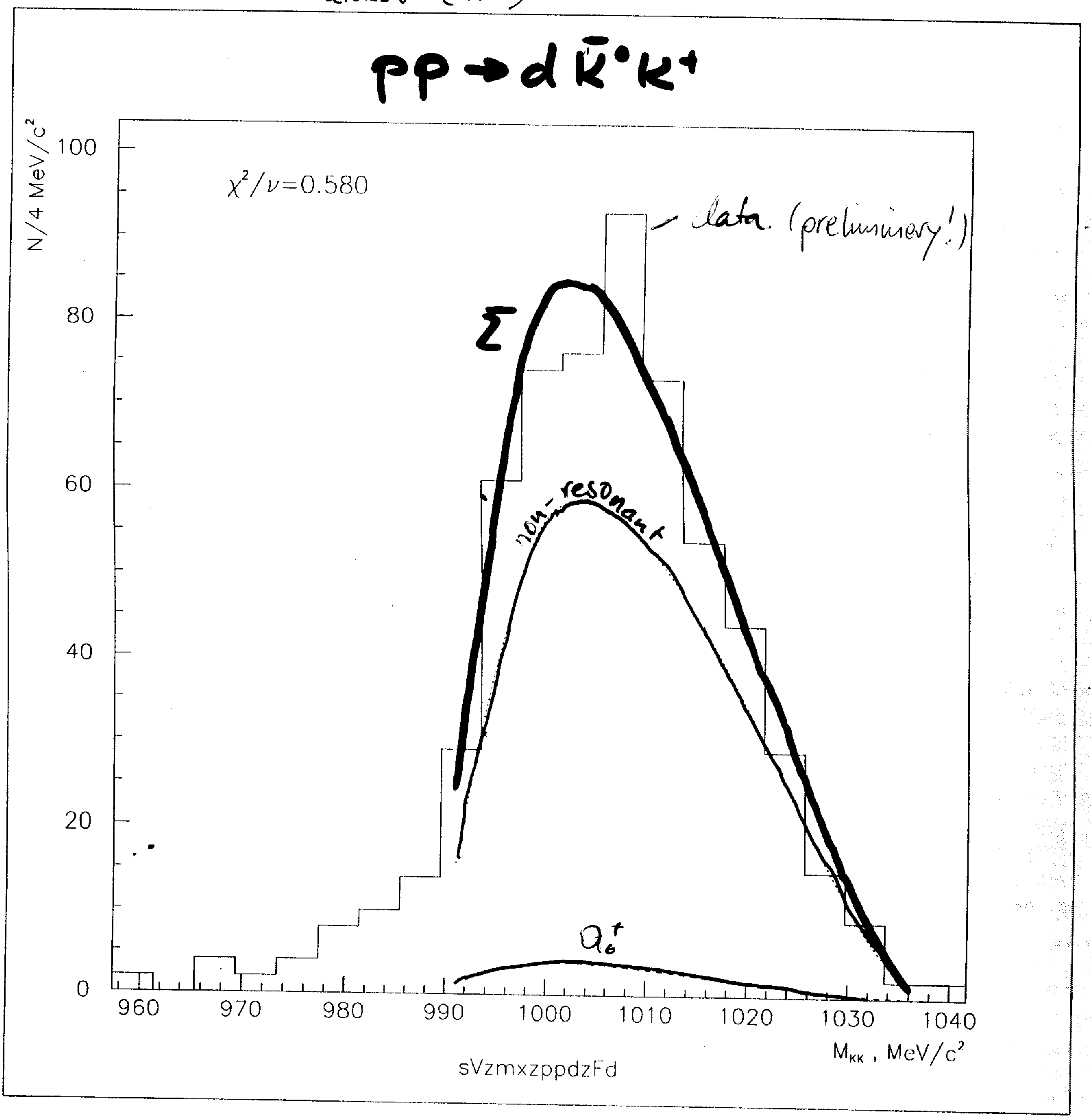

Fig. 3

The p-wave background →
→ good description of the shape of $K\bar{K}$-mass spectrum, but
a_0 can not be excluded also.

Real background

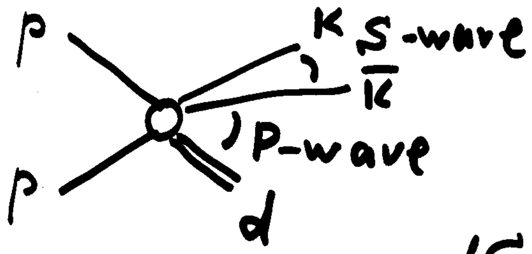

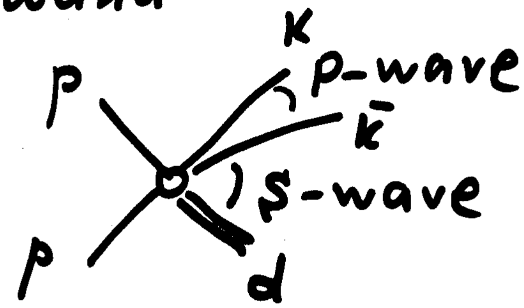

$$k^3 \cdot q \leftarrow \frac{d\sigma}{dm_{K\bar{K}}} \rightarrow k \cdot q^3$$

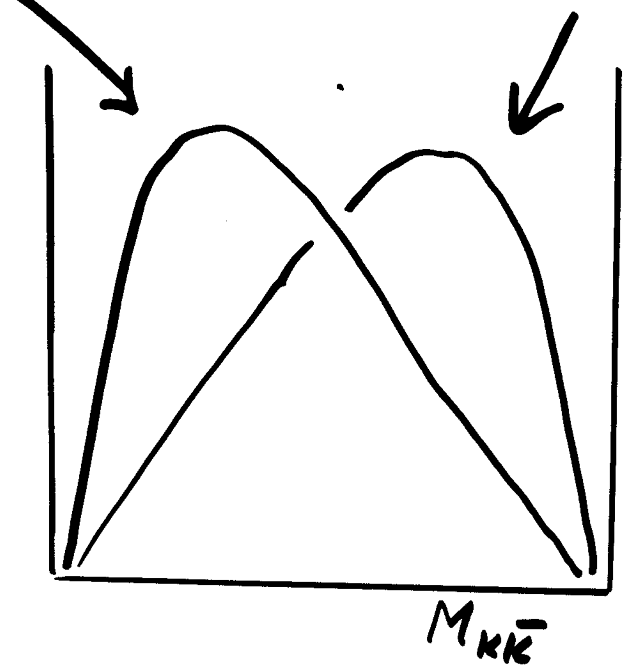

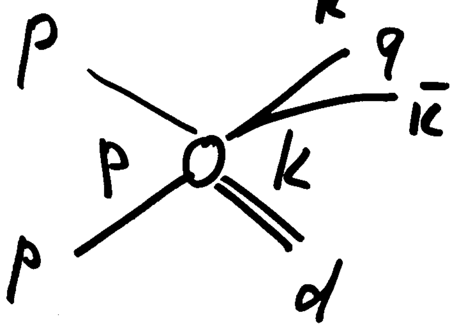

q, k - relative momenta

a_0 by Missing Mass

$$p + p \rightarrow d + a_0^+ \rightarrow d + \pi^+ + \eta$$

(software) conditions:

very preliminary missing mass distributions!!!

- * π^+ in sidewall
- * particle in FD with cut on TOF ($\rightarrow$ d in FW)
- * cut on momentum (1800-2700 MeV)
- * cut on missing mass (pp,dπ^+)

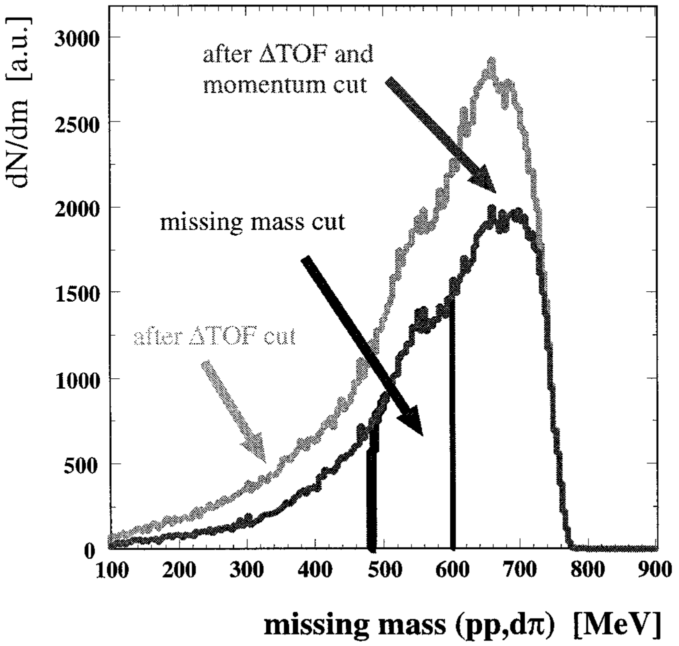

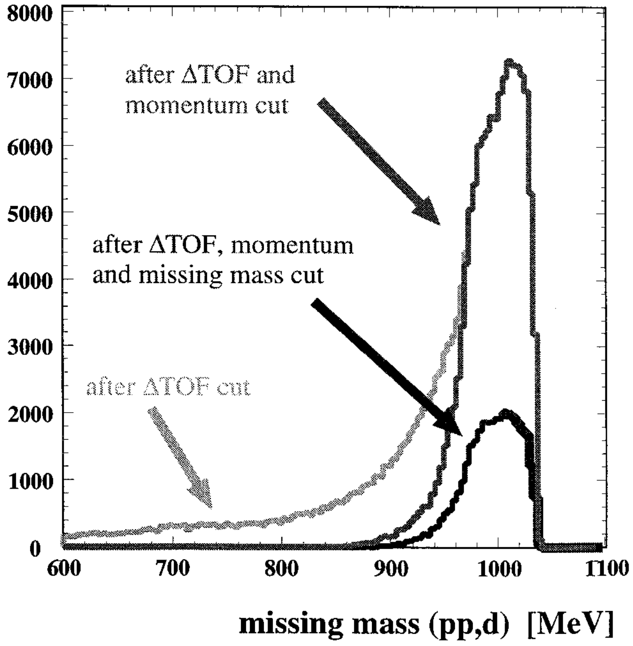

Cross Section

number of events

'non-decay' probability

branching ratio

$$\sigma = \mathbf{n / (L_{int} * \varepsilon_{geo} * \varepsilon_{decay} * \varepsilon_{det} * \Gamma)}$$

detection efficiency

geometrical acceptance

time integrated luminosity
of the cluster jet target

1. number of events: **n=560**

all results preliminary!!!

2. 'non-decay' probability:
by simulations:

K^+ : 30 %
π^+ : 90 %

3. branching ratio[*]:

$a_0^+ \to K^+ + \overline{K}^0$: 12 %
$a_0^+ \to \pi^+ + \eta$: 88 %

[*] A. Abele et al., Phys. Rev. D57 (1998) 3860, with phasespace correction

Cross Section

$$\sigma = \ n / (L_{int} * \varepsilon_{geo} * \ \varepsilon_{decay} * \varepsilon_{det} * \Gamma)$$

4. luminosity:

$p(2.65\ GeV) + p \rightarrow p + p$

S.Dymov → $L = 1.4 - 1.9 * 10^{31}\ s^{-1}cm^{-2}$
(first estimate during beam time; one run only)
P.Fedorets → $L = 2.68 * 10^{31}\ s^{-1}cm^{-2}$
(most recent value; for one run only)

$p(0.5\ GeV) + p \rightarrow d + \pi^{+}$

V.Koptev → $L = 4.5 * 10^{30}\ s^{-1}cm^{-2}$
(different beam energy)

→ $L \sim 1.0 * 10^{31}\ s^{-1}cm^{-2}$

⟶ $L_{int} = L * \Delta t$
$= L * \ 55.1\ h$

all results preliminary!!!

Cross Section

$$\sigma = n / (L_{int} * \varepsilon_{geo} * \varepsilon_{decay} * \varepsilon_{det} * \Gamma)$$

5. geometrical acceptance:

GEANT simulations

ε_{geo} ($K^+ + d$) : 9.4 %
ε_{geo} ($\pi^+ + d$) : 0.4 %

6. detection efficiency

$$\varepsilon_{det} = \varepsilon_{SD\text{-}MWPC} * \varepsilon_{\Delta E\text{-}Cut} * \varepsilon_{FD\text{-}MWPC}$$

$\varepsilon_{SD\text{-}MWPC} = 96$ %

$\overline{\varepsilon}_{\Delta E\text{-}Cut}$(tel. 11-15) = 56 %

$\overline{\varepsilon}_{FD\text{-}MWPC} = 25$ %

all results preliminary!!!

→ $\sigma = (0.62 +/- ?)\ \mu b$

a_0^+ - Production Cross Section

$$\sigma = n / (L_{int} * \varepsilon_{geo} * \varepsilon_{decay} * \varepsilon_{det} * \Gamma)$$

n = 560

$L = 1 \cdot 10^{31}\ cm^{-2}s^{-1}$

$\varepsilon_{geo} = 9.4\ \%$

$\varepsilon_{decay} = 0.30\ \%$

$\varepsilon_{det} = 13.4\%$

$\Gamma = 12\%$

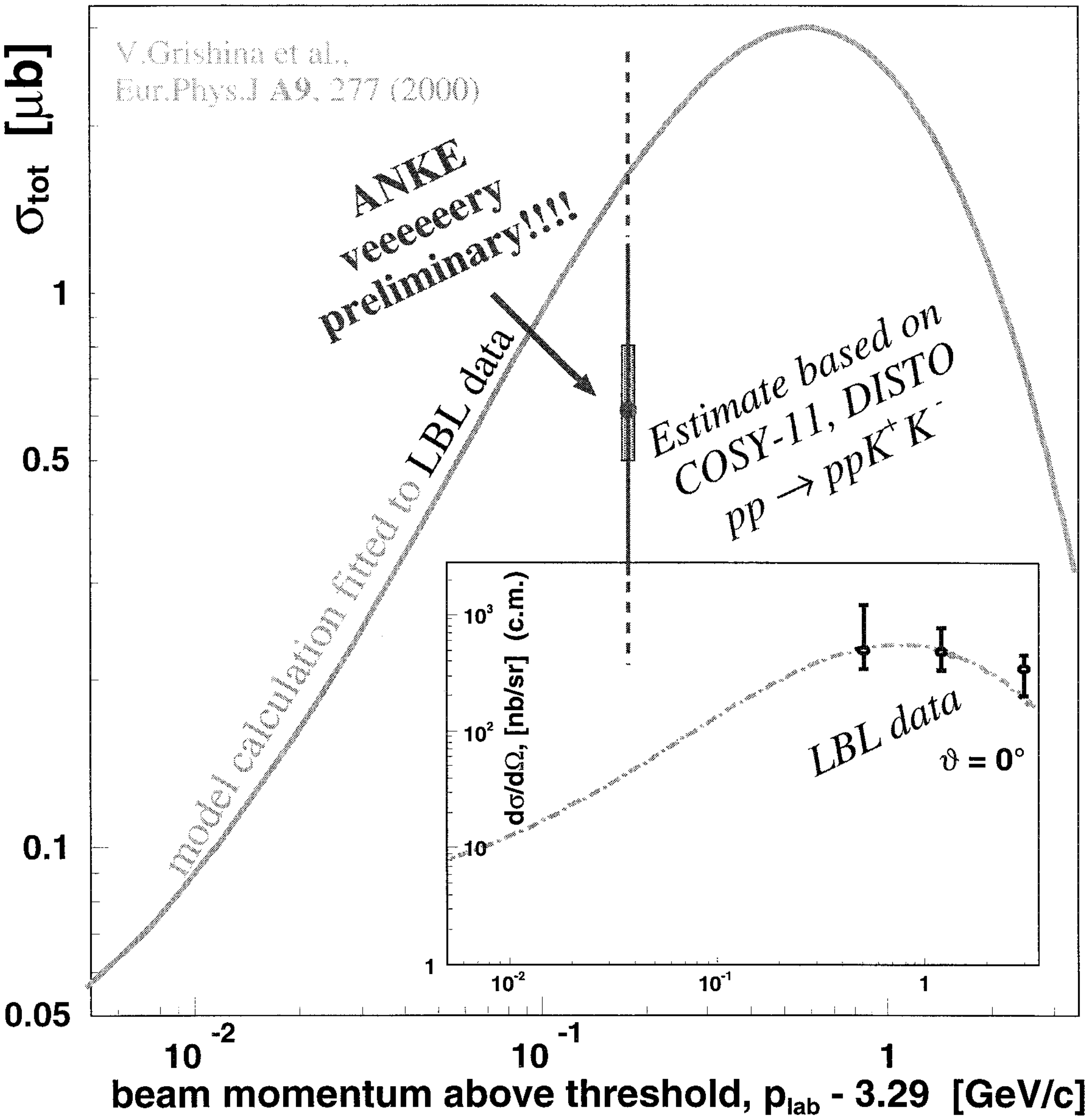

Resume of a_0^+ Beam Time

- p(2.65 GeV) p $\to dK^+\bar{K}^0$ and $\to d\pi^+\eta$ events have been identified (in total ~2000 expected)
- Interpretation as pp $\to da_0^+$
  $\to \pi^+\eta$
  $\to K^+\bar{K}^0$
  seems justified
- a_0^+ -production cross section is rather large
  $\sigma_{tot} \sim 0.6\ \mu b$
- Data analysis is in progress ...!
- Systematic studies of scalar mesons are possible with ANKE

- ANKE + detectors for negatively charged particles:

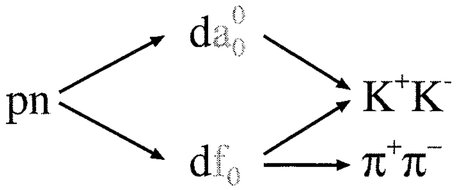

pn
da_0^0
df_0
K^+K^-
$\pi^+\pi^-$

Outlook

a_0^+: → data analysis is going on

- **π/μ channel**
- **efficiency studies**
- **simulations to compare data and model**

a_0^0/f_0:

- **first tests during next beam time in August 2001 (ω production on the n)**
- **3 weeks of beam time in beginning of 2001**

Analysis of the data on a_0-meson production from the ANKE experiment

A.E.Kudryavtsev

Institute of Theoretical and Experimental Physics
117259 Moscow
Russia

Recent results on the reaction

$$pp \to K^+\bar{K}^0 d \tag{1}$$

at $T_p = 2.645$ GeV/c, obtained in the current experiment at ANKE spectrometer [1], are analysed phenomenologically. The purpose of the analysis is to answer the question whether these data give evidence for production of scalar a_0^+ meson in the $K\bar{K}$ channel. The experimental $K^+\bar{K}^0$-mass spectrum from the reaction (1) is shown in Fig.1 (histogram).

There are some arguments for resonance solution of this problem:

i) The number of events observed in ANKE experiment [1] is in correspondence to what follows from theoretical estimations. Those theoretical predictions were based on the estimation of the production rate for a_0^+ meson in a simple meson exchange model, see, ref. [2] for more details.

ii) Theoretical estimations for nonresonance background [2] are expected to be strongly suppressed in comparison with what is seen at ANKE experiment.

iii) The observed $K^+\bar{K}^0$-effective mass spectrum looks like a resonance or a rather sharp bump.

Note that arguments *i)* and *ii)* are model dependent. The modern effective meson-nucleon theories of strong interactions are not able to predict cross sections for production of heavy mesons ($m_a \sim 1$ GeV) with high accuracy. What about argument *iii)*, the allowed $K\bar{K}$-mass interval is rather narrow ($991.4 < M_{K\bar{K}} < 1037.3$ MeV). That is why the phase volume limitations should already reproduce a resonance-like bump in the $K\bar{K}$-mass spectrum. The complicating point of the situation is in the following: the expected width of a_0 meson ($\Gamma_a \sim 80$ MeV) is larger that the allowed $K\bar{K}$-mass interval $\Delta m \sim 40$ MeV. That is why great efforts are to be performed to make distinction between resonance and nonresonance solutions.

Let us consider first the case, when the reaction amplitude is considered to be constant. Then the shape of the $K\bar{K}$-spectrum is given by phase space factor, i.e.

$$\frac{d\sigma}{dm} = N\, k\, q\,. \tag{2}$$

Here m is the mass of the $K^+\bar{K}^0$ system, k is the deuteron reaction c.m. momentum, q is the relative momentum of kaons in the $K\bar{K}$ system, and N is normalization constant. The distribution (2) is shown in Figure 1 by dotted curve. As it is seen from Figure, this phase space dependence is inconsistent with the experimental data. Hereafter, when describing the visible $K\bar{K}$ spectrum, we take into account experimental mass resolution by convoluting the theoretical expressions for $d\sigma/d\Omega$ with gaussian:

$$\frac{d\sigma}{dm} = \int g(m,m')\,\frac{d\sigma}{dm'}\,dm'\,, \tag{3}$$

where

$$g(m,m') = \frac{1}{\sigma\sqrt{2\pi}}\exp\left[-\frac{(m-m')^2}{2\sigma^2}\right]\,. \tag{4}$$

Gaussian parameter $\sigma = \sigma(m)$ was chosen in correspondence to experimental mass resolution function $\delta m(m)$, taken from ref [3]. According to gaussian parametrization of experimental resolution we took $\sigma(m) = \delta m(m)/2.36$.

Note that phase space dependence of differential cross section (2) discussed above corresponds to the production of final deuteron and a_0 meson in s wave. However, s-wave channel in the reaction $pp \to da_0^+$ is forbidden due to parity and angular momentum conservations and the Pauli principle [2, 4].

Consider first the case, when $K^+\bar{K}^0$ system has angular momentum $l = 0$, i.e. kaons are produced in s wave. Then the $K\bar{K}$ system should be produced in p wave with respect to deuteron. Then the reaction amplitude is to have a linear dependence on momentum k and we get instead of (2):

$$\frac{d\sigma}{dm} = \tilde{N}\, k^3\, q. \tag{5}$$

The distribution (5) being convoluted with the experimental resolution according to the prescription (3), is shown in Figure 1 by solid line. As it seen, it is in reasonable agreement with the experimental data and gives $\chi^2/d.f. = 0.89$ (hereafter χ^2 procedure is applied to the mass interval 990 MeV $\leq m \leq$ 1038 MeV, for which the number of events in each bin is high enough).

In the case when the $K^+\bar{K}^0$ system has angular momentum $l = 1$, we get quite a different expression for differential cross section:

$$\frac{d\sigma}{dm} = \tilde{\tilde{N}}\, k\, q^3\,, \tag{6}$$

which corresponds to the production of deuteron in s wave with respect to the $K\bar{K}$ system. The distribution, which corresponds to the expression (6), is shown by dashed-dotted line in Figure 1. As it seen, it is inconsistent with the experimental data.

That is why we conclude that in the ANKE experiment at $T_p = 2.645$ GeV/c^2, the $K\bar{K}$ system is produced mainly in s wave.

So later on we shall limit ourself by suggestion that the $K\bar{K}$ system is produced only in s wave and shall compare resonance and nonresonance production hypotheses with the experimental data.

Consider first the case of a pure resonance production of $K\bar{K}$ system, i.e. through the chain

$$pp \to a_0^+\, d \to K^+\bar{K}^0\, d\,. \tag{7}$$

For this resonance production mechanism the differential cross section has the form

$$\frac{d\sigma}{dm} = N\, |A|^2\, k^3\, q\,, \tag{8}$$

where $A = (m - m_a + i\Gamma(m)/2)^{-1}$ and m_a is nominal mass of a_0^+ meson. For the width $\Gamma(m)$ we use the analytic expression, suggested by Flatte [5]:

$$\Gamma(m) = g_1 q_1 + g\, q\,, \tag{9}$$

where q_1 is relative momentum in the $a_0 \to \pi + \eta$ decay channel, taken at $m = m_a$. We use the parameters m_a = 1001 MeV, $g_1 = 0.243$ and $g = 0.221$ for a_0^+ meson from the ref [6]. The result of the χ^2-fit to the experimental data is shown by dashed line in Figure 1. The description of the data is quite reasonable ($\chi^2/d.f. = 1.01$).

So we conclude that both alternative ways for description of the experimental $K\bar{K}$-mass spectrum (resonance and nonresonance) look reasonable.

Now let us consider the case when the production matrix elements includes both resonance and nonresonance terms. In this case we get

$$A = \frac{1}{m - m_a + i\Gamma(m)/2} + Be^{i\phi}, \tag{10}$$

where B and ϕ are constant. In what follows we shall vary parameters B and ϕ to get better description of the data.

One example of the fit ("best fit") to the data with the amplitude A in the form (10) is given in Figure 2. The parameters B and ϕ are presented in the Table. The description of the data is quite reasonable ($\chi^2/d.f. = 0.546$). Solid, dashed and dotted curves in Figure 2 represent total, resonance and background contributions, respectively. We see that for this case resonance contribution dominates.

However, the value $\chi^2/d.f.$ is rather smooth function of parameters B and ϕ (no strong minimum of χ^2 functional). One can essentially increase the value B and obtain similar to the best fit description of the data with good values for $\chi^2/d.f.$ The example of the description is presented in Figure 3 and corresponds to the value $\chi^2/d.f. = 0.58$. In this case background dominates and resonance contribution is suppressed. Both results, presented in Figures 2 and 3, are summarized in the Table.

	B, MeV^{-1}	ϕ, deg	x_R	x_B	$\chi^2/d.f.$
Fig.2 (best fit)	0.005	15	1.006	0.065	0.546
Fig.3 (fixed B)	0.080	-140	0.044	0.720	0.580

Here: x_R and x_B are relative weights of resonance and background contributions,

$$x_n = \sigma_n/\sigma \quad (n = R, I, B),$$

and $\sigma = \sigma_R + \sigma_I + \sigma_B$. Subscripts R, I and B correspond to contributions of the resonance, interference and background terms, respectively, and $x_R + x_I + x_B = 1$.

We conclude that the description of the data with matrix element, taken as the sum of resonance and nonresonance terms (10), is excellent. At the same time both versions presented in Figures 2 and 3 reproduce experimental data well. So we can not prefer one of this version to another. Thus, for the moment it is impossible to separate resonance hypothesis from nonresonance one.

Notice that if nonresonance contribution to the cross section is large, as in the version, shown in Figure 3, the genesis for such a large background remains questionable. Existing theoretical estimations for background predict smaller value [2]. May be large background is influenced by the induced decay of the produced a_0^+ mesons. In this case the inelastic $a_0 d \to K\bar{K}d$ cross section is large, what corresponds to the molecular hypothesis of a_0 meson [7].

Note that the width of a_0^+ meson is large, $\Gamma_a \approx 80$ MeV, and is comparable with the studied $K\bar{K}$-mass interval $\Delta m \approx 40$ MeV. For the present statistics (number of events $N_{ev} \approx 600$) we can not separate resonance from nonresonance hypotheses ($\chi^2/d.f.$ is approximately the same for both cases). But if statistics of the experiment will increase, we get opportunity to separate these hypotheses. This statement is illustrated in Figure 4, in which the dashed curves correspond to ratios $f_1(m)/f_0(m)$ (Figure 4a) and $f_2(m)/f_0(m)$ (Figure 4b). Here we use the notations $f_i(m) = d\sigma_i/dm$ $(i = 0, 1, 2)$ for $K\bar{K}$-mass distributions. The subscripts $i = 1$ and $i = 2$ correspond to pure nonresonance (5) and pure resonance (8) hypotheses for matrix element, respectively. The case $i = 0$ corresponds to the some ideal distribution, which we shall identify with our "best fit" solution, given by solid curve in Figure 2. The dotted curves show the error bars, which are given for the present statistics and correspond to the expressions $1 \pm 1/\sqrt{f_0(m) \cdot \Delta m}$, and the bin is: $\Delta m = 4$ MeV. It is seen that the decrease of errors by factor 3 should clarify the situation and confirm or disconfirm one of these two hypotheses.

Conclusions

Existing experimental data [1] on the reaction $pp \to K^+\bar{K}^0 d$ may be described quite reasonable under suggestion that all kaons are produced through formation of a_0^+ resonance. Another possible solution with nonresonance production mechanism also gives reasonable description of the data. Nonresonance production of $K\bar{K}$ system with angular momentum $l = 1$ may be excluded at present level of statistics. Future increase of statistics may help in getting the correct solution of the problem.

The authors are thankful to S.Dymov and V.Kleber for useful discussion of the experimental situation. The authors are also thankful to M.Büscher and H.Ströher for their interest to this work and useful remarks.

References

[1] V.Kleber. The talk given at this ANKE 2001 Meeting. June 2001, Gatchina. M.Büscher (spokesperson). Status report for COSY experiment #55, March 16, 2001.

[2] V.Yu.Grishina, L.A.Kondratyuk, E.L.Bratkovskaya, M.Büscher and W.Cassing. Nucl-th/0007074, 2000.

[3] H.Junghans. In. Proc. of ANKE 2000 Workshop, Berichte des Forschungszentrum Jülich 3801, p.261.

[4] A.E.Kudryavtsev, V.E.Tarasov. In. Proc. of ANKE 2000 Workshop, Jülich 3801, p.151; JETP Lett., **72**, N.8, 2000, pp.410-414; nucl-th/0102053, Feb 2001.

[5] S.M.Flatte. Phys.Lett. **63**, 224 (1976).

[6] S. Teige, B.B. Brabson, R.R. Crittenden, *et al.*. Phys.Rev.D **59**, 012001 (1999).

[7] J.Weinstein and N.Isgur, Phys.Rev.D **41**, 2236 (1990).

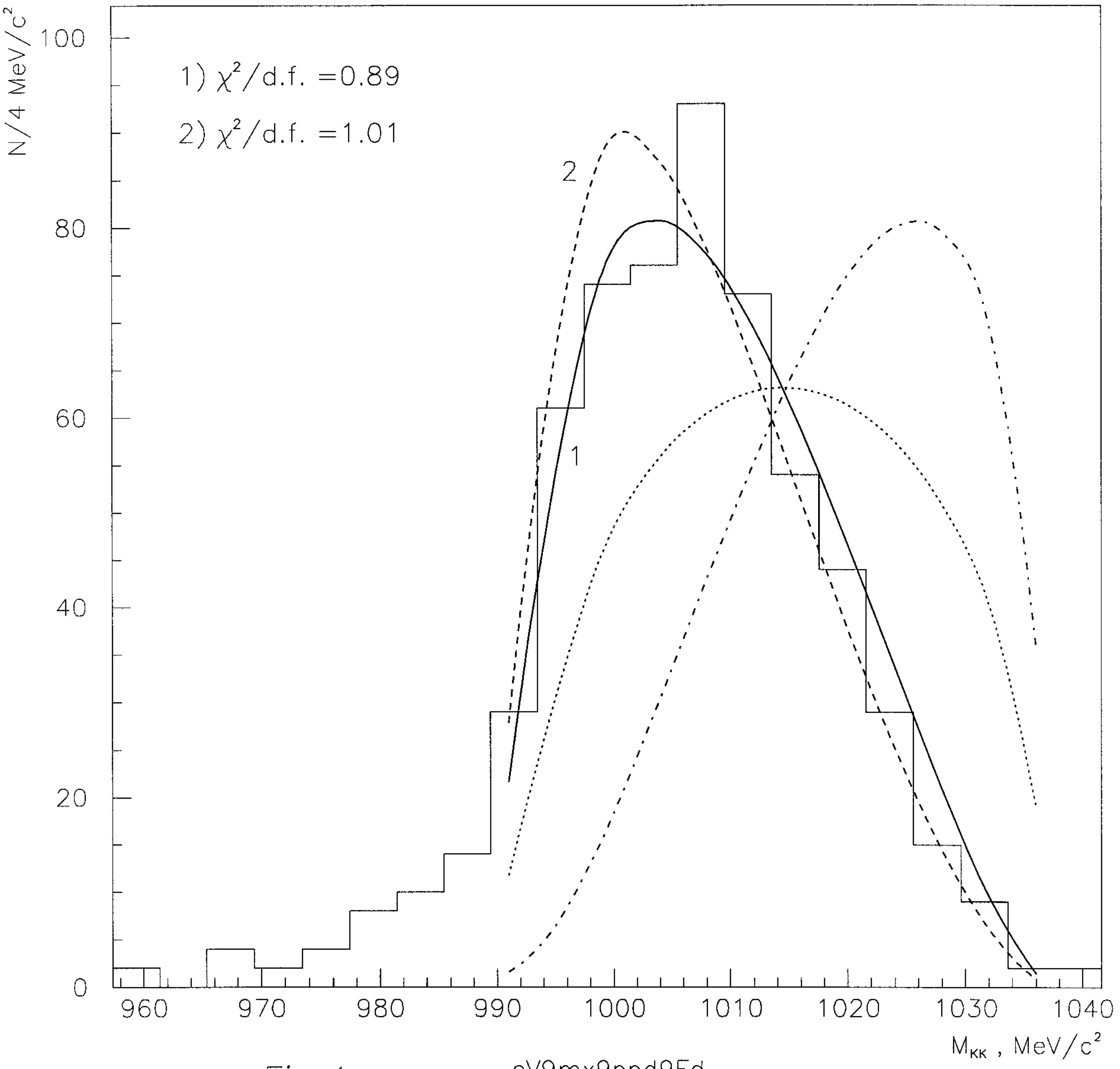

Fig.1

sV9mx9ppd9Fd

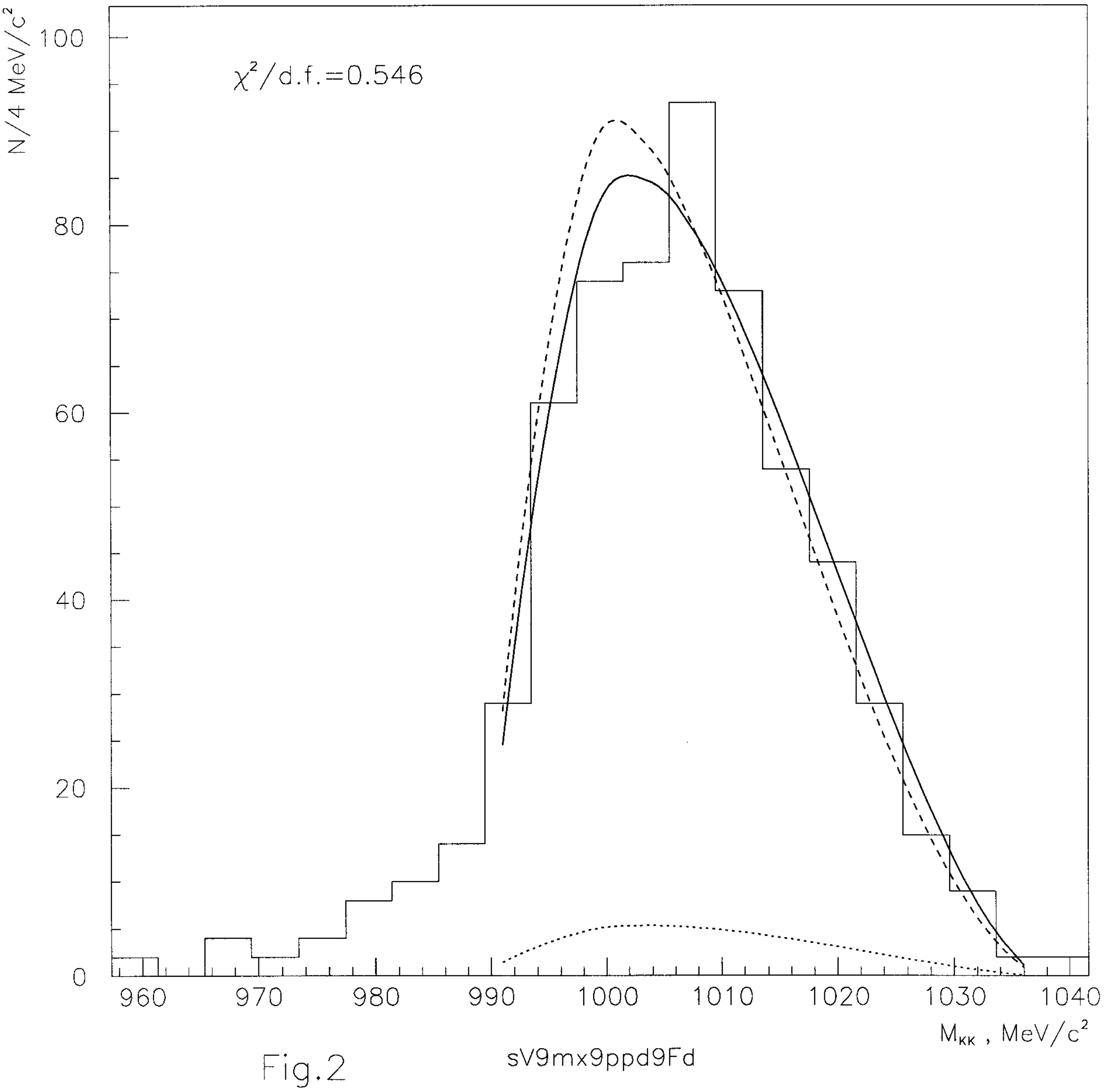
N/4 MeV/c^2
0
20
40
60
80
100
χ^2/d.f.=0.546
960
970
980
990
1000
1010
1020
1030
1040
M_{KK} , MeV/c^2
sV9mx9ppd9Fd

Fig.2

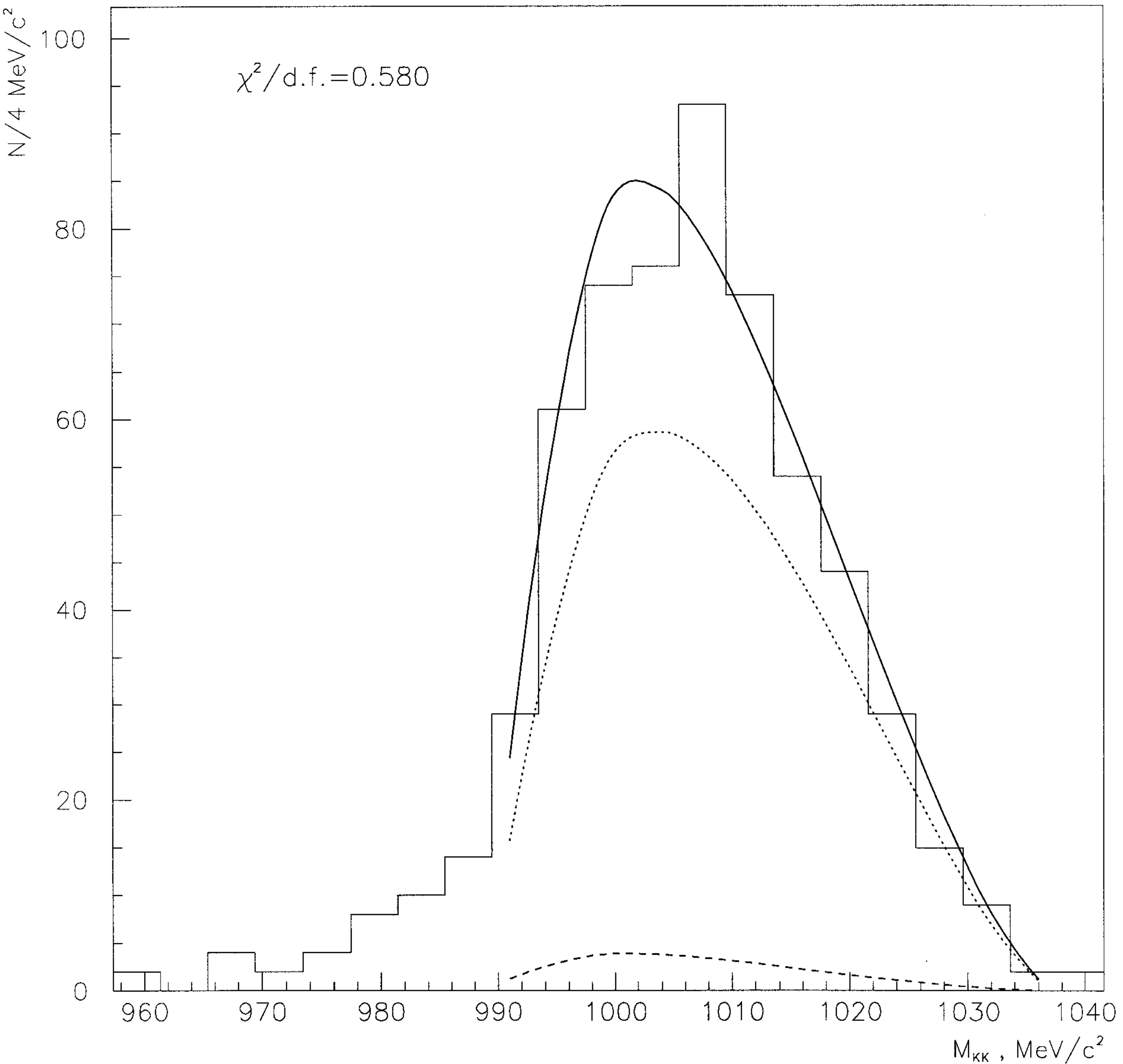

Fig.3

sV9mx9ppd9Fd

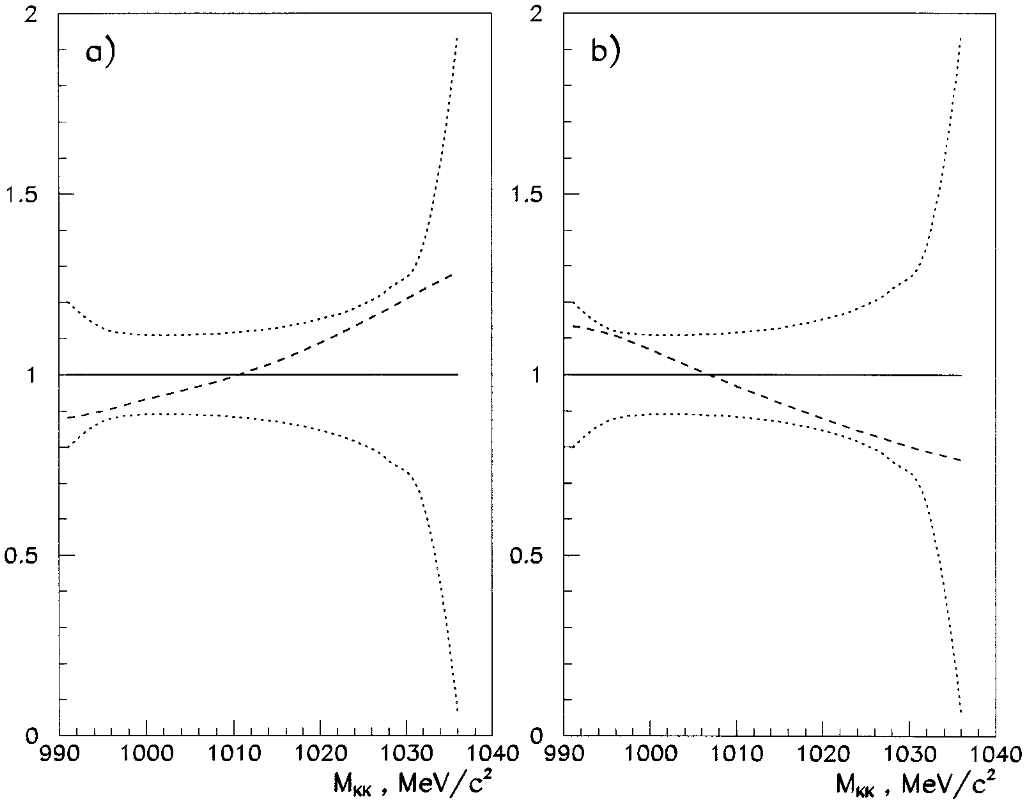

Fig.4

The analysis of the data on the a_0^+ production (ANKE exp)

V. Chernishov, V. Tarasov, A. Kudryavts

$pp \to d a_0^+$

$\quad \hookrightarrow K^+\bar{K}^0$

$\quad \hookrightarrow \pi^+\eta$ (?)

$(pp \to d K^+\bar{K}^0)$
??

$991.4 < M_{KK} < 1037.3$

$\Gamma_a \sim 80$

$T_p = 2.645$ GeV

$\sigma_{Theor} \sim 1\,\mu b$ (V. Grishina et al.)

Arguments for the resonance solution:

1) $N(K^+\bar{K}^0) \sim$ that follows from theoretical predictions

2) Background is expected to be suppressed

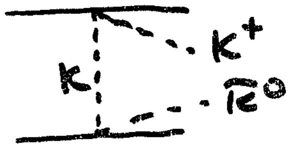

3) $K^+\bar{K}^0$ effective mass spectrum looks like resonance

1) + 2) → theoretical calculation predict only order of magnitudes for such $q^2 \gg 1\,GeV^2$: different theor models, ISI factor was not included

3) Phase Volume is limited → $K^+\bar{K}^0$ eff. mass spectrum looks naturally like "bump"

$$m(K^+\bar{K}^0) = m(K^+) + m(\bar{K}^0) + E_{cm}$$

$$\frac{d\sigma}{dm_{KK}} = \frac{1}{j}|M|^2 \cdot \underbrace{K \cdot q}_{\overset{\uparrow}{p.v.}}$$

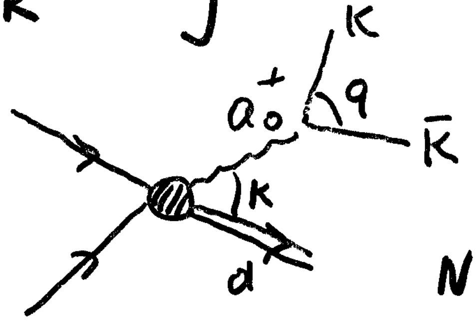

1) |M| is constant

2) $M \sim K$ $\quad pp \to \underbrace{da_0^+}_{\text{P-wave}}$ Near threshold $|M|^2 \sim |K|^2$

I=1, S=1, L=1 → NN are fermions

$$\frac{d\sigma}{dm_{KK}} \sim |A|^2 \cdot K^3 \cdot q$$

3) We have resonance production (not coustant)

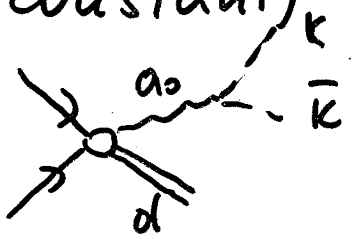

$$A \sim \frac{1}{m - \bar{m} + i\frac{\Gamma}{2}(m)}$$

(Flatte)

$$\boxed{\text{Figure } 1}$$

$A = \text{const}$ $\quad \chi^2/\nu = 0.89$

$$A = \frac{1}{m - \bar{m} + i\frac{\Gamma(m)}{2}} \qquad \chi^2/\nu = 1.01$$

$$M = \frac{1}{m - m_a + i\frac{\Gamma(m)}{2}} + Be^{i\phi}$$

B, ϕ-coustants

Better desqription (we have 2 parameters)

B	ϕ	$\chi^2/d.f.$	
0.005	15°	0.546	Fig 2
0.080	-140°	0.580	Fig3

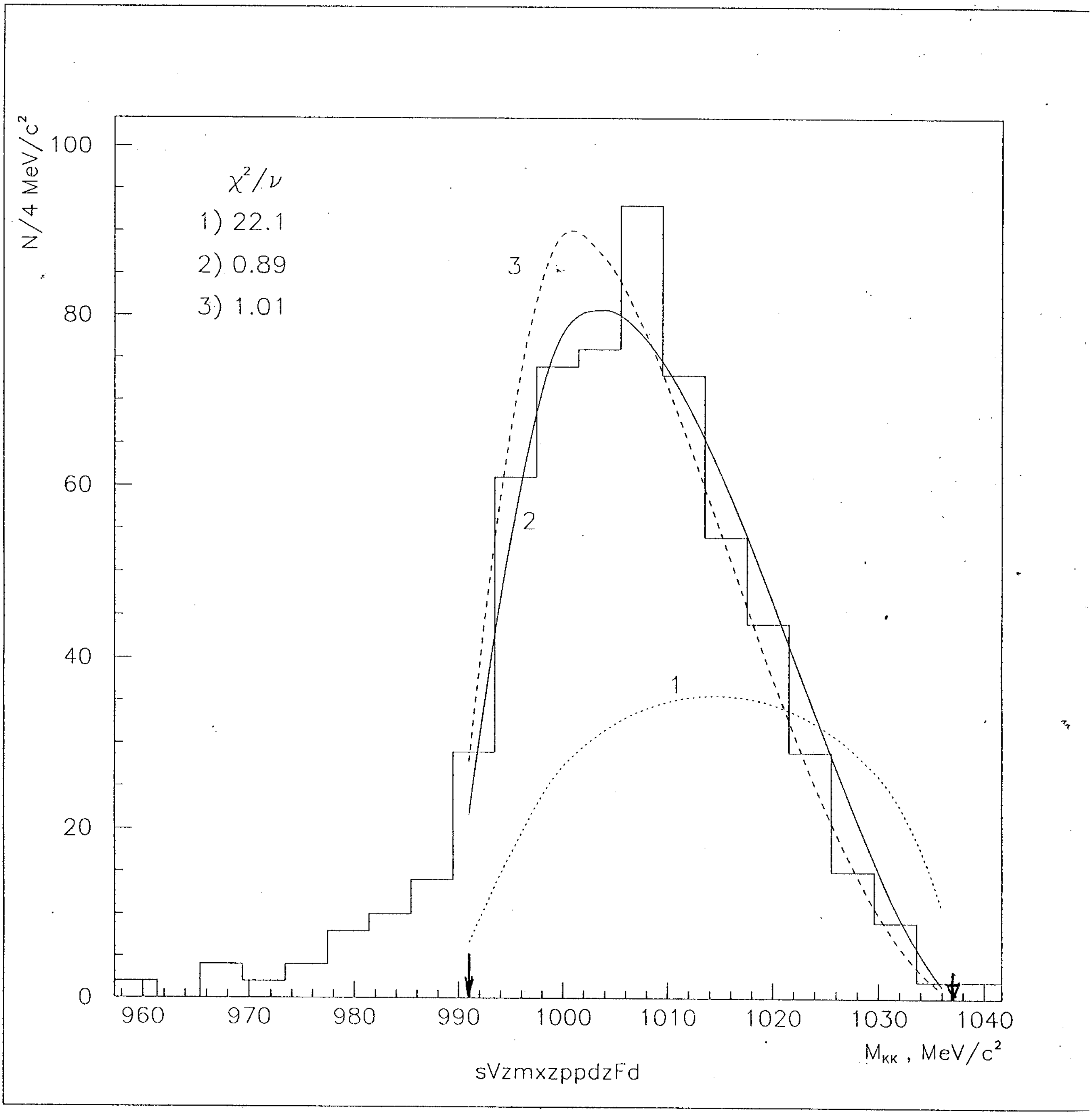
N/4 MeV/c^2
100
80
60
40
20
0
χ^2/ν
1) 22.1
2) 0.89
3) 1.01
3
2
1
960
970
980
990
1000
1010
1020
1030
1040
M$_{KK}$, MeV/c^2
sVzmxzppdzFd

Fig. 1

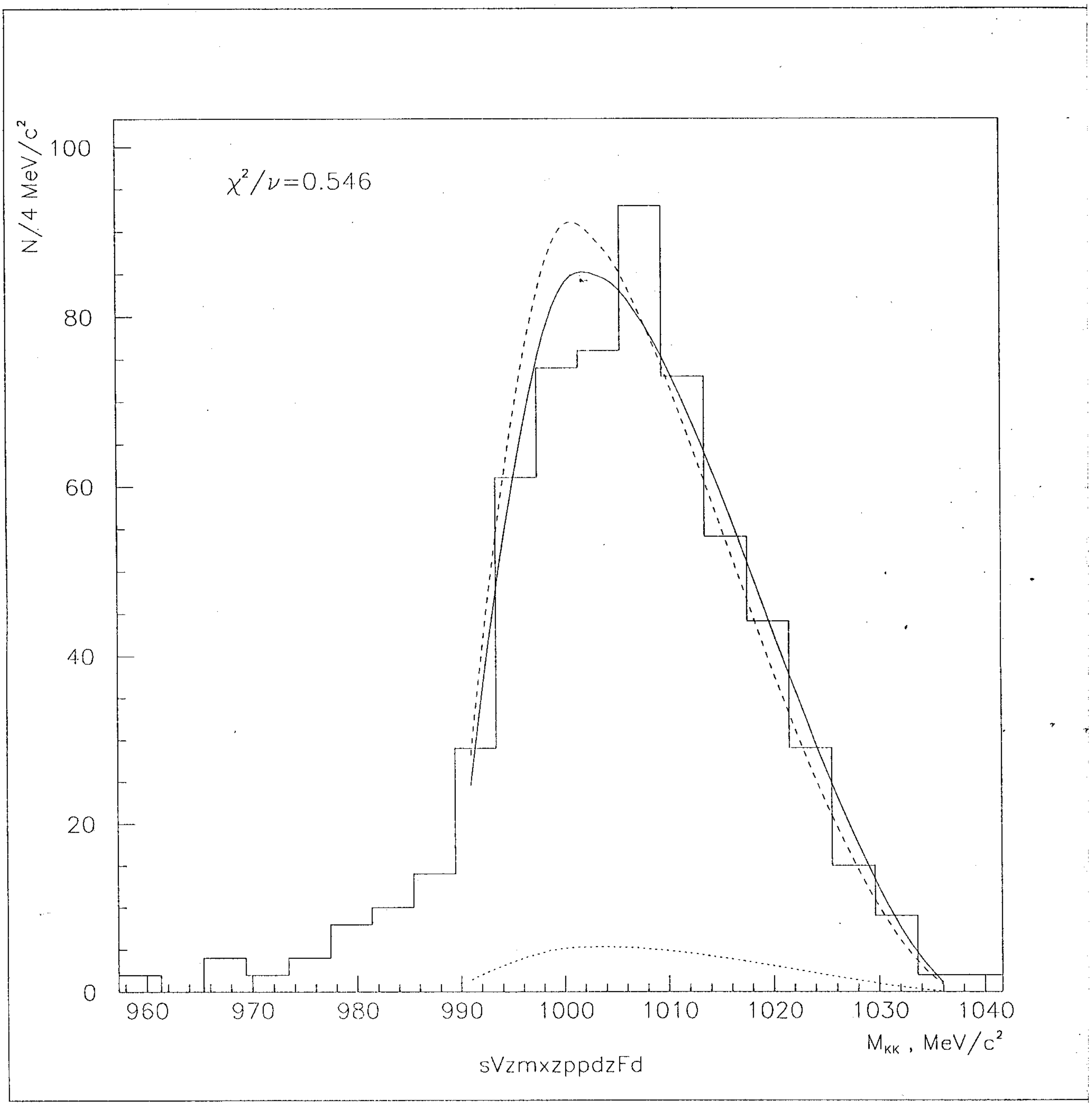
χ^2/ν=0.546
N/4 MeV/c^2
0
20
40
60
80
100
960
970
980
990
1000
1010
1020
1030
1040
M$_{KK}$, MeV/c^2
sVzmxzppdzFd

Fig.2

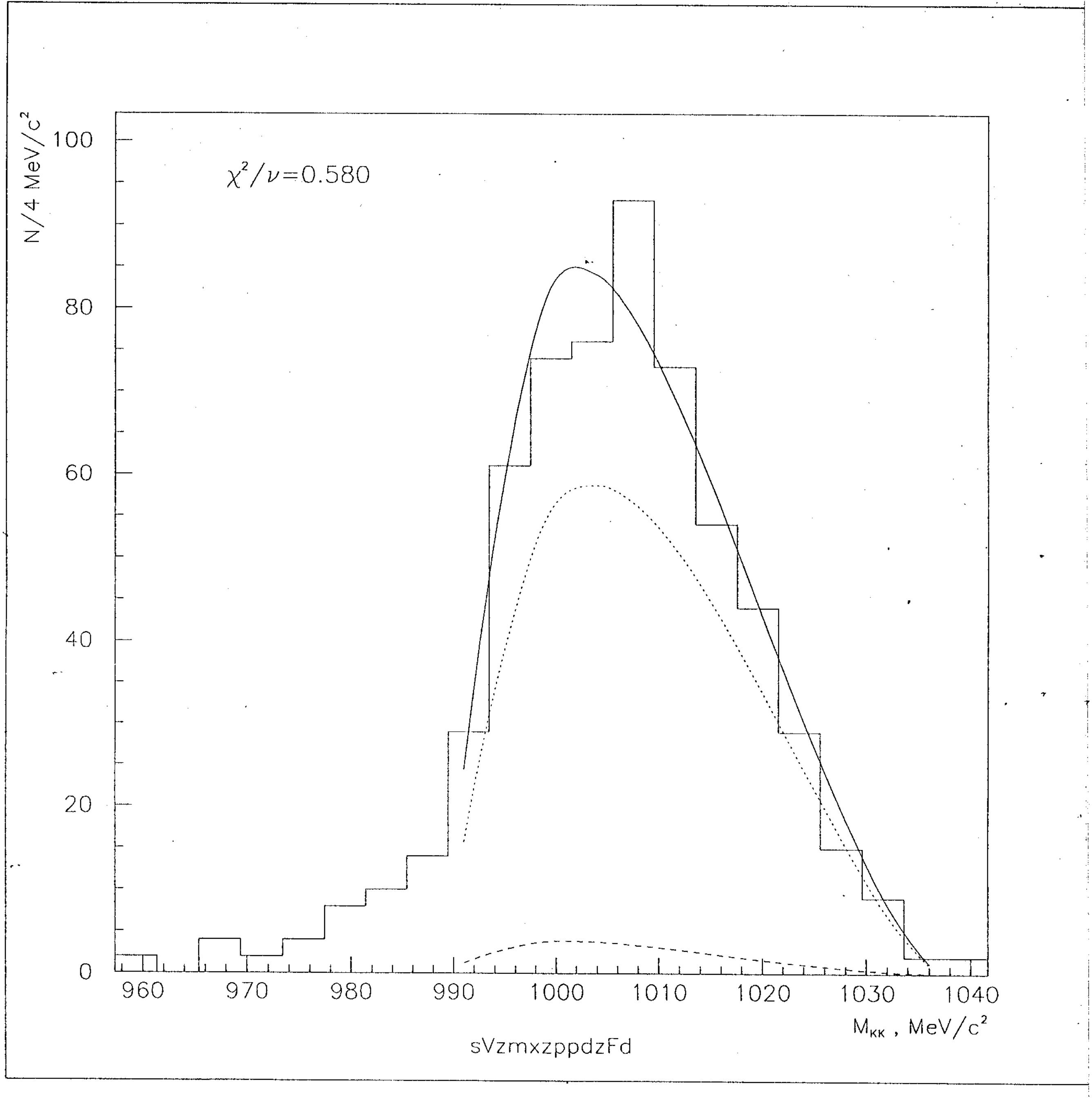
N/4 MeV/c²
100
80
60
40
20
0
χ²/ν=0.580
960
970
980
990
1000
1010
1020
1030
1040
M_KK , MeV/c²
sVzmxzppdzFd

Fig. 3

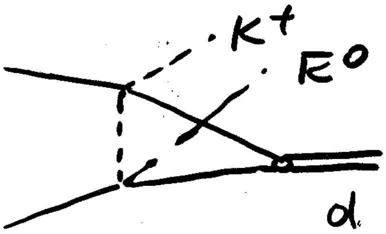

? The background is small.

Hypothesis: a_0 induced background

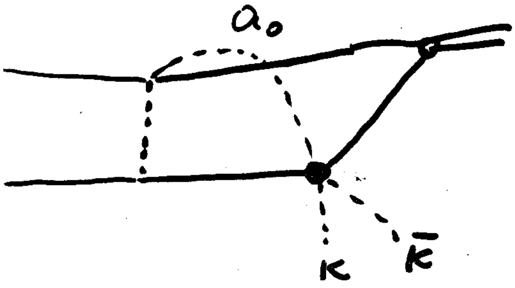

? looks like background (molecular hypothesis)

Preconclusions:

1) Statistics is to be improved

2) $\pi^+\eta$ is more preferrable $\underline{\Delta m_{\pi\eta} > \Gamma_{a_0}}$

$\eta \to 2\gamma$

3) Binnie's method

$pp \to dX$

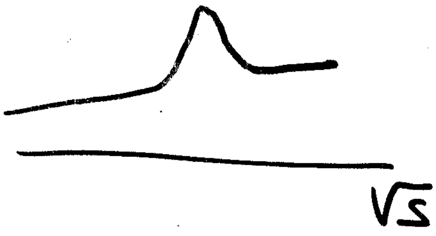

$\sqrt{s}, T_p$ P_d is fixed

4) $pd \to p_s(a_0^0 d)$

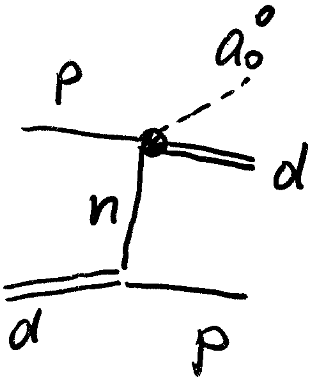

5) $\underline{a_0^0 \to f_0}$ Asymmetry

Planned $a_0(980)/f_0(980)$ measurements at ANKE

M.Büscher

Institut für Kernphysik
Forschungzentrum Jülich
52425 Jülich
Germany

Status report for COSY experiment #55 "Study of $a_0^+(980)$ mesons at ANKE" and **Proposal** "Investigation of neutral scalar mesons a_0/f_0 with ANKE"

M. Büscher (**Spokesperson**), M. Hartmann, V. Kleber, R. Koch,
R. Schleichert, H. Ströher
Institut für Kernphysik, Forschungszentrum Jülich,
D-52425 Jülich, Germany

V. P. Chernyshev, P. Fedorets, L. A. Kondratyuk
Institute of Theoretical and Experimental Physics,
117259 Moscow, Russia

Ye. S. Golubeva, V. Grishina
Institute of Nuclear Research, 117312 Moscow, Russia

V. Koptev, S. Mikirtychiants, M. Nekipelov
High Energy Physics Dept., Petersburg Nuclear Physics Institute,
188350 Gatchina, Russia

A. Khoukaz, N. Lang
Institut für Kernphysik, Universität Münster,
Wilhelm-Klemm-Str. 9, D-48149 Münster, Germany

S. Dymov, V. Komarov, G. Macharashvili
Lab. of Nuclear Problems, Joint Institute of Nuclear Research,
141980 Dubna, Russia

I. Zychor
The Andrzej Soltan Institute for Nuclear Studies,
PL-05400 Swierk, Poland

E.L. Bratkovskaya, W. Cassing
Institut für Theoretische Physik, Universität Giessen,
D-35392 Giessen, Germany

and the ANKE collaboration

March 16, 2001

Abstract

During two weeks of beam time in Jan./Febr. 2001, the production of a_0^+-mesons in the reaction $p(2.645\text{GeV})p \to da_0^+$ has been studied at the ANKE spectrometer. About 1000 correlated dK$^+$ (dπ^+) events have been identified which can be interpreted in terms of $a(980)$-meson production followed by a decay $a_0^+ \to K^+\overline{K^0}$ ($\to \pi^+\eta$). These count rates allow systematic investigations of the scalar mesons and we propose **3 weeks** of measurements of the neutral scalar mesons produced in a deuteron target $pn \to da_0^0/f_0$. The mesons will be identified by measuring their decay into $\pi^+\pi^-$- and K^+K^--mesons in coincidence with the fast deuteron. This requires the use of the detection system for negatively charged ejectiles which will be available at ANKE in the beginning of 2002.

Contents

1 Introduction

This proposal is a continuation of the studies on a_0^+ production described in COSY proposal #55 [1, 2] which was approved during the 14th and 20th meeting of the COSY-PAC. The corresponding measurements were carried out during two weeks of beam time in Jan./Febr. 2001. After a first analysis of the data, about 1000 events from reactions $p(2.645\mathrm{GeV})p \to dK^+\overline{K^0}$ and $\to d\pi^+\eta$ have been identified. Based on the theoretical considerations outlined in the proposal [1, 2] these events are assigned to a_0^+-production followed by a decay into $K\bar{K}$ or $\pi\eta$. The number of identified a_0^+-mesons is in good agreement (within a factor of 2) with the predicted values in [2]. **We conclude that these moderately large counting rates allow systematic studies of the scalar $\mathbf{a_0^+}$-meson.**

This proposal foresees the investigation of the *neutral* scalar mesons a_0 and f_0 produced in the reactions $pn \to da_0^0/f_0$ at maximum COSY energy ($T = 2.645$ GeV or higher). Based on the experience of the a_0^+ beam time (see Sect. 3 for first results from the data analysis) and on our cross section estimates for the a_0^0/f_0 (see Sect. 4.1.2) it is estimated that within three weeks of beam time a few thousand a_0^0 and f_0 events can be identified.

The cluster-jet target with D_2 as target material will be used which will supply the effective neutron target. The mesons will be identified via their decay into pions and kaons ($a_0^0 \to K^+K^-$ and $f_0 \to \pi^+\pi^-/K^+K^-$). This requires the use of detectors for negatively charged ejectiles. This detector will be installed and commissioned in the second half of 2001 (the latter is planned to be done parasitically during the beam time on subthreshold K^+-production, see beam request for COSY proposal #18 for this PAC meeting). Thus the measurements can be performed in the beginning of 2002. In addition, a target-near semiconductor counter will be installed which allows for spectator tagging and will supply luminosity monitoring.

The detectors and on-line trigger will be set up such that high quality data on (at least) the following reactions can be expected in parallel: *i)* $pd \to {}^3\mathrm{H}\ a_0^+$ and $pd \to {}^3\mathrm{He}\ a_0^0$ (see below for physics motivation); *ii)* $pn \to d\omega/\phi$ (see approved COSY proposal #75 [3]); *iii)* $pn \to n\Lambda(\Sigma)K^+$ (requires the use of a neutron detector).

2 Physics case

The scalar meson sector plays a very important role in the physics of hadrons since its carries the quantum numbers of the vacuum. Nevertheless, the structure of the lightest scalar mesons $a_0(980)$ and $f_0(980)$ is not completely understood yet and is an important topic of hadronic physics (see e.g. [4, 5, 6, 7, 8, 9, 10, 11] and references therein). It has been discussed that they could be either "Unitarized $q\bar{q}$ states", "Four-quark cryptoexotic states", $K\bar{K}$ molecules or vacuum scalars (Gribov's minions). Nowadays, theory gives preference to the $q\bar{q}$ model (see [12, 13, 14]), but other options cannot be ruled out so far. Since there is a strong mixing between the uncharged $a_0(980)$ and the $f_0(980)$ due to a coupling to $K\bar{K}$ intermediate states [6], it is important to study independently the uncharged and charged components of the $a_0(980)$ because the latter ones do not mix with the $f_0(980)$ and preserve their original quark content. Furthermore, it is generally expected that the different $a_0(980)/f_0(980)$ production cross sections in πN and NN reactions will provide valuable information on their internal structure.

The Branching Ratios (BR's) of the two main a_0-decay channels ($\eta\pi$ and $K\bar{K}$) are still unclear: the $\eta\pi$ mode is quoted by the PDG [15] as 'dominant' and the $K\bar{K}$ mode as 'seen'. Its full width is not fixed and can be in the interval from 50 to 100 MeV. The situation with the f_0 is even less clear. While its width can vary from 40 to 100 MeV, the value of $BR(f_0 \to K\bar{K})$ is not yet fixed. Experimental data on the reaction $\pi^- p \to n2K_s^0$ (see p.418 of Ref.[15]) give evidence that the ratio $\Gamma(\pi\pi)/[\Gamma(\pi\pi)+\Gamma(K\bar{K})] \simeq 0.7\div 0.8$; data on K^+K^- meson production can only be described using $BR(f_0 \to K\bar{K}) \simeq 2\%$ [16].

As it was suggested long ago in Ref. [17] the dynamical interaction of the $a_0(980)$ and $f_0(980)$ with the nearby $K\bar{K}$ thresholds can give rise to a significant a_0-f_0 mixing. Different aspects of mixing dymanics and possibilities to measure this effect were discussed in Refs.[18, 19, 20, 21]. Furthermore, it was suggested recently in Ref.[11] that new data from the WA102 collaboration at CERN [22] on the central production of f_0 and a_0 in the reaction $pp \to p_s X p_f$ give evidence that the f_0–a_0 mixing intensity is is as large as $|\xi|^2 = (8 \pm 3)\%$.

Experimental information on the mixing effect is also very important for a better understanding of the nature of the f_0/a_0 states, whether they really have a common origin and what it is. Understanding the f_0-structure is also crucial for identifying the dynamics associated with the scalar glueball.

As it is shown in Ref.[23] possible tests of a_0-f_0 mixing can be done measuring isospin violation effects in the reactions

$$pp \to da_0^+ \ (a), \quad pn \to da_0^0 \ (b),$$

$$pd \to \ ^3\mathrm{H}\ a_0^+ \ (c), \quad pd \to \ ^3\mathrm{He}\ a_0^0 \ (d)$$

and

$$dd \to \ ^4\mathrm{He}\ a_0^0 \ (e)$$

near the corresponding thresholds. If the mixing intensity is as large as (8±3)%, then the isospin violation in the ratio of the differential cross sections of the reactions $pp \to da_0^+$ and $pn \to da_0^0$ as well as in the forward-backward asymmetry in the reaction $pn \to da_0^0$ not far from threshold can be as large as (50–100)%. A similar isospin violation is expected in the ratio of the differential cross sections of the reactions $pd \to {}^3\mathrm{H}\ a_0^+$ and $pd \to {}^3\mathrm{He}\ a_0^0$. The isospin violating effects can also be measured in the reactions $pn \to df_0$ and $dd \to {}^4\mathrm{He}\ a_0$.

The a_0-meson can decay into $\pi\eta$ or $K\bar{K}$ and the f_0 into $\pi\pi$ or $K\bar{K}$. As it will be shown in Sect. 4.1.3, the best way to observe isospin-violation effects is to identify a_0-production through its decay into $\pi\eta$. Nevertheless, a measurement of such effects in the K^+K^- decay channel is also very promising: there are serious arguments (see above) that $BR(f_0 \to K\bar{K})$ is quite small. If $\sigma(f_0) \times BR(f_0 \to K^+K^-)$ is smaller than $\sigma(a_0^0) \times BR(a_0^0 \to K^+K^-)$ (which seems to be the case) then the observation of isospin violation in the reactions $pp \to da_0^+ \to dK^+\bar{K}^0$ and $pn \to da_0^0 \to dK^+K^-$ will mostly be related to f_0/a_0 mixing. Consistency of the analysis can be checked comparing cross sections and angular distributions for all these reactions. Another possibility to observe isospin violation is to measure the f_0 decay into $\pi^+\pi^-$.

It is also very interesting to measure the cross sections of the elementary reactions $pp \to ppa_0^0$, $pp \to pna_0^+$, $pn \to ppa_0^-$ and $pn \to pna_0^0$. The $NN \to NNa_0$ cross sections for different isospin channels would help to understand the mechanism of the a_0 production that can also shed light on its internal structure.

The program of f_0/a_0 physics planned so far for ANKE includes the following items:

i) measurement of the cross sections and angular distributions for the reactions $pp \to da_0^+$ and $pn \to da_0^0/f_0$ detecting a_0 via its $K\bar{K}$, $\pi\eta$ decays and f_0 through its $\pi^+\pi^-$ and $K\bar{K}$ decays;

ii) measurement of the cross sections for the reactions $pd \to {}^3\mathrm{H}\ a_0^+$ and $pd \to {}^3\mathrm{He}\ a_0^0$ detecting a_0 through its $K\bar{K}$ and $\pi\eta$ decays;

iii) measurement of the cross sections $dd \to {}^4\mathrm{He}\ a_0^0/f_0$ detecting a_0 through its $K\bar{K}$, $\pi\eta$ decays and f_0 through its $\pi^+\pi^-$, $K\bar{K}$ decays;

iv) measurement of the cross sections of the elementary reactions $pp \to ppa_0^0$, $pp \to pna_0^+$, $pn \to ppa_0^-$ and $pn \to pna_0^0$.

The reaction $p(2.645\ \mathrm{GeV})p \to da_0^+$ has already been measured at ANKE in Jan./Feb., 2001. This new proposal foresees measurements at a similar beam energy using a *deuteron target* (as an effective neutron target) and *detectors for (positively and negatively) charged ejectiles.* In addition, target-near semiconductor counters can be used for proton-spectator tagging and luminosity monitoring.

3 Preliminary results of the a_0^+ beam time

During two weeks of beam time in Jan./Feb. 2001, the production of a_0^+-mesons in the reaction $pp \to da_0^+$ has been studied at ANKE (see [1, 2] for a detailed description of the experiment). It was planned to measure simultaneously the two decay channels of the a_0^+-meson to $K^+\overline{K^0}$ and $\pi^+\eta$. Figure 1 shows the principal layout of the experiment. The decay kaons (pions) were measured in the K^+-telescopes (telescopes and side wall counters) in coincidence with fast deuterons. The latter were detected in the forward detection system (FD) which is located close to the beam pipe of COSY.

The K^+-telescopes allow to unambiguously discriminate K^+-mesons against the background of mainly target pions and protons and scattered particles, see e.g. [24] and status report for proposal #18 presented to this PAC meeting.

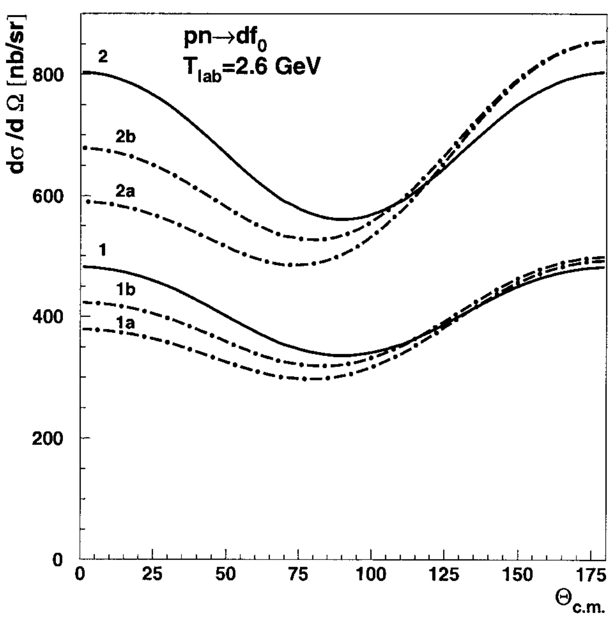

Figure 9: Differential cross section of the reaction $pn \to df_0$ at $T_p = 2.6$ GeV as a function of $\Theta_{\text{c.m.}}$. The notation of the curves is the same as in Fig.8.

(which would correspond to isospin conservation) might be 100% or more. Only in the case $|D_f|^2 \ll |D_a|^2$ the difference of $|R_{dc}|^2$ from 0.5 will be small. However this possibility looks very unlikely. If we consider a two-step model of the reactions $pd \to {}^3\text{He}\ a_0^0$ and $pd \to {}^3\text{He}\ f_0$, involving the subprocesses $pp \to d\pi^+$ and $\pi^+ n \to p\ a_0/f_0$ (see e.g. Ref.[34, 35]), then we find

$$\frac{\sigma(pd \to {}^3\text{He}\ a_0^0)}{\sigma(pd \to {}^3\text{He}\ f_0)} \simeq \frac{\sigma(\pi^+ n \to p\ a_0^0)}{\sigma(\pi^+ n \to p\ f_0)}. \tag{15}$$

According to Ref.[30] $\sigma(\pi^+ n \to p\ a_0) = \sigma(\pi^- p \to n\ a_0) \simeq 0.5 \div 1$ mb at 1.75–2 GeV/c. A similar value of $\sigma(\pi^- p \to n\ f_0)$ can be found using the results of Ref.[16]. According to this paper $\sigma(\pi^- p \to n\ f_0 \to nK^+K^- \simeq 6-8\ \mu$b at 1.75-2 GeV/c and $BR(f_0 \to K^+K^-) \simeq 1\%$, which means that $\sigma(\pi^- p \to n\ f_0) \simeq 0.6-0.8$ mb. Thus we expect $|D_a| \sim |D_f|$ near threshold. This would imply that the effect of isospin violation in the ratio R_{dc} can, in fact, be quite large. Using once more the arguments of the two-step model we can write

$$R(a_0/\eta') = \frac{|D_a|^2}{|T(pd \to {}^3\text{He}\ \eta')|^2} \simeq \frac{|T(\pi^- p \to p\ a_0^0)|^2}{|T(\pi^- p \to p\ \eta')|2}. \tag{16}$$

Taking $\sigma(\pi^- p \to a_0^0 n) \simeq 0.6$ mb at 1.75 GeV/c and using the near threshold value $\sigma(\pi^- p \to \eta' n) = (0.35\pm0.03)\ q^{\eta'}_{\text{c.m.}}\ \mu$b (where $q^{\eta'}_{\text{c.m.}}$ is in MeV/c) [36] we find that $R(a_0/\eta') \simeq 1$. Therefore using the experimental data on the reaction $pd \to {}^3\text{He}\ \eta'$ [37] we get for the reaction $pd \to {}^3\text{He}\ a_0^0$ near the threshold:

$$\frac{q^{proton}_{\text{c.m.}}}{q^{He}_{\text{c.m.}}} \times \frac{\text{d}\sigma_{\text{c.m.}}}{\text{d}\Omega} \simeq 0.9 \text{ nb/sr} \tag{17}$$

The energy behaviour of the differential cross section for the reaction $pd \to {}^3\text{He}\ \eta'$ was calculated within the two-step model in Ref.[35]. A similar energy behaviour (as functions of the c.m. energy release $Q = \sqrt{s} - \sqrt{s_{\text{th}}}$) is also expected for the differential cross sections of the reactions $pd \to {}^3\text{He}\ a_0^0$ and $pd \to {}^3\text{He}\ f_0$.

4.3 Reactions dd → ^{4}He a_0^0 and dd → ^{4}He f_0

Direct production of the a_0 in the reaction $dd \to\ {}^4He\ a_0^0$ is forbidden and can be only due to f_0-a_0 mixing:

$$\frac{\sigma(dd \to {}^4\text{He}\ a_0^0)}{\sigma(dd \to {}^4\text{He}\ f_0)} = |\xi|^2. \tag{18}$$

Therefore it is very interesting to study the reaction

$$dd \to {}^4\text{He}\ (\pi^0\ \eta) \tag{19}$$

near the f_0-production threshold. Any signal of reaction (19) will be related to isospin breaking. It is expected to be much more pronounced near the f_0 threshold as compared with the region below this threshold. An interesting point is that in case of a_0-production the two deuterons in the initial state and the outgoing ^{4}He a_0^0 may be both in S-wave. Thus, compared to the isospin-violating process $dd \to {}^4\text{He}\ \pi^0$ where the initial deuterons must be in P-wave, the cross section might be larger since no rearangement of the nucleon wave functions is involved.

The measurements require a deuteron beam with momenta of $p_d \sim 3.7$ GeV/c (to be compared with the current maximum momentum of COSY, $p_{max} \sim 3.4$ GeV/c) and the detection of the π^0 and η in the final state via their decay into photons. No beam time for this reaction is requested for in the framework of this proposal. As soon as the technical requirements can be fulfilled we will present a more detailled request and present it to PAC.

4.4 Elementary reactions pp → ppa_0^0, pp → pna_0^+, pn → ppa_0^- and pn → pna_0^0

Let us consider, following Ref.[38], a_0^0, a_0^+, a_0^- production in the reactions $pp \to ppa_0^0$ (1), $pp \to pna_0^+$ (2), $pn \to ppa_0^-$ (3) and $pn \to pna_0^0$ (4) within the π-exchange model. For the elementary $\pi N \to Na_0$ transition amplitude we take into account different mechanisms (denoted by "α") corresponding to t-channel diagrams with $\eta(550)$- and $f_1(1285)$-meson exchanges ($\alpha = t(\eta)$, $t(f_1)$) alone whereas s and u-channel graphs with intermediate nucleon ($\alpha = s(N)$, $u(N)$).

The invariant amplitude of $NN \to NNa_0$ reaction is the sum of four terms coming from diagrams with permutations of nucleons in the initial and final states

$$\begin{aligned}
&\mathcal{M}^{\pi}_{j(\alpha)}[ab;cd] = \\
&\xi^{\pi}_{j(\alpha)}[ab;cd]\mathcal{M}^{\pi}_{\alpha}[ab;cd] + \xi^{\pi}_{j(\alpha)}[ab;dc]\mathcal{M}^{\pi}_{\alpha}[ab;dc] \\
&\xi^{\pi}_{j(\alpha)}[ba;dc]\mathcal{M}^{pi}_{\alpha}[ba;dc] + \xi^{\pi}_{j(\alpha)}[ba;cd]\mathcal{M}^{\pi}_{\alpha}[ba;cd]
\end{aligned} \tag{20}$$

with coefficients $\xi^{\pi}_{j(\alpha)}$ presented in Table 1.

Reaction j	mechanism α	$\xi^{\pi}_{j(\alpha)}[ab;cd]$	$\xi^{\pi}_{j(\alpha)}[ab;dc]$	$\xi^{\pi}_{j(\alpha)}[ba;dc]$	$\xi^{\pi}_{j(\alpha)}[ba;cd]$
$pp \to ppa_0^0$	$(t(\eta), t(f_1))$	$+1/\sqrt{2}$	$-1/\sqrt{2}$	$+1/\sqrt{2}$	$-1/\sqrt{2}$
	$(s(N))$	$+1/\sqrt{2}$	$-1/\sqrt{2}$	$+1/\sqrt{2}$	$-1/\sqrt{2}$
	$(u(N))$	$+1/\sqrt{2}$	$-1/\sqrt{2}$	$+1/\sqrt{2}$	$-1/\sqrt{2}$
	Regge	0	0	0	0
$pp \to pna_0^+$	$(t(\eta), t(f_1))$	$-\sqrt{2}$	0	0	$+\sqrt{2}$
	$(s(N))$	0	$+\sqrt{2}$	$-\sqrt{2}$	0
	$(u(N))$	$+2\sqrt{2}$	$-\sqrt{2}$	$+\sqrt{2}$	$-2\sqrt{2}$
	Regge	-1	$+1$	-1	$+1$
$pn \to ppa_0^-$	$(t(\eta), t(f_1))$	$+1$	-1	0	0
	$(s(N))$	-2	$+2$	-1	$+1$
	$(u(N))$	0	0	$+1$	-1
	Regge	$+1$	-1	-1	$+1$
$pn \to pna_0^0$	$(t(\eta), t(f_1))$	-1	0	$+1$	0
	$(s(N))$	-1	-2	$+1$	$+2$
	$(u(N))$	-1	$+2$	$+1$	-2
	Regge	0	$-\sqrt{2}$	$+\sqrt{2}$	0

Table 1: Coefficients in Eq.(20) for different mechanisms of the $pp \to ppa_0^0$, $pp \to ppa_0^+$, $pn \to ppa_0^-$ and $pn \to pna_0^0$ reactions.

As it was shown in Ref.[30] in the region of a few GeV the dominant mechanisms of a_0 production in the reaction $\pi N \to a_0 N$ are u-channel nucleon and t-channel f_1-meson exchanges which give cross sections for a_0 production of about 0.3 – 0.4 mb. Similar cross sections ($\simeq$ 0.4 – 1 mb) are predicted by the Regge model with conspiring ρ_2 (or ρ_2 and b_1) exchanges, normalized to the Brookhaven data at 18 GeV/c [39]. The contributions of s-channel nucleon and t-channel η -meson exchanges are small and can be neglected. The contribution of the f_1 exchange to the cross section of the reaction $pp \to da_0^+$ appeared to be small and the data of Ref.[32] can be described by the u-channel exchange mechanism alone. If the u-channel exchange will be dominant also in the reaction $NN \to NNa_0$ then we would expect $\sigma_1 : \sigma_2 : \sigma_3 : \sigma_4 \simeq 1 : 10 : 1 : 5$ (neglecting interference between different terms in Eq.(20). If the dominant contribution will be due to $\rho_2 - b_1$ Reggeon exchange, then $\sigma_1 : \sigma_2 : \sigma_3 : \sigma_4 \simeq 0 : 2 : 2 : 2$. Correspondingly for f_1-exchange we would have $\sigma_1 : \sigma_2 : \sigma_3 : \sigma_4 \simeq 1 : 2 : 1 : 1$. The most striking ratio $\sigma_2 : \sigma_1 \simeq 10$ we have for the u -channel mechanism. However in any case σ_1 appears to be suppressed as compared with σ_2. The cross sections of the reactions (2) and (3) are expected to be the same for the Regge mechanism, but if the u-channel is dominant we expect $\sigma_2 \gg \sigma_3$. Therefore measurements of the $NN \to NNa_0$ cross section for different charge channels would help to understand the mechanism of the a_0 production.

Recently the COSY-11 collaboration [40] reported cross section $\sigma(pp \to ppK^+K^-) \simeq 2$ nb at Q=17 MeV. According to the fit to the COSY-11 and DISTO data (see Fig. 8 in Ref.[40]) we get $\sigma(pp \to ppK^+K^-) \simeq 20$ nb at Q=50 MeV. Dividing this value by $BR(a_0^0 \to K^+K^-) \simeq 0.1$ we can estimate an upper limit for $\sigma(pp \to ppa_0^0)$ at $Q = 50$ MeV to be about 200 nb. Then, as it follows from Table 1, the upper limit on the cross section $\sigma(pp \to pna_0^+)$ is expected to be considerably (up to a factor 10) larger. We remind for comparison that our prediction for the cross section of the reaction $pp \to da_0^+$ (which was the basis for the count-rate estimates in proposal #55 [2]) is about 1 μb at $Q = 50$ MeV.

5 Detection scheme and rate estimates

Based on the experience of the last ANKE beam time, the number of assigned $pp \to da_0^+$ events from Sect. 3 and the cross-section calculations from Sect. 4.1.2, a brief estimate of the expected count rates and possible background in case of the neutral scalar mesons is presented in this section.

In order to observe scalar meson production in pn collisions, a deuteron cluster-jet target will be used. For the unambiguous identification of a_0^0/f_0-production on the neutron one either has to

- pin down the quasi-free reaction on the neutron with the help of spectator-proton detection, $pd \to p_{\rm sp}dX$, and to detect at least one charged decay product of the meson with ANKE, or
- measure all particles in the exit channel of the reaction $pn \to dS \to dm_1m_2\ldots$, where S denotes the produced scalar meson and the m_i its decay products.

The first technique has already been applied at ANKE for the detection of π^0- and ω-production on the neutron. However, for the present proposal we prefer the second method, i.e., detection of the K^+K^-- and $\pi^+\pi^-$-pairs from a_0^0/f_0-decay. The reason is that currently the target-near spectator counters are rather small. Thus the acceptance for the detection of scalar mesons at ANKE is larger if one uses the detectors for negatively charged ejectiles (to be installed in fall 2001) in coincidence with the already well understood detectors for π^+- and K^+-mesons. Nevertheless, during the beam time the spectator counters will be installed for luminosity monitoring as well as for spectator-proton detection. As in the case of the a_0^+-meson, the fast deuteron will be detected in the forward detection system.

Our simulations gave the following results for the acceptances of a_0^0/f_0-detection, as compared to the a_0^+, and for the expected count rates:

$\mathbf{a_0^0/f_0 \to K^+K^-}$ The geometrical acceptance of ANKE for the detection of K^+K^--pairs is (almost) equal to the single K^+ efficiency. This is due to the fact that only those K^+-mesons are detected with c.m. emission angles of ~ 0° or ~ 180°. Close to threshold the coincident K^--mesons must have emission angles of ~ 180° or ~ 0° and are also within the ANKE angular acceptance. The momentum range covered by the negative-particle detectors fully overlaps the momenta of the K^--mesons from a_0^0/f_0-decay. Consequently, losses are dominantly due to K^--decay-in-flight between target and detectors. Thus, the total acceptance for K^+K^--pairs from a_0^0/f_0-decay is estimated to be 30% of the value for $a_0^+ \to K^+\overline{K^0}$ events. The cross section for $f_0(a_0^0)$-production in pn-collisions is predicted to be ~ 5 times larger (~ 2 times smaller) than of a_0^+-production in pp collisions. Therefore, the expected count rates are roughly 2 times larger (5 times smaller) for the $f_0(a_0^0)$ as compared to the rates in the a_0^+ beam time and within the requested beam time of three weeks a few thousand events should be observed. We expect that the background in this decay channel containing open strangeness should be comparable to the case of *pp*-collisions where it is probably negligible.

$f_0 \to \pi^+\pi^-$ According to our simulation calculations, the detection efficiency for the $\pi^+\pi^-$-pairs from f_0-decay is $\sim 10^{-4}$. This is about one order of magnitude less than for the π^+-mesons from a_0^+-decay. Since the cross section for f_0-production is expected to be ~ 5 times larger, it is expected that within three weeks of beam time up to 1000 $f_0 \to \pi^+\pi^-$ events can be detected. In the $d\pi^+$ missing-mass spectrum of Fig.4 there is no peak around the pion mass. Thus the number of $d\pi^+\pi^0$ events in pp reactions is smaller than the number of detected a_0^+-mesons. It is concluded that for the case of $pn \to d\pi^+X$ reactions, the background in the π^- region should also be smaller than the signal from $f_0 \to \pi^+\pi^-$ events (the latter having a larger production cross section than the a_0^+).

6 Overview of possible experiments

Possible reaction channels with the production of scalar mesons which might be investigated at COSY are summarized in Table 2. An advantage of the measurements proposed here is that a few reaction channels can be observed in the same experiment. This is especially useful for the reactions with ^{3}He and ^{3}H in the exit channel: for a quasi-free pn reaction at a beam energy of $T = 2.645$ GeV, the maximum accessible mass is $m_{\text{max}} = 1.036$ GeV (this value is slightly higher if Fermi motion of the neutron is taken into account). In case of the reaction $pd \to {}^3\text{He}\ X$ the maximum mass is $m_{\text{max}} \sim 1.4$ GeV. Thus a much wider coverage of the a_0 resonance without phase-space restrictions is possible or, in other words, this allows the measurement of the a_0^0/f_0 excitation function at two energies during the same beam time.

Entrance	Exit channel					Comments
channel	Baryons	a_0^-	a_0^0	a_0^+	f_0	
$p+p$	pp		σ<2 nb		σ<2 nb	COSY 11, Q=17 MeV
$p+p$	pn			x		
$p+p$	d			p wave$^{(*}$		ANKE, Jan. 2001
$p+n$	pp	x				(this proposal)
$p+n$	nn			x		
$p+n$	pn		x		x	
$p+n$	d		p wave$^{(*}$		s wave$^{(*}$	this proposal
$p+d$	^{3}He		x		x	this proposal
$p+d$	^{3}H			x		this proposal
$d+d^{(*}$	^{4}He$^{(*}$		via f_0		x	isospin violation(?)
Decay channels		$\pi^-\eta$	$\pi^0\eta$	$\pi^+\eta$	$\pi^+\pi^-$ $\pi^0\pi^0$	
		K^-K^0	K^+K^- $K^0\overline{K^0}$	$K^+\overline{K^0}$	K^+K^- $K^0\overline{K^0}$	

$^{(*}$ Isospin restrictions: $I(d+d)=0, I(^4\text{He})=0, I(d\,a_0)=1, I(d\,f_0)=0$

Table 2: Overview over the possible reactions with production of scalar mesons

7 Beam-time request

Summarizing, we apply for the following amount of beam time: **Three weeks** to study the production of a_0^0- and f_0-mesons in the reaction $pn \rightarrow da_0^0/f_0$ at maximum COSY energy (T = 2.645 GeV or higher, if possible). It is expected that a few thousand mesons can be identified by detection of their decay products, $a_0^0 \rightarrow K^+K^-$ and $f_0 \rightarrow \pi^+\pi^-/K^+K^-$ in coincidence with the fast deuteron. From the measurement of the f_0 c.m. angular distribution information about the isospin-violating a_0-f_0 mixing can be expected. In addition, the production of other mesons in pn collisions (e.g. the $\phi(1020)$) will be studied simultaneously.

References

[1] V. Chernyshev et al., COSY proposal #55 "Study of a_0^+ mesons at ANKE" (1997) *available via www:* `http://ikpd15.ikp.kfa-juelich.de:8085/doc/Anke.html`; L.A. Kondratyuk et al. *Preprint ITEP* **18-97**, Moscow (1997).

[2] M. Büscher et al., Beam-time request for COSY proposal #55 "Study of a_0^+ mesons at ANKE" (2000) *available via www:* `http://ikpd15.ikp.kfa-juelich. de:8085/doc/Anke.html`.

[3] M. Büscher et al., COSY proposal #75, "Study of ω- and ϕ-meson production in the reactions $pd \to dVp_{\rm sp}$ at ANKE" (1998) *available via www:* `http://ikpd15.ikp.kfa-juelich. de:8085/doc/Anke.html`.

[4] F.E. Close et al., Phys. Lett. **B 319** (1993) 291.

[5] M. Genovese et al., Nuovo Cim. **107A** (1994) 1249.

[6] G. Janssen, B. Pierce, K. Holinde and J. Speth, Phys. Rev. **D 52** (1995) 2690.

[7] V.V. Anisovich et al., Phys. Lett. **B 355** (1995) 363.

[8] N. A. Törnqvist, Phys. Rev. Lett. **49** (1982) 624.

[9] K. Maltman, "Scalar Meson Decay Constats and the Nature of the $a_0(980)$", Review talk at Hadron-99, Beijing, Aug. 24–28, 1999; hep-ph/0005155.

[10] S. Narison, "Gluonic Scalar Mesons Hybrids from QCD Spectral Sum Rules", Review talk at Hadron-99, Beijing, Aug. 24–28, 1999; hep-ph/9909470; Nucl. Phys. Proc. Suppl. **86** (2000) 242.

[11] F. E. Close, A. Kirk, Phys. Lett. **B489** (2000) 24.

[12] L. Montanet, Nucl. Phys. B (Proc. Suppl.) **86** (2000) 381.

[13] V.V. Anisovich, L. Montanet, V.N. Nikonov, Phys. Lett. **B 480** (2000) 19.

[14] S. Narison, hep-ph/0012235.

[15] C. Caso et al. (Particle Data Group), Eur. Phys. J. **C 15** (2000) 1.

[16] E.L. Bratkovskaya et al., Eur. Phys. J. **A4** (1999) 165.

[17] N.N. Achasov, S.A. Devyanin and G.N. Shestakov , Phys. Lett. **B88** (1979) 367.

[18] O. Krehl, R. Rapp and J. Speth, Phys. Lett. **B390** (1997) 23.

[19] B.O. Kerbikov and F. Tabakin, Phys. Rev. **C 62** (2000) 064601.

[20] N.N. Achasov and G.N. Shestakov, Phys. Rev. **D56** (1997) 212.

[21] G. Janssen, "Meson-Meson-Prozesse in der starken Wechselwirkung", Dissertation Universität Bonn, Berichte des FZJ Jül-3065J, Jülich (1995).

[22] D. Barberis et al., **B 488** (2000) 225.

[23] V.Yu. Grishina et al., publication in preparation.

[24] S.Barsov et al., Acta Phys. Polonica B **31**, 2159 (2000).

[25] V.Yu. Grishina et al., Annual Report of the IKP 2000, *available via www:* `http://ikpd15.ikp.kfa-juelich.de:8085/doc/Anke.html`.

[26] H. Müller et al., Annual Report of the IKP 2000, *available via www:* `http://ikpd15.ikp.kfa-juelich.de:8085/doc/Anke.html`.

[27] A. Kudryavtsev and V.E. Tarasov, JETP Lett. **72** (2000) 410.

[28] V.Yu. Grishina et al., Phys. Lett. **B475**, 9 (2000).

[29] V.Yu. Grishina, L.A. Kondratyuk, M.Büscher, Phys. Atom. Nucl. **63** (2000) 1824.

[30] V.Yu. Grishina et al., Eur. Phys. J. **A9** (2000) 277.

[31] M. Kirchbach, D.O. Riska, Nucl. Phys. **A 594** (1995) 419.

[32] M.A. Abolins et al., Phys. Rev. Lett. **25** (1970) 469.

[33] V. Mull and K. Holinde, Phys. Rev. C 51 (1995) 2360.

[34] G. Fäldt and C. Wilkin, Phys. Lett. **B354** (1995) 20.

[35] L.A. Kondratyuk and Yu.N. Uzikov, JETP Lett. **63** (1996) 1.

[36] D.M. Binnie et al. Phys. Rev. **D 8** (1973) 2789.

[37] R. Wurzinger et al., Phys. Lett. **B 374** (1996) 283.

[38] E.L. Bratkovskaya et al., publication in preparation.

[39] A.R. Dzierba, in Proceedings of the Second Workshop on Physics and Detectors for DAΦNE'95, Frascati, 1995, edited by R. Baldini et al., Frascati Physics Series **4**, 99 (1996).

[40] C. Quentmeier et al., nucl-ex/0103001.

Proposal #97

"Investigation of neutral scaler mesons a_0^0/f_0 with ANKE"

Maybe a better title would be:

$pn \rightarrow \begin{matrix} dX \\ nY \end{matrix}$ @maximum COSY energy

$X =$
- a_0^0/f_0 (motivation follows)
- ω/ϕ (accepted COSY proposal #75)
- η'
-
-

$Y =$
- $K^+ \Lambda/\Sigma$
-
-

$pd \rightarrow {}^3He\ a_0^0/f_0$ (Note:
larger a_0^0/f_0 masses accessible!!)

$pd \rightarrow {}^3H\ a_0^+$

M.Büscher, 4/01

Why a_0^0/f_0? new proposal

Final goal:
what is the nature of the
light scalar mesons a_0/f_0 ?

Observables:

- Mass distributions of a_0's and f_0
- Decay coupling constants
  (Branching ratios)
- Test of isospin relations
  for various channels/targets (e.g. pd → $^3H\ a_0^+$ / $^3He\ a_0^0$)
- Mixing $a_0 \leftrightarrow f_0$
-
-

Proposal #55
$pp \to d a_0^{\times}$

Production of neutral scalar mesons:

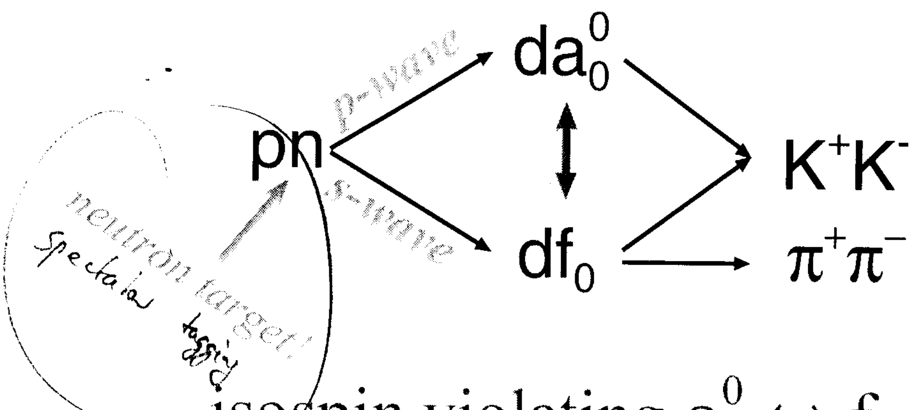

isospin violating $a_0^0 \leftrightarrow f_0$ mixing

How to measure $pd(n) \rightarrow d\, a_0^0/f_0\, p_{sp}$

Spectator tagging:

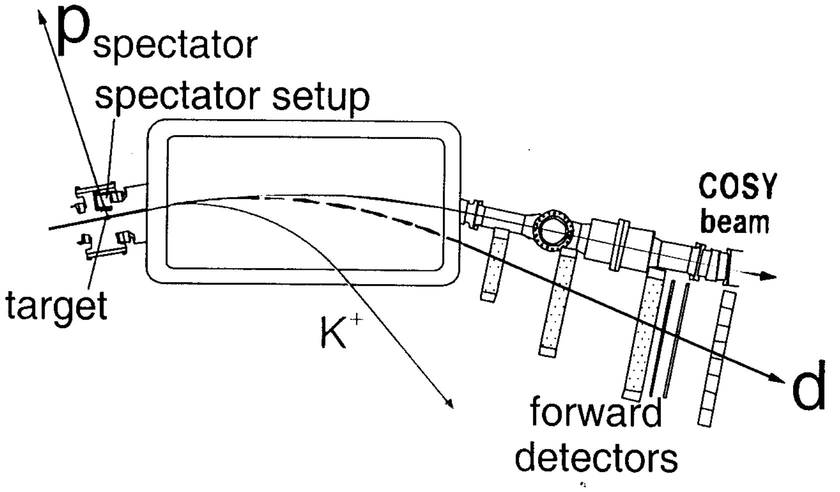

$pn \rightarrow d\, K^+\, X$
(analogous to
$pp \rightarrow d\, K^+\, X$)

Exclusive measurement of a_0^0/f_0 decay:

needs detectors for
negatively charged ejectiles
(installation in summer 2001,
commissioning → beam request 70.1)

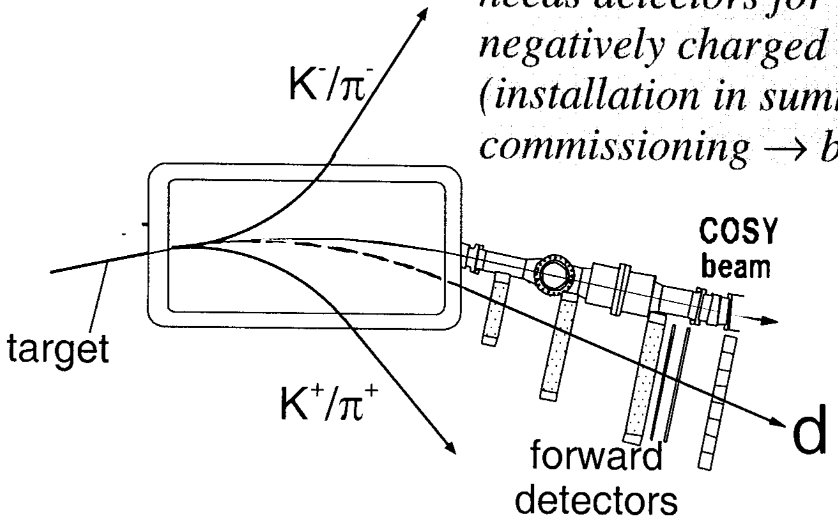

$pd \rightarrow d\, K^+K^-\, X$
$pd \rightarrow d\, \pi^+\pi^-\, X$

Both techniques will be used

M.Büscher, 4/01

Rate estimates

Expected cross sections:

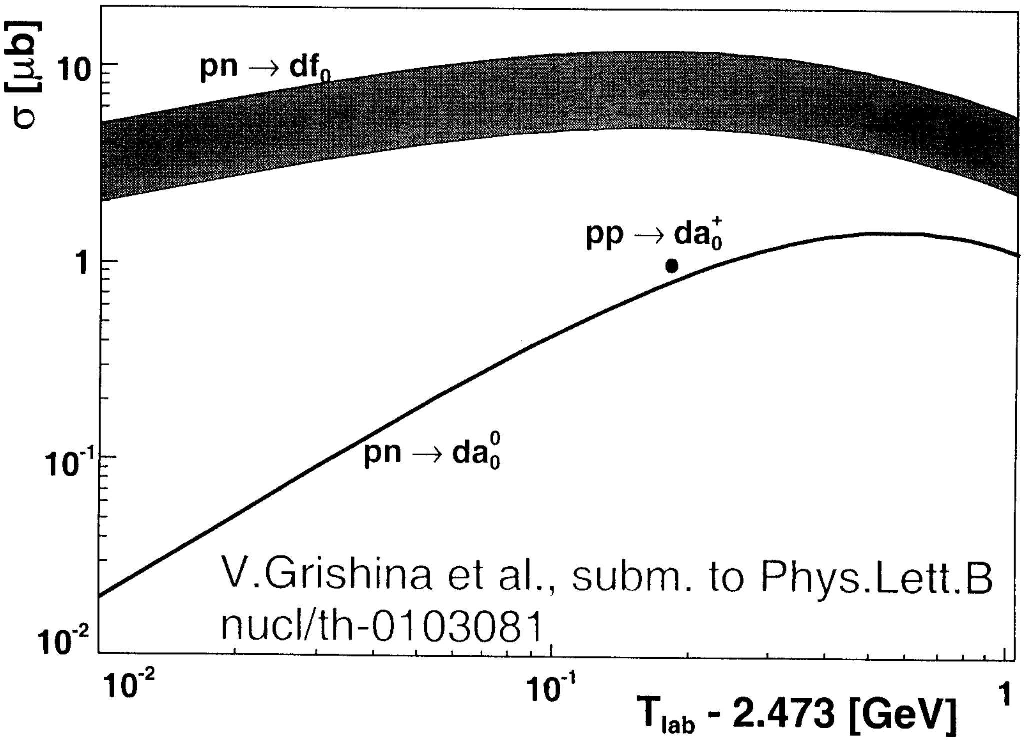

V.Grishina et al., subm. to Phys.Lett.B
nucl/th-0103081

Acceptances:

$$A(\mathrm{pn} \rightarrow \mathrm{d}\ a_0^0 \rightarrow \mathrm{d}\ K^+K^-)$$

$$\sim 0.3 \cdot A(\mathrm{pp} \rightarrow \mathrm{d}\ a_0^+ \rightarrow \mathrm{d}\ K^+\ X)$$

$$A(\mathrm{pn} \rightarrow \mathrm{d}\ f_0^0 \rightarrow \mathrm{d}\ \pi^+\pi^-)$$

$$\sim 0.1 \cdot A(\mathrm{pp} \rightarrow \mathrm{d}\ a_0^+ \rightarrow \mathrm{d}\ \pi^+\ X)$$

→ in 3 weeks of beam time
as many events as
during the a_0^+ beam time

Effects of isospin violation

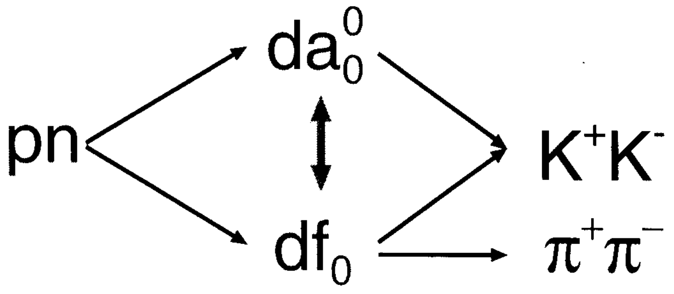

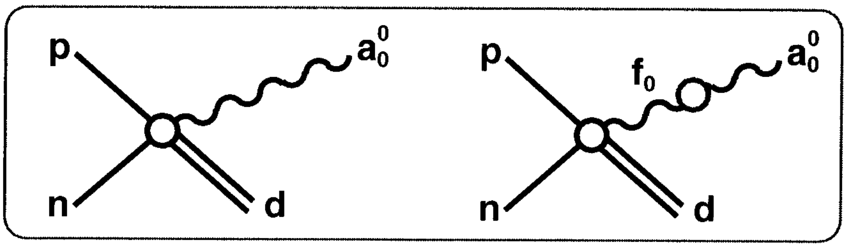

$a_0^0 \leftrightarrow f_0$ mixing disturbs angular distributions

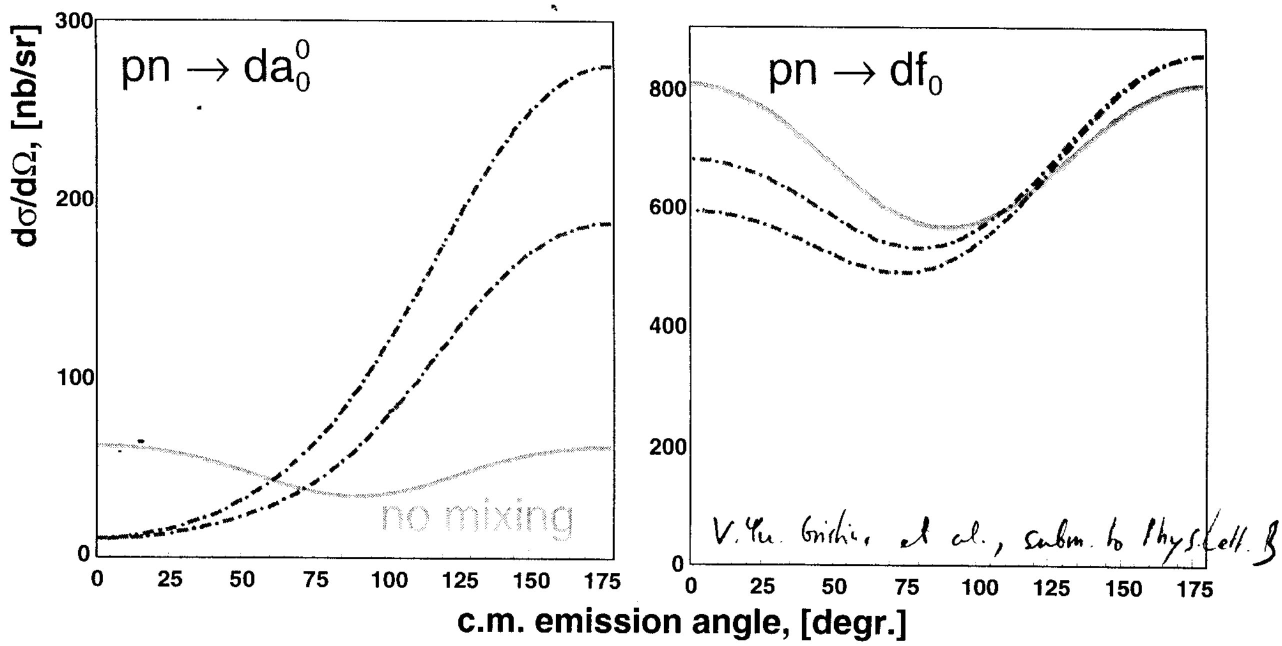

V. Yu. Grishina, et al., subm. to Phys.Lett. B

Assumptions:

$R = \sigma(f_0)/\sigma(a_0^0) = 2.4$

Mixing intensity $|\xi|^2 = (8 \pm 3)$ %

(F.E.Close et al., Phys.Lett.B 489 (2000) 24)

The reaction dd → ^{4}He a_0^0

dd → ^{4}He a_0^0 is forbidden, if isospin is conserved

isospin-breaking mechanism

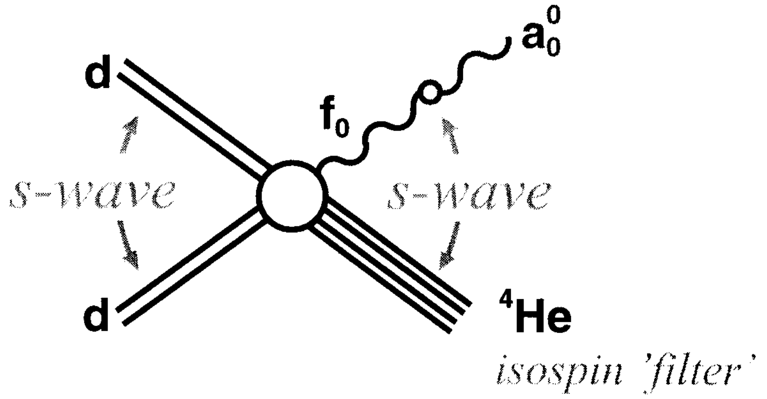

- **Observation of dd → ^{4}He $\pi^0\eta$**
  = indication of isospin violation !
- **Needs photon detection**
- **p_{beam} ~ 3.7 GeV/c !**
- **Possible advantage compared to dd → ^{4}He π^0**

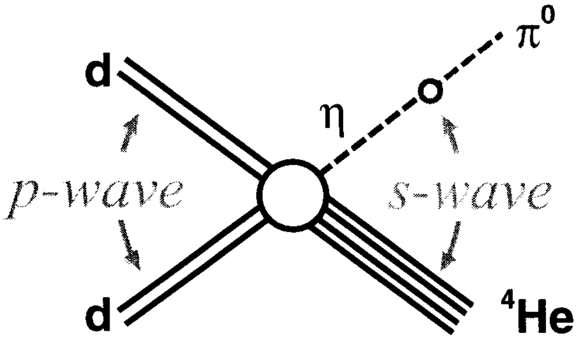

Beam-time request

Reactions to be measured:

$$pn \rightarrow d\, a_0^0/f_0 \rightarrow d\, K^+K^-$$
$$\rightarrow d\, f_0 \quad \rightarrow d\, \pi^+\pi^-$$

(...and many others!!)

Required beam time:

3 weeks

(A few 1000 events can be collected)

When?

Beginning of 2002

(Needs K^-/π^- detectors)

Thank you for your attention!

M.Büscher, 4/01

Hyperon production in $pp \to pK^{+}Y$ reactions at 2.65 GeV

P.Kravtchenko

High Energy Physics Department
Petersburg Nuclear Physics Institute
188350 Gatchina
Russia

Hyperon production in $pp \rightarrow pK^+Y$ reaction at 2.65 CeV.

Polina Kravtchenko,PNPI

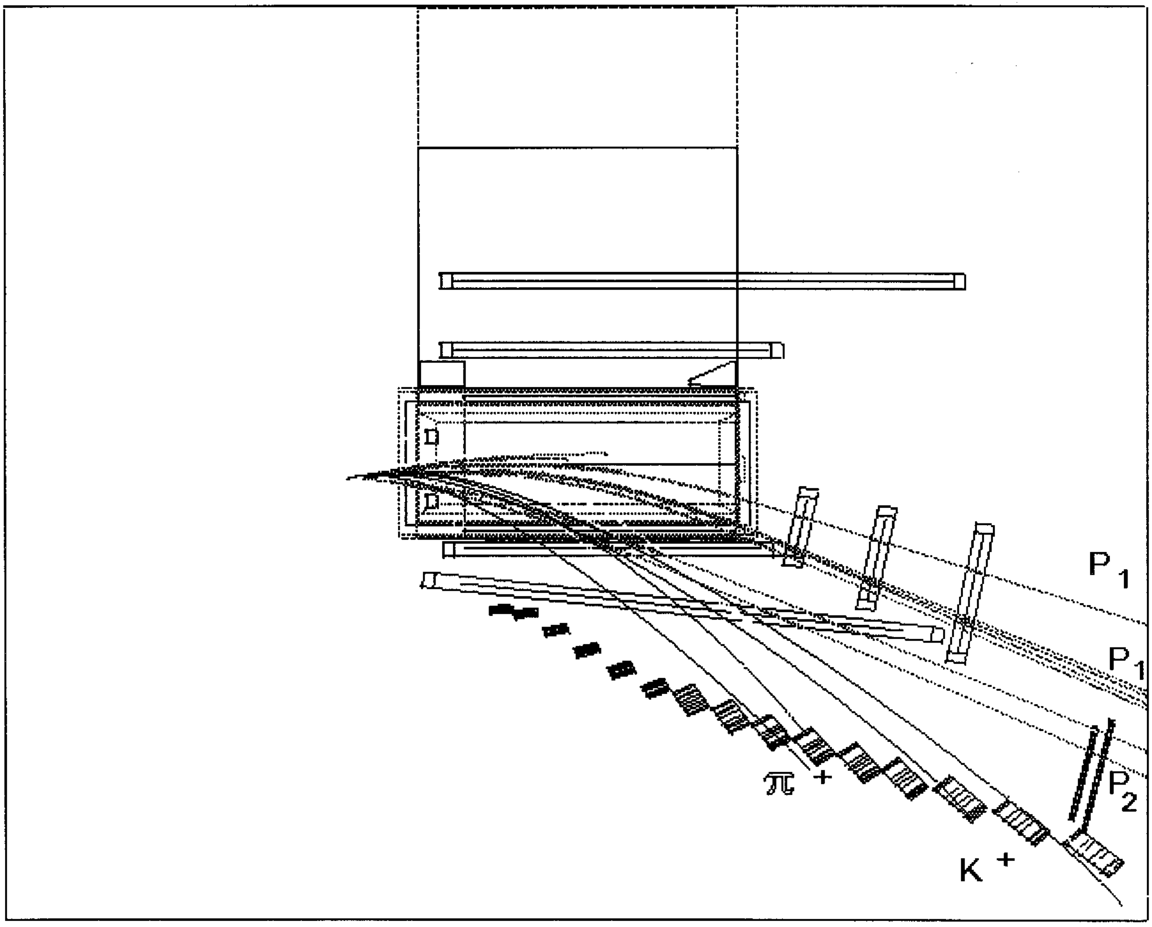

- 2.65 GeV is below the threshold of Λ(1520) production
- 2.65 GeV is at threshold of Σ(1480) 1[J^P?], $\Gamma = 30 - 80MeV$ $\overline{K}N/\Lambda\pi = 0.7 \pm 0.5$; $\Lambda\pi/\Sigma\pi = 0.8 \pm 0.5$
- 2.65 GeV is above the threshold of Φ(1020),K^+K^-,Λ(1405),Σ(1385)
- **The threshold of Φ(1020) - 2.60Gev**
  - $pp \rightarrow pp\Phi, \Phi \rightarrow K^+K^-$
  - $pp \rightarrow ppK^+K^-$
  - $\sigma_{tot} \leq 0.1 \mu b$, $M_{Kp}^{min} = m_p + m_K = 1435MeV$

Missing mass spectrum

Experimental data
preselected data file Run3276-3369ka.Sd.noScal.FD.gz

Trigger conditions

- p in FD;
- K^+ in telescope (TOF(Sa-So)$\approx \pm 0.7ns$, $delayVe > 1.5ns$)
- $\Delta t(K^+p) = t_0 \pm 1.5ns$
- vert.angle $= \theta_v \pm 2.5deg$

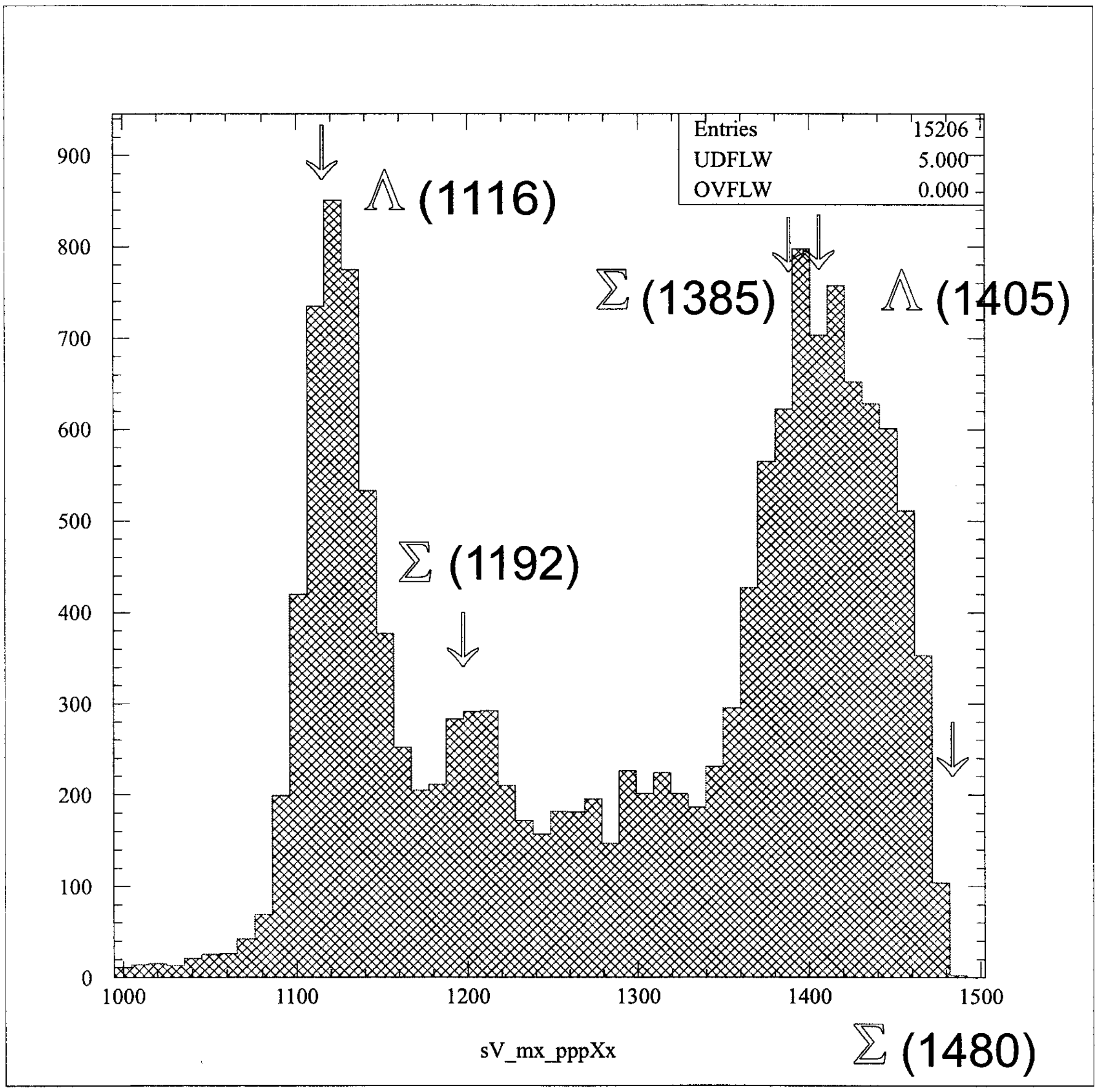

Light hyperons (Particle Data)

$\Lambda(1116)0(\frac{1}{2}^+)$

$$pp \to K^+p\Lambda \to \pi^0 n(35\%), \quad \sigma^{tot}_{Laget} = 29\mu b,$$
$$\to \pi^- p(65\%), \quad \sigma^{tot}_{exp} = 40 \pm 10\mu b$$

Phys.Let.B,v259,n1-2,p24(1991)

$\Sigma^0(1193)1(\frac{1}{2}^+)$

$$pp \to K^+p\Sigma^0 \to \gamma\Lambda \to \pi^0 n(35\%), \quad \sigma^{tot}_{Laget} = 5.5\mu b$$
$$\to \pi^- p(65\%), \quad \sigma^{tot}_{exp} = 10 \pm 5\mu b$$

$$(\frac{\sigma^{tot}_{\Lambda}}{\sigma^{tot}_{\Sigma^0}})_{Laget} = 5.2 \qquad (\frac{\sigma^{tot}_{\Lambda}}{\sigma^{tot}_{\Sigma^0}})_{exp} = 4.0 \pm 2.5$$

$$(\frac{\sigma^{tot}_{\Lambda}}{\sigma^{tot}_{\Sigma^0}})_{COSY11(\epsilon=60MeV)} = 7.5 \pm 3.5$$

no π^+pK^+ combinations

$\Sigma^+(1189)1(\frac{1}{2}^+)$

$$pp \to K^+n\Sigma^+ \to \pi^0 p(51\%), \quad \sigma^{tot}_{Laget} = 24.5\mu b$$
$$\to \pi^+ n(48\%), \quad (\frac{\sigma^{tot}_{\Sigma^+}}{\sigma^{tot}_{\Sigma^0}})_{Laget} = 4.5$$

$$(\frac{\sigma^{\Sigma^+}}{\sigma^{\Sigma^0}})_{K^+p(fromdecay)} = 4.5 * \frac{0.51}{0.65} = 3.5\mu b$$

Missing mass spectra for light hyperons

$$pp \to K^+ p(M_x = Y \to p\pi^-)$$

Simulation

Most of the simulations are done in the frame of standart statmodel

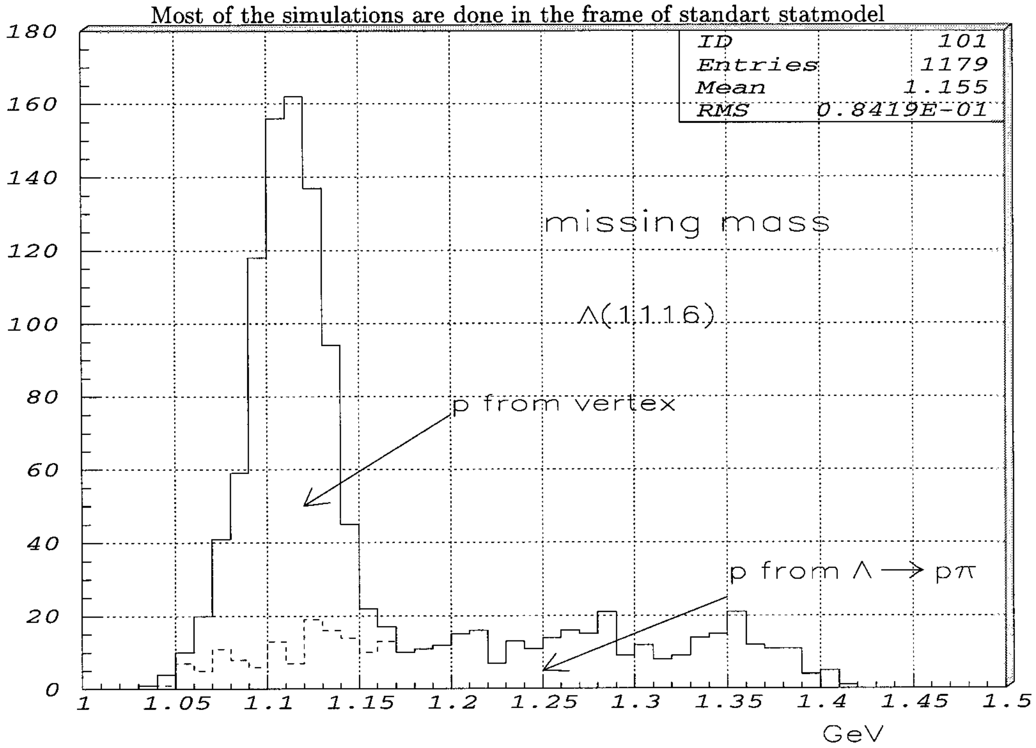

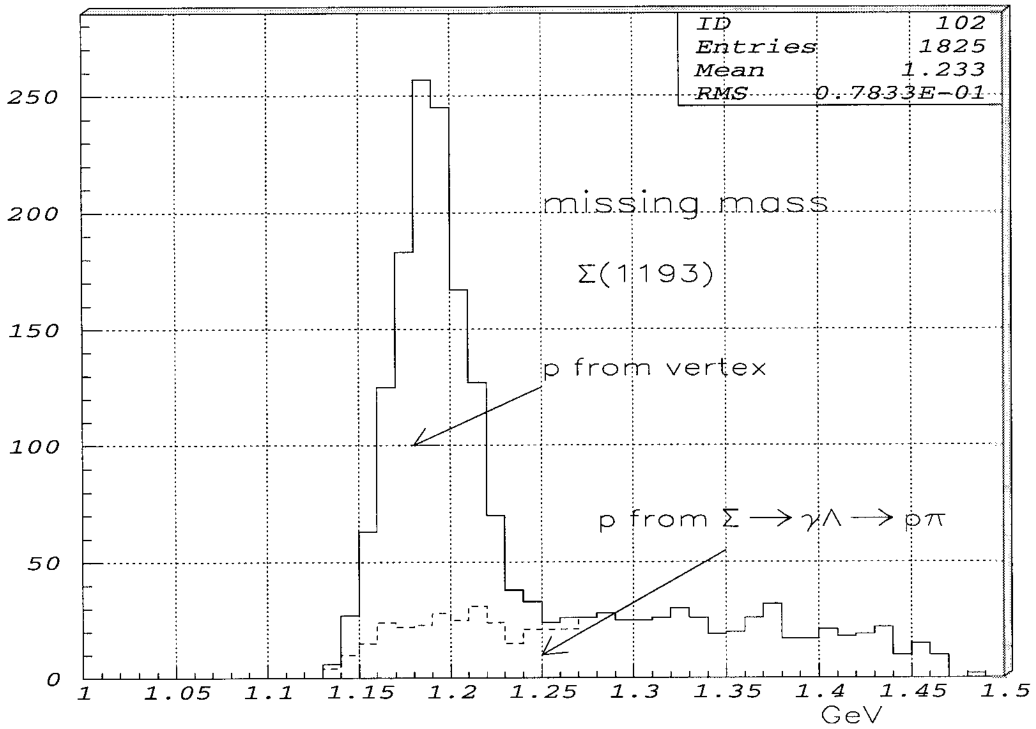

Simulation program was developed with the help from O.Grebenyuk, V.Nelyubin and I.Zychor.

Summary missing mass spectra

Simulation for $pp \rightarrow pK m_x$

Sum of $\Lambda(1116)$ and $\Sigma(1193)$

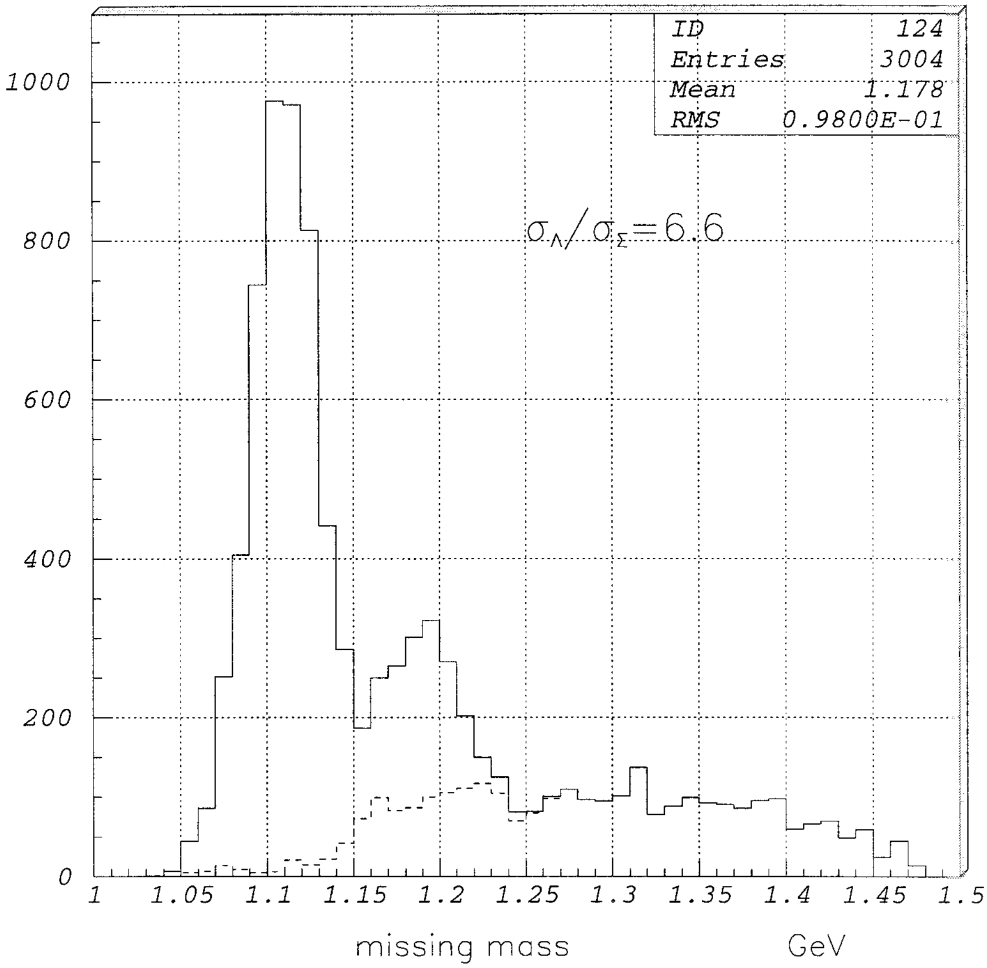

Summary missing mass spectrum for light hyperons

This figure was calculated in the frame
of OPE+OKE+FSI model.

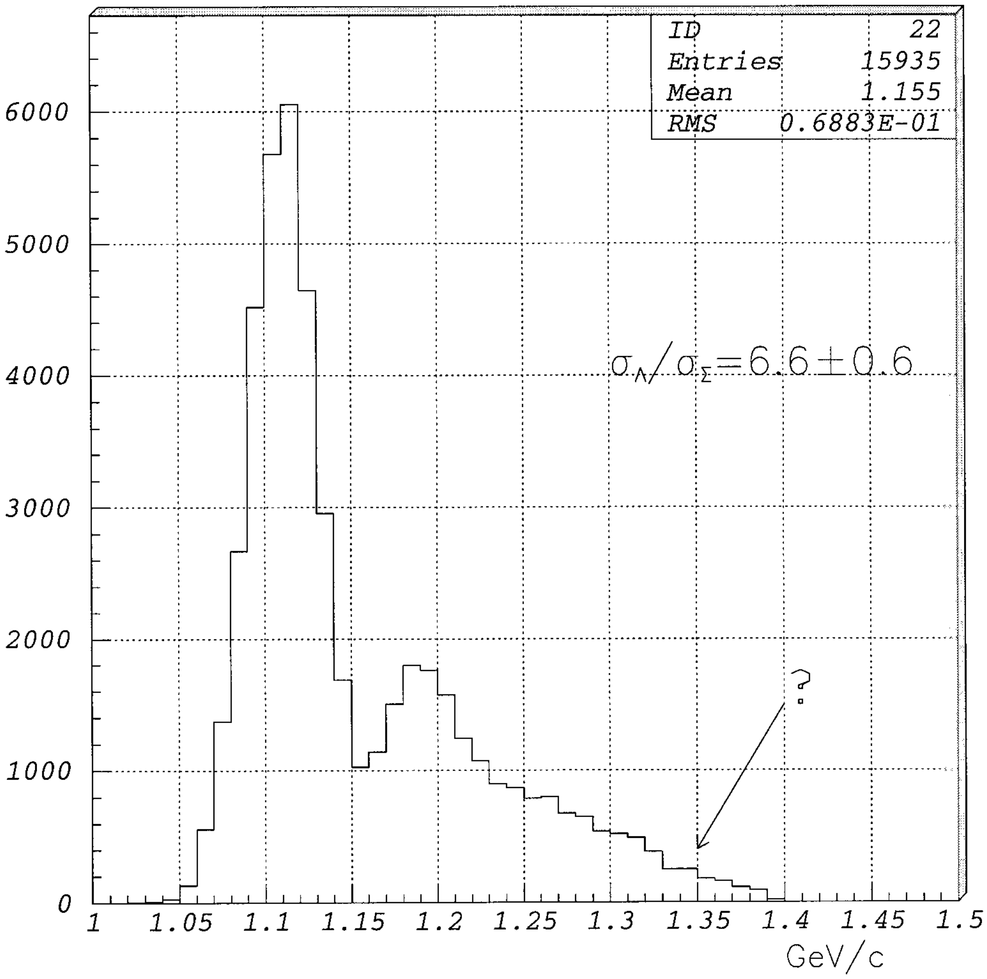

What is in the experimental spectrum (page 2) above 1.25 GeV: the effect of heavy hyperons or events from some background processes???

Background of additional π production.

- $pp \rightarrow K^+ NY\pi\ ,Y\ = \Lambda(1116)$
  $M_{min}^{\pi^0\Lambda} = 1255MeV$
  $M_{max}^{\pi^0\Lambda} = 1480MeV$
  $< M_{\Lambda\pi} >= 1327MeV$
- $pp \rightarrow K^+ NY\pi\ ,Y\ = \Sigma(1193)$
  $M_{min}^{\pi^0\Sigma^0} = 1330MeV$
  $M_{max}^{\pi^0\Sigma^0} = 1480MeV$
  $< M_{\Sigma\pi} >= 1405MeV$
- $pp \rightarrow K^+ NY\pi\pi$
  $< M_{Y\pi\pi} >= 1440MeV$

$$\sigma_{pp \rightarrow K^+ NY\pi} = \sigma_{K^+ NY} * \alpha$$

$\alpha = \frac{1}{3}$ from $K^- p \rightarrow N\Lambda$,
$\alpha = 1$ from $\pi p \rightarrow K\Lambda$

Summary missing mass spectrum $pp\to K^+pM_x$
for light hyperons including the background
of one additional pion production.
Simulations

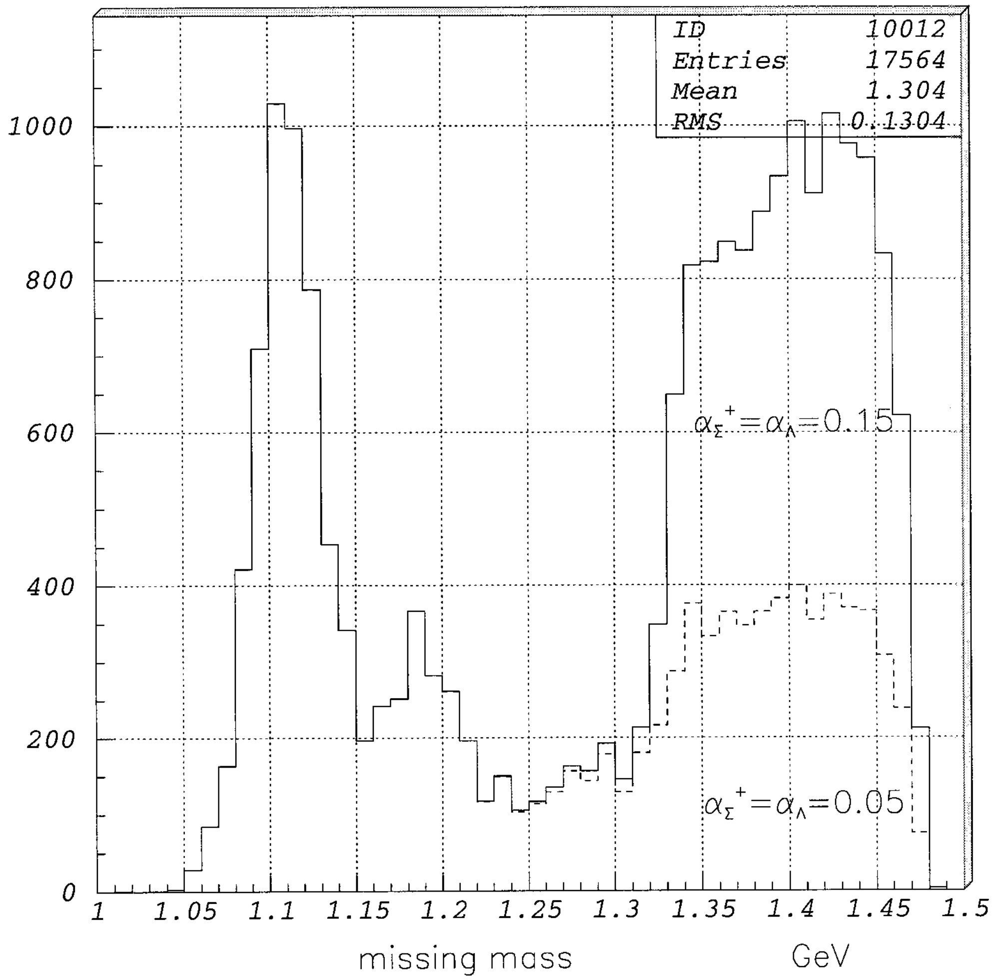

$$\frac{\sigma_\Lambda}{\sigma_\Sigma} = 6.6\pm1.0 \qquad \sigma_{\Sigma^+}\approx\sigma_\Lambda\gg\sigma_{\Sigma^0}$$

The background at $M_x > 1.3GeV$ cOmes from seven $pp- > K^+pY\pi$ reactions with $\sigma^{tot}_{sum(KNY\pi)}\approx 4*\alpha*\sigma^{tot}_{Kp\lambda}$. A solution with $\alpha = 0.15$ (seems reasonable) will fit the experimental data in this region.

As an alternative to this is the request of $\sigma^{tot}_{KpY^*} \approx 0.3*\sigma^{tot}_{KpY}$. This is hardly possible because for $m_Y < m_{Y\pi} < m_{Y^*}$ is expected that $\sigma^{tot}_{Y} > \sigma^{tot}_{Y\pi} > \sigma^{tot}_{Y^*}$. Moreover,if near threshold energy dependences of Y and Y^* production are similar, than $\sigma^{tot}_{Y^*} < 0.1\sigma^{tot}_{Y}$ is expected.

So, from this spectrum no reasonable conclusion can be done about Y^* production but good description of experimental data for $M_x < 1.25$GeV

Heavy hyperons (Particle Data)

$\Lambda(1405)0(\frac{1}{2}^{-}), \Gamma = 50MeV$

$$\begin{aligned} pp &\rightarrow K^+p\Lambda^*\rightarrow\pi^0\Sigma^0\rightarrow\gamma\Lambda\rightarrow\pi^0 n(35\%) \\ &\qquad\qquad\qquad\qquad\qquad\;\;\rightarrow\pi^- p(65\%), \\ pp &\rightarrow K^+p\Lambda^*\rightarrow\pi^-\Sigma^+\rightarrow\pi^0 p(51\%) \\ &\qquad\qquad\qquad\qquad\;\;\rightarrow\pi^+ n(48\%), \\ pp &\rightarrow K^+p\Lambda^*\rightarrow\pi^+\Sigma^-\rightarrow\pi^- n \end{aligned}$$

$\Sigma^0(1385)1(\frac{3}{2}^{+}), \Gamma = 35MeV$

- 88% $$\begin{aligned} pp &\rightarrow K^+p\Sigma^{0*}\rightarrow\pi^0\Lambda^0\rightarrow\pi^- p(65\%) \\ &\qquad\qquad\qquad\qquad\;\;\rightarrow\pi^0 n(35\%), \end{aligned}$$
- 12% $$\begin{aligned} pp &\rightarrow K^+p\Sigma^{0*}\rightarrow\pi^0\Sigma^0\rightarrow\gamma\Lambda, \quad \boxed{C - G\equiv 0} \\ &\qquad\qquad\;\;\rightarrow\pi^-\Sigma^+\rightarrow\pi^0 p(51\%) \\ &\qquad\qquad\qquad\qquad\;\;\rightarrow\pi^+ n(48\%), \\ &\qquad\qquad\;\;\rightarrow\pi^+\Sigma^-\rightarrow\pi^- n \end{aligned}$$

$\Sigma^+(1385)1(\frac{3}{2}^{+}), \Gamma = 35MeV$

- 88% $$\begin{aligned} pp &\rightarrow K^+n\Sigma^{+*}\rightarrow\pi^+\Lambda^0\rightarrow\pi^- p(65\%) \\ &\qquad\qquad\qquad\qquad\;\;\rightarrow\pi^0 n(35\%), \end{aligned}$$
- 12% $$\begin{aligned} pp &\rightarrow K^+n\Sigma^{+*}\rightarrow\pi^0\Sigma^+\rightarrow\pi^0 p(51\%) \\ &\qquad\qquad\qquad\qquad\;\;\rightarrow\pi^+ n(48\%), \\ &\qquad\qquad\;\;\rightarrow\pi^+\Sigma^0\rightarrow\gamma\Lambda^0\rightarrow\pi^- p(65\%) \\ &\qquad\qquad\qquad\qquad\qquad\quad\;\rightarrow\pi^0 n(35\%), \end{aligned}$$

$K^+p_1(M_x = p_2 + x)$ **correlations**

Experimental data

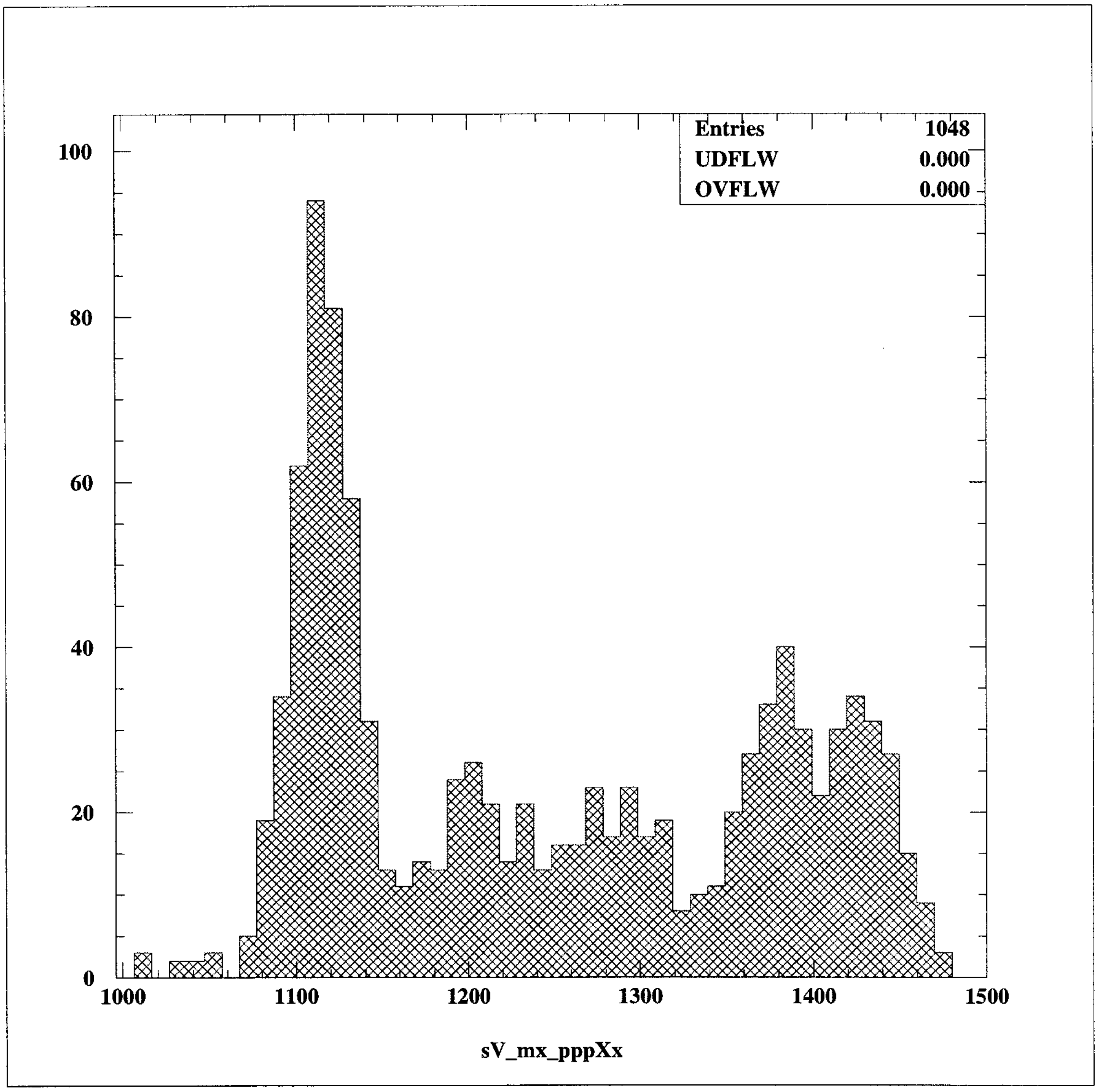

- p_1 in FD;
- p_2 in tel and SW-Sa;
- MWPC1 and 2 are not used;
- p_2 momentum is not analyzed.

Why MWPC1 and MWPC2 were not used to analyse p2.

$$pp- > K^+p1(Mx = p2 + x) \qquad T_p = 2.65GeV$$

A. Trigger is the same as on page 10
but p2 is only in SW-Sa combinations
Conclusion: in comparison to page 10
1.only 40% provide light hyperons
but p1 is mostly from vertex.
2.more than 90% provide
$M_x > 1.3GeV$

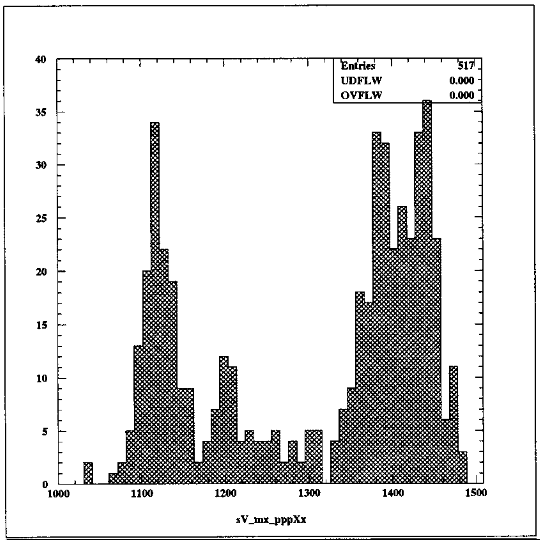

B. Trigger is the same as A but
MWPC1 and MWPC2 were used
to analyse p2
Conclusion: only 45% of p2 from SW-Sa
providing $M_x > 1.3GeV$
are analysed by MWPC1 and MWPC2

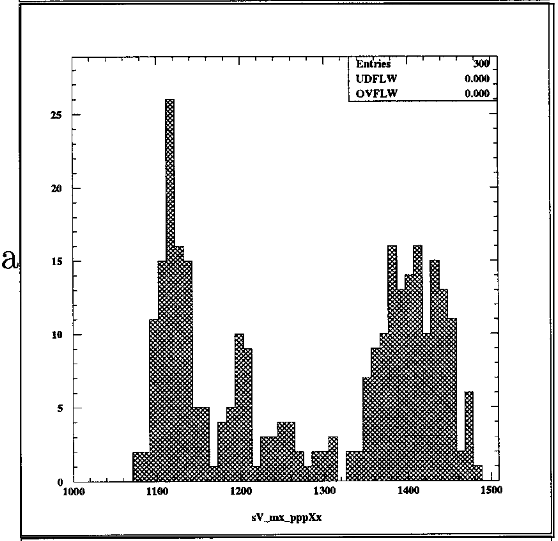

C. Trigger is the same as on page 10
but p2 is in SW-Sa combinations and
in SW but via the exit D2 window
Conclusion:
total gain for analysed K^+p1p2 events
can be at least 4 times if to improve
MWPC1-MWPC2 geometry

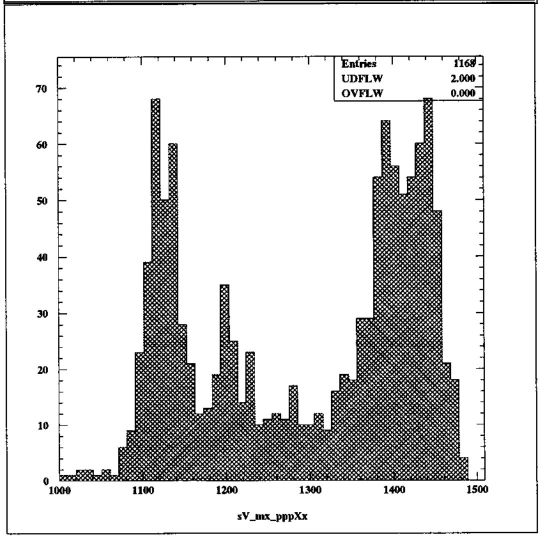

$pp- > p_1p_2(M_x = K^+ + x) \qquad T_p = 2.65GeV$

A. Trigger is the same as on page 10
but MWPC1 and MWPC2 are used
$M_x > 850$ is from:
light hyperons with additional pion
heavy hyperons
$pp- > ppK^+K^-$
$pp- > pp\phi$

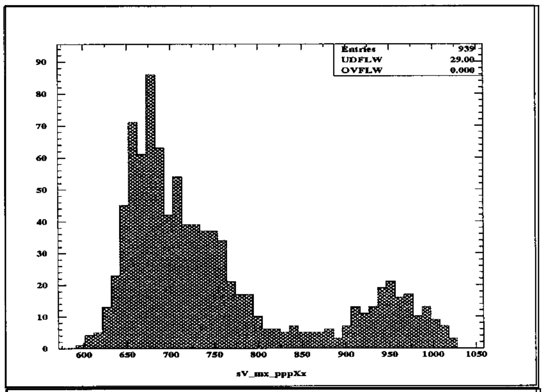

B. Trigger is the same in A
but p2 is only in SW-Sa
Conclusion: 90% with $M_x > 850$
are from p2 in SW-Sa

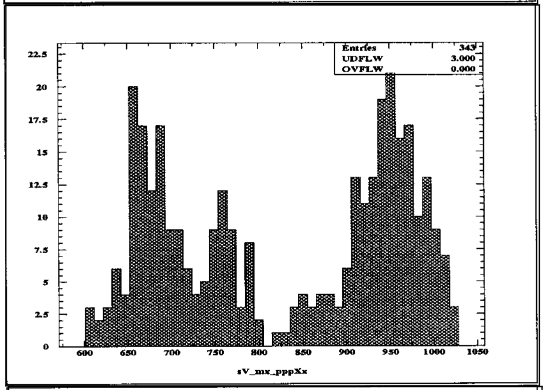

C. Trigger is the same as in B
but p2 are only in SW(4-6)-Sa and
p1 is in FD(4-8)
Conclusion:practically all the events
with $M_x > 0.97GeV$ survived

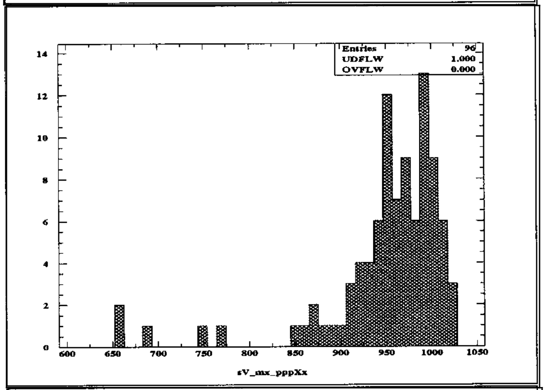

D. The same as C but
$850MeV < M_x < 1030MeV$
Experimentally was confirmed a trivial
result: near threshold of the reaction
ejectiles with $m_{p1} = m_{p2} < M_x$
will have $< P_{p1} >=< P_{p2} > \sim 1GeV/c$
which are the upper(lower) acceptances
limits of SW(FD), restricted by the
MWPCs frames

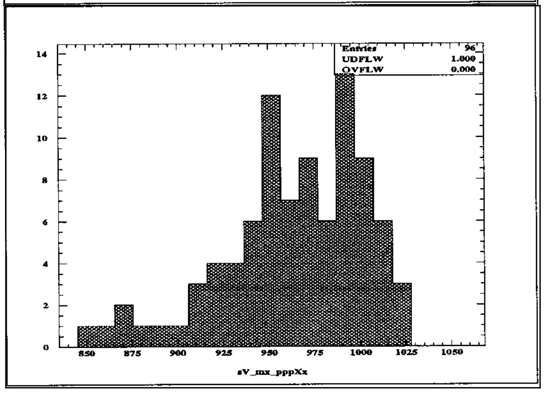

$K^+p_1(M_x = p_2 + x)$ correlations
Simulation

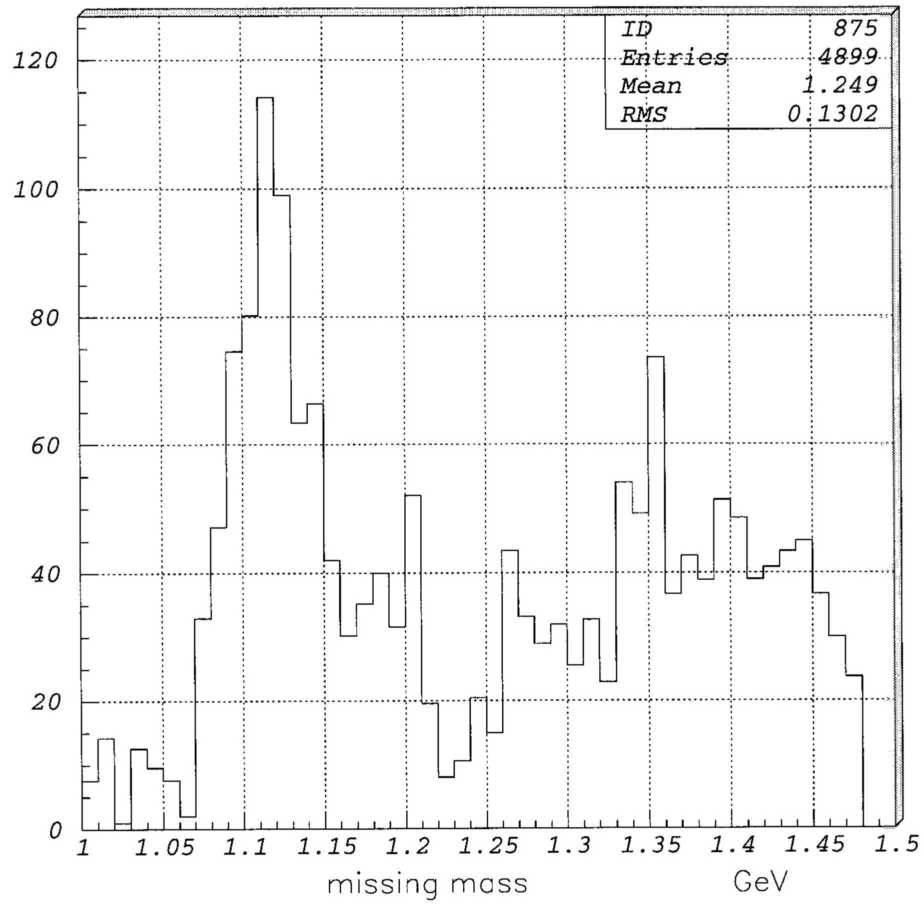

Only the reactions with light hyperon production with and without background single pion production. The α was taken as $\alpha = 0.15$

$pp \to K^+p(\Lambda \to \pi^- p)$	$pp \to K^+p(\Sigma^0 \to \gamma\Lambda \to \pi^- p)$

$pp \to K^+p\pi^0(\Lambda \to \pi^- p)$	$pp \to K^+p\pi^+\pi^-(\Lambda \to \pi^- p)$
$pp \to K^+p\pi^0(\Sigma^0 \to \gamma\Lambda \to \pi^- p)$	$pp \to K^+p\pi^+\pi^-(\Sigma^0 \to \gamma\Lambda \to \pi^- p)$
$pp \to K^+p\pi^-(\Sigma^+ \to \pi^0 p)$	$pp \to K^+p\pi^0\pi^-(\Sigma^+ \to \pi^0 p)$

Pion background can explain experimental data at $M_x > 1.3 GeV$. Improvement can be after all three particles (K^+,p_1 and p_2) are analyzed??

$K^+p(M_x = \pi^+ + x)$ correlation

Experimental data

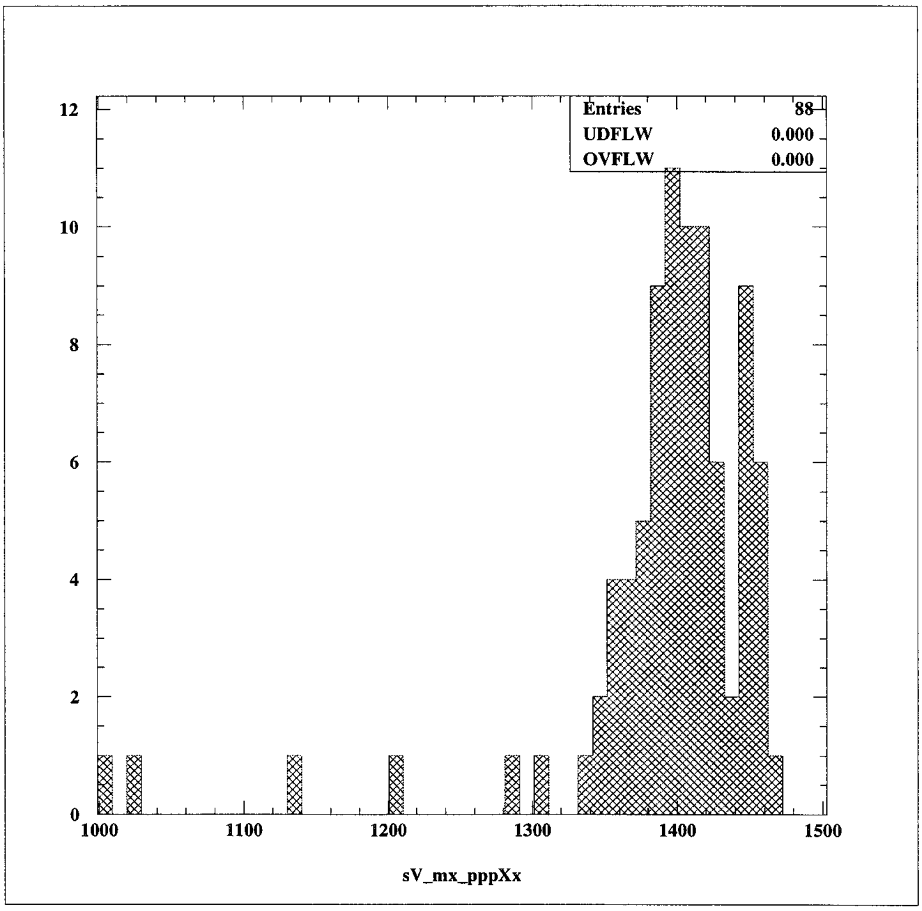

K^+ in tel, p in FD;

π^+ in tel (MWPC1 and 2 were not used for pion selection)

no processes : $pp \rightarrow K^+p\Lambda, \quad pp \rightarrow K^+p\Sigma^0$

should be seen :

$pp \rightarrow K^+p\Lambda^* \rightarrow Kp_1\pi^+\pi^-n$
$pp \rightarrow K^+p\Lambda^* \rightarrow Kp_1\pi^+\Sigma^-$
$pp \rightarrow K^+p\Sigma^{0*} \rightarrow Kp_1\pi^+\pi^-n$
$pp \rightarrow K^+p\Sigma^{0*} \rightarrow Kp_1\pi^+\Sigma^-$
$pp \rightarrow K^+n\Sigma^{+*} \rightarrow Kp_2\pi^+\pi^-n$

practically no background at $M_x < 1.300GeV$ - perfect!!!

$K^+p(M_x = \pi^+ + x)$ **correlation**

Experimental data

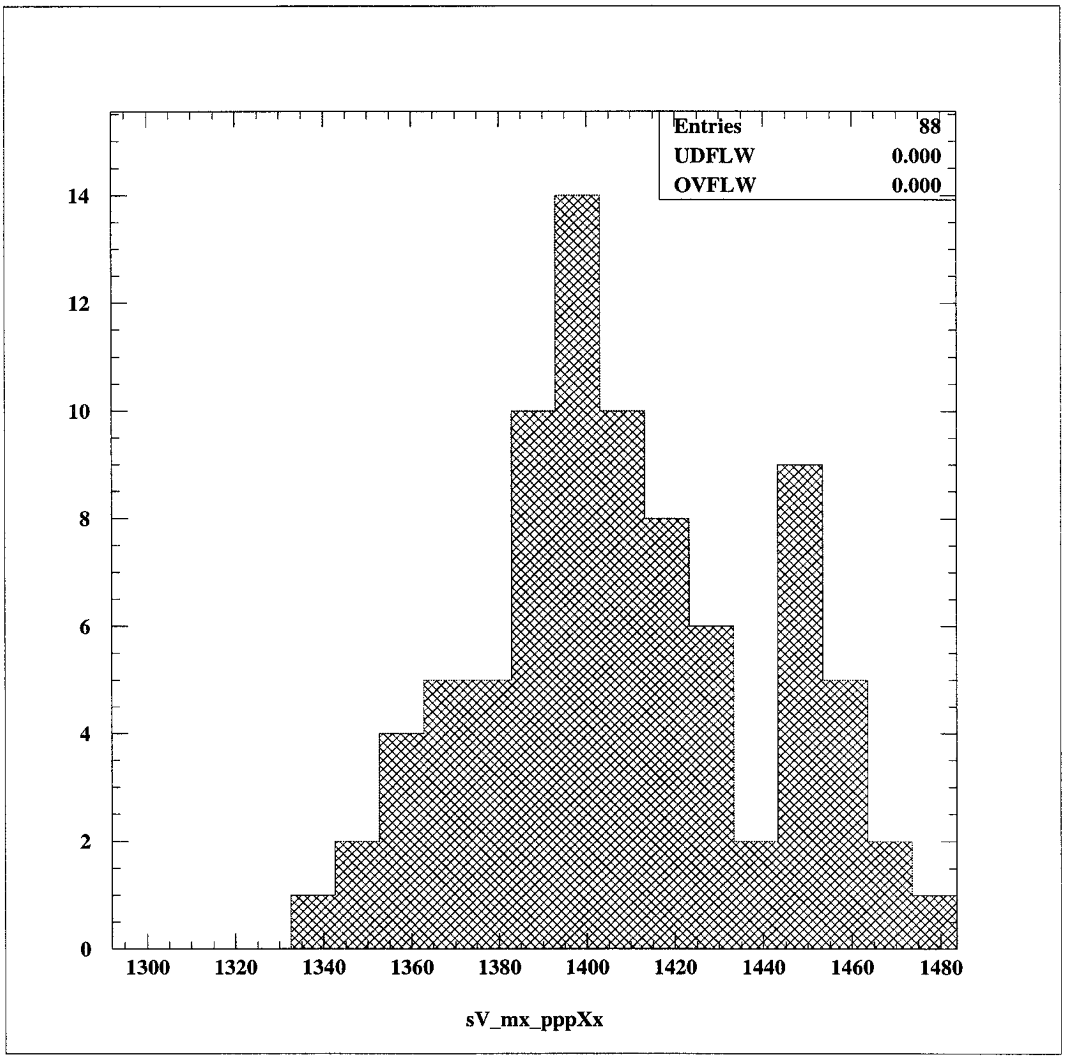

$1.3 < M_x < 1.5$ $\Gamma_{\Lambda^*} \approx 35 - 40 MeV$

Two peaks are obvious: at $\sim 1400 MeV$ and

at $\sim 1450 MeV$

π^+ spectrum from Y^* decay simulations

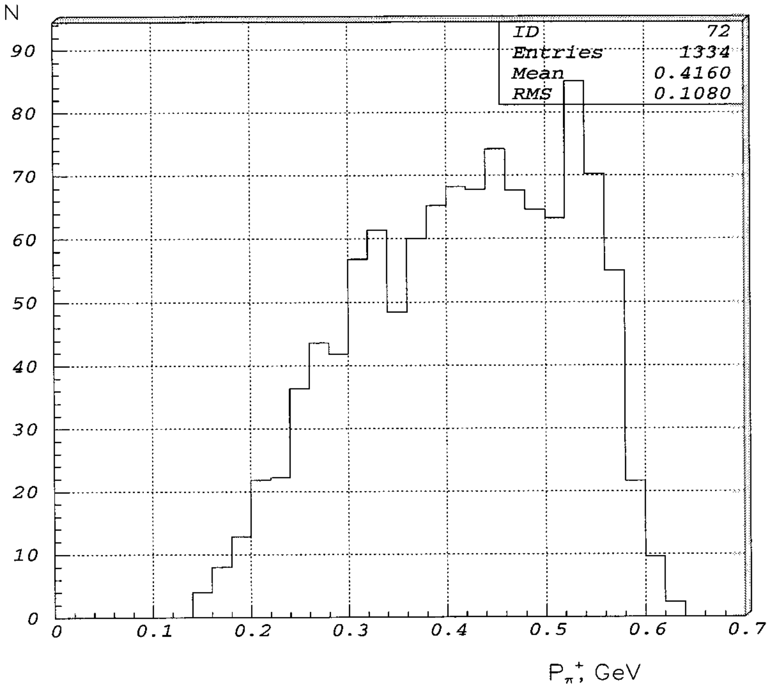

Experiment

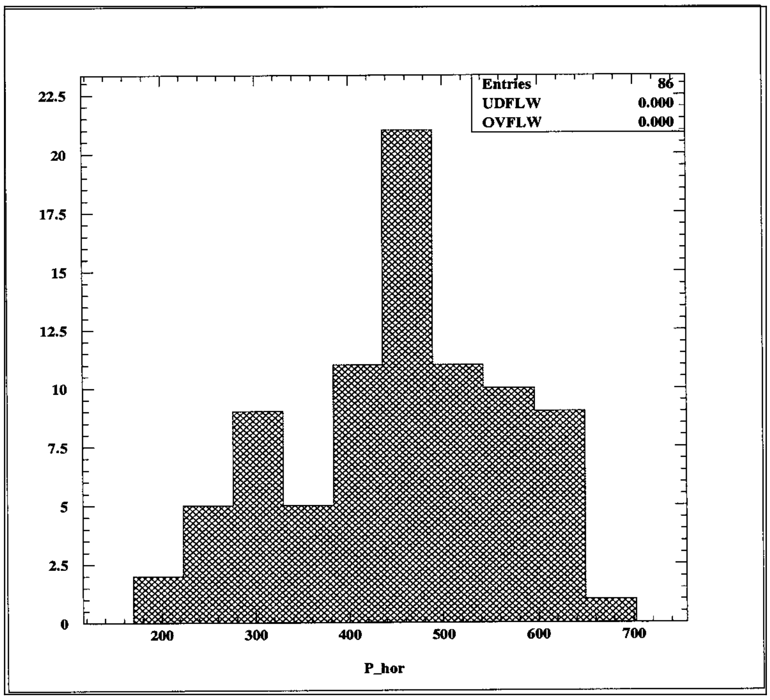

All the pions are in telescopes!!

$K^+p(M_x = \pi^+ + x)$ correlation
Simulation

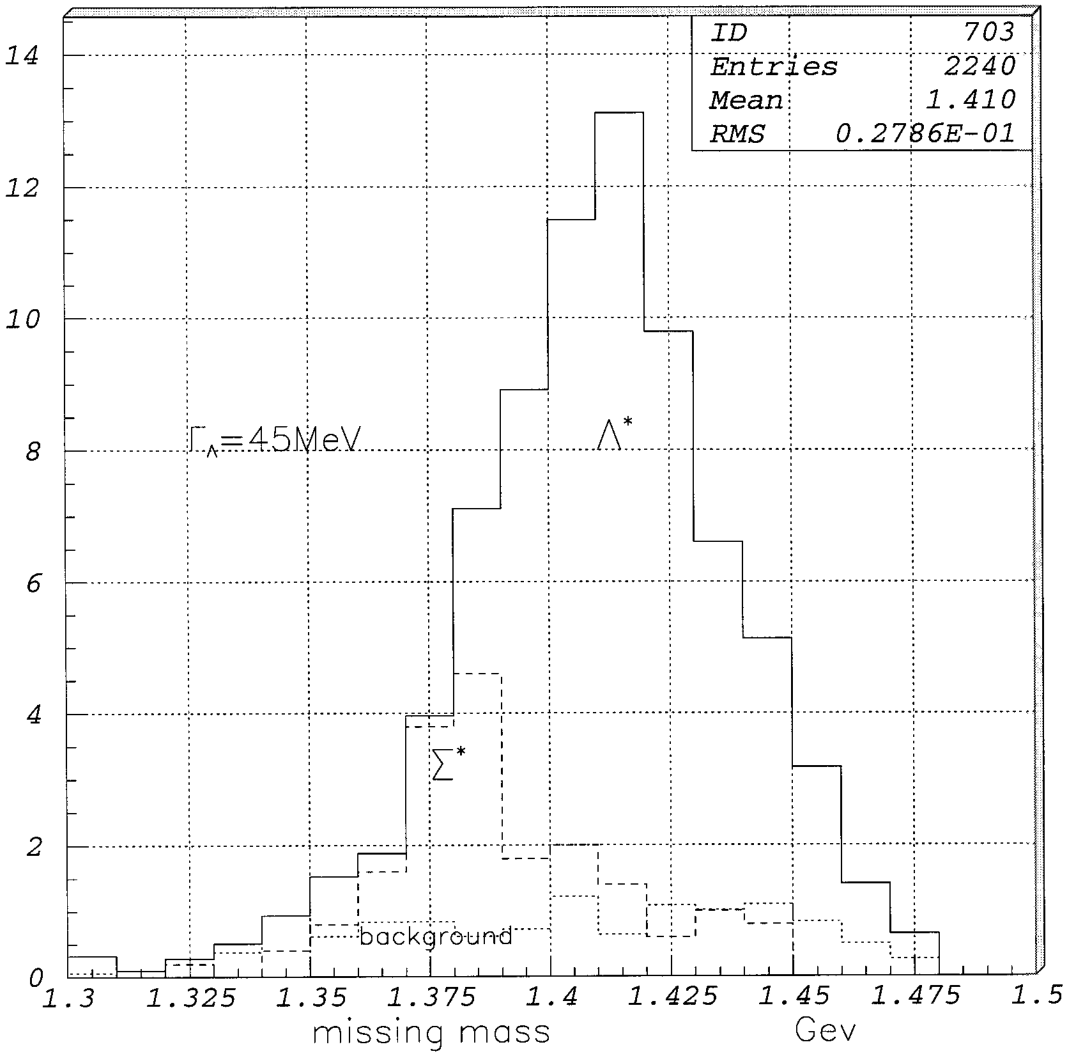

$$\alpha_{\Sigma^+} \approx \alpha_\Lambda \approx 0.07$$

$$\frac{\sigma_\Lambda}{\sigma_{\Lambda^*}} = 55 \pm < 30\%, \qquad \frac{\sigma_\Lambda}{\sigma_{\Sigma^*}} = 35 \pm ?$$

but simulated distribution is wider, Γ_Λ should be $< 45MeV$

$pp \rightarrow KNY\pi\pi$ is not yet considered (it should give a peak around 1440MeV (see p.7))

$$\boxed{K^-p \rightarrow \pi^-\Sigma^+(1660) \rightarrow \pi^-\pi^+\Lambda(1405)}$$

Data from literature

JPG, 17, 289(1991)

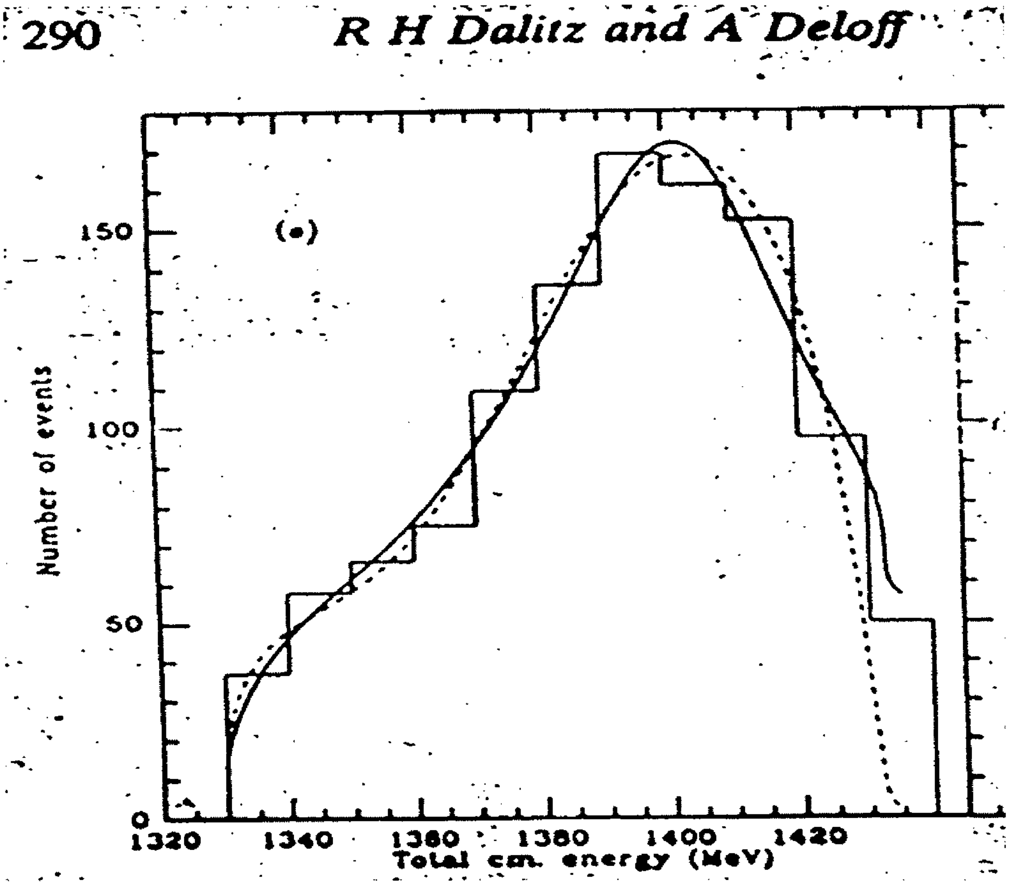

290 *R H Dalitz and A Deloff*

$$\Gamma = 50MeV$$

Conclusion:

1. $\frac{\sigma^{tot}_{Kp\Lambda}}{\sigma^{tot}_{Kp\Sigma}} = 6.6 \pm 1.0$

This result is more or less reliable,since checked in the frame of two models.

2. $\frac{\sigma^{tot}_{Kp\Lambda}}{\sigma^{tot}_{Kp\Lambda(1405)}} = 55 \pm 18$ and $\frac{\sigma^{tot}_{Kp\Lambda}}{\sigma^{tot}_{Kp\Sigma(1385)}} = 35 \pm ?$

Only statmodel was use to get this result.Since $T_p = 2.65 GeV$ is close to the thresholds of $\Sigma(1385)$ and $\Lambda(1405)$ production the Y^*N final state interaction must be important.

- Peak (??) at 1450MeV can be connected with $pp \rightarrow K^+ N \pi\pi Y$ or $pp \rightarrow K^+ p \Sigma(1480)$. The last reaction is of the top interest, because propertis of $\Sigma(1480)$ practically are not known.
  Analysis of these assumptions is in progress.
- In oder to understand the nature of this peak one needs:
  - Higher energy 2.70GeV or better 2.75GeV;
  - 10 times more statistics.

3. To make more effective studies of heavy hyperon production and $pp- > ppK^+K^-$ processes in a Kpp coincidence experiment in is desirable to improve MWPC's geometry,say,to change two sets of MWPCs (FD and SD) to a single one.

$pp \to K^+p \cdots \quad T_p \approx 2.65\ GeV$

1

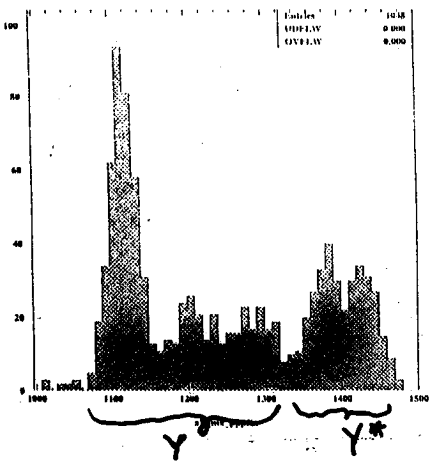

$pp \to K^+_{tel}\ p_{FD}\ M_X(p^{+x}_{tel+SW-Sa})$

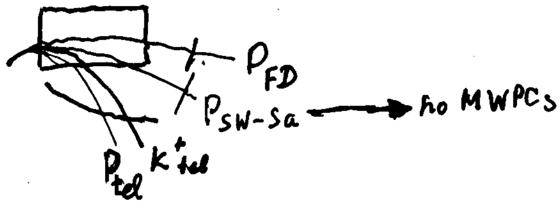

2

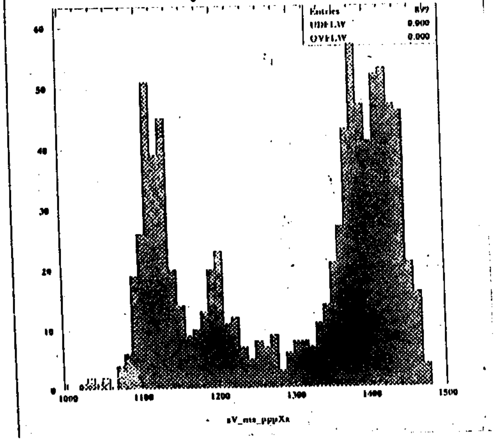

$pp \to K^+_{tel}\ p_{FD}\ M_x(p^{+x}_{any\ SW})$

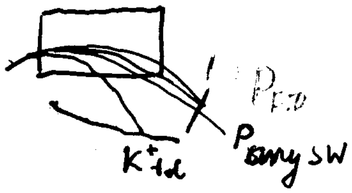

3

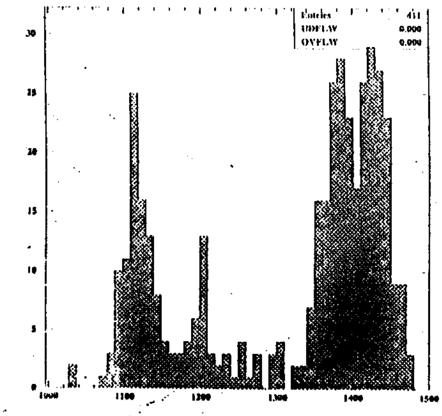

$pp \to K^+_{tel}\ p_{FD}\ M_x(p^{+x}_{SW-Sa})$

4

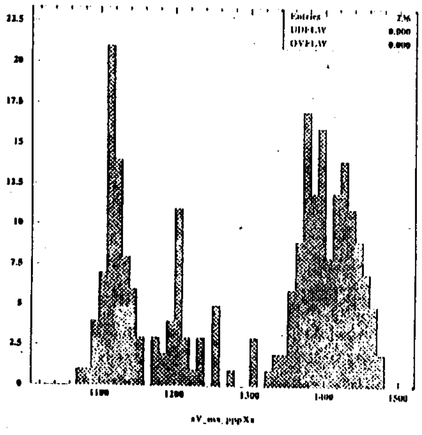

$pp \to K^+_{tel} \cdot p_{FD} \cdot M_x(p^{+x}_{SW-Sa-MWPCs})$

M_x

$$\frac{N_{Y*}(2)}{N_{Y*}(1)} \approx 0.8 \qquad \frac{N_{Y*}(3)}{N_{Y*}(2)} = 0.5$$

$$\frac{N_{Y*}(4)}{N_{Y*}(2)} = 0.3$$

Status of the pellet target at ANKE

V.Chernyshev

Institute for Theoretical and Experimental Physics
117259 Moscow
Russia

Status of pellet target for ANKE.

V. Chernyshev (ITEP)

- Principle of operation
- Work participants
- Present status of set-up
- Obtained results.
- Conclusions and plans.

Participants of activity at IKP and responsibility:

A.Boukharov	gas supply and diagnostic	MPEI
A.Balanutsa	vacuum	ITEP
W.Borgs	infrastructure	IKP
M.Buescher	physics program	IKP
V.Chernetsky	cryostat and cooling	ITEP
V.Chernyshev	project responsible	ITEP
M.Chumakov	PC control and DAQ	ITEP
A.Dmitriev	pellet production theory	MPEI
P.Fedorets	data analysis	ITEP
A.Gerasimov	mechanics	ITEP
V.Goryachev	diagnostic and control	ITEP
L.Gusev	electronic	ITEP
S.Podchasky	cryostat and cooling	ITEP

Test setup of the ANKE PELLET TARGET, Nov.2000

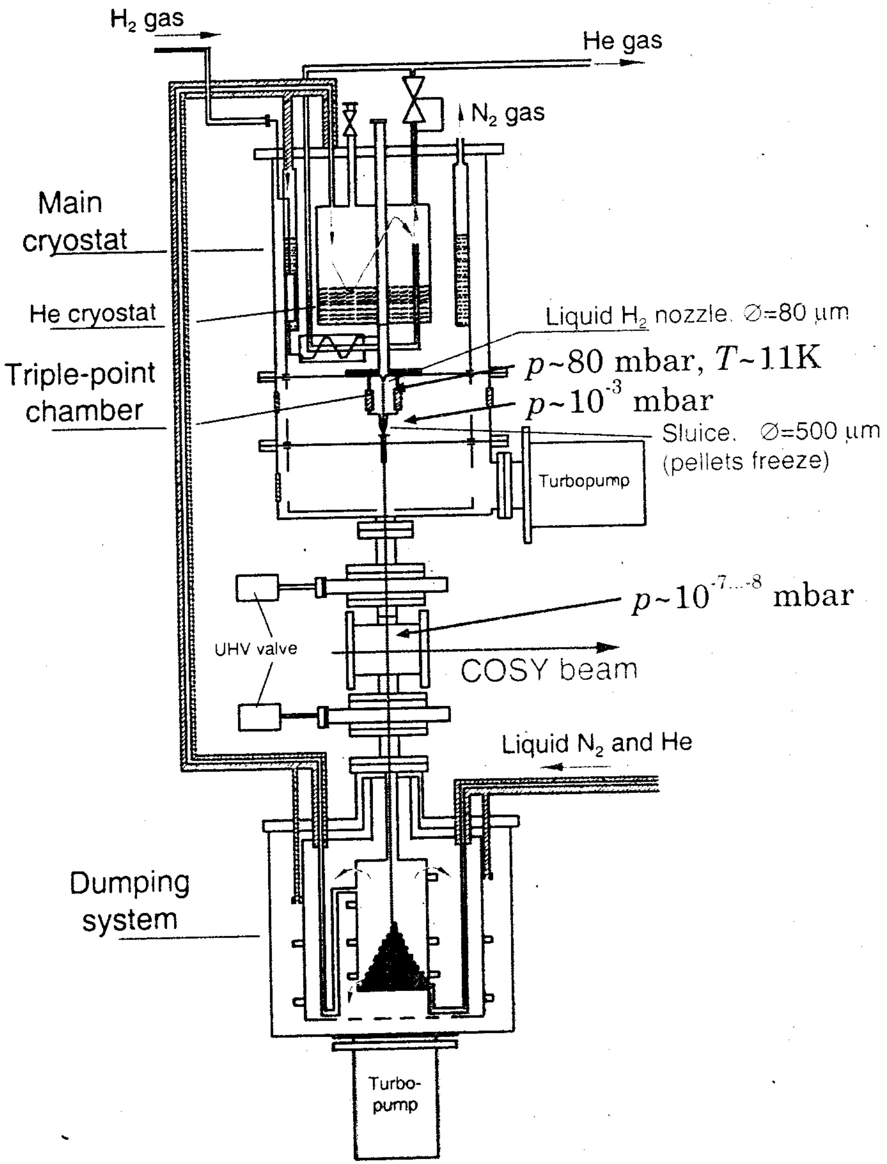

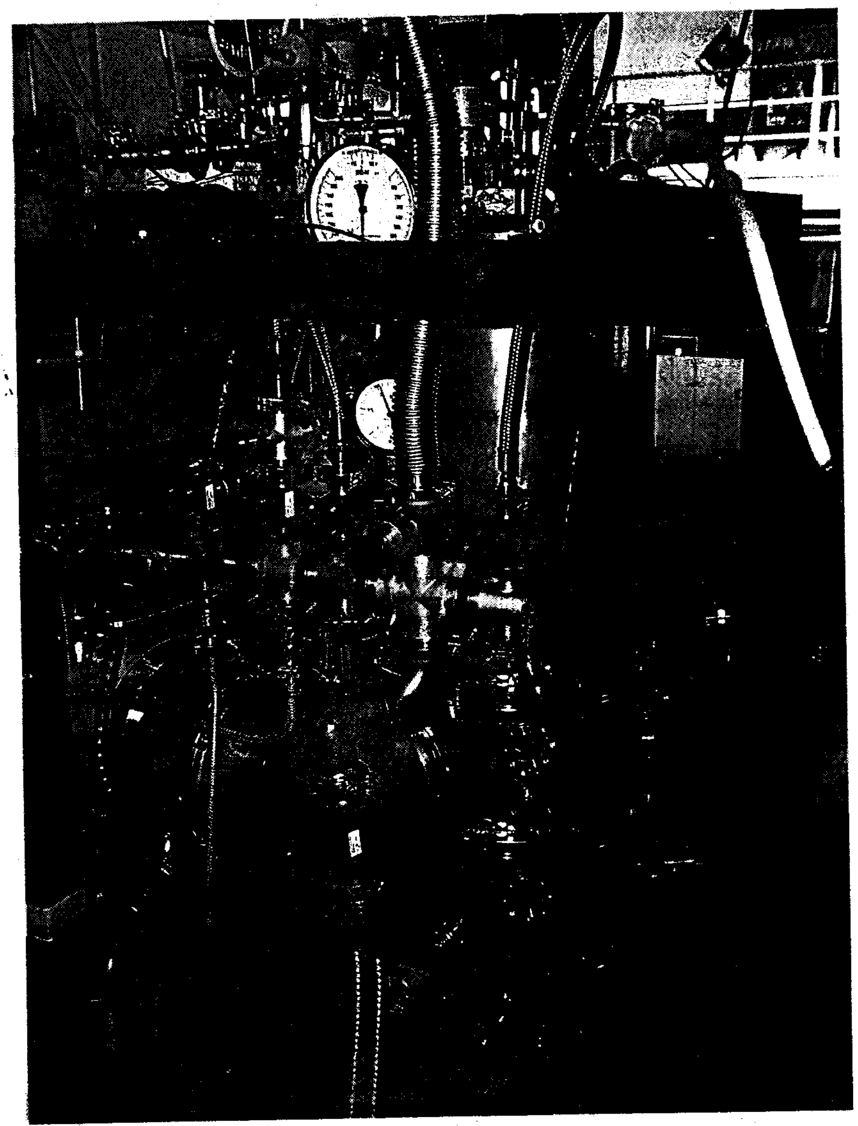

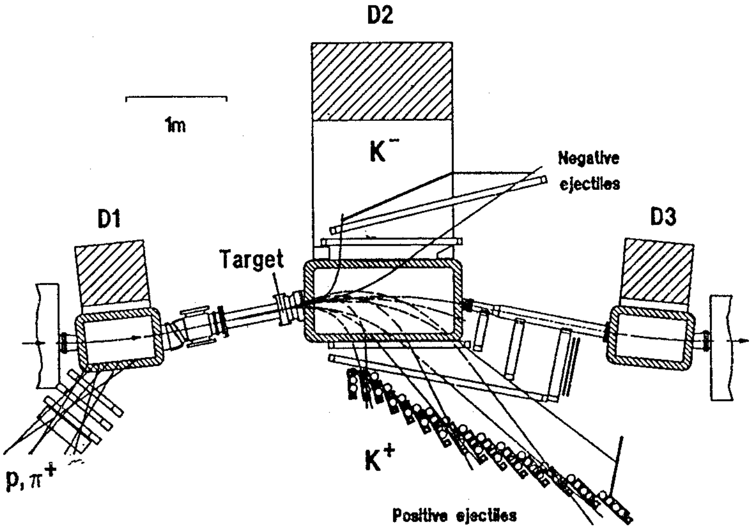

Figure 7: Layout of the setup at the ANKE spectrometer

Table 2: Densities of the ITEP frozen-pellet target with hydrogen as target material, a COSY-beam diameter of 2 mm, a beam intensity of $n = 3 \cdot 10^{10}$ and under the assumption that one pellet is in the beam

Diameter of pellet (μm)	Mass (g)	Total number of atoms per pellet	Luminosity ($cm^{-2}s^{-1}$)
20	$3 \cdot 10^{-10}$	$1.8 \cdot 10^{14}$	$2.8 \cdot 10^{32}$
40	$2.3 \cdot 10^{-9}$	$1.4 \cdot 10^{15}$	$2.2 \cdot 10^{33}$
60	$8 \cdot 10^{-9}$	$4.8 \cdot 10^{15}$	$7.4 \cdot 10^{33}$

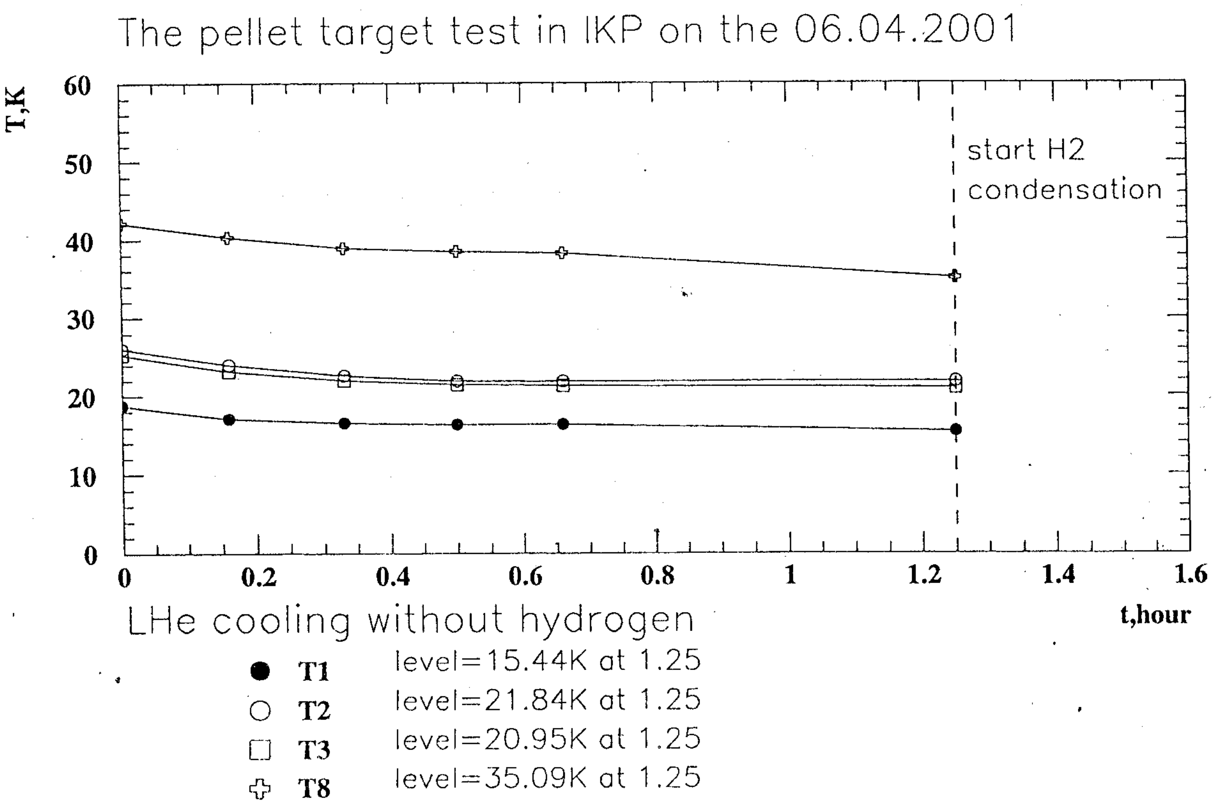
The pellet target test in IKP on the 06.04.2001
T,K
60
50
40
30
20
10
0
start H2
condensation
0
0.2
0.4
0.6
0.8
1
1.2
1.4
1.6
t,hour
LHe cooling without hydrogen
● T1 level=15.44K at 1.25
○ T2 level=21.84K at 1.25
□ T3 level=20.95K at 1.25
✣ T8 level=35.09K at 1.25

The pellet target test in IKP on the 06.04.2001

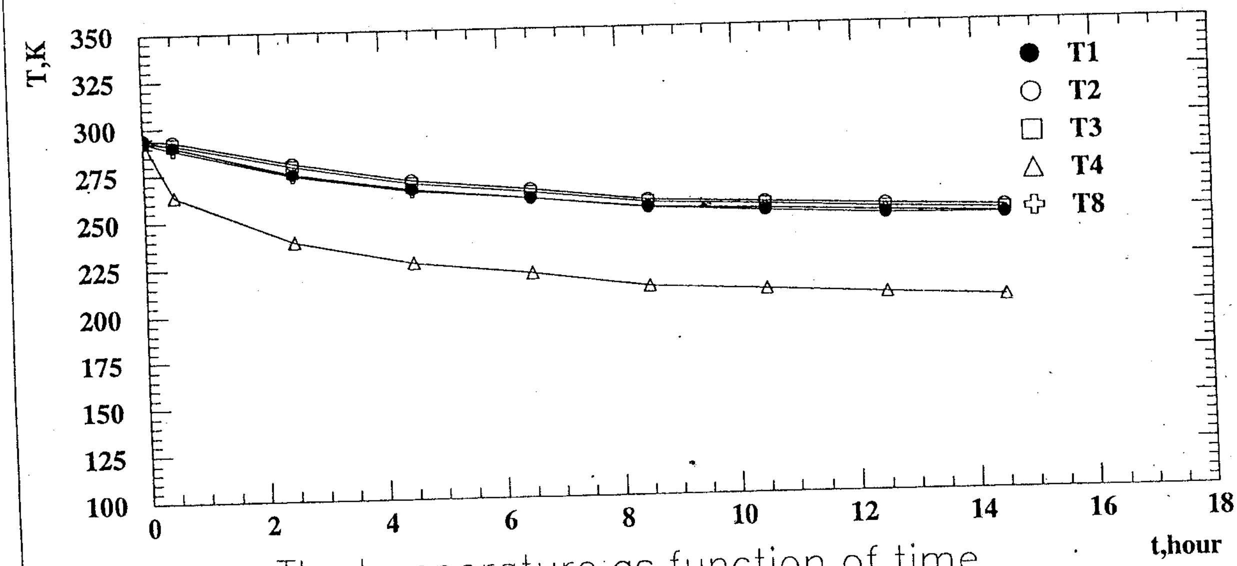

The temperature as function of time
LN cooling

●	**T1**	level=247.1K at 14.5
○	**T2**	level=251.2K at 14.5
□	**T3**	level=249.8K at 14.5
△	**T4**	level=203.6K at 14.5
✣	**T8**	level=247.8K at 14.5

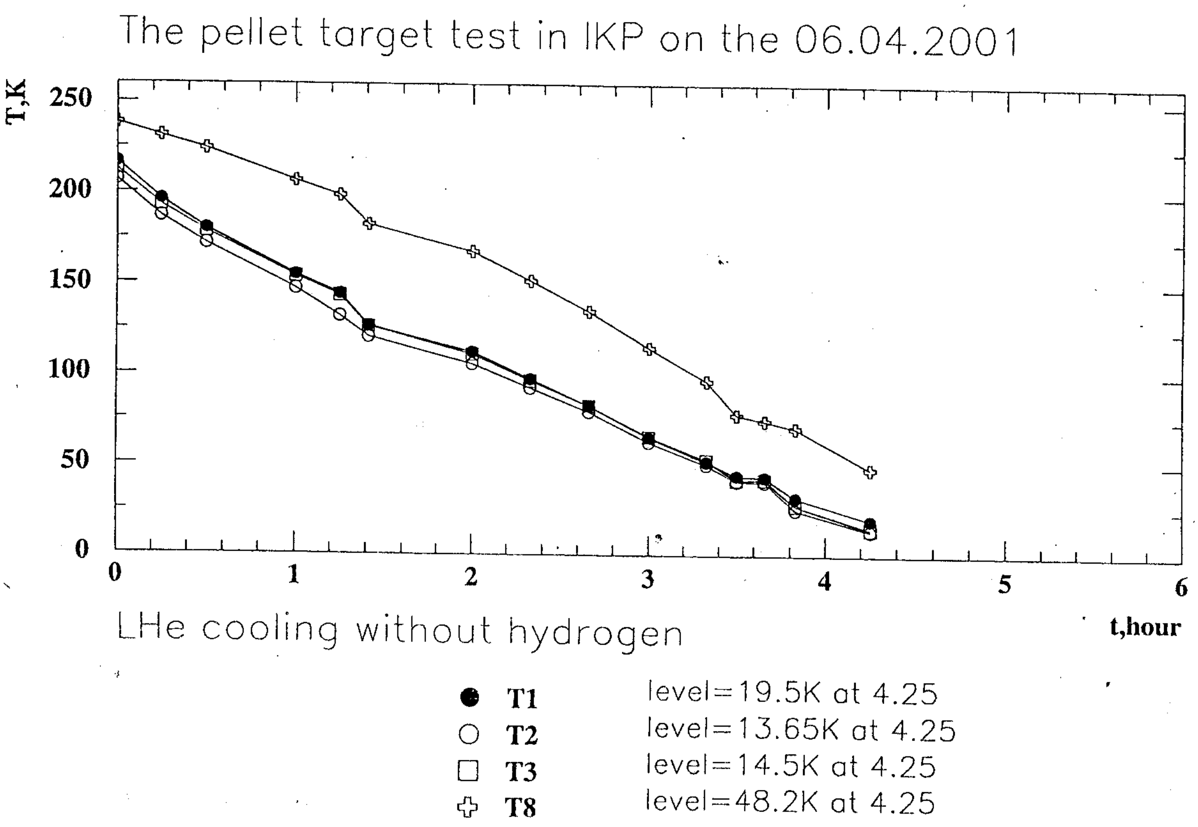

The pellet target test in IKP on the 06.04.2001
T,K
250
200
150
100
50
0
0
1
2
3
4
5
6
t,hour
LHe cooling without hydrogen
● T1 level=19.5K at 4.25
○ T2 level=13.65K at 4.25
☐ T3 level=14.5K at 4.25
✚ T8 level=48.2K at 4.25

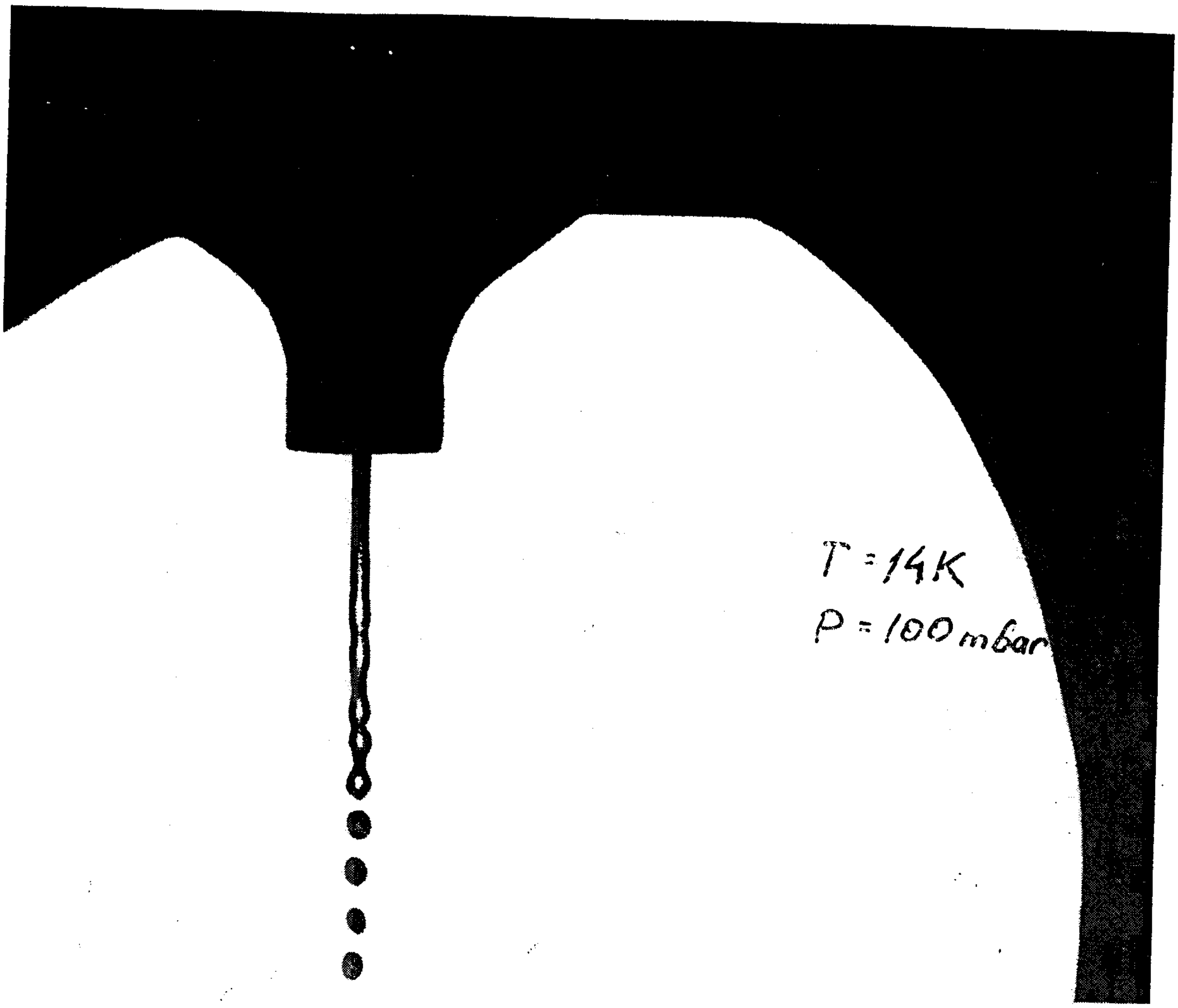
T = 14K
P = 100 mbar

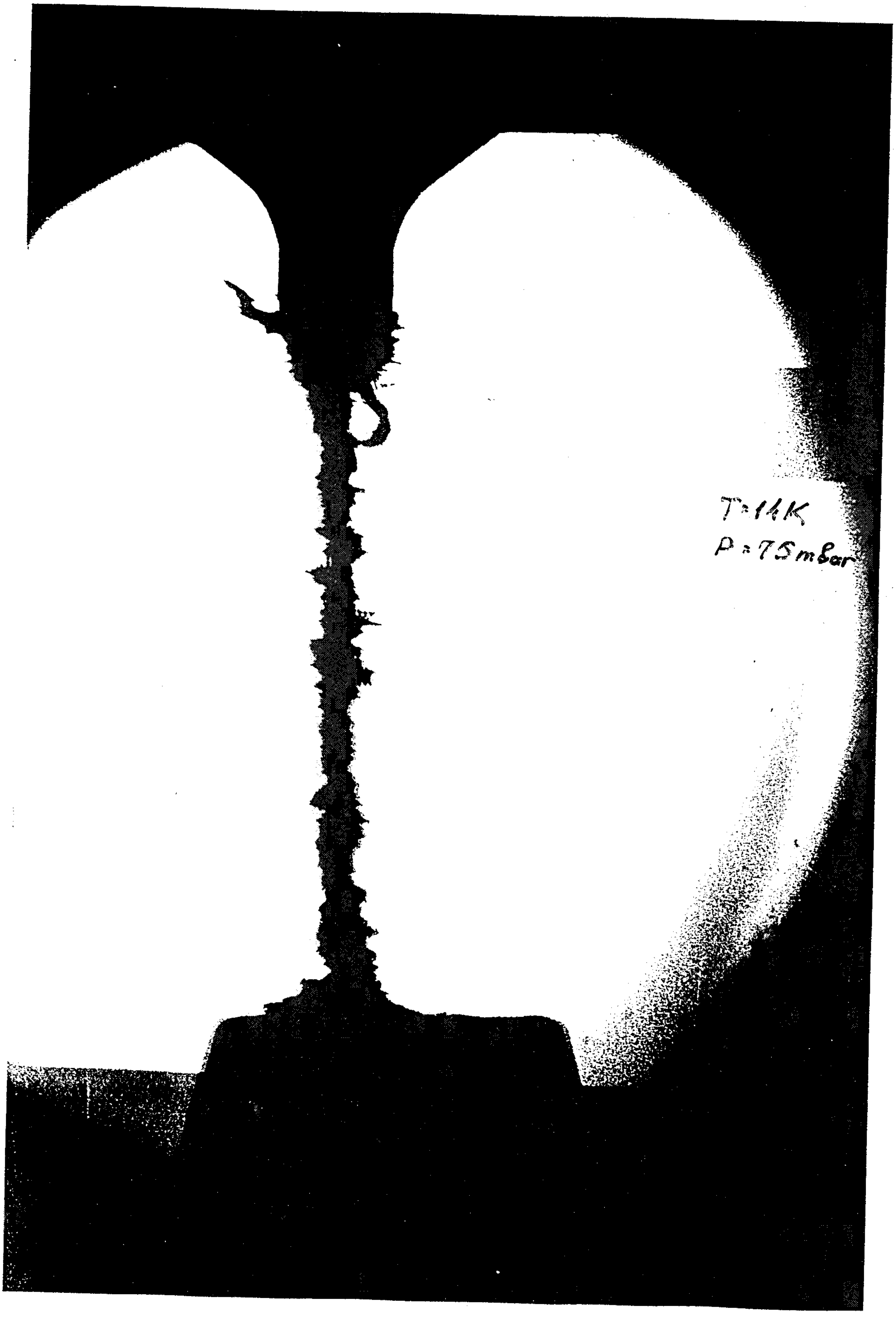
T=14K
P=75mbar

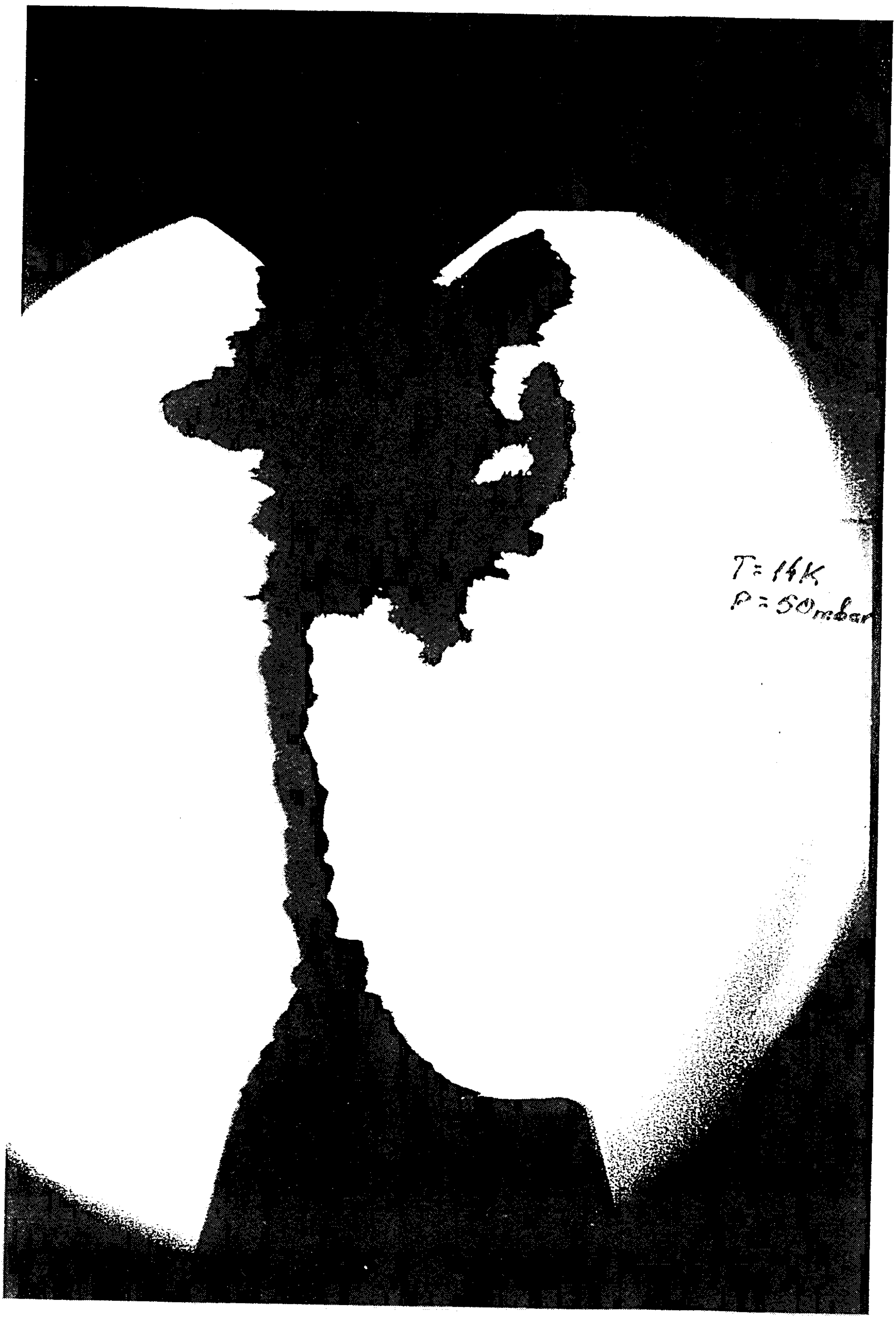

T=14K
P=50mbar

Short summary

1. Controlled (60 μm diameter) liquid hydrogen jet generation is realized
2. Mono-size droplet flow is obtained. Droplet generation system tested
3. The regimes of stable jet generation measured
4. DAQ prototype tested.

NN correlations: Pauli principle and FSI

I.Seluzhenkov

Moscow State Engineering Physics Institute
115409 Moscow
Russia
and
Institute of Theoretical and Experimental Physics
117259 Moscow
Russia

Low energy reactions with more than two identical nucleons in the exit channel are discussed. A simplest examples of such reactions are pion double and single charge exchange reactions on ^{3}He. In all these reactions, from the one hand, cross section should be strongly suppressed by the Pauli principle, and from another hand, must be increased by the nucleon-nucleon final state interaction.

In this report I will try to prove the following statement: suppression of the cross section due to the Pauli exclusion principle becomes ineffective as soon as the final state interaction between outgoing nucleons is taken into account.

NN correlations: Pauli Principle and FSI

Low energy reactions with more than two identical nucleons in the exit channel.

Examples:

- $\pi^- \, {}^3\mathrm{He} \rightarrow \pi^+ \, n \, n \, n$
- $\pi^+ \, {}^3\mathrm{He} \rightarrow \pi^0 \, p \, p \, p$
  etc.

The main effects:

- Pauli exclusion principle
- NN final state interaction
  (Migdal-Watson effect)

Main statement:
suppretion due to the Pauli exclusion principle gets ineffective by the NN FSI

Experiment:
cross section at $T_\pi = 70$ MeV:

$\pi^+ \, {}^3\mathrm{He} \rightarrow \pi^0 \, p \, p \, p \quad 2.7 \pm 0.6$ mb
$\pi^+ \, {}^2\mathrm{H} \rightarrow \pi^0 \, p \, p \quad 4.8 \pm 1.0$ mb

Pion single charge exchange reaction

$$\pi^+ + {}^3\text{He} \to \pi^0 + p\ p\ p$$

Naive estimate gives:

$$d\sigma \sim \langle v_{\rm N}\rangle^2$$

Simplified **amplitude:**

$$M \sim \sum_{ijk} \epsilon_{ijk}\ \ (\bar{u}_i(A + B\hat{q})U)\ \ \left(\bar{u}_j C\gamma_5 \bar{u}_k^T\right)$$

u, U – *bespinors*, $C = \gamma_2\gamma_0$, A and B are *constants.*

Realistic **amplitude**:

has the same form with A and B *smooth functions* of kinematic variables.

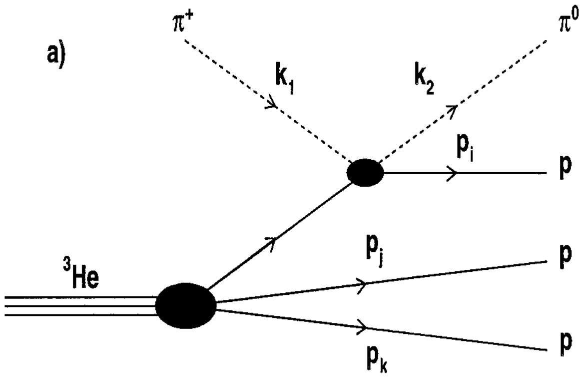

In terms of two-component spinors:

$$M \sim \sum_{ijk} \epsilon_{ijk} \left(\varphi_j^+ \left\{ 1 + i\boldsymbol{\sigma} \frac{[\mathbf{p}_j \mathbf{p}_k]}{(E_j + m)(E_k + m)} \right\} \sigma_2 \varphi_k^* \right) \times$$

$$\times \left(\varphi_i^+ \left\{ A + q_0 B - iB\boldsymbol{\sigma} \frac{[\mathbf{p}_i \mathbf{q}]}{E_i + m} \right\} \phi \right)$$

Easy to see, that:

$$\sum_{ijk} \epsilon_{ijk} \left(\varphi_j^+ \sigma_2 \varphi_k^* \right) \left(\varphi_i^+ \phi \right) = 0$$

Thus:

$$d\sigma \sim \langle v_{\mathrm{N}} \rangle^2$$

At the incoming pion energy $T_\pi \sim 50$ MeV, $\langle v_{\mathrm{N}} \rangle \sim 1/10$, and suppression of $d\sigma$ by two orders of magnitude.

NN final state interaction

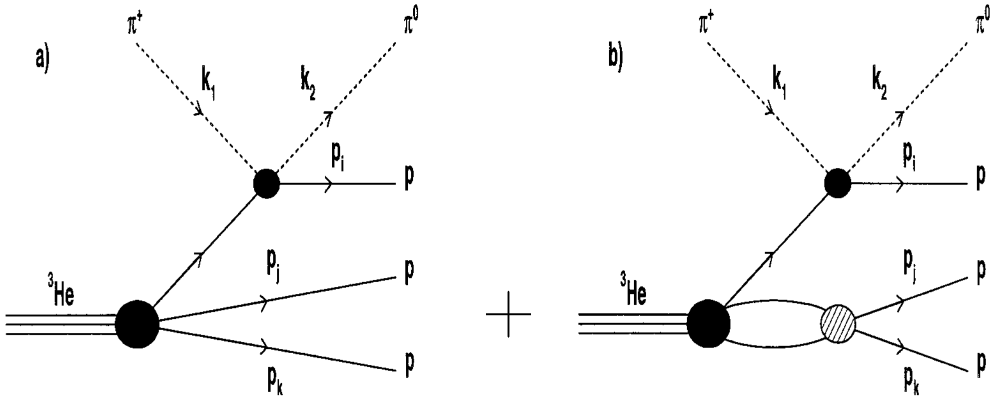

The amplitude of the reaction

$$M \sim \sum_{ijk} \epsilon_{ijk}(\bar{u}_i(A + B\hat{q})U)(\bar{u}_j C\gamma_5 \bar{u}_k^T)\left(1 + R^{-1} \cdot f_{jk}\right)$$

f_{jk} – NN–scattering amplitude of the pair of nucleons in relative S–wave.

In this case

$$\sum_{ijk} \epsilon_{ijk} \left(\varphi_j^+ \sigma_2 \varphi_k^*\right) \left(\varphi_i^+ \phi\right) f_{jk} \neq 0$$

NN–scattering amplitude at low energies has a form

$$f_{12} \approx -\frac{1}{a^{-1} + i|\mathbf{p}_{12}|}$$

In the considered energy region

$$\frac{i}{2} f_{12} \approx -\frac{1}{|\mathbf{p}_1 - \mathbf{p}_2|} = \sum_{l_1=l_2=l} \left(\frac{p}{P}\right)^l P_l(\cos\theta)$$

$p = \min\{\mathbf{p}_1, \mathbf{p}_2\}$, $P = \max\{\mathbf{p}_1, \mathbf{p}_2\}$,
θ is the angle between $\mathbf{p}_1$ and $\mathbf{p}_2$,
$l_1 = l_2 = l$ orbital momentum of either nucleons in the ${}^1S_0$-pair relative to the “third” nucleon.

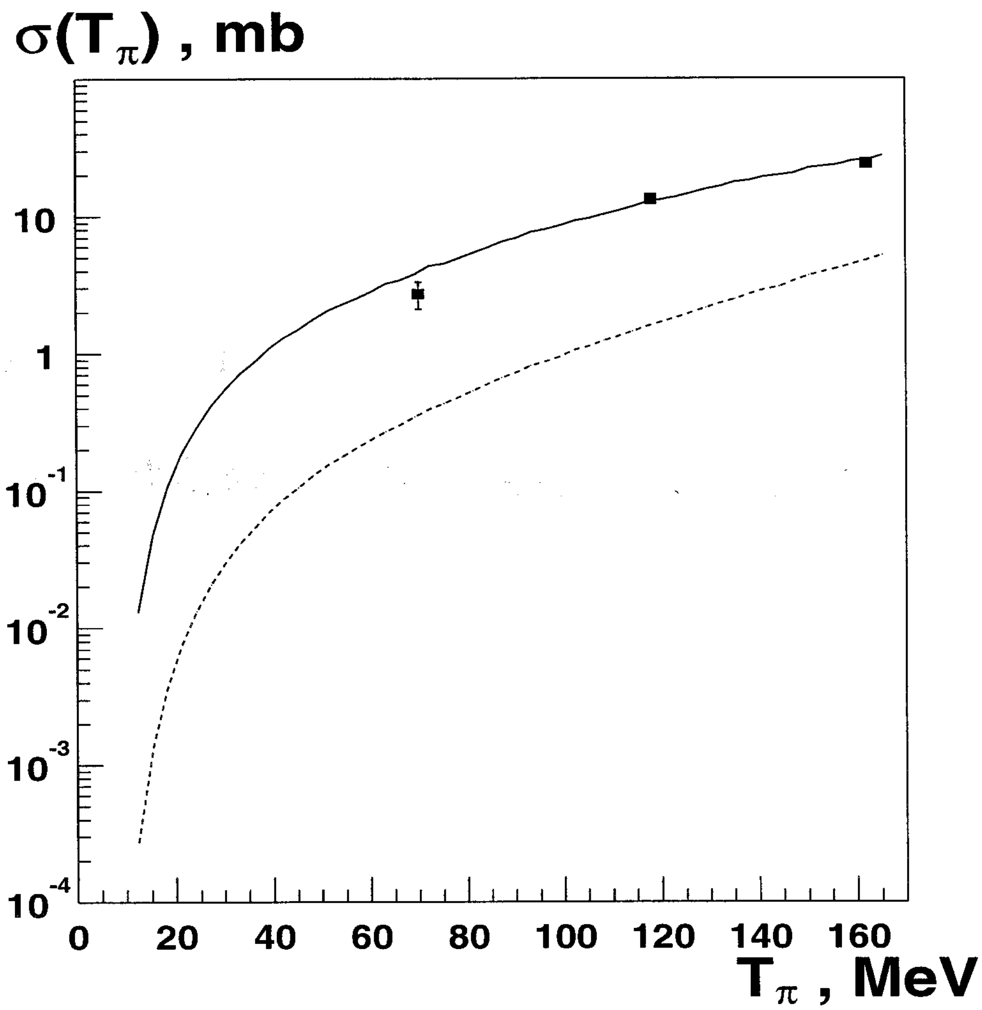

Cross section of the reaction $\pi^+\ {}^3\text{He} \to \pi^0\ p\ p\ p$ **with** (**solid** curve) and **without** (**dotted** curve) NN **final state interaction** taken into account. Exp. points : A. Lehmann et al. (LADS Collaboration) Phys. Rev. **C60**, 024603 (1999).

Analysis of experimental data on ω-meson production (September 2000 beam time)

S.Barsov

High Energy Physics Department
Petersburg Nuclear Physics Institute
188350 Gatchina
Russia

The analysis of experimental data on the ω-meson production taken in September,2000 beam time.

The current status and proposal for the next beam time.

S.Barsov for the ANKE collaboration.

Reaction: p d $\rightarrow$ p_{sp} d ω

Experiment:

- **Beam - 2.77 GeV/c. Target - deuterium cluster target. The D2 - 7.4°.**
- **p_{sp} in SP** (The telescope of three silicon detectors:
  1 - 60μm(no strip), 2 - 300μm(strip - 1mm), 3 - 5mm(strip - 0.234mm)).
  Total energy ranges: (1&2) - 2.5MeV...6MeV; (1&2&3) - 7MeV...30MeV;
  Resolution(σ) - 0.2MeV; Energy calibration - 3%.
  Angular range: ϕ: -10°...+10°; Θ: 80°...110°;
  $\Delta\Theta$: (1&2) - 4°...5°, (2&3) - 1°...3°.
- **d in FD** (The forward detector system: two planes of scintillators - FDH(8, 9), Cherenkov's detectors: Ce(8upp, 8low), 2 MWPC).
  Momentum range: 0.9 GeV/c...2.77 GeV/c.
  Resolution at 2.76 GeV/c (σ_p/p) - 2.3% (with 3 wire + strip planes).
  (σ_p/p) = 1.3% (with 4 wire planes) is available for a small part of the total statistics.
  Angular range depends on momentum: $\Delta\phi$: 2π ...40°; Θ: 0°...10°; $\Delta\Theta$: 0.2°
  Energy loss calibration is done for 5 scintillators in each plane - FDH(5, 5)
  Momentum dependent Ce efficiency calibration is done for 12 Cherenkov's detector - Ce(6upp, 6low)
- **Main trigger:** hardware coincidence FDH&SP(300μm).
- **Statistics** on tapes: $38.2 \cdot 10^6$ / 39 hours.

Selection for the analysis:

- **SP:** 2.5 - 5 MeV, total angular range. 80% of available spectator protons.
- **FD:** 1.5 - 2.3 GeV/c , FDH(5, 5), Geom.cut. 60% of the available **FD** acceptance - mostly, because of geometrical cuts applied on Ce detectors in order to avoid an edge inefficiency.
- **Statistics** after selection: 28175

Measurement for background:

- **Beam - 2.5 GeV/c. Target - deuterium cluster target. The D2 - 7.4°.**
- **Statistics** on tapes: $11.6 \cdot 10^6$ / 7 hours.
- **Statistics** after selection: 8037

Sept.2000. 2.77GeV/c. D-target.
SP: 2.5 - 5 MeV, Θ > 95°.
FD: 2.5-3.5 GeV/c, FDH(5, 5), Geom. cuts.
Quasi-free pn elastic scattering.

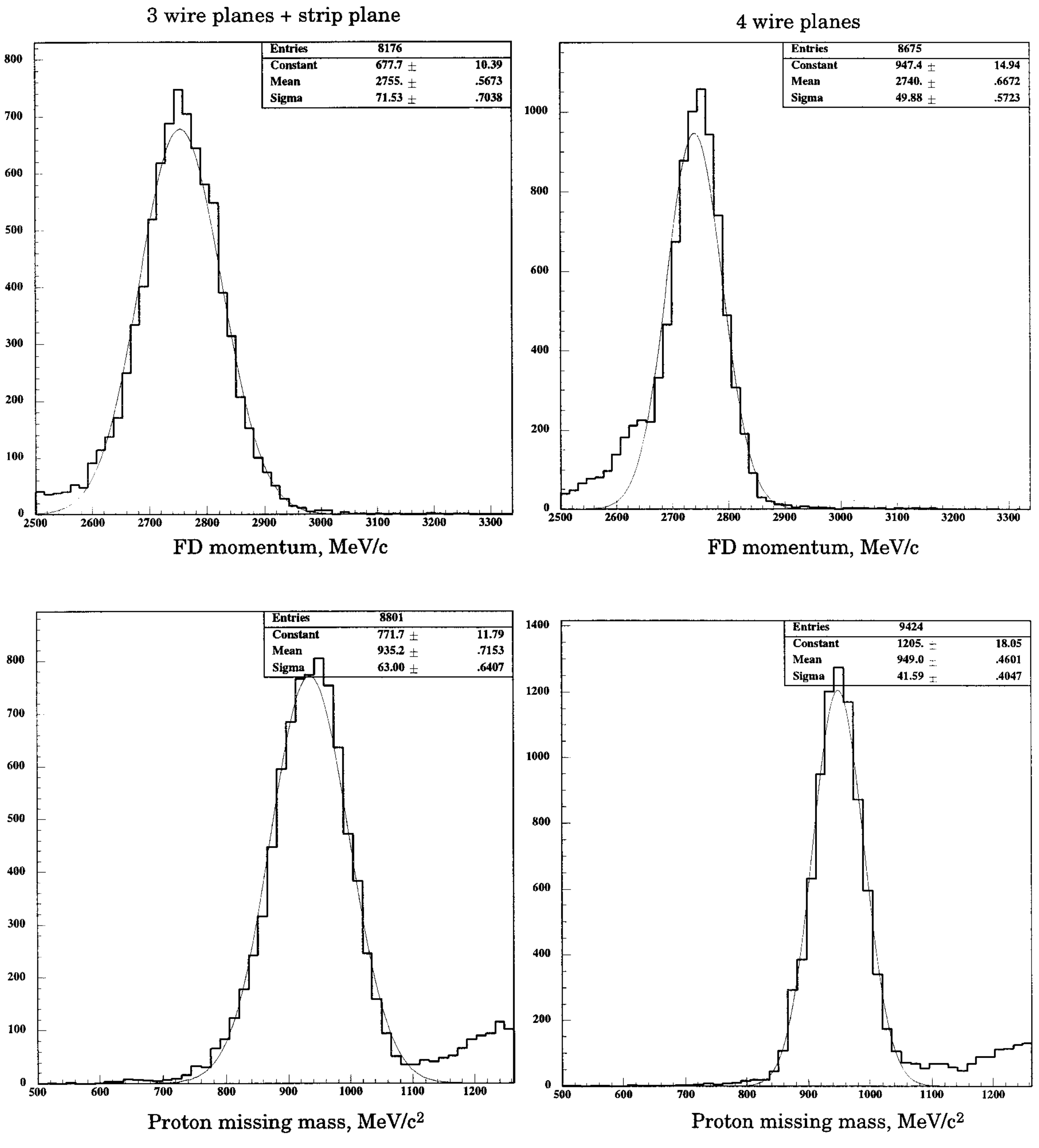

This is a test on the missing mass reconstruction procedure. The expected FWHM of the ω-meson peak in an experimental missing mass distribution is calculated to be of 30-35 MeV/c^2. It is mostly contributed by the uncertainty of Θ_{SP} (18-20MeV/c^2) and by the uncertainty of p_{FD} (22-23MeV/c^2). The significant improvement of the **FD** momentum resolution is expected for the next beam time.

Sept.2000. 2.77GeV/c. D-target. Total statistics.
SP: 2.5 - 5 MeV.
FD: 1.5-2.3 GeV/c, FDH(5, 5), Geom. cuts.

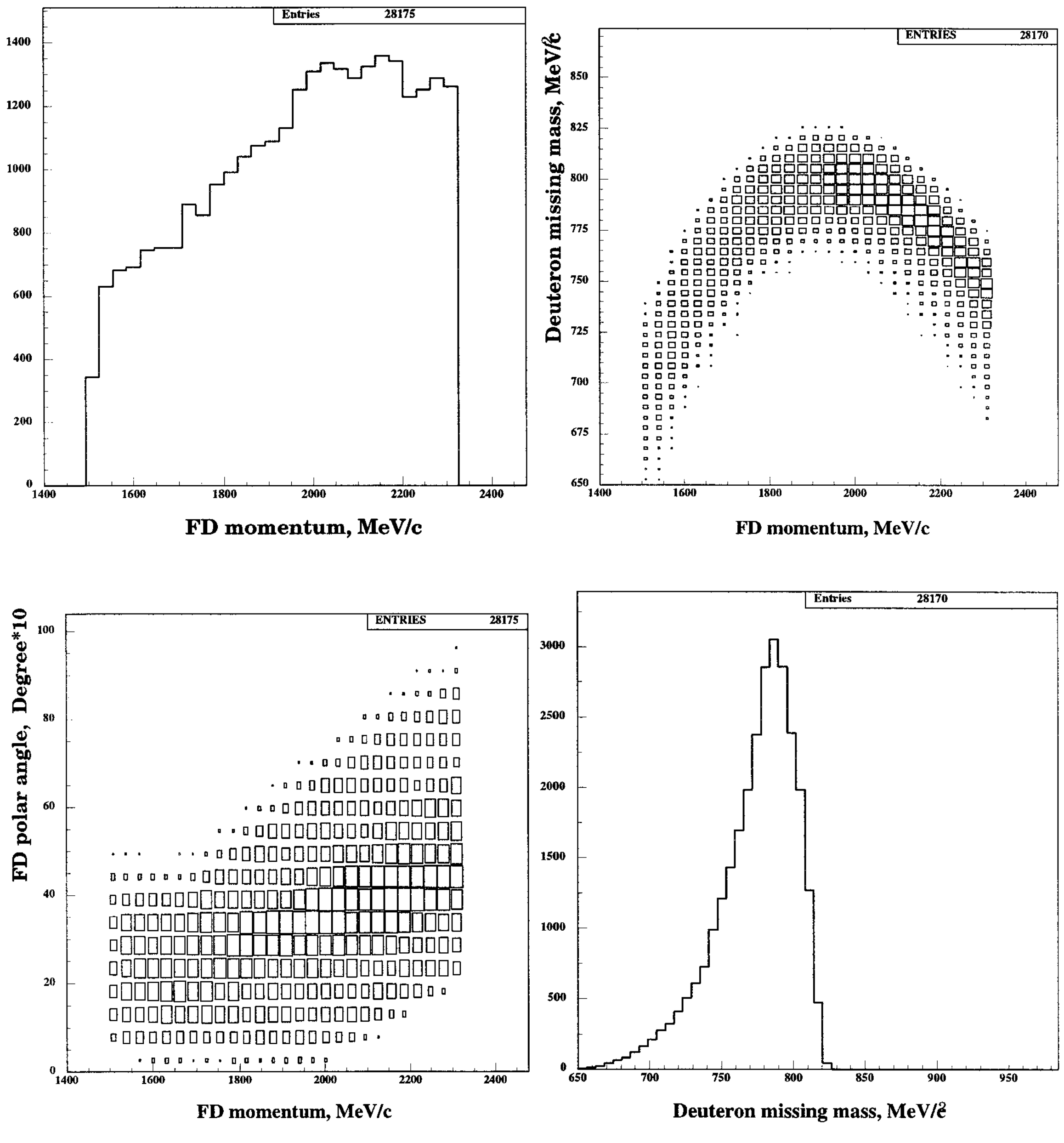

Distributions for all selected events. Actually, almost all particles detected in **FD** are protons from the pion production. The missing mass is reconstructed under the assumption that all they have the deuteron mass. It is seen that under experimental conditions protons misidentified as deuterons produce a peak near the position of the ω-meson mass.

Sept.2000. 2.77GeV/c. D-target. Total statistics.
SP: 2.5 - 5 MeV.
FD: 1.5-2.3 GeV/c, FDH(5, 5), Geom. cuts, Ce(5, 5)

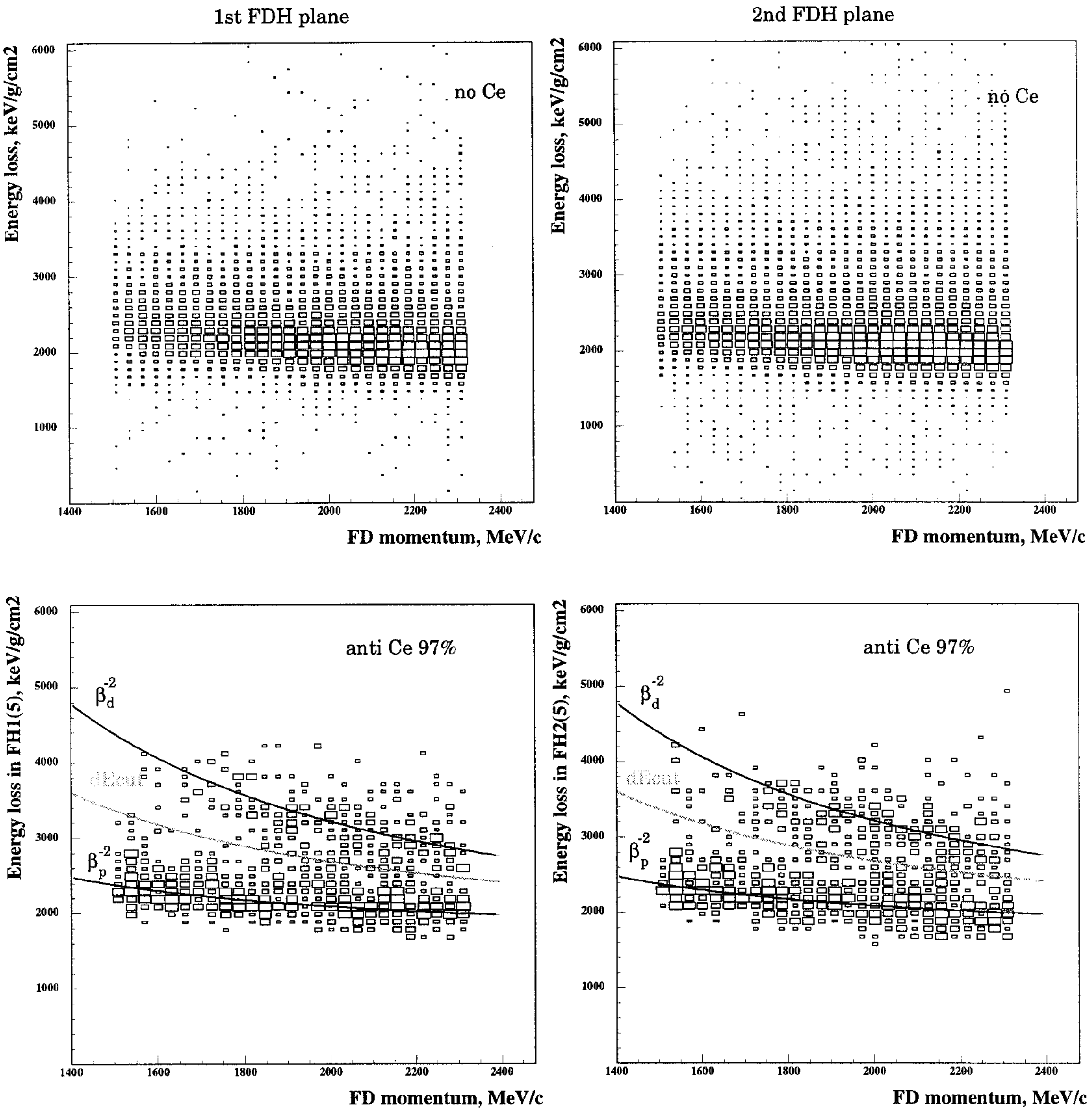

The selection of deuterons means the suppression of protons which, in average, produce higher signal amplitudes in Cherenkov's detectors and have lower energy loss in scintillators than deuterons of the same momentum. So, requirements to a particle to be accepted as deuteron are the anticoincidence with the Cherenkov's detector signal (antiCe) and the energy loss above some value (dEcut). The efficiency of all Ce detectors for protons are equalized with help of individual software thresholds. It is also momentum independent due to an automatic shift of these thresholds using individual momentum dependences of the efficiency measured for each detector.

2.77GeV/c. SP:2.5-5MeV. FD:1.5-2.3GeV/c, dEcut(FDH2) = 2.1MeV/g/cm2.
Energy loss is projected along the deuteron band.

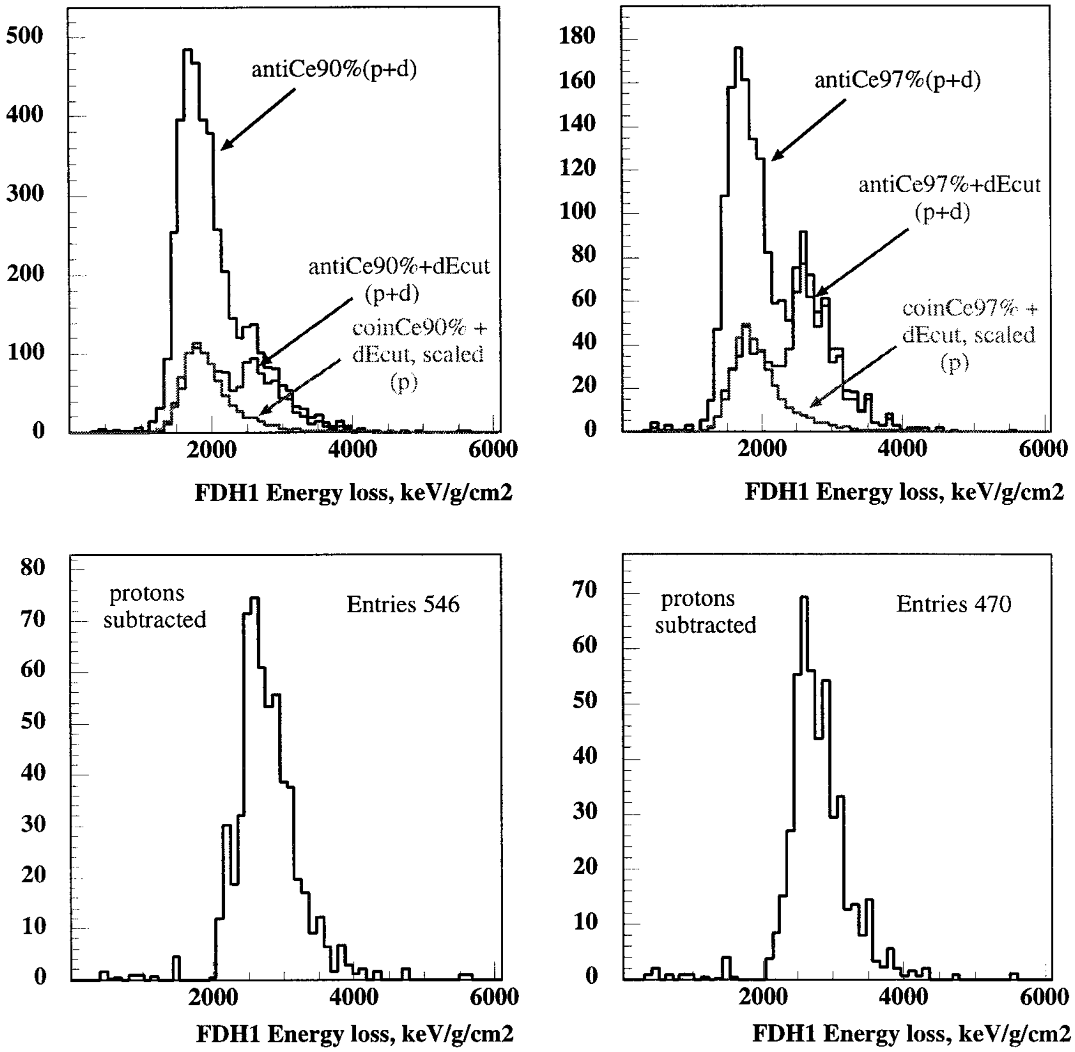

The energy loss in the first **FDH** plane projected along the deuteron band. The dEcut $\geq$ 2.1 MeV$/g/cm^2$ is applied on energy loss spectra in the second **FDH** plane also projected in the same way. Spectra obtained in the coincidence with Ce detector's signals (i.e., for protons) are scaled to maxima of proton peaks.

The uncertainty of the subtraction increases with the decreasing of the Ce efficiency because of the tail of energy loss distribution. One can decrease the contribution of this tail applying dEcut (double dEcut) on both the FDH planes. Then the number of deuterons and the contribution of protons above these cuts can be calculated as it is shown in the next page.

Sept.2000, 2.77GeV/c, D-target, Total statistics.
SP: 2.5-5MeV; FD: 1.5-2.3GeV/c, FDH(5,5), Ce(5,5), Geom.cut, dEcut.

a) Number of particles detected by FD scintilators within Ce geometrical cuts.

c) Number of particles undetected by Ce and accepted by dEcuts after subtraction of proton fraction.

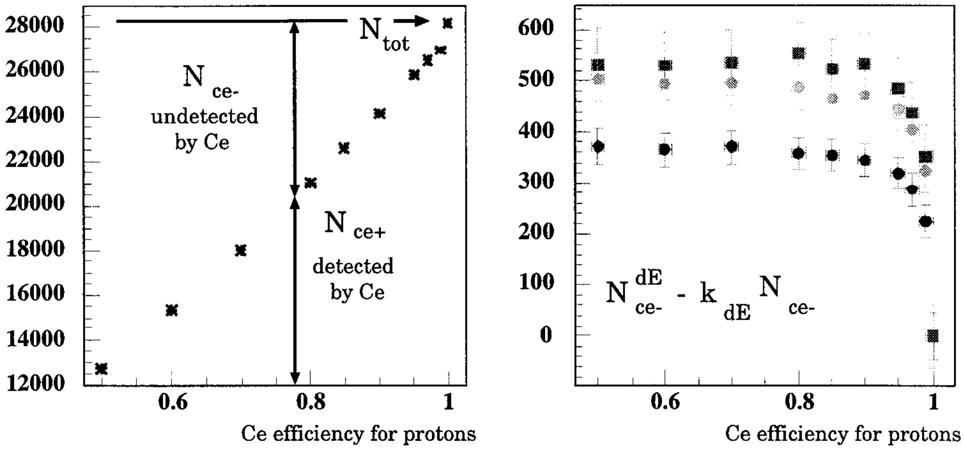

b) Fraction of particles detected by Ce and accepted by deuteron dEcuts
$N^{dE}_{ce+} / N_{ce+} = k_{dE}$

d) The relative change of the number of "deuterons" presented above.

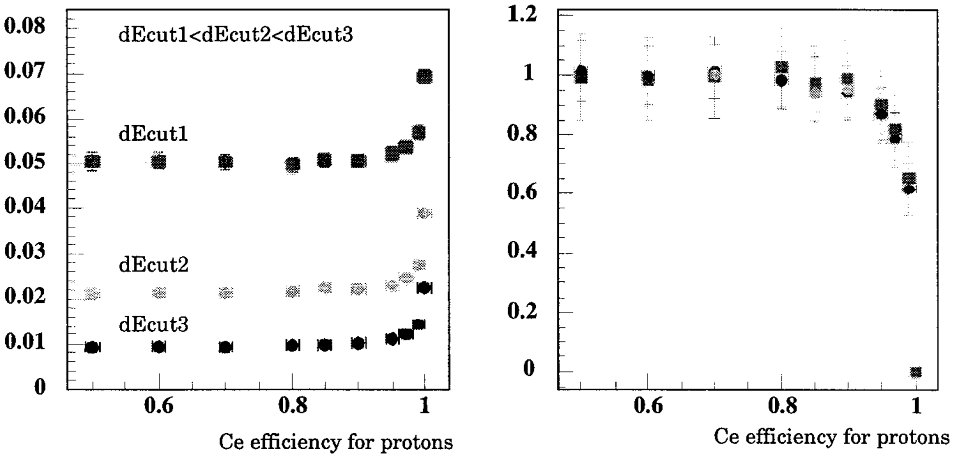

** At the Ce efficiency 1.0 Ce detectors are switched off.

It is seen that the calculated number of deuterons is saturated with the decreasing of the Ce efficiency as well as with the shift of dEcuts from the deuteron band towards the proton band. (The dEcut2 was shown before in (Energy loss vs. momentum) dependences. The dEcut1 is shifted from the dEcut1 towards the proton band in 150keV. The dEcut3 is shifted from dEcut1 towards the deuteron band in the same 150keV.)

The decrease of the number of deuterons with the increasing of Ce efficiency for protons (i.e., with decreasing of thresholds) shows that deuterons still produce the Ce signals with low amplitudes. The Ce efficiency for deuterons was investigated with help of protons of the 1.1GeV/c momentum to be, in average, of 25-30%. This corresponds to the observed relative change

Sept.2000. 2.77GeV/c. D-target. Total statistics.
SP: 2.5 - 5 MeV.
FD: 1.5-2.3 GeV/c, FDH(5, 5), Geom. cuts, Ce(5, 5), dEcut.

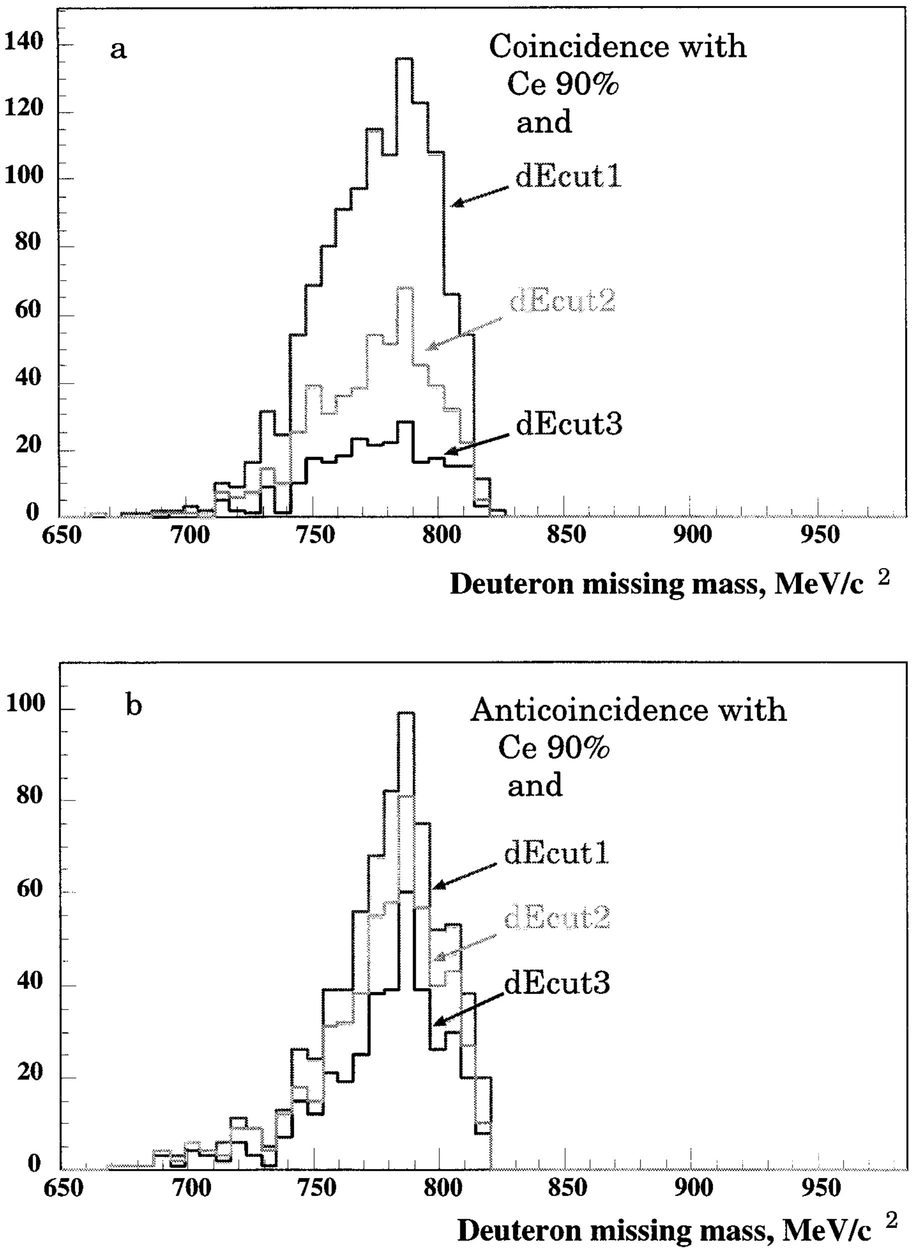

Using the k_{dE} coefficient one can scale an experimental proton distribution obtained for particles which were detected by Ce detectors (i.e., in coincidence with Ce signals) and subtract it from the same experimental distribution obtained for particle which were not detected by Ce detectors (i.e., in anticoincidence with Ce signals). Of course, both these distribution must be produced with the same dEcut and the Ce efficiency. Such missing mass distributions obtained for the same dEcuts which were just mentioned are presented.

Sept.2000. 2.77GeV/c. D-target. Total statistics.
SP: 2.5 - 5 MeV.
FD: 1.5-2.3 GeV/c, FDH(5, 5), Geom. cuts, Ce(5, 5), dEcut.

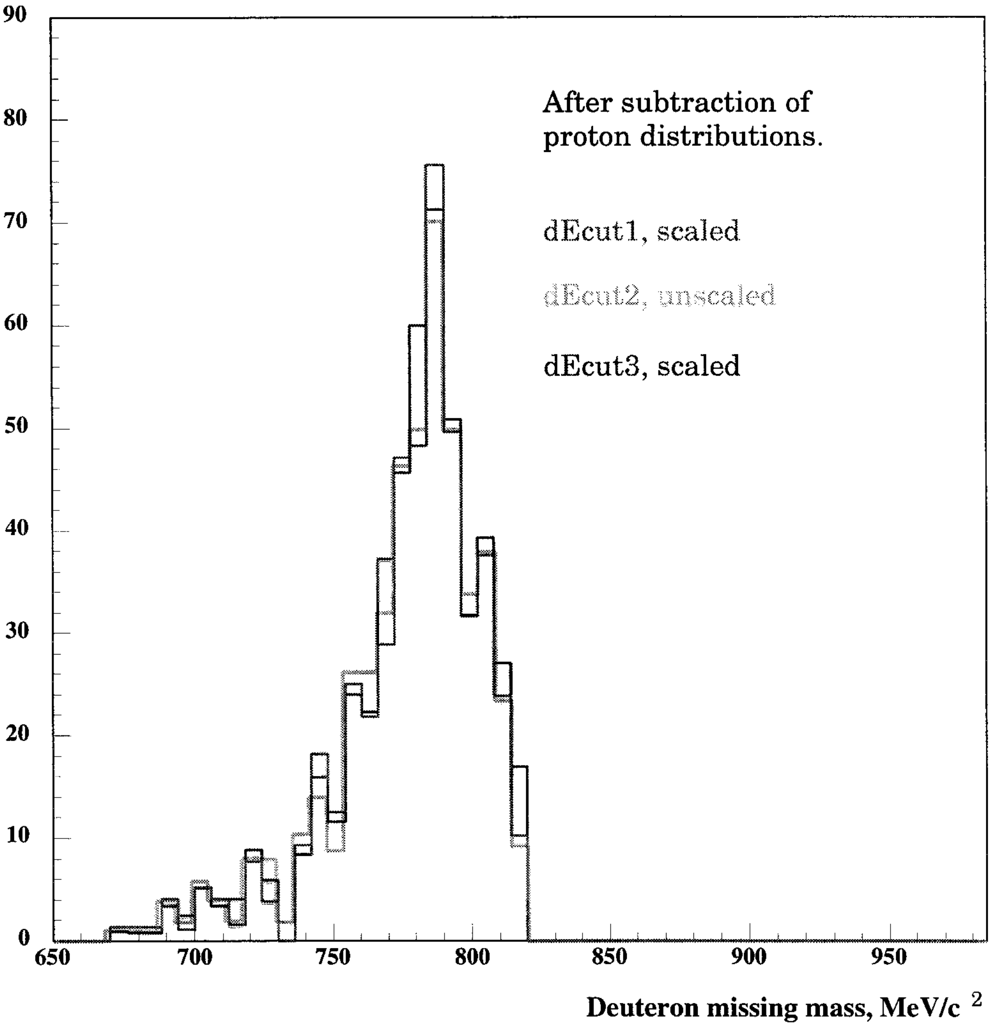

The result of the subtraction is shown. Distributions obtained for different dEcuts are scaled using the total number of deuterons calculated for each of them. Distribution for dEcut2 is not scaled.

Sept.2000. 2.77GeV/c. D-target. Total statistics.
SP: 2.5 - 5 MeV.
FD: 1.5-2.3 GeV/c, FDH(5, 5), Geom. cuts, Ce(5, 5)

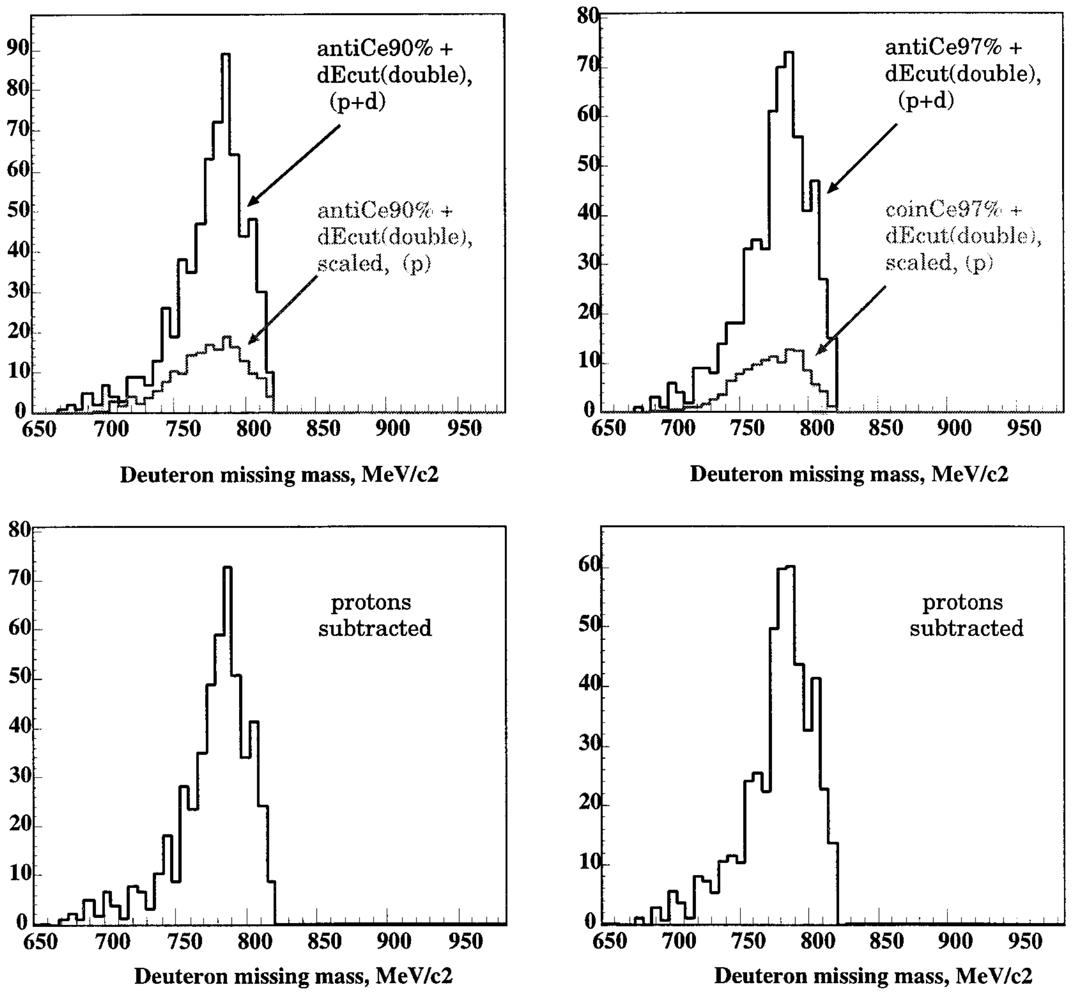

Missing mass distributions for different Cherenkov's efficiencies. The double double dEcut$\geq$ 2.1 MeV$/g/cm^2$ (i.e.,for both the **FDH1** and the **FDH2** planes) in energy loss spectra projected along the deuteron band was used. In the case of the 97% Ce efficiency part of Ce detectors have minimal possible thresholds.

Despite of different sets of statistics selected due to different dEcuts and Ce efficiencies the shape of missing mass distributions remains the same within statistical errors. It demonstrates a pronounced peak at the ω-meson mass. The width of the peak corresponds to the expected FWHM.

Sept.2000. 2.77GeV/c. D-target. Total statistics.
SP: 2.5 - 5 MeV.
FD: 1.5-2.3 GeV/c, FDH(5, 5), Geom. cuts, Ce(5, 5), dEcut.

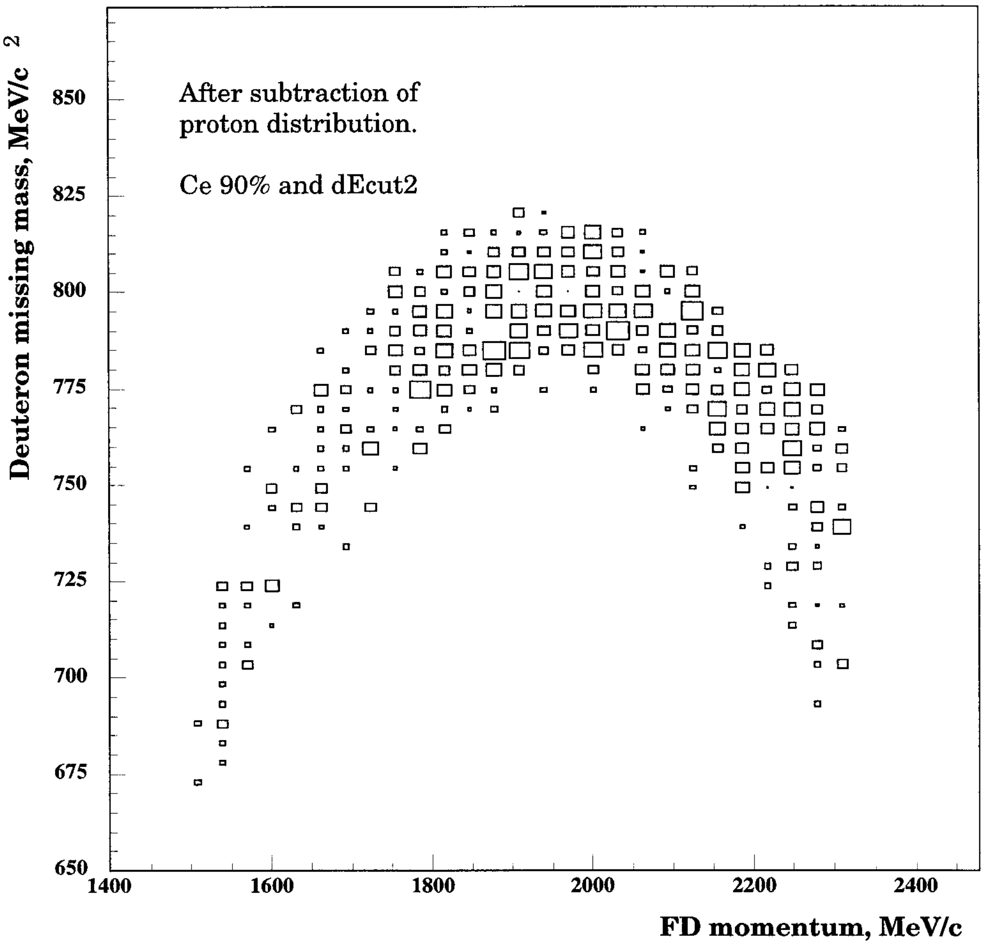

However, the two-dimensional plot doesn't show a clear evidence for the band related to the ω-meson. This is obviously related to the background of deuterons from the non-resonant pion production as well as from the ρ-meson production.

Sept.2000. 2.5GeV/c. D-target. Total statistics.
SP: 2.5 - 5 MeV.
FD: 1.5-2.3 GeV/c, FDH(5, 5), Geom. cuts, Ce(5, 5), dEcut.

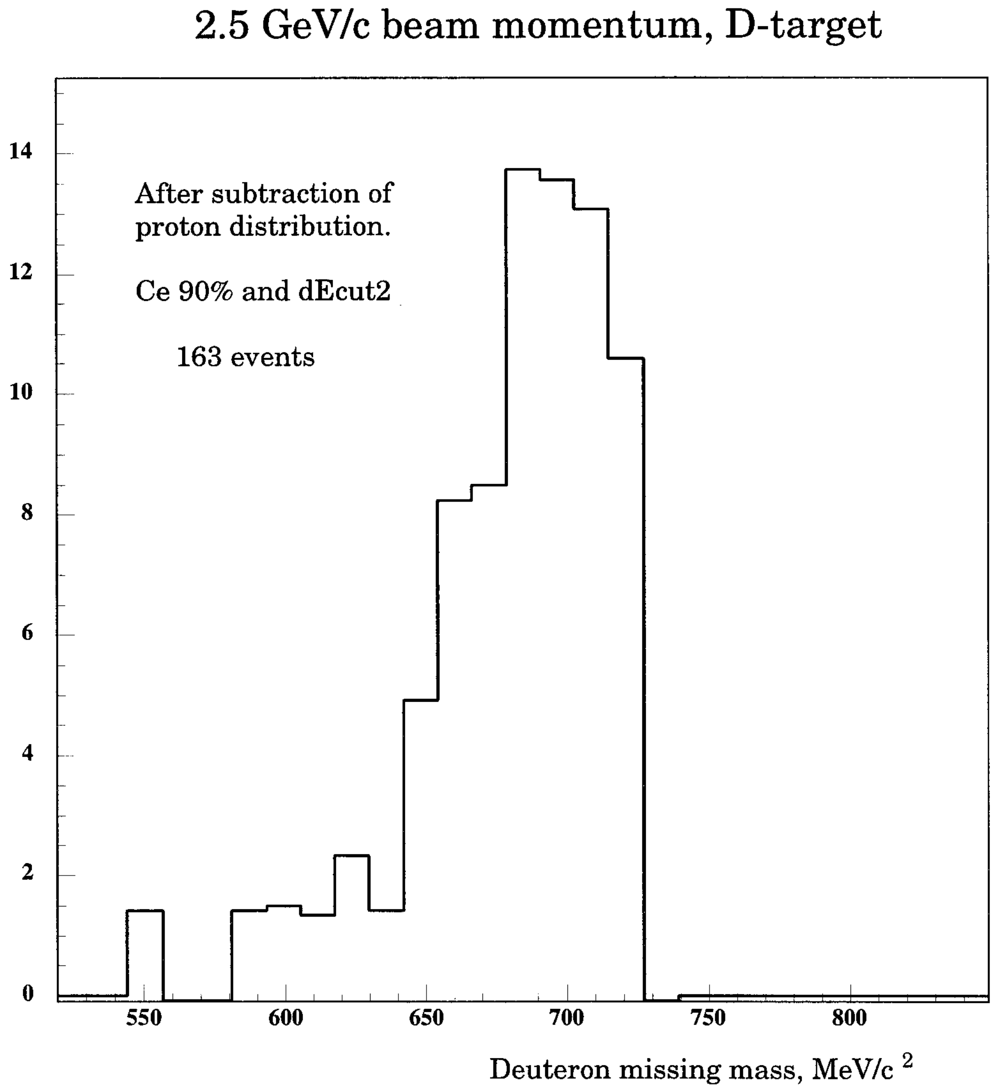

The data taken at the beam below the ρ-meson production threshold were treated in the same way as the data taken at the 2.77GeV/c beam momentum. Because of limited **SP** and **FD** angular acceptances deuterons from the non-resonant pion production also produce a peak in the end of the missing mass distribution though the width of the peak is almost twice larger than the expected for ω-meson.

Sept.2000. 2.77GeV/c. D-target. Total statistics.
SP: 2.5 - 5 MeV.
FD: 1.5-2.3 GeV/c, FDH(5, 5), Geom. cuts, Ce(5, 5), dEcut.

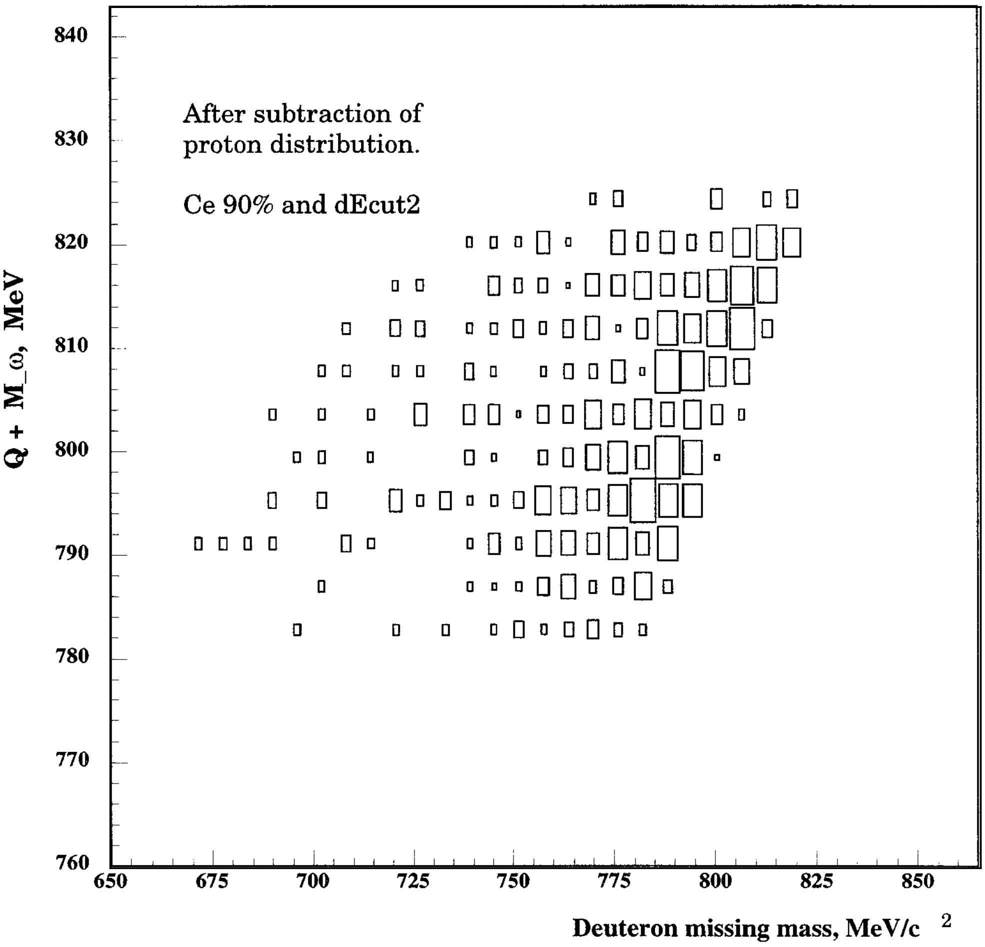

At the moment the subtraction of the deuteron background using the distribution obtained at the 2.5GeV/c beam momentum doesn't seem to be reliable because of the lack of data on the non-resonant pion production. It is not possible to verify an extrapolation to the 2.77GeV/c because the background is practically hidden under the probable ω-meson peak. The reason is that the angular acceptance of the **SP** determines the Q value range within 40Mev. It is necessary either to shift the upper edge of the missing mass distribution or to increase the angular range of **SP** in order to solve the problem of the deuteron background subtraction.

Summary and the next beam time preparation.

The selection of deuterons from protons directly coming from the target is developed. The procedure is based on the good calibration of Cherenkov's detector efficiencies as well as on the good energy calibration and the good energy resolution of **FDH** scintillators. The quality of calibrations is strongly dependent on the quality of the **FD** momentum reconstruction.

The developed procedure of the deuteron selection allows to subtract a rest of proton background from any experimental distribution using the scaling as described above. After such a subtraction the shape of deuteron missing mass distribution doesn't depend on the applied dEcut.

The deuteron missing mass distributions has a pronounced peak positioned at 785 MeV/c^2 that is in a good agreement with the expected $m_\omega = 782.6$ MeV/c^2. The width of peak is 30-35 MeV/c^2 (FWHM) which corresponds to the expected one taking into account the experimental uncertainties of missing mass reconstruction.

The proposal for the next beam time based on the results is following:

- to repeat the measurement of the ω-meson production at the **2.806 GeV/c** beam momentum shifting the edge of the deuteron missing mass spectrum up to 835 MeV/c^2. It seems, to be reasonable to keep the existing spectator detector in the same position as before. Due to the better (hopefully less than 1.3%) **FD** momentum resolution the FWHM of the ω-meson peak is expected to be of 25MeV/c^2. At this beam momentum the maximal outgoing polar angle of deuteron is not more than 10°. At the 2.77GeV/c beam momentum it was 8°. So, the deuteron acceptance is estimated to be about 20-30 % less than before. The decreasing of the acceptance will be partially compensated by an increasing of the production cross section.

- to take data at the **2.600 GeV/c** beam momentum in order investigate the background distribution just below the ω-meson production threshold. It is important that the statistics of this measurement must be high enough.

Future spectator and vertex counters for ANKE

A.Mussgiller

Institut für Kernphysik
Forschungzentrum Jülich
52425 Jülich
Germany

For the ANKE beam time in August of 2001, during which the production of ω-mesons from pn collisions will be studied, a new, second generation, spectator detector will be installed at ANKE. The new setup will have a telescope structure with a 65 μm first detector layer, a 300 μm second layer and a 5.5 mm thick third layer. In contrast to the already existing setup [3], the first two detector layers will be double-sided, allowing the measurement of the both the θ- and the ϕ-angle of the spectator. With this information it will be possible to determine the track of the particles which will result in a higher precision of the measurered spectator momentum and thus in an improved missing-mass resolution.

The horizontally aligned strips of the second layer (measuring the ϕ-angle) will not be used for measuring the energy of the particles. They will be equipped with special amplifying electronics, that will allow for time-of-flight (TOF) determination. In coincidence with the TOF information from the forward detection system of ANKE, the proton-deuteron separation can easily be improved. Although the energy information from these strips will not be given, the position information will be available.

The TOF channels of the new setup will be read-out by standard TDC modules. For all other strips the newly developed integrated chip read-out will be used [1]. In this case special amplifier chips are located inside the vacuum close to the detector. Each chip has 32 input channels and a maximum of 10 chips can be connected to a chain, giving the data as a serial stream of analog data. The analog data stream is sampled by standard VME ADC modules [2]. The second and third detector layers of the new spectator setup are also equipped with in-vacuum trigger chips which allow to get a trigger signal from the setup itself.

In order to be able to correct common mode noise it will probably not be possible to use the zero suppression function of the ADC modules. Since common mode is highly depending on shielding and the environment, a final decision can only be made once the setup is installed at ANKE. In case zero suppression cannot be used the amount of data will be rather high resulting in a high dead time. The estimated event rate that can be handled by the new read out system without zero suppression is between 200 events/s and 300 events/s.

The new spectator setup will be installed together with the existing setup to increase the acceptance. For final adjustments and in order not to disturb data taking it will be set up as a separate read-out system in the beginning of the beamtime and will later be integrated in the ANKE data acquisition.

References

[1] A. Mussgiller. Setup and test of a vacuum-compatible read-out system for silicon-strip-detectors. Master's thesis, Fachhochschule München, 2000.

[2] C.A.E.N. spa. *Technical Information Manual - Mod. V 550 (2 Channel C-Rams)*, 1.0 edition, 4 1998.

[3] S.Barsov. *Talk given during this ANKE meeting,*

Spectator Detector 2001

- Improve deuteron identification by TOF
- Improve spectator angular resolution by x,y detectors

- TOF FD/spectator 1ns ≤ FWHM !!!
- double sided silicon-strip detectors with self-triggering front-end chips

3 layer x,y detector telescope

- 65um, ΔE-proton ≥ 2.5MeV
- 300um, E-proton ≤ 6 MeV
- 5500um, E-proton ≤ 40 MeV

The new Spectator Setup

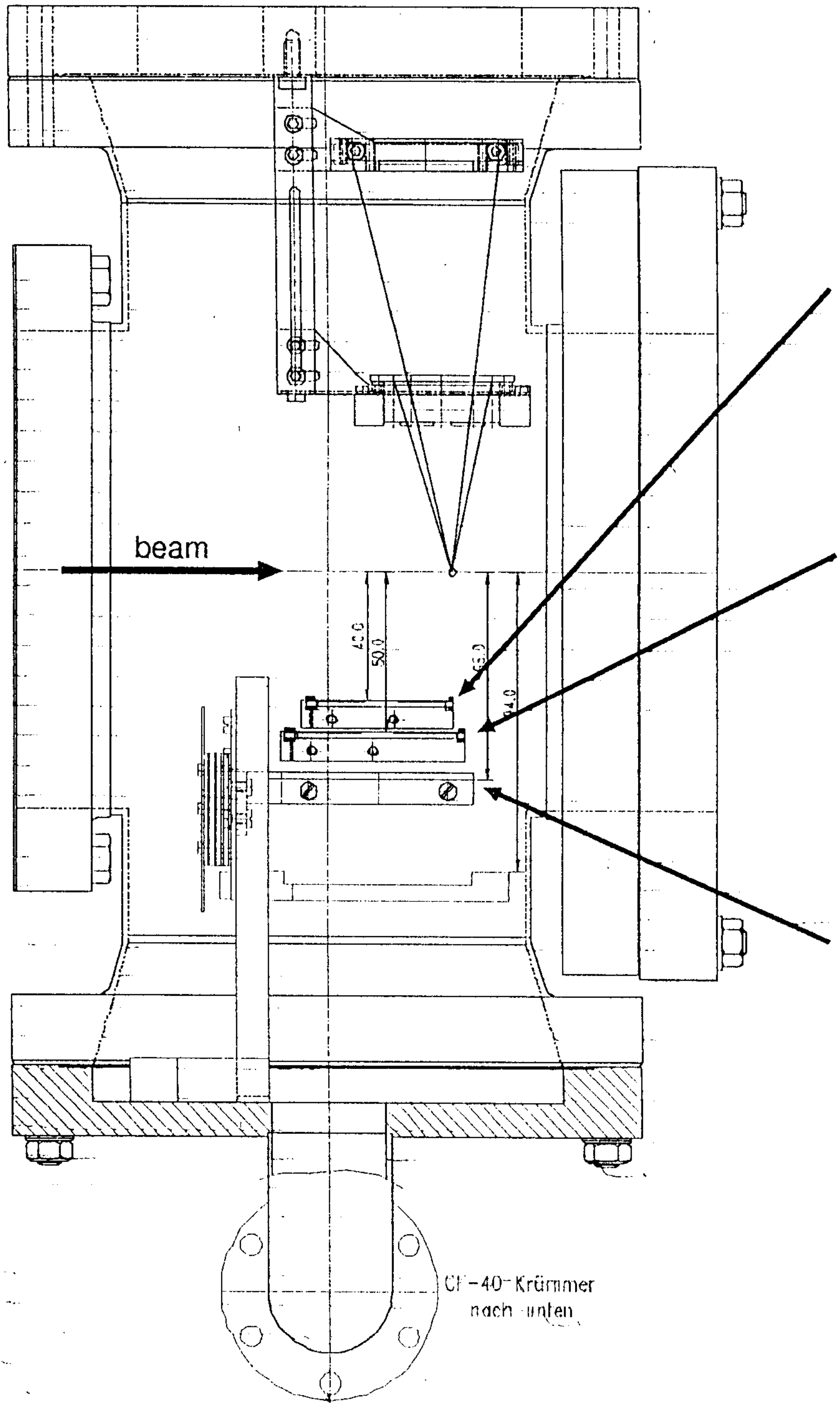

1. Layer

- 65 µm thickness
- 1mm pitch
- 40 strips in Y direction
- 40 strips in Z direction
- 40mm x 40mm

2. Layer

- 300 µm thickness
- 1mm pitch in Y direction
- 0.2mm pitch in Z direction
- 60 strips in Y direction for TOF measurement
- 250 strips in Z direction for energie measurement
- 60mm x 50mm

3. Layer

- 5000 µm thickness
- 235 µm pitch
- 100 strips in Y direction
- 200 strips in Z direction
- 23.5mm x 47mm

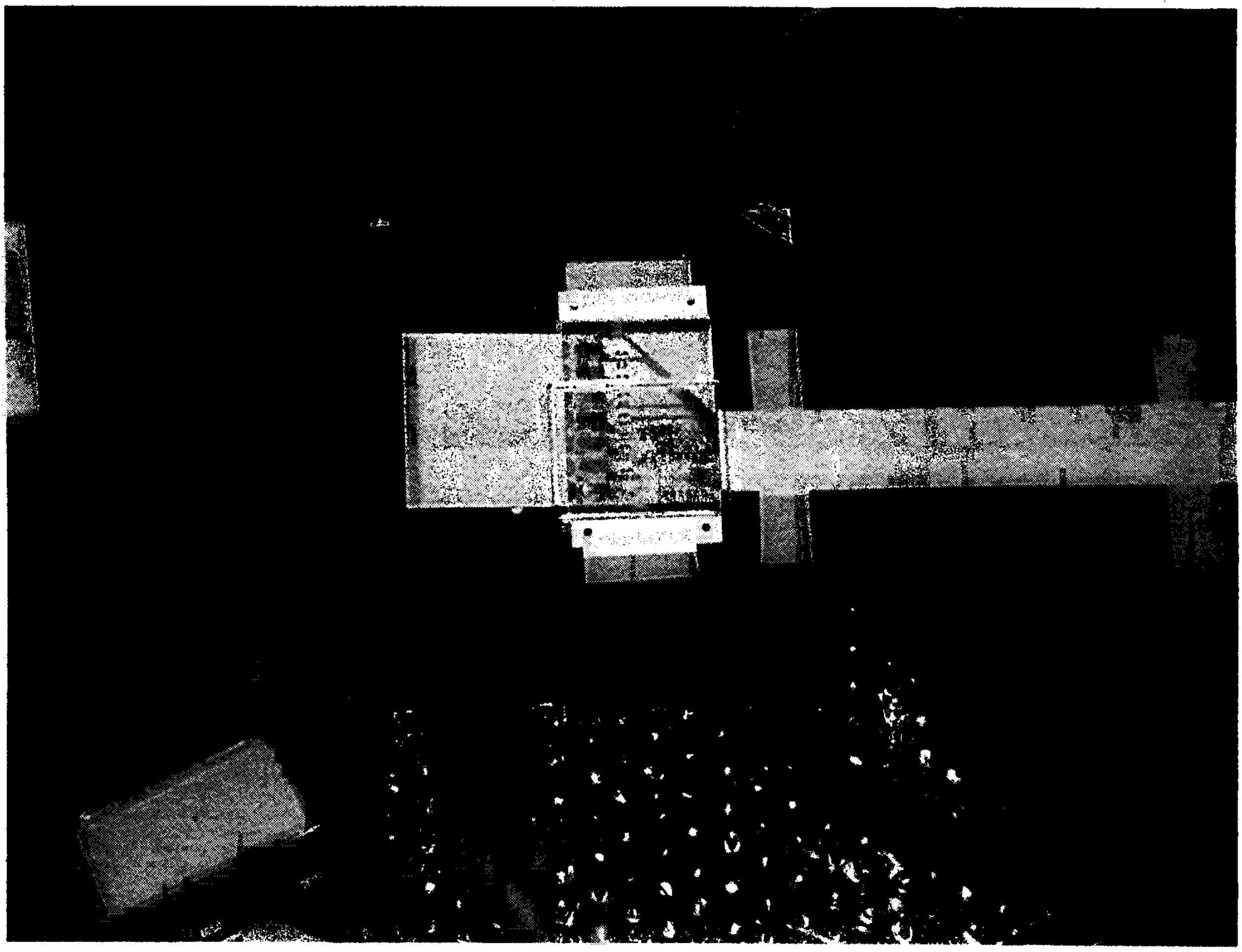

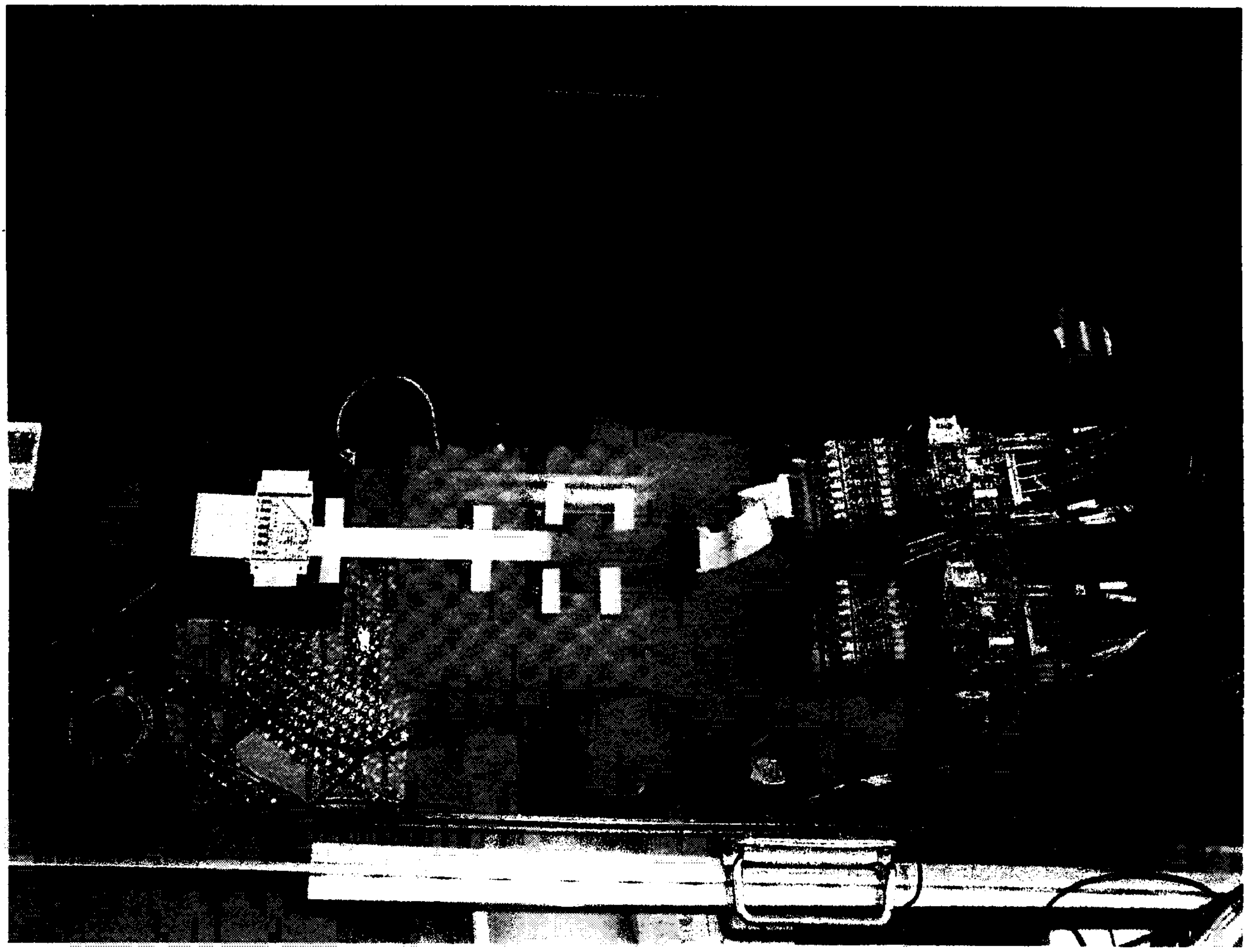

The ANKE Silicon Vertex Detector

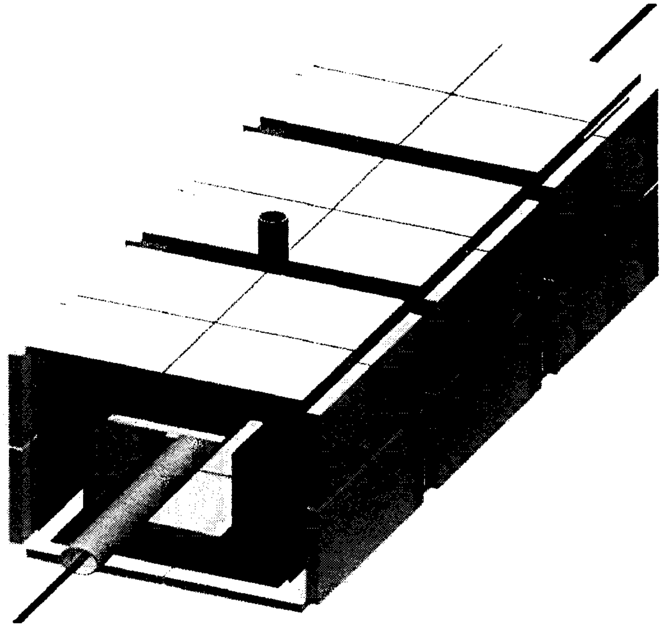

Vertex Reconstruction
- MIP Tracking ($\Delta p/p \leq 1\%$)
- ΔE deuteron identification
  Spectator Proton Tagging/Tracking
- $\Delta E/E$ particle identification,
  2-40MeV protons
- TOF particle identification,
  FWHM < 1ns
- Polarimeter (pp-elastic)

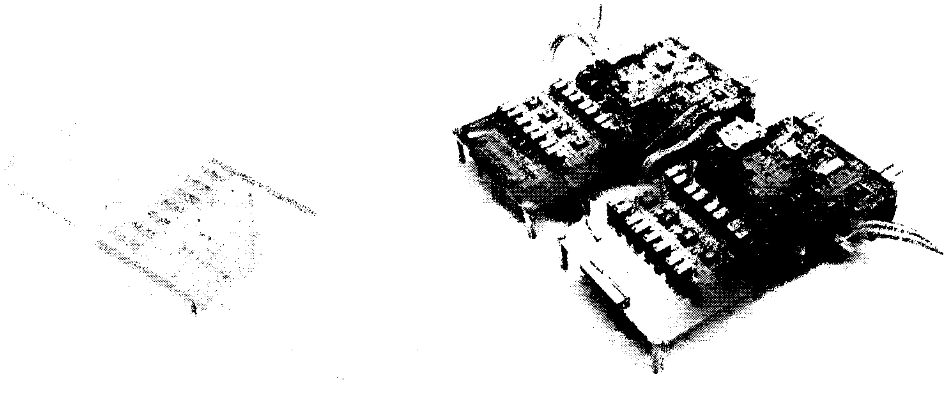

Future prospects at COSY–Jülich

H.Ströher

Institut für Kernphysik
Forschungzentrum Jülich
52425 Jülich
Germany

At COSY, experimental investigations of hadron physics with hadronic probes are performed in order to obtain precision information for meson and hyperon production, on their interactions with nucleons, about baryon excited states and nuclear structure. The ultimate goal is to gain a fundamental, intellectually satisfying understanding of "strong QCD", i.e. how QCD makes hadrons.

In order to strive for precision by improved luminosity, COSY is continuously improved and expanded: the number for polarized protons in COSY has now reached a level of more than 10^{10} at a degree of polarization of more than 60%. An (as yet) unpolarized deuteron beam is available with momenta up to 3 GeV/c and intensities of 5 x 10^{10}. A new injector (SC linac) will replace the current cyclotron to push the intensity to the space charge limit also for polarized beams.

At ANKE, one of the internal experiments in the COSY ring, the following physics programs are being/will be pursued:

1. Nuclear targets (V. Koptev, M. Hartmann et al.)
   K^+ production in p+A collisions were one of the initial motivations to build ANKE. The first phase of the program (measurement of cross sections and A-dependences at both subthreshold and higher energies) has almost been completed - first results have been published in Phys. Rev. Lett. The next phase (correlation studies) will probably start in 2002. In future it is planned to extend these studies to the production of vector mesons (ω, ϕ) in the nuclear environment. In preparing for these measurements the negative particle detection system will be implemented into ANKE.

2. Deuteron breakup (V. Komarov, F. Rathmann et al.)
   Also being an early proposal, the program has recently started with an unpolarized measurement. The next step will be the use of a polarized proton beam incident on an unpolarized cluster jet proton beam. In the near future, the ABS (plus a storage cell) will be employed for double polarization experiments. This, however, requires a serious COSY-beam development. Also a vertex detector is necessary which is in the planning stage.

3. Scalar mesons (M. Büscher et al.)
   Being a relatively new program, a first experiment aiming to measure pp$\rightarrow$ d a_0^+ has been conducted sucessfully. The hope is to detect the scalar meson in its two decay channels (K^+K^- and η π). Next will be measurements of proton-deuteron reactions.

4. Neutron target (R. Schleichert et al.)
   Since no free neutron targets are available the best way to study proton-neutron interactions is by means of the spectator–proton tagging technique, using a deuteron target. This program has recently started with a measurement of pd $\rightarrow$ p_{sp} d ω, and will be extended to other mesons as well.

5. Photon detector (V. Hejny et al.)
   The proposal to build a compact electromagnetic calorimeter with a large solid angle at ANKE has recently been accepted. First detector modules have been ordered and will be tested later this year.

6. Deuteron beam
   This new possibility at COSY will certainly be exploited in future ANKE proposals, for example d + d$\rightarrow \pi^0 + \alpha$.

In conclusion it can be stated that an exciting period for first class physics experiments at COSY (and in particular at ANKE) lies ahead - everybody interested is invited to attend !

Priorities for following measurements with open strangeness production

1. Measurements with proton target, T~2.7 GeV (i.e. as high as possible)

Reactions to be investigated:

$pp \to d\, a_0^+ (\to K^+K^0)$

$\to pp\, \phi, a_0^0/f_0 (\to K^+K^-)$

$\to pK^+ Y$ $(Y=\Lambda(1405), \Sigma(1480)$

Trigger on delayed K^+ events
K^- detection needed
Remaining 3 weeks of beam time from proposal #55 can be used
Beam request for PAC, Nov. 2001; beam time in spring 2002
Responsible for preparation of request: M.Büscher, M.Hartmann, V.Koptev

2. Measurements with deuteron target, T~2.7 GeV (i.e. as high as possible)

Reactions to be investigated:

$pn \to d\, \phi, a_0^0/f_0 (\to K^+K^-)$

$pd \to {}^3He/\, \phi, a_0^0/f_0 (\to K^+K^-)$

$\to {}^3H\, a_0^+ (\to K^+K^0)$

Trigger on delayed K^+ events
K^- detection needed
3 weeks of beam time granted (proposal #97)
Beam request for PAC, spring 2002; beam time in fall 2002
Responsible for preparation of request: M.Büscher
First parasitic test in Aug. 2001: $p(2.0\ GeV)d \to K^+ X$

3. Measurements with heavier targets, T~2.7 GeV

Reactions to be investigated:

$pA \to \phi X$ $(A = C, \ldots, Au)$

New proposal will be prepared by: M.Hartmann